2010

Behavior characterization and development of LRFD resistance factors for axially-loaded steel piles in bridge foundations

Sherif Sayed Abdelsalam
Iowa State University

Behavior characterization and development of LRFD resistance factors for axially-loaded steel piles in bridge foundations

by

Sherif S. AbdelSalam

A dissertation submitted to the graduate faculty

in partial fulfillment of the requirements for the degree of

DOCTOR OF PHILOSOPHY

Major: Civil Engineering (Geotechnical Engineering)

Program of Study Committee:
Sri Sritharan, Major Professor
Muhannad T. Suleiman
Fouad S. Fanous
Thomas J. Rudolphi
Jeramy C. Ashlock
Charles T. Jahren

Iowa State University

Ames, Iowa

2010

DEDICATION

The author devotes this thesis to his father Dr. Sayed AbdelSalam for his support and inspiration throughout this work, as well as his mother, sister, and brother for their unconditional support and understanding that helped the author to get through all the challenges and successfully complete this thesis.

TABLE OF CONTENTS

LIST OF FIGURES

LIST OF TABLES

ABSTRACT

The Federal Highway Administration (FHWA) mandated utilizing the Load and Resistance Factor Design (LRFD) approach for all new bridges initiated in the United States after October 1, 2007. Consequently, significant efforts have been directed by Departments of Transportation (DOTs) in different states towards the development and implementation of the LRFD approach for the design of bridge's deep foundations. The research presented in this thesis is aimed at establishing the LRFD resistance factors for the design of driven pile foundations by accounting for local soil and pile construction practices. Accordingly, regional LRFD resistance factors have been developed for different static analysis methods, incorporating more efficient in-house and combinations of suitable pile design methods, following the AASHTO LRFD calibration framework. Typical calibration framework was advanced in the research presented in this thesis to incorporate the effects of layered soil systems and to reduce the uncertainties associated with soil variation along pile embedment.

To achieve the calibration process successfully, the following three major tasks were accomplished as part of the research presented here: (1) completion of nationwide and statewide surveys of different state DOTs and Iowa county engineers, respectively, to obtain necessary information regarding current pile design and construction practices, the extent of LRFD implementation and regional calibration, as well as to learn of existing local practices; (2) calibration of the LRFD resistance factors for bridge deep foundations, based on the local database (PIle LOad Tests in Iowa [PILOT-IA]), was developed as part of the project and contained data from 82 load-tested steel H-piles, as well as adequate soil profile information; and (3) conduction often full-scale instrumented pile static load tests that cover different local soil regions, accompanied by various soil in-situ tests, including standard penetration test (SPT), cone penetration test (CPT), borehole shear test (BST), and push-in-pressure-cells, in addition to soil laboratory tests with soil classification, 1-D consolidation, CU-Triaxial tests, and direct shear test (DST).

In addition, the AASHTO LRFD calibration framework only addresses pile design at the strength limit state; however, more comprehensive and practical design recommendations should account for the strength and serviceability limit states, simultaneously. For this

purpose, two different levels of advanced analysis to characterize the load-displacement response of piles subjected to axial compressive loads were used. The first level of analysis was based on an improved load-transfer method (or t-z model), attained as follows: (a) establishing a modification to the Borehole Shear Test equipment (mBST), that, for the first time, allows for a direct field measurement of the soil-pile interface properties for clay soils; (b) establishing a modification to the Direct Shear Test (mDST), that allows for an accurate and simple laboratory measurement of the soil-pile interface for sands; and (c) adapting a new Pile Tip Resistance (PTR) laboratory test that can measure practically the pile end-bearing properties. The improved t-z analysis uses the measured soil-pile interface properties from the mBST and/or the mDST for different soil layers, and also uses the end-bearing properties of the soil under the pile tip from the PTR laboratory measurements. The t-z analysis showed significantly improved characterization for the pile load-displacement behavior and load distribution along the pile length, compared to field test results. The second level of analysis was based on finite elements (FE), where the Mohr-Coulomb soil constitutive properties were adjusted, using a sensitivity analysis based on various laboratory soil tests, such as the mDST and CU-Triaxial tests. After improving the reliability of the different analytical models in characterizing the behavior of axially-loaded steel piles, a new LRFD displacement-based pile design approach was provided in this thesis, utilizing the improved analytical models.

CHAPTER 1: INTRODUCTION

1.1. Background

Driven pile foundations are frequently used in the United States to support bridge structures and their capacity can be estimated using three types of analytical methods. They are static analysis methods, dynamic analysis methods, and dynamic formulas. The static methods, developed empirically or semi-empirically using data from field testing of piles, are widely used and recommended by different codes for the design of bridge's deep foundations. In contrast, dynamic analysis methods and dynamic formulas are typically not employed as design methods, but used to control pile driving during the construction stage. While the dynamic methods are examined in companion studies by Roling (2010) and Ng (in process), the research in this thesis focuses on the design and response characterization of axially-loaded pile foundations. In this process, an estimate of the number and/or length of piles are established by using one of several static methods available in the literature. Each method has advantages and limitations, and the selection of the most appropriate method for a specific design problem depends upon the site geology, pile type, extent of available soil parameters, local design, and construction practices.

For a selected static method, the pile design may be achieved using the Working Stress Design (WSD) approach, Load Factor Design (LFD), or the Load and Resistance Factor Design (LRFD) approach. The WSD approach has been used in engineering practice since the early 1800s, in which the actual loads anticipated from the structure are compared with the capacity of the foundations, ensuring an adequate factor of safety (FS). Generally, engineers assumed the FS based on different levels of control in the design and construction stages. Particularly for deep foundations, experience and subjective judgment are greatly important for selecting the appropriate FS (Paikowsky et al., 2004). However, it has long been recognized that pile designs based on the WSD approach cannot ensure consistent and reliable performance of substructures (Goble, 1999). This major drawback of the WSD stems from ignoring various sources and levels of uncertainties associated with loads and capacities of deep foundations, causing highly conservative FS to be used (Paikowsky et al., 2004). In general, the uncertainties associated with structural resistances are minimal compared to

those found in the parameters defining the geotechnical resistances. In the latter case, the uncertainties arise, due to the large variation of the soil properties and non-homogeneity, fluctuation of the ground water table, and variable soil strength-deformation behavior (Paikowsky et al., 2004). This causes large inconsistencies in determining pile resistance, depending on the extent of soil investigation, design methodology, and construction control (Becker and Devata, 2005).

To overcome this large inconsistency in the design of pile foundations, the LRFD approach was introduced to quantify various uncertainties using probabilistic methods, which aim to achieve engineered designs with a chosen level of reliability. In the LRFD approach, loads are multiplied by load factors, usually greater than unity, and capacities are multiplied by resistance factors smaller than unity. A simple definition of failure in this framework is when the factored loads exceed factored capacities. To avoid failure, the probabilistic approach used for the LRFD development allows for determining the overlap area between the probability density functions (PDFs) of loads and resistances. The overlap area is limited to an acceptable level that defines the acceptable risk of failure.

There are several advantages of using the LRFD approach over the WSD method for designing deep foundations. The most important advantage is handling the uncertainties associated with different design parameters by utilizing a rational framework of probability theory, leading to a constant degree of reliability. Consequently, the LRFD provides consistent design reliability for the entire structure, when it is applied to both superstructure and substructure, thus improving the overall design and construction process. Paikowsky et al. (2004) indicated LRFD designs could result in cost-effective pile foundations, even though they were developed to yield reliabilities equal to or higher than those provided by the WSD approach. Furthermore, the LRFD pile design approach does not require the same amount of experience and engineering judgment as required for the WSD approach.

Since the mid-1980s, the LRFD approach has been progressively developed, established, and implemented for the design of structural elements; however, its application to geotechnical designs has been relatively slow (DiMaggio et al., 1998). This could be due to the dissimilarities between the LRFD and past WSD design practices, as well as the lack

of pile load test databases required to develop the LRFD resistance factors (Withiam et al., 1998).

1.1.1. LRFD implementation

In 2000, the Federal Highway Administration (FHWA) mandated all new bridges initiated in the United States after October 1, 2007, must follow the LRFD approach. Consequently, significant efforts have been directed by Departments of Transportation (DOTs) in different states towards the development and application of the LRFD approach to foundation design. After developing several versions of specifications to design deep foundations using the LRFD approach, the 2007American Association of State Highway and Transportation Officials (AASHTO) specifications were released, based on studies conducted by Barker et al. (1991), Paikowsky et al. (2004), and Allen et al. (2005). However, several code users indicated the AASHTO recommended LRFD resistance factors led to inappropriate pile designs that conflicted with their past experiences—it yielded unnecessarily conservative pile designs (Moore, 2007). Furthermore, AASHTO does not provide resistance factor recommendations for all static methods, different combinations of methods, or local "in-house" methods developed by the DOTs in different states. The obvious reason for these limitations is that AASHTO specifications are aimed at establishing design guidelines at the national level, accounting for the large variation in soil properties (Paikowsky et al., 2004). To collect detailed information regarding current practices and the extent of LRFD implementation for the design of bridge's deep foundations, a nationwide survey was conducted among state DOTs as part of this study, which revealed that utilizing regionally-calibrated LRFD resistance factors for specific soil conditions would increase pile design capacity by more than 50%, which will likely reduce the overall cost of bridge foundations.

To attain more cost-effective bridge foundations, the FHWA permitted establishing regionally-calibrated LRFD resistance factors to minimize any unnecessary conservatism built into the pile's design. Regionally-calibrated LRFD resistance factors can be developed for a specific geographical region with unique soil conditions and construction practices. The development of such resistance factors for a given pile type and geological region requires

the existence of adequate local static load test data, as well as quality soil investigations. According to survey outcomes, at least 18 state DOTs have developed their regional resistance factors based on local databases to improve the cost-effectiveness of deep foundations.

The development of such regional resistance factors should be conducted in a manner consistent with the 2007 AASHTO LRFD calibration framework, as required by the FHWA. However, the AASHTO calibration framework provides resistance factors for three general soil groups: sand, clay, and mixed soils. In fact, it is atypical to only have one soil type at a site, but these groups represent the predominant soil types present along the pile's embedded length. Nevertheless, suitable criteria for defining the extent of a specific soil type to classify the site as sand or clay site is not clearly defined in AASHTO. Foye et al. (2009) stated the current LRFD calibration framework discarded various sources of uncertainties, contributing to the observed scatter in soil properties; hence, provided resistance factors for pipe piles driven into clean sand soils, separated for the skin-friction and end-bearing components of the pile's total resistance. Recently, McVay et al. (2010) indicated the current design code involved indistinct averaging due to the reliance placed on constant resistance factors that ignored the effects of soil variation along the shaft's embedment. Consequently, a major part of this research is dedicated to 1) developing the LRFD resistance factors for the design of driven steel H-piles for different soils in the state of Iowa and 2) advancing the calibration process to avoid the aforementioned AASHTO shortcomings regarding the effect of soil variation.

1.1.2. Pile settlement

The pile serviceability limit state is defined by the prescribed permissible settlements and/or differential settlements based on the structural serviceability requirements. According to the 2007 AASHTO LRFD specifications, the pile serviceability limits should be checked during the design stage and shall be consistent with the type of structure, structure performance, magnitude of transient loads, and the structure's anticipated service life. However, the design specification only provides resistance factors for axially-loaded piles at the strength limit state. Consequently, the pile settlements typically checked after

determining the design's capacity, which may require several design iterations to satisfy the pile strength and serviceability requirements (Misra and Roberts, 2006). According to Abu-Hejleh et al. (2009), pile settlement may control the design of bridge foundations, due to the existence of large structural loads that need to be adequately supported without experiencing excessive deformations, especially when the piles are embedded in highly deformable soils. Therefore, the typical design sequence approach may not be efficient when the serviceability limit state governs the bridge pile design, considered a disadvantage of the current LRFD design framework.

A design methodology based on determining the load-displacement behavior of the pile can easily incorporate both strength and serviceability limit states in the pile's design process. However, static analysis methods only provide the pile nominal capacity at failure without determining the corresponding settlement. Therefore, characterizing the load-displacement behavior of axially-loaded piles requires adapting more appropriate and comprehensive techniques compared to traditional static methods. The most accurate way to measure the actual load-displacement behavior is to conduct a pile static load test (SLT), a very expensive and time consuming field test (Misra and Roberts, 2006). Another approach would be to establish suitable analytical models that can accurately predict the pile load-settlement behavior. Researchers have attempted different analytical approaches to model the pile's behavior under monotonic axial loads. The most important parameters that control the accuracy of these approaches are soil properties and soil-pile interface parameters dependent on the pile material and construction techniques, several are empirical and/or semi-empirical in nature and rely on field and/or laboratory conventional soil tests (Roberts et al., 2008). According to Guo and Randolph (1998), the analytical models used to characterize pile behavior can be classified into three major categories: (1) approximate closed-form solutions, (2) one-dimensional numerical algorithms, and (3) boundary or finite element (FE) approaches.

The first two categories depend on load-transfer analysis, an iterative technique for solving the nonlinear differential equations of the transferred stresses and displacements along the pile embedded length using the finite-difference method (Coyle and Reese, 1966; and Suleiman and Coyle, 1976). Pile analytical models, based on load-transfer analysis, can

also be identified as the "t-z" models, where the "t" refers to transferred loads at a specific depth along the pile embedment length, and "z" refers to the corresponding vertical displacement of the pile with respect to the surrounding soil. In the t-z model, the pile is divided into several segments and is replaced by elastic springs. The surrounding soil is represented as a set of nonlinear springs, with one spring depicting the behavior of end-bearing at the pile tip (Misra and Chen, 2004; Alawneh, 2006; Roberts et al., 2008). According to El-Mossallamy (1999), the t-z models do not require significant soil testing to develop the soil-pile interface parameters in comparison to the efforts needed to develop the FE models. Moreover, the t-z analysis has been widely used and considered very acceptable for modeling bridge deep foundations subjected to axial compressive loads (Misra and Chen, 2004; Alawneh, 2006; Misra and Roberts, 2006; and Roberts et al., 2008). However, the stiffness of the nonlinear springs required for the t-z analysis (load-transfer curves) are commonly approximated, based on empirical or semi-empirical correlations to field or laboratory soil tests, such as Standard Penetration Test (SPT) or Cone Penetration Test (CPT). This may introduce significant bias into the reliability design computation; hence, reducing the anticipated LRFD resistance factors for such biased analysis (Roberts et al., 2008).

The most accurate way to determine the *t-z* and *q-w* curves, respectively, required to model the skin-friction and end-bearing in the t-z analysis, is by conducting an instrumented SLT on piles. Since performing a SLT is costly and time consuming, it would be more practical to utilize in-situ and/or laboratory tests that measure the *t-z* and *q-w* curves accurately and efficiently. Nevertheless, these tests should provide an actual measure of the soil-pile interface parameters without using any empirical correlations. Essentially, in practice, no straightforward test is available that can be used to directly measure the soil-pile interface properties. However, a few studies have been conducted in an attempt to measure the soil-pile interface friction angle using the direct shear test (DST) apparatus. For example, Reddy et al. (2000) and Pando et al. (2002) placed metallic plates into the lower half of the DST shear box, while the upper half was filled with sand. They compared the test results with the costly soil-pile-slip test results. Both studies showed the DST can be efficiently used to obtain relative values of the interface friction angle to estimate the skin-friction of steel

piles driven into sand soils. However, none of the previous studies used the DST to measure the *t-z* curves or simulate the pile load-displacement response. Furthermore, this approach was not used to study the properties of pile-cohesive soil interfaces, as the DST was mainly developed to measure the shear strength properties of sand soils. On the other hand, there has not been a simple and cost-effective test established to directly measure the *q-w* curve required for modeling pile end-bearing using the t-z analysis.

Although the t-z analysis may provide an accurate estimate of the load-displacement response of axially-loaded piles, it does not determine the stresses and strains induced in the surrounding soil continuum. To confirm the induced stresses and strains in the soil continuum are not extended beyond the model boundaries—not affecting potential neighbouring structures—using a more sophisticated FE analysis may be considered.

The FE analysis has been extensively used over the past three decades in studying soil-structure interaction problems and numerous constitutive models have been developed to model the soil continuum and the soil-pile interface (El-Mossallamy, 1999). According to El-Mossallamy (1999), the soil and the interface element constitutive properties are the most important parameters that control the accuracy of the FE analysis dependent on the pile material and construction techniques, several of which are approximated, based on empirical correlations to conventional field and/or laboratory soil tests (Misra and Chen, 2004). According to De-Gennaro et al. (2006) and Engin et al. (2007), the soil-pile interface properties as well as the soil modulus, approximated based on empirical correlations, largely dictate the FE results. This may require utilizing more sophisticated soil constitutive models in the analysis to avoid the aforementioned problems, which are expensive and may require completion of complex and time consuming soil tests (De-Gennaro et al., 2006; and Engin et al., 2007). However, conducting a sensitivity analysis that differentiates between potential sources of error in the FE simulation, based on direct measurement of the soil-pile interface properties and the soil elastic modulus, may facilitate the adjustment of the FE model for specific soil and pile conditions. The adjusted FE model may provide an improved and efficient prediction of the load-displacement response for axially-loaded pile foundations.

1.2. Scope of Research

The overall scope of the research presented in this thesis is to develop regionally-calibrated LRFD resistance factors for the design of bridge pile foundations in Iowa that incorporate more efficient in-house static methods and overcome the AASHTO limitations associated with ignoring the effect of soil variation. In addition, the recommended LRFD pile design approach should account for the strength and serviceability limit states mainly achieved by adapting two different levels of analysis to characterize the load-displacement response of piles subjected to axial compressive loads, based on direct measurements of the soil-pile interface properties. In the context of the described scope above, the objectives formulated for the study presented in this thesis are as follows:

1. Complete a nationwide survey of different state DOTs to collect detailed information on pile analysis and design approaches used, pile drivability, design verification, and quality control. The survey is the first conducted on the LRFD topic following the FHWA mandate. The results can provide essential information regarding pile design and construction practices, the extent of LRFD implementation, and the benefits of adapting regionally-calibrated resistance factors.
2. Contribute to 10 full-scale instrumented pile static load tests (SLTs) that cover different soil regions and geological formations in the state of Iowa. Each of the 10 tests includes in-situ soil investigations using SPT, CPT, Borehole Shear Test (BST), and push-in-pressure-cells to monitor the change in the lateral earth's pressure and pore water pressure during and after pile driving. Moreover, complete laboratory soil tests for each site, including soil classification, Atterburg limit, 1-D consolidation, Consolidated Undrained (CU) Triaxial test, and Direct Shear Test (DST) were conducted. Results from the aforementioned tests can be utilized to improve the accuracy and efficiency of different analytical models that characterize the behavior of axially-loaded pile foundations. Moreover, field test results can be used to verify and monitor the performance of the intended regionally-calibrated LRFD resistance factors and add to the existing local database.
3. Modify the Borehole Shear Test (mBST) to directly measure the *t-z* curves along the soil-pile interface for cohesive soils in the field. Use the mBST field measurements to

model pile load-displacement behavior using the t-z analysis and compare the results with the analysis based on empirical correlations to CPT data, as well as the actual results obtained from the pile SLT data. The mBST is the first field test used to accurately measure the *t-z* curves, required for the t-z analysis of axially-loaded piles, in cohesive soils, in a cost-effective way.

4. Modify the Direct Shear Test (mDST) to measure the soil-pile interface for cohesionless soils and develop a Pile Tip Resistance (PTR) test to measure the end-bearing properties required for t-z analysis in the laboratory. Conduct t-z analysis, based on the mDST and PTR results, and compare these results with the actual pile SLT data. The mDST and the PTR are the first tests used to accurately and efficiently measure the *t-z* and *q-w* curves, respectively, required for t-z analysis, which can separately characterize the skin-friction and end-bearing behaviors of axially-loaded piles driven into cohesionless soils.
5. Evaluate the existing Mohr-Coulomb soil constitutive model, using FE analysis aimed to simulate the behavior of axially-loaded piles, as well as the surrounding soil continuum. Measure the properties of the interface element and the soil elastic modulus in the laboratory by means of the mDST and CU-Triaxial tests, respectively. Recommend any needed adjustments to the FE model and to the typical estimation procedures for the soil constitutive properties using empirical correlations from the CPT test results. The adjusted FE model can be used to accurately predict the pile load-displacement response and the stress-strain behavior in the soil medium.
6. Develop LRFD preliminary recommendations and design guidelines for bridge pile foundations in Iowa that focus on the strength limit state and incorporate in-house methods into the design process. The regional LRFD resistance factors can be calibrated, based on the database (PIle LOad Tests in Iowa [PILOT-IA]) locally developed as part of this project by Roling et al. (2010), containing 264 pile load test results as well as comprehensive soil data.
7. Advance the LRFD calibration process to avoid the AASHTO shortcomings regarding the effect of soil variation along the pile length and use combinations of

static methods. The advanced LRFD-based pile design can increase the overall cost-effectiveness of bridge foundations compared to the AASHTO recommended design.

8. Develop the LRFD resistance factors that account for the strength and serviceability limit states using the pile vertical load-displacement relationship predicted by means of the improved t-z analysis, based on the actual measurements of the mBST and mDST in clay and sand soils, respectively. This method can provide a displacement-based LRFD design approach for bridge pile foundations.

1.3. Thesis Outline

This thesis follows a paper format and consists of eight chapters including five papers. Each paper that appears as a chapter includes related literature review, analysis and findings, conclusions, and recommendations. Following this introduction chapter, a general literature review regarding the basic principles of the LRFD approach, as well as different static analysis methods, is provided in Chapter 2. Finally, Chapter 8 summarizes the most significant research outcomes and provides future work recommendations. The contents of each chapter are summarized below.

- Chapter 1 – Introduction: A brief overview on the LRFD implementation and pile settlement, in addition to the scope of research and thesis outline, is presented.
- Chapter 2 – Literature Review: A detailed review and background information on the principles and the development of the LRFD resistance factors for geotechnical uses are provided. The typical resistance factors calibration framework and the associated construction control aspects are discussed. Also the basic principles of different static analysis methods used for the design of bridge deep foundations are presented.
- Chapter 3 – Current Design and Construction Practices of Bridge Pile Foundations with Emphasis on Implementation of LRFD: Major findings from the nationwide survey conducted on the current deep foundation practice, pile analysis and design, pile drivability, design verification, and quality control, are summarized. This chapter provides essential information regarding the current national pile design and construction practices, the extent of LRFD implementation, and the benefits of adapting regional resistance factors for the design of bridge deep foundations.

- Chapter 4 – Modeling Axially-loaded Friction Steel Piles using the Load-Transfer Approach, Based on a Modified Borehole Shear Test: Introduction to the mBST equipment and modifications are presented. Procedures of measuring the soil-pile interface properties using the mBST are summarized. Moreover, this chapter introduces an improved load-transfer analytical model (t-z model) based on actual mBST field measurements of the soil-pile interface properties in clay soils. Finally, the predicted load-displacement responses, as well as the load distribution along the pile length, are compared with results from t-z models, based on empirical correlations with CPT data, as well as with field measured responses from three load tested piles driven into cohesive soils.
- Chapter 5 – Improved t-z Analysis for Vertically-Loaded Piles in Cohesionless Soils Based on Laboratory Test Measurements: Introduction to the proposed mDST and PTR test equipment is presented. Procedures of measuring the soil-pile interface properties along the shaft embedment, as well as the load-penetration curve at the end-bearing soil under the pile tip, are summarized. Moreover, this chapter introduces a comprehensive load-transfer analytical model (t-z model) based on actual mDST and PTR laboratory measurements of the soil-pile interface properties in sandy soils. Finally, the predicted load-displacement responses, as well as the load distribution along the pile length, are compared with field-measured responses from two load tested piles driven into cohesionless soils.
- Chapter 6 – Pile Response Characterization Using the Finite Element Approach: Evaluation of the Mohr-Coulomb soil constitutive model using a FE analysis to simulate the behavior of axially-loaded piles and the surrounding soil continuum is presented. A sensitivity analysis based on the mDST and CU-Triaxial laboratory soil tests is provided, which describes the effect of changing the soil-pile interface properties and the soil elastic modulus on overall pile behavior. The chapter then introduces an adjusted FE model, based on actual measured soil constitutive properties. Finally, the predicted load-displacement responses, as well as the load distribution along the pile length, are compared with field-measured responses from four load tested piles driven into cohesive and cohesionless soil layers.

- Chapter 7 – An Investigation of the LRFD Resistance Factors with Consideration to Soil Variability and Pile Settlement: Preliminary regionally-calibrated LRFD resistance factors, design guidelines, and recommendations for Iowa soils are presented. An enhanced calibration framework that accounts for soil variability along the pile length as well as includes combinations of static methods is presented. Furthermore, a displacement-based LRFD pile design approach that accounts for the strength and serviceability limit states is suggested, utilizing the improved t-z analysis, based on soil-pile interface measurements from the mBST and mDST tests.
- Chapter 8 – Conclusions and Recommendations: This research's major outcomes are summarized in addition to the suggested future work.

1.4. References

AASHTO LRFD Bridge Design Specifications (2007). Customary U.S. Units, 4th edition, 2008 Interim, Washington, D.C.

Abu-Hejleh, N., DiMaggio, J., and Kramer, W. (2009). "AASHTO Load and Resistance Factor Design Axial Design of Driven Pile at Strength Limit State." Transportation Research Board 88th Annual Meeting, 2009, Paper #09-1034, Washington D.C.

Alawneh, A. S. (2006). "Modeling Load–Displacement Response of Driven Piles in Cohesionless Soils under Tensile Loading." *Computers and Geotechnics,* No.32.

Allen, T. M. (2005). "Development of Geotechnical Resistance Factors and Downdrag Load Factors for LRFD Foundation Strength Limit State Design." *FHWA-NHI-05-052,* Federal Highway Administration, U.S. DOT, Washington, DC.

Barker, R. D., Rojiani, J. K., Tan, O. P., Kim, S. C. (1991). "NCHRP Report 343: Manuals for the Design of Bridge Foundations." *TRB*, National Research Council, Washington, D.C.

Becker, D. E., and Devata, M. (2005). "Implementation and Application Issues of Load and Resistance Factor Design (LRFD) for Deep Foundations." *Proceeding: Sessions of the Geo-Frontiers 2005 Congress*, January 24-26, 2005, Austin, Texas.

Coyle, H.M. and Reese, L.C. (1966). "Load Transfer for Axially-loaded Piles in Clay." *Journal of Soil Mechanics and Foundation Engineering Division*, 92(2), 1- 26.

De Gennaro, V., Said, I., and Frank, R. (2006). "Axisymmetric and 3D Analysis of Pile Test using FEM." *Numerical Methods in Geotechnical Engineering*, 2006 Taylor & Francis Group, London, ISBN 0-4 15-40822.

DiMaggio, J., Saad, T., Allen, T., Passe, P., Goble, G., Christopher, B., Dimillio, A., Person, G., and Shike, T. (1998). "FHWA Summary Report of the Geotechnical Engineering Study Tour -GEST." *FHWA International Technology Scanning Program*.1998.

El-Mossallamy, Y. (1999). "Load-settlement Behavior of Large Diameter Bored Piles in Over-consolidated Clay." Proc. of the 7th Int. symp. on numerical models in geotechnical engineering - NUMOG VII, Graz, Rotterdam, Balkema.

Engin, H. K., Septanika, E. G., and Brinkgreve, R. B. (2007). "Improved Embedded Beam Elements for the Modeling of Piles." *Proc. 10th Int. Symp. on Numerical Models in Geotechnical Engineering – NUMOG X*, Rhodes, Greece.

Goble, G. (1999). "NCHRP Synthesis of Highway Practice 276: Geotechnical Related Development and Implementation of Load and Resistance Factor Design (LRFD) Methods." *TRB*, National Research Council, Washington, D.C.

Guo, W. D. and Randolph, M. F. (1998). "Vertically Loaded Piles in Non-homogeneous Media." *Inter. Journal for Numerical and Analytical Methods in Geomechanics*, Vol. 21, 507-532.

Misra, A. and Chen, C. H. (2004). "Analytical solutions for Micropile Design under Tension and Compression." *Geotechnical and Geological Engineering*, 22(2), 199-225.

Misra, A. and Roberts, L.A. (2006). "Probabilistic Analysis of Drilled Shaft Service Limit State Using the "t-z" Method." *Canadian Geotechnical Journal*, 1324-1332 (2006).

Moore, J. (2007). "AASHTO LRFD Oversight Committee (OC) - update 2007." New Hampshire DOT, AASHTO Load and Resistance Factor Design (LRFD) Bridge Specifications.

Ng, W. K. (in process). "Dynamic Pile Driving Characterization and its Contribution to Load Resistance Factor Design (LRFD) of Vertically Loaded Piles." PhD Dissertation, Iowa State University, United States – Iowa

Paikowsky, S. G. with contributions from Birgisson, B., McVay, M., Nguyen, T., Kuo, C., Baecher, G., Ayyub, B., Stenersen, K., O'Malley, K., Chernauskas, L., and O'Neill,

M. (2004). “Load and Resistance Factor Design (LRFD) for Deep Foundations.” *NCHRP Report number 507*, TRB, Washington D.C.

Pando, M., Filz, G., Dove, J., and Hoppe, E. (2002). “Interface Shear Tests on FRP Composite Piles.” *ASCE International Deep Foundations Congress*, Orlando, FL, Vol.2, 1486-1500.

Reddy, E. S., Chapman, D. N., and Sastry, V. V. (2000). “Direct Shear Interface Test for Shaft Capacity of Piles in Sand.” *Geotechnical Testing Journal*, Vol. 23, No. 2, pp. 199–205.

Roberts, L. A., Gardner, B. S., and Misra, A. (2008). “Multiple Resistance Factor Methodology for Service Limit State Design of Deep Foundations using t-z Model Approach.” *Proceeding: Geo-Congress 2008*, New Orleans, LA.

Roling, J. M. (2010). “Establishment of a Suitable Dynamic Formula for the Construction Control of Driven Piles and its Calibration for Load and Resistance Factor Design.” Master’s Dissertation, Iowa State University, United States - Iowa.

Suleiman I. B. and Coyle H. B. (1976). “Uplift Resistance of Piles in Sand.” *Journal of Geotechnical Engineering*, ASCE 1976; 102(GT5):559–62.

Withiam, J., Voytko, E., Barker, R., Duncan, M., Kelly, B., Musser, S., and Elias, V. (1998).“LRFD of Highway Bridge Substructures.” *FHWA HI-98-032*. FHWA.

CHAPTER 2: LITERATURE REVIEW

This chapter provides a detailed review and background information on the principles and the development of the Load and Resistance Factor Design (LRFD) approach for geotechnical uses. In addition, the chapter summarizes the typical resistance factors calibration framework and the associated construction control aspects. Moreover, the principles of different analysis methods used for the design of bridge deep foundations are presented herein with emphasis on static methods. Finally, review on different criteria used to determine the pile nominal capacity from the load-displacement response is presented.

2.1. Allowable Stress Design

Starting in the early 1800s until the mid 1950s, the Allowable Stress Design (ASD) approach has been used in the design of structures and substructures, where the actual loads anticipated from the structure were compared to the foundation capacity (or resistance) and an adequate Factor of Safety (FS) was ensured. According to Paikowsky et al. (2004), a pile design, based on the ASD approach, cannot ensure consistent and reliable performance of foundations. This major drawback of the ASD is due to ignoring the various sources and levels of uncertainty associated with loads and capacities of deep foundations. Consequently, the selected FS for deep foundations used to be highly conservative. However, the FS can be typically reduced when extreme load combinations, such as including impact and seismic loads, are used in the design (Allen, 2005). Generally, engineers assumed the FS, based on different levels of confidence in the design and construction control. Particularly in the design of deep foundations, experience and subjective judgment were greatly dependent in selecting the appropriate FS (Paikowsky et al., 2004). As stated by Becker and Devata (2005), loads and capacities are probabilistic and not deterministic in nature. Thus, artificial FS should be replaced by a probability-based design approach that better deals with rational geotechnical properties.

2.2. Load and Resistance Factor Design

Since the mid-1950s, the Load and Resistance Factor Design (LRFD) approach has been developed for the design with the objective of ensuring a uniform degree of reliability throughout the structure. The basic hypothesis of the LRFD is quantifying the uncertainties based on probabilistic approaches, which aims to achieve engineered designs with consistent levels of reliability (or probability of failure). In the LRFD approach, different load types and combinations are multiplied by load factors, while resistances are multiplied by resistance factors, where the factored loads should not exceed the factored resistances. There are several advantages of using the LRFD approach over the ASD approach for designing deep foundations. The most important advantage is handling the uncertainties associated with design parameters by utilizing a rational framework of probability theory, leading to a constant degree of reliability. Consequently, the LRFD provides a consistent design approach for the entire structure (i.e., superstructure and substructure), which improves the overall design and construction perspective. Furthermore, the LRFD approach does not require the same amount of experience and engineering judgment in the design process as required in the ASD approach.

2.2.1. Basic principles

In the LRFD approach, loads are multiplied by load factors usually greater than unity, while capacities are multiplied by resistance factors less than unity. A simple definition of failure is when the factored loads exceed the factored capacities. The basic equation of the LRFD-based design can be expressed as follows:

$$\varphi_i R_i \geq \sum \gamma_i Q_i , \qquad [2.1]$$

where R_i is the resistance, φ_i is the resistance factor, Q_i is structural load, and γ_i is the load factor. The uncertainties associated with resistances and loads can be defined through the distribution of their Probability Density Functions (PDFs). As seen in Figure 2.1, the probabilistic approach used for the LRFD development allows for determining the overlap area between the PDFs of loads and resistances. This overlap area is statistically restricted to a certain acceptable level, which defines the acceptable risk of failure. According to Kyung

(2002), the overlap area depends on: 1) the relative position of the PDFs, determined by μ_Q and μ_R (i.e., the mean bias for loads and resistances, respectively); 2) the dispersion of the PDFs, determined by σ_Q and σ_R (i.e., the standard deviation for loads and resistances, respectively); and 3) the shape of the PDFs.

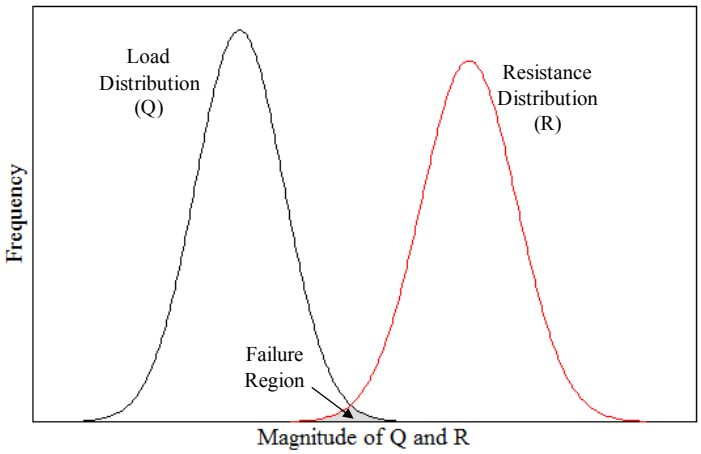

Figure 2.1: LRFD failure criterion between loads and resistances PDFs

2.2.2. Implementation

Over the past two decades, significant efforts have been directed towards development and application of the LRFD approach in geotechnical engineering. In 1989, the American Association of State Highway and Transportation Officials (AASHTO) developed their first geotechnical LRFD specifications. In the early 1990s, the Federal Highway Administration (FHWA) Manual for the Design of Bridge Foundations was released, followed by the National Cooperative Highway Research Program (NCHRP) Report 343 by Barker et al. (1991). Later on, the NCHRP Report 343 became the basis for the foundation section of the 1994 AASHTO Bridge Design Specifications (AASHTO, 1994). They were used in the foundations of offshore structures (Hamilton and Murff, 1992; Tang, 1993), as well as general foundations design (Kulhawy et al., 1996). The 1994 AASHTO Specifications focused more on load uncertainties than resistance uncertainties and did not include many subjective factors unique to geotechnical practice.

The 2004 AASHTO-LRFD Design Specifications (AASHTO, 2004) were also developed, based on the report by Barker et al. (1991). However, the LRFD resistance factors

were based on reliability theory and fit to the FS of the ASD approach. It was found the LRFD resistance factors calibrated by fitting to ASD did not provide the desired level of reliability (Withiam et al., 1998). To overcome this problem, the NCHRP and FHWA funded further research resulting in two major reports by Paikowsky et al. (2004) and Allen et al. (2005). The 2007 AASHTO-LRFD bridge design specifications (2008 revised interims) include the outcomes of study by Allen et al. (2005), in addition to the details provided by Barker et al. (1991) and Paikowsky et al. (2004).

Although the LRFD approach to designing structural elements has been well established and implemented in design codes around the world, its application to geotechnical design has been relatively slow (DiMaggio, 1999). This enforced the FHWA to mandate the usage of the LRFD approach in the design of bridges initiated in the United States after October 1, 2007. Despite the FHWA mandated deadline, not all State DOTs have adopted the LRFD in their foundation designs. This could be due to the conservatism of the LRFD bridge design specifications which increase the cost of foundations, given the design specifications account for the large variation in soil parameters, as well as different levels of uncertainty associated with determining the capacity of deep foundations (Paikowsky et al., 2004). Consequently, regionally-calibrated resistance factors are permitted in LRFD to minimize the unnecessary conservatism built into the design, provided these factors are developed in a consistent manner with the approach suggested in the 2007 AASHTO-LRFD Specifications. Two different calibration techniques were used to develop the LRFD geotechnical resistance factors. The first is by fitting to ASD and the second is by using reliability theory. The following sections provide a brief discussion on both techniques.

2.2.3. Calibration by fitting to ASD

According to Allen (2005), fitting a new design approach to an old one is initially valid at the beginning of mandating a new design specification that depends on a different design philosophy. In case of LRFD, calibration by fitting to ASD is used if the data required for the statistical analysis is not available. In this case, the obtained LRFD resistance factors by fitting to the ASD method should be only used as a benchmark to provide the same degree of safety the ASD used to provide. However, this does not satisfy the LRFD reliability based

requirements. Calibration by fitting can be performed using the following equation:

$$\varphi = \frac{\gamma_{DL}\,{}^{DL}/_{LL} + \gamma_{LL}}{({}^{DL}/_{LL}+1)FS} \quad [2.2]$$

where,

φ =Resistance factor

γ_{DL} =Load factor for Dead Loads (DL)

γ_{LL} =Load factor for Live Loads (LL)

DL/LL =Dead load to live load ratio assumed according to Table 2.1.

From Eq. [2.2], it can be noted the resistance factor mainly depends on the DL to LL ratio. The DL/LL ratio could range between 1.0 and 4.0 for bridge structures, depending on the bridge span and other factors. Barker et al. (1991) recommended a DL/LL ratio of 3.0 for bridge structures. On the other hand, Paikowsky et al. (2004) suggested the ratio should be within the range of 2.0 to 2.5, adding this range is reasonable and can be applicable for long span bridges. According to Allen (2005) and Paikowsky et al. (2004), the DL/LL ratio has a small influence on the LRFD resistance factors, when calibrated based on reliability theory. This will be discussed later in this chapter. Allen (2005) considered a DL/LL ratio of 3.0 to be consistent with the previous work completed by Barker (1991) and, hence, can directly compare with the earlier resistance factors presented in Table 2.2. In the State of Iowa, the DOT uses a DL/LL ratio of 1.5. However, as previously mentioned, the differences in the DL/LL ratio do not greatly influence the values of the calibrated resistance factors. In case of DL/LL = 3.0, a more simplified correlation between the LRFD resistance factor and the ASD factor of safety can be adopted, where Eq. [2.2] can be rewritten as:

$$FS = \frac{\gamma_{DL}\frac{DL}{LL} + \gamma_{LL}}{\varphi\left(\frac{DL}{LL}+1\right)} \quad [2.3]$$

Which means in the case of DL/LL = 3.0 and using the 2004 AASHTO load factors:

$$\varphi = \frac{1.25(3.0)+1.75}{(3.0+1)FS} = \frac{1.375}{FS} \quad [2.4a]$$

And, in the case of DL/LL = 3.0 and using the load factors from Barker et al. (1991):

$$\varphi = \frac{1.30(3.0)+2.17}{(3.0+1)FS} = \frac{1.518}{FS} \quad [2.4b]$$

Table 2.1: Load factors used for LRFD resistance factors calibration by fitting to ASD

Load Type	Recommended LRFD Load Factors (after Barker et al., 1991)	Recommended LRFD Factors (after 2004 AASHTO specifications)
Dead Load	1.30	1.25
Live Load	2.17	1.75

Table 2.2: Resistance factors and corresponding FS using calibration done by fitting to ASD with a DL/LL=3.0 (after Allen et al., 2005)

Factor of Safety	Resistance Factor	
	Recommended LRFD Factors (after Barker et al., 1991)	Recommended LRFD Factors (after 2004 AASHTO specifications)
1.5	1.00	0.92
1.8	0.84	0.76
1.9	0.80	0.72
2.0	0.76	0.69
2.25	0.67	0.61
2.5	0.61	0.55
2.75	0.55	0.50
3.0	0.51	0.46
3.5	0.43	0.39
4.0	0.38	0.34

2.2.4. Calibration using reliability theory

The objective of reliability theory is to limit the probability of structure failure (P_f), i.e., probability of loads exceeding their resistances, to a certain acceptable extent. As shown in Figure 2.1, Q and R are two PDFs representing the loads and resistances, respectively. As previously discussed, the area of overlap between the two PDFs is considered as failure. By subtracting the two PDFs (i.e., R - Q), the area to the left of the zero axis is considered the failure region (see Figure 2.2). In this case the probability of failure can be replaced by the reliability index (β). The reliability index stands for the number of standard deviations (σ) representing the distance between the zero axis and the mean of R - Q. The general process used by Barker et al. (1991) and Paikowsky et al. (2004) to develop the regionally calibrated

LRFD resistance factors based on the reliability theory is as follows:

- Gather data required for statistical analysis.
- Calculate parameters, such as the mean, standard deviation, and Coefficient of Variation (COV) for load and resistance PDFs.
- Determine best-fit of each PDF (e.g., normal, lognormal).
- Select appropriate statistical method for calibration.
- Select a target, β, based on the margin of safety required in design specifications and consider the recommended levels of reliability used for geotechnical designs.
- Use recommended load factors provided in the design code.
- Calculate regionally-calibrated LRFD resistance factors.

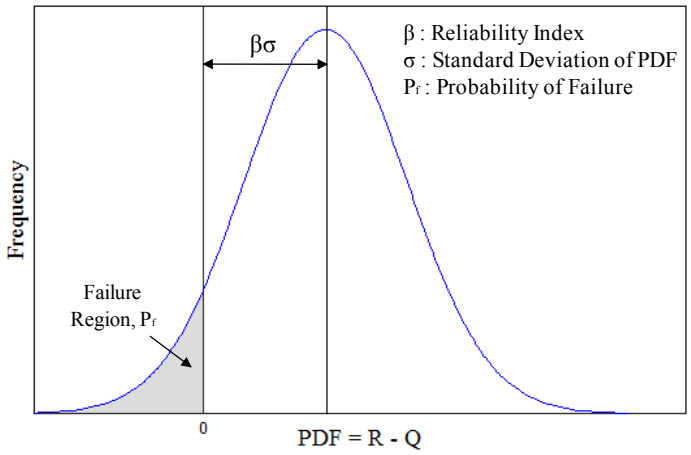

Figure 2.2: Probability of failure and reliability index (after Withiam et al., 1998)

Several statistical methods with different degrees of sophistication have been used for the LRFD resistance factors calibration, depending on the desired degree of accuracy. According to Kyung (2002), the most commonly used methods are the First Order Second Moment (FOSM) and First Order Reliability Methods (FORM). According to Allen et al. (2005), a straightforward technique is the FOSM. In FOSM, the random variables are represented by their first two moments, i.e., the mean (μ) and standard deviation (σ), while the Coefficient of Variation (COV) can be calculated by dividing the standard deviation by the mean. Paikowsky et al. (2004) performed this analysis using both methods (FOSM and FORM) and concluded the difference between them is relatively small, as it did not exceed

10% on average, where the FOSM provides slightly conservative resistance factors. Moreover, the existing 2007 AASHTO-LRFD specifications are based on the FOSM, assuming a lognormal distribution of the loads and resistances PDFs. According to Allen et al. (2005), another advanced method, Monte Carlo simulation, has been used for performing reliability analyses. Allen et al. (2005) as well as Nowak and Collins (2000) have shown all of these advanced methods should produce similar results to each other, which may indicate that using a less sophisticated approach like the FOSM would provide close results to other more sophisticated approaches. The following section provides a mathematical derivation of the basic equations of the FOSM method.

2.2.4.1 First Order Second Moment (FOSM)

Scott and Salagado (2003) indicated the lognormal distribution better represents and models the transient loads and fully characterizes it by its first two moments. They added the magnitude of the transient loads and resistance found in geotechnical problems cannot take negative values, and the lognormal distribution can better represent their product even if the variables themselves are not log-normally distributed. Therefore, and with accordance to the 2007 AASHTO-LRFD specifications, the load and resistance PDFs are assumed to follow lognormal distributions. The following provides a derivation of the FOSM basic Eq. [2.25] necessary to calculate the LRFD resistance factors:

According to Figure 2.2, failure occurs when the loads exceed the resistance. Since the PDFs are assumed to follow the lognormal distribution, the probability of failure will be:

$$P = P\left[(\ln Q_R - \ln Q_L) < 0\right] \quad [2.5]$$

The mean bias for the loads and resistance will be the ratio between the mean predicted and the nominal (actual), respectively, as follows:

$$\lambda_L = \frac{\bar{Q}_L}{Q_{L_n}} \quad [2.6]$$

$$\lambda_R = \frac{\bar{Q}_R}{Q_{R_n}} \quad [2.7]$$

Assuming that both follow a lognormal distribution and are statistically separate and independent variables, therefore, the mean difference will be:

$$\overline{U} = \ln \overline{Q}_R - \ln \overline{Q}_L \quad [2.8]$$

On the other hand, for the lognormal distributed PDFs, the standard deviation for the difference between loads and resistances will be:

$$\sigma_U = \sqrt{\sigma^2_{\ln\, Q_L} + \sigma^2_{\ln\, Q_R}} \quad [2.9]$$

Also, by considering the relationship between the standard deviation and the COV for a lognormal distribution:

$$\sigma^2_{\ln Q_L} = \ln(1 + COV^2_{Q_L}) \quad [2.10]$$

$$\sigma^2_{\ln Q_R} = \ln(1 + COV^2_{Q_R}) \quad [2.11]$$

According to Macgregor (1976), in case the COV < 0.6, the previous expressions can be approximated as follows:

$$\sigma^2_{\ln Q_L} = COV^2_{Q_L} \quad [2.12]$$

$$\sigma^2_{\ln Q_R} = COV^2_{Q_R} \quad [2.13]$$

From Figure 2.2, the reliability index, β, is simply the ratio of the mean and standard deviation (Allen, 1975; Macgregor, 1976; Becker, 1996) as follows:

$$\beta = \frac{\ln \overline{Q}_R - \ln \overline{Q}_L}{\sqrt{\sigma^2_{\ln Q\, L} + \sigma^2_{\ln Q\, R}}} \quad [2.14]$$

By substituting from Eqs. [2.12 and 2.13] in Eq. [2.14] as follows:

$$\beta = \frac{\ln \overline{Q}_R - \ln \overline{Q}_L}{\sqrt{COV^2_{Q_L} + COV^2_{Q_R}}} \quad [2.15]$$

$$\ln \overline{Q}_R - \ln \overline{Q}_L \geq \beta \sqrt{COV^2_{Q_L} + COV^2_{Q_R}} \quad [2.16]$$

Lind (1971) has shown that:

$$\sqrt{COV^2_{Q_L} + COV^2_{Q_R}} = \alpha\, COV_{Q_L} + \alpha\, COV_{Q_R}, \quad [2.17]$$

where α is a separation coefficient having a value between 0.707 and 1.0, depending on the ratio COV_{QR}/COV_{QL} (after Lind, 1971). By adapting the equation below:

$$\ln \overline{Q}_R - \ln \overline{Q}_L = \ln\left(\frac{\overline{Q}_R}{\overline{Q}_L}\right) \quad [2.18]$$

By substituting from Eqs. [2.17 and 2.18] in Eq. [2.16] as follows:

$$\ln\left(\frac{\overline{Q}_R}{\overline{Q}_L}\right) \geq \beta\alpha\, COV_{Q_L} + \beta\alpha\, COV_{Q_R} \quad [2.19]$$

$$\therefore \frac{\overline{Q}_R}{\overline{Q}_L} \geq e^{(\beta\alpha\, COV_{Q_L} + \beta\alpha\, COV_{Q_R})} \quad [2.20]$$

By rearranging Eq. [2.20] as follows:

$$\overline{Q}_R\left(e^{-\beta\alpha\, COV_{Q_R}}\right) \geq \overline{Q}_L\left(e^{\beta\alpha\, COV_{Q_L}}\right) \quad [2.21]$$

From Eqs. [2.6 and 2.7], Eq. [2.21] will be:

$$Q_{R_n}\,\lambda_R\left(e^{-\beta\alpha\, COV_{Q_R}}\right) \geq Q_{L_n}\,\lambda_L\left(e^{\beta\alpha\, COV_{Q_L}}\right) \quad [2.22]$$

Based on Eqs. [2.21 and 2.22], one can assume the LRFD factors for load and resistance are φ_L and φ_R, respectively, as follows:

$$\varphi_R = \lambda_R\left(e^{-\beta\alpha\, COV_{Q_R}}\right) \quad [2.23]$$

$$\varphi_L = \lambda_L\left(e^{\beta\alpha\, COV_{Q_L}}\right) \quad [2.24]$$

By separation of the loads into dead loads (DL) and live loads (LL), and by rearranging the formula according to the recommended AASHTO-LRFD Probabilistic characteristics of random variables for loads (after Nowak, 1999; Paikowsky et al., 2004), Eqs. [2.22, 2.23, and 2.24] can be rewritten as follows:

$$\varphi_R = \frac{\lambda_R\left(\frac{\gamma_{DL}\,Q_{DL}}{Q_{LL}} + \gamma_{LL}\right)\sqrt{\frac{\left(1+COV^{\,2}_{Q_{DL}} + COV^{\,2}_{Q_{LL}}\right)}{\left(1+COV^{\,2}_{Q_R}\right)}}}{\left(\frac{\lambda_{Q_{DL}}\,Q_{DL}}{Q_{LL}} + \lambda_{Q_{LL}}\right)\exp\left\{\beta_T\sqrt{\ln\left[\left(1+COV^{\,2}_{Q_R}\right)\left(1+COV^{\,2}_{Q_{DL}} + COV^{\,2}_{Q_{LL}}\right)\right]}\right\}} \quad [2.25]$$

where,

γ_{DL} =Load factor for dead loads (see Table 2.3)

γ_{LL} =Load factor for live loads (see Table 2.3)

$\lambda_{Q_{DL}}$ =Bias for dead loads (see Table 2.3)

$\lambda_{Q_{LL}}$ =Bias for live loads (see Table 2.3)

$\frac{Q_{DL}}{Q_{LL}}$ =Dead load to live load ratio (usually ranging from 1.5 to 3.5 for bridge structures)

Table 2.3: AASHTO random variables for loads (after Nowak, 1999)

Load Type	Load Factor (γ_D, γ_L)	Load Bias (λ_{QD}, λ_{QL})	Load COV (COV_{QD}, COV_{QL})
Dead Load (D.L.)	1.25	1.05	0.1
Live Load (L.L.)	1.75	1.15	0.2

From Eq. [2.25], it can be noticed the mean bias (or the mean), the standard deviation, as well as the COV are all utilized in the FOSM equation. Therefore, a higher COV would probably yield a higher LRFD resistance factor, which may seem unclear. Actually, it is important to highlight the fact that a higher resistance factor does not necessarily reflect a higher efficiency of the design capacity of a pile foundation. According to McVay et al. (2000), the efficiency of the different design methods cannot be reflected from the value of the resistance factor. McVay et al. demonstrated an efficiency factor—the ratio of resistance factor to the bias of the method (φ/λ). This factor represents a better understanding of the efficiency of different design methods and provides a sense of the economy of each method in different soil and pile types. Using this efficiency factor, McVay avoided the misconception between the economy of the different design methods and the high values of LRFD resistance factors.

2.2.5. Target reliability index

In LRFD specifications, the targeted reliability index (β) is defined as the measure of safety associated with a probability of failure (P_f). The probability of failure represents the probability for the condition at which the resistance multiplied by the resistance factors will be less than the load multiplied by the load factors (Paikowsky et al., 2004). Rosenbleuth et al. (1972) presented an approximate relation between the probability of failure and the reliability index as follows:

$$P_f = 460e^{-4.3\beta} \quad [2.26]$$

Baecher (2001) showed this relation is not accurate for β less than 2.5, which is within the preferable range of β for foundations. According to Meyerhof (1970), β is in a limited range of 3 to 3.6 for foundations, which was reduced for driven piles, due to its redundancy in a range from 2.0 to 2.5 (Barker et al., 1991), as the failure of one pile does not necessarily imply the pile group will fail. In contrast, the reliability indices expected for the design of bridge foundations, based on the ASD method, could be in the range of 1.5 to 4.7 (Mertz, 2007). In the NCHRP report 507 (by Paikowsky et al., 2004), the following recommendations were provided for reliability indices and associated P_f for LRFD resistance factors calibration:

- For redundant piles, defined as 5 or more piles per pile cap, the recommended probability of failure is $P_f = 1\%$, corresponding to a target reliability index of $\beta = 2.33$.
- For non-redundant piles, defined as 4 or fewer piles per pile cap, the recommended probability of failure is $P_f = 0.1\%$, corresponding to a reliability index of $\beta = 3.00$.

2.3. Framework for Calibration

First, the development of the LRFD resistance factors requires an adequate pile load test database. This database should include reliable data conducted at the same region (State) of the desired LRFD calibration to account for the unique and different levels of variation in soil and geology, as well as design and construction practices. However, if the anticipated regional database is not available, the usage of another database to similar conditions that can effectively represent the local conditions is accepted. Following the procedures provided in the NCHRP-507 report by Paikowsky et al. (2004) and the FHWA-NHI report by Allen (2005), the framework of developing the LRFD geotechnical resistance factors can be essentially summarized as follows:

1. Develop a comprehensive and reliable pile static load test database, including: a) sufficient soil parameters and profiles; b) pile properties and geometry; c) pile driving information (or drilled shaft information), such as hammer properties and dates of driving (dates of EOD and BOR); and d) an acceptable static load test data, i.e., accepted load-displacement relationship at the pile head, which indicates the pile

failure load or the pile ultimate capacity in the field. The database should include a large number of data points so it can be successfully used for the LRFD calibration.

2. Sort the database into different groups. Each group should represent a specific soil and pile type. For example, an appropriate group would represent load tests conducted on driven steel H-piles in sand. The precision and efficiency of the expected LRFD resistance factors is higher whenever the number of variables among each group is limited. As previously indicated, the number of data points within each group must be sufficient for the analysis.
3. Measure the capacity of piles for all groups, using the load-displacement relationship obtained from the load test results. Consistency of the selected criterion of calculating the piles' ultimate capacity is required for all data points, i.e., when selecting Davisson's criterion (Davisson, 1972), it should be used for all piles within all groups.
4. Calculate the nominal capacity of piles for all groups, using any desired static or dynamic analysis methods or dynamic formulas. Also, in-house methods can be used to calculate the nominal capacity and, therefore, LRFD resistance factors of a specific in-house method can be considered in the calibration.
5. Determine the bias of the used methods or the pile actual to nominal capacity ratios, for all groups.
6. Determine the distribution of the Probability Density Functions (PDFs) within each group in the database, i.e., normal or lognormal distributed. Also, determine the best-fit for each dataset, using any of the available statistical distribution identification tests, such as the Anderson Darling test.
7. Select the appropriate reliability approach that will be used for the LRFD resistance factors calibration, such as the FOSM or the FORM approaches. This depends on the degree of sophistication anticipated in the analysis.
8. Calculate the parameters required for the desired reliability approach; for example, the mean and standard deviation, if the FOSM approach is selected. Also, select the target reliability index, DL/LL ratio, and the dead and live load factors, based on the AASHTO recommendations.

9. Calculate the regional LRFD resistance factors, and then compare these results to the resistance factors calibrated by fitting to the ASD factor of safety. Also, determine the efficiency factors for each group.
10. Check the reliability and consistency of the calibrated resistance factors by means of full-scale pile load tests in different soil types, representing all groups of the database. Then, develop recommendations for the LRFD-based design for bridge pile foundations.

Figure 2.3 represents a flowchart showing the previous steps of the LRFD resistance factors calibration. As seen on the figure, the static analysis methods are used during the design stage of the project, while the dynamic analysis and dynamic formulas take place during the construction stage of the project. A discussion on the main difference between these two stages and the construction control aspects are provided later in this chapter.

2.4. Current AASHTO-LRFD Specifications

The source of the initial resistance factors provided by the earlier 2004 AASHTO-LRFD specifications was the NCHRP Report 343 by Barker et al. (1991). Resistance factors were calibrated using a combination of reliability theory and fitting to ASD, which, according to Allen (2005), did not meet the objective of providing a consistent level of safety in design. The 2006 as well as the current 2007 AASHTO-LRFD bridge design specifications depend on the NCHRP Report 507 by Paikowsky et al. (2004) and the FHWA-NHI report by Allen (2005). As previously indicated, the calibration framework used to develop the geotechnical resistance factors in the NCHRP, as well as the FHWA reports, was mainly based on the reliability theory.

As will be discussed in the next section, there are three different methods of analysis that can be used to estimate the pile nominal capacity: 1) static analysis methods, 2) dynamic analysis, and 3) dynamic formulas. From the geotechnical aspect, the nominal pile design capacity can be defined as the maximum calculated axial compressive load that the soil-pile system can handle without excessive settlement. This capacity is calculated during the design or construction stages of the foundation, depending on the soil and pile properties, as well as the pile driving conditions. The 2007 AASHTO-LRFD specifications provided resistance

factors for the three pile analysis methods (static and dynamic analysis, as well as dynamic formulas) in different soil types and according to different levels of site variability and construction control.

2.4.1. Static methods

Different static analysis methods are used to estimate the number and length of piles required to release the bidding and contracting documents during the initial design stage. Selecting the appropriate static method requires a sufficient knowledge of the site subsurface conditions and implication to the deep foundation type. As can be seen from Table 2.4, the current AASHTO specifications provide the LRFD resistance factors for single axially loaded piles using six different static analysis methods in sand, clay, and mixed soils. It also provides the geotechnical LRFD resistance factors for uplift capacity of single piles. The AASHTO resistance factors were mainly developed from load test results obtained on piles with diameters of 600 mm (23.6 inch) or less. The pile nominal capacity calculated using different static analysis methods should be multiplied by the appropriate resistance factors presented in Table 2.4 (adapted from the 2007 AASHTO-LRFD specifications). The recommended AASHTO factors are based on redundant pile groups, i.e., pile groups of five or more piles. As described in the AASHTO (2007) Section 10.5.5.2.3 for driven piles, if the pile group contains less than five piles, the resistance factors should be reduced by 20% to reflect a higher target reliability index, $\beta_T = 3.0$ or more.

2.4.2. Dynamic methods

Tables 2.5, 2.6, and 2.7 are adapted from the AASHTO (2007) LRFD Bridge Design Specifications for dynamic analysis methods. Referring to Tables 2.5, 2.6, and 2.7, the resistance factors are verified by means of pile SLTs and dynamic tests or wave equation analyses (WEAP), depending on the site variability and the number of static and dynamic tests conducted at the site. Generally, the resistance factors increase as the reliability of the field verification methods increase (Allen, 2005). As described in AASHTO (2007) Section 10.7.3.8.2, the SLT is the best way to determine the pile actual (nominal) capacity, which shall not be performed before five days after driving. The SLT shall follow the procedures

specified in ASTM D 1143 (ASTM, 2007) for the Quick Load Test Method unless other longer test methods are needed. The Davisson failure criterion is recommended for piles with diameters smaller than 600 mm (23.6 inch). A resistance factor of 0.65 should be used if the pile design verification method is dynamic tests with signal matching (CAPWAP) at Beginning of Restrike (BOR) and using the minimum number of dynamic tests in the field, depending on site variability. AASHTO (2007) recommended the CAPWAP should be performed evenly within a pier and across the entire structure to justify use of the specified resistance factors. On the other hand, a resistance factor of 0.40 should be used if the design capacity is verified by means of WEAP at End of Drive (EOD) conditions.

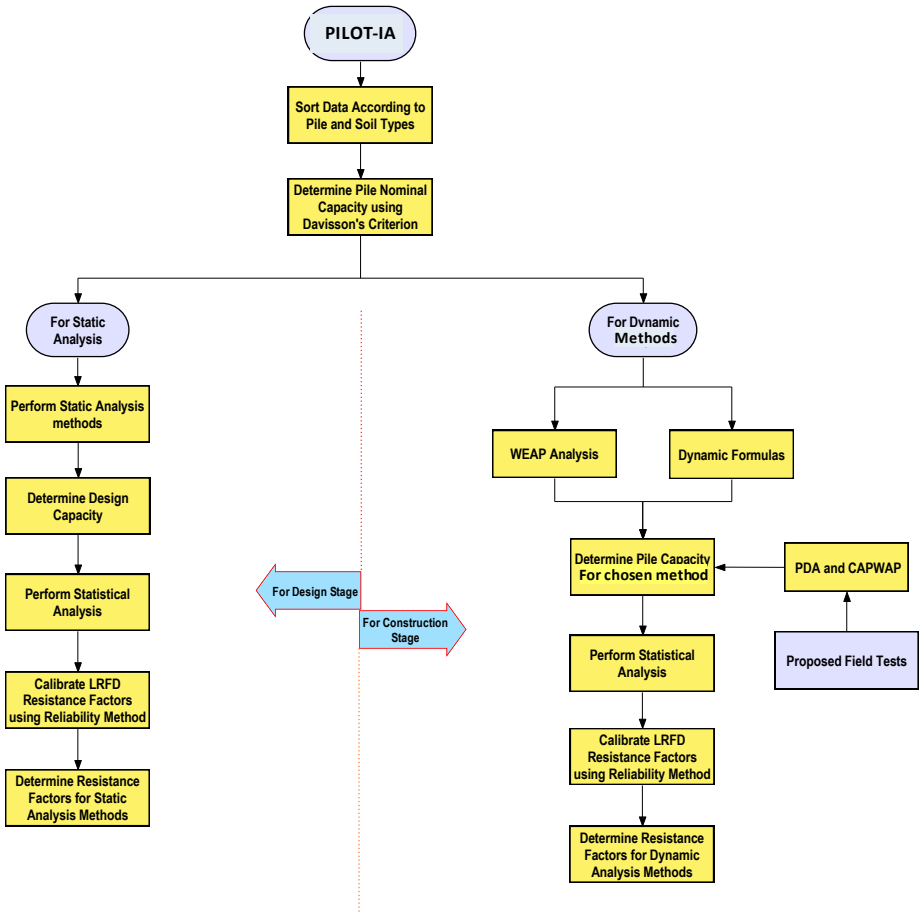

Figure 2.3: Framework of the LRFD resistance factors calibration for design and construction methods of analysis

Table 2.4: LRFD resistance factors for static analysis methods (after 2007 AASHTO)

Condition/Resistance Determination Method		φ
Nominal Resistance of Single Pile in Axial Compression – Static Analysis Methods, φ_{stat}	Skin Friction and End Bearing: Clay and Mixed Soils: α-method (*Tomlinson, 1987; Skempton, 1951*) β-method (*Esrig & Kirby, 1979; Skempton, 1951*) λ-method (*Vijayvergiya & Focht, 1972; Skempton, 1951*) Skin Friction and End Bearing: Sand Nordlund/Thurman Method (*Hannigan et al., 2005*) SPT-method (*Meyerhof*) CPT-method (*Schmertmann*) End bearing in rock (*Canadian Geotech. Society, 1985*)	 0.35 0.25 0.40 0.45 0.30 0.50 0.45
Block Failure, φ_{bl}	Clay	0.60
Uplift Resistance of Single Pile, φ_{up}	Nordlund Method α-method β-method λ-method SPT-method CPT-method Load test	0.35 0.25 0.20 0.30 0.25 0.40 0.60
Group Uplift Resistance, φ_{ug}	Sand and clay	0.50
Horizontal Geotechnical Resistance of Single Pile or Pile Group	All soils and rock	1.0
Structural Limit State	Steel piles: See the provisions of Article 6.5.4.2 in 2007 AASHTO LRFD specifications Concrete piles: See provisions of Article 5.5.4.2.1.1 in 2007 AASHTO LRFD specifications Timber piles: See the provisions of Article 8.5.2.2 and 8.5.2.3 in 2007 AASHTO specifications	
Pile Drivability Analysis, φ_{da}	Steel piles: See the provisions of Article 6.5.4.2 in 2007 AASHTO LRFD specifications Concrete piles: See the provisions of Article 5.5.4.2.1 in 2007 AASHTO LRFD specifications Timber piles: See the provisions of Article 8.5.2.2 in 2007 AASHTO LRFD specifications In identified above, use φ identified as "resistance during pile driving"	

Table 2.5: LRFD resistance factors for dynamic analysis (after 2007 AASHTO)

Condition/Resistance Determination Method		Resistance Factor
Nominal Resistance of Single Pile in Axial Compression - Dynamic Analysis and Static Load Test Methods, φ_{dyn}	Driving criteria established by static load test(s) in combination with dynamic testing or wave equation analyses.	Values in Table 2.6*
	Driving criteria established by dynamic test with signal matching at beginning of re-drive (BOR) conditions only of at least one production pile per pier, but no less than the number of tests per site.	0.65
	Wave equation analysis, without pile dynamic measurements or load test, at end of drive conditions only.	0.40

*Reduces 20 percent for non-redundant pile groups

Table 2.6: The φ for number of static load tests conducted per site (after 2007 AASHTO)

Number of Static Load Tests per Site	Resistance Factor, φ		
	Site Variability		
	Low	Medium	High
1	0.80	0.70	0.55
2	0.90	0.75	0.65
3	0.90	0.85	0.75
More than or equal 4	0.90	0.90	0.80

Table 2.7: Number of dynamic tests with signal matching analysis per site to be conducted during production pile driving (after 2007 AASHTO)

Site Variability	Low	Medium	High
Number of Piles Located Within Site	**Number of Piles with Dynamic Tests and Signal Matching Analysis Required (BOR)**		
Less than or equal 15	3	4	6
16-25	3	5	8
26-50	4	6	9
51-100	4	7	10
101-500	4	7	12
More than 500	4	7	12

2.5. Regionally-Calibrated Resistance Factors

Several code users indicated the recommended resistance factors led to inappropriate design that conflicted with their past experiences (Goble, 1999). Moreover, the current version of the AASHTO-LRFD specifications has other shortcomings. For example, they do not provide resistance factors for all static analysis methods for pile design, including obviously the "in-house" methods developed by different DOTs (Kyung et al., 2002). Since the design specifications were developed for general use, the AASHTO-LRFD bridge design specifications account for large uncertainties in soil properties, resulting in conservative resistance factors (Paikowsky et al., 2004). In addition, AbdelSalam et al. (2008) revealed: 1) the 2007 AASHTO-LRFD design specifications do not distinguish between different pile types used in practice and 2) development of regionally calibrated LRFD resistance factors, as permitted by AASHTO, for specific soil conditions, pile types, and construction practices would help overcome the aforementioned limitations and result in more cost-effective pile foundations.

The regionally-calibrated LRFD resistance factors can be obtained for a specific geographical region with unique soil conditions and construction practices. The development of such resistance factors for a given pile type and geological region requires the existence of adequate static load test data, as well as good quality soil parameters from in-situ testing. With the existence of such data, regionally-calibrated resistance factors can be developed following the approach suggested in the LRFD Specifications (2007 AASHTO-LRFD Specifications). As a part of this study, a nationwide survey was conducted in 2008, indicating that at least five state DOTs have developed their own regionally-calibrated resistance factors, based on reliability theory to improve the cost-effectiveness of deep foundations. The survey indicated about 13 state DOTs are in a transition stage from ASD to LRFD, where they have adopted preliminary regionally-calibrated resistance factors by fitting to the ASD. A full preview of the survey's outcomes is presented in Chapter 3 of this thesis. From here arise the importance and the necessity of developing regionally-calibrated resistance factors for Iowa DOT.

2.5.1. Background summary

In 2000, Liang and Nawari investigated the AASHTO-LRFD resistance factors for driven piles using a pile static load test database, which covered a spectrum of variations in soil formations, as well as different pile types and geometry. Liang and Nawari (2000) studied the LRFD resistance factors for 11 different static analysis methods suitable for determining the pile design capacity and their results were compared to ASD factor of safety. These results indicated the resistance factors ranged between 0.69 and 0.55 at β=2.0 for most of the static methods they used. They also provide design tables indicating the resistance factors for different β values. This study proved that utilizing regionally-calibrated LRFD resistance factors could lead to a significant gain in the pile design capacity.

Other studies were conducted to evaluate the assumptions considered in the AASHTO-LRFD code to develop the resistance factors; for example, using the same load factors developed for structural members to provide design consistency (Withiam et al., 1997). A study was developed by Scott et al. (2003) to assess the usage of the typical load factors in the calibration of the LRFD for substructures, as they employed the First Order Second Moment (FOSM) reliability, based analysis to calculate the load factors, and compared these results to different load factors presented in various design codes. Different load combinations were applied in the strength limit state and the average values they calculated showed good agreement with AASHTO and U.S. codes. As a conclusion, the FOSM reliability-based analysis was found to be a good statistical approach for calculating the LRFD resistance factors. Scott et al. (2003) assumed a lognormal Probability Density Function (PDF) in the FOSM analysis. According to Ellingwood et al. (1980), the lognormal distribution is more precise for modeling transient loads than the normal distribution. Moreover, the lognormal distribution represents the product of several positive random variables, even if these variables do not follow lognormal distributions.

As a part of the previous work completed to evaluate the performance of the AASHTO-LRFD resistance factors in unique soil types, Thibodeau and Paikowsky (2005) conducted a large load test program, which included 23 statically-load tested piles in distinctive subsurface conditions containing glacio-delatic silt and sand deposits. The main concern of this study was the difficult subsurface conditions, which yield higher pile static

capacity predictions than expected. Thibodeau and Paikowsky (2005) found the over-prediction of static methods was due to the overestimation of soil properties for the glacio-delatic deposits. Accordingly, a local calibration for the LRFD resistance factors was recommended for this specific soil type for more efficiency. However, despite the over-prediction of typical static analysis methods, they acknowledged the recommended resistance factors in the NCHRP 507 performed better than the ASD specifications at that time, where for some cases the ASD factor of safety was less than unity.

Abu-Hejleh et al. (2009) demonstrated the LRFD design procedures for driven H-piles and cast-in-place pipe piles to help with interpretation of AASHTO-LRFD design specifications for driven piles into the design and construction practice. The study mainly focused on the geotechnical strength limit state for a single pile. Abu-Hejleh et al. (2009) highlighted the importance of performing field verification tests (i.e., dynamic tests), which can account for pile setup, relaxation, and soil plugging for steel H-piles. In their study, setup was reported in sand for steel H-piles. However, normally setup occurs in cohesive soils for displacement piles. Moreover, static analysis methods were considered to be more accurate and recommended in soft silty clays and hard rocks, and it was conservatively assumed that static analysis predictions correspond to BOR conditions. As for the pile structural limit state, Abu-Hejleh et al. (2009) assumed a resistance factor of 0.5 and 0.6 at hard driving conditions for steel H-piles and cast-in-drilled-hole piles, respectively. These resistance factors were slightly increased in case of easy driving. The study illustrated the significant cost savings when using LRFD instead of ASD in the design of pile foundations, demonstrating numerical examples, especially when local calibration of the LRFD resistance factors is considered. Finally, Abu-Hejleh et al. (2009) were concerned about evaluating the serviceability limit in the LRFD design of foundations, especially when large loads are permitted in the strength limit states.

Many calibration frameworks have been conducted, based on reliability analysis using large databases. However, Foye et al. (2009) indicated that reliability analyses, based on databases, do not necessarily account for uncertainties caused by soil variation, soil testing techniques, and the analysis model used to calculate the foundation capacity. Foye et al. (2009) developed the LRFD resistance factors for driven pipe piles in sand by isolating

various sources of uncertainties using two design approaches. The first approach used direct design method, and the second used the property-based design method. Direct methods are those depending on direct correlation with soil in-situ tests, while the property-based design methods depend on laboratory and field test results. The LRFD resistance factors were separated for skin-friction and end bearing components. Foy et al. (2009) indicated the direct method is more accurate than the property-based method and gives higher LRFD resistance factors, as the property-based method requires assuming several soil properties. Foye et al. (2009) claimed the calibration technique, used in the NCHRP-507 (Paikowsky et al., 2004), is based on a lumped database, as it did not discriminate between the various sources of uncertainty contributing to the observed scatter between prediction and measurements. Recently, McVay et al. (2010) indicated the design specifications depend on constant resistance factors that ignore the effect of soil variation along the shaft, involving spatial averaging. For this reason, they developed design charts for single and group of pile layouts, considering the effect of soil variability for the shaft and tip resistance components.

Separating the skin-friction and end-bearing components of the pile resistance and developing the corresponding resistance factors is a crucial topic ignored in many codes. In 2002, Kuo et al. developed resistance factors for a database consisting of 185 drilled shafts by only considering the skin friction, and then compared the differences when considering the total resistance. One of their conclusions was the difference in the values of the resistance factors for only the total or the skin-friction components of the pile capacity depends more on the pile type, installation technique, and soil profile. However, in 2008, Lai et al. separated the resistance components using conventional static analysis methods and developed the resistance factors, based on a database containing 13 load tested steel piles. Nevertheless, only few studies have addressed this issue, as separating the shaft and tip resistances requires conducting SLTs on instrumented piles, which are quite expensive and time consuming.

In addition to the previous findings, there is an evident disadvantage of the current geotechnical LRFD practice, as it only accounts for the strength limit states. Starting in 1994, Green observed various technical problems that arose while using the Ontario LRFD code, and recommended an improved communication between the structural and geotechnical engineers to ensure that serviceability and strength limits are properly identified. In 1996,

Goble indicated the need for additional research to include the serviceability limit states into the LRFD code. Scott and Salgado (2003) identified the importance of this issue, especially for cohesive soils where the settlement is not immediate and using the unity resistance factor recommended by the AASHTO for serviceability checks may not be adequate. Consequently, several studies were conducted on this topic during the last few years. Some were based on predicting the pile load-displacement relationship, and selecting the design capacity and the corresponding settlement in a reliability-based manner. The load-transfer method (t-z method) has been extensively used to model load-displacement curves and perform the reliability analysis of deep foundations (Misra and Roberts, 2006; Misra et al., 2007). In 2008, Robert et al. developed a practical LRFD method for the simultaneous design of deep foundations at both the strength and service limit states, using the t-z method. Recently, Abu-Hejleh et al. (2009) developed the LRFD design for drilled shafts, based on the Cone Penetration Test (CPT) data for serviceability limits, indicating that settlement can control the design in particular soil types, especially when large loads are permitted.

2.5.2. State DOTs implementation

The FHWA mandated all new bridges initiated in the United States after October 1, 2007, must follow the LRFD approach. Since then, there has been a general move among State DOTs toward the increased use of the LRFD in structural and geotechnical design practices. In 1997, the Florida Department of Transportation (FDOT) developed a LRFD Code for their bridge design (Passe, 1997). Although no probabilistic analysis was performed in the calibration process, the FDOT was a pioneer among the state DOTs in implementing the LRFD for geotechnical applications. In 2002, North Carolina Department of Transportation (NCDOT) developed resistance factors in a framework of reliability theory for axially-loaded driven piles. After this, many other states have calibrated their own LRFD resistance factors. According to a recent survey by AbdelSalam et al. (2008), responses obtained from more than 30 DOTs revealed that more than 50% of the state DOTs are currently using the LRFD method for pile design, while only 30% of the DOTs are still in a transition phase from the ASD method to the LRFD. Their study also revealed about 30% of the DOTs that employ the LRFD for piles have utilized their regionally-calibrated resistance

factors to improve the cost-effectiveness of pile foundations, which means that at least five state DOTs have adopted regionally-calibrated resistance factors based on reliability theory and 13 state DOTs among those, who are still in a transition stage to the LRFD, have adopted preliminary, regionally-calibrated resistance factors by fitting to the ASD.

2.6. Construction Control of Deep Foundations

In this section of the chapter, the difference between the pile design and construction stages is presented. This is followed by a simplified definition for the construction control of bridge deep foundations. Finally, the possibility of considering the construction control aspects during the design stage is discussed.

2.6.1. Design versus construction stages

Site investigation and soil parameters determination are the first step in the design stage of any bridge project. Soil parameters are commonly evaluated by performing laboratory and/or field tests, such as SPT and CPT, depending on the soil type and the desired degree of accuracy. The second step in the design stage is identifying the possible foundation schemes, based on the results of the investigation, load requirements, importance of the structure, and local experience. The third step is calculating the capacity of the selected type of foundation, and determining the length and number of the needed piles. In order to perform this step, static analyses take place. In the case of driven piles, a dynamic analysis (WEAP) can be considered for hammer evaluation, feasibility of installation, and structural adequacy of the pile. Therefore, the design stage's main purpose is performing structural and geotechnical analyses to provide a reasonable estimate for the required foundation type, length, number, and size. Hence, this process will serve in assembling the bidding documents concerning the bridge's substructure.

In the construction stage, design verification and construction control should be achieved by means of SLT and/or dynamic analysis. The assigned capacity and the final specifications should be determined from the construction stage. The difference between the pile designed capacity and the measured capacity in the field should not be large, and should maintain the same degree of reliability. In some important projects, the design stage relies on

pile SLT and/or dynamic analysis instead of performing static analysis (Paikowsky et al., 2004). Figure 2.4 provides a flowchart that briefly describes the typical design and construction cycle. As shown in Figure 2.4, after performing the static analysis for determining the preliminary pile design capacity, a pile deformation analysis takes place to ensure the design capacity does not lead to an excessive settlement or deformations to the structure. As previously mentioned, the construction stage takes place after releasing the bidding (contracting) documents, where the design verification is performed by means of SLT, or PDA and CAPWAP. Regarding the practices of deep foundations, it was found that Iowa DOT has slightly different design and construction practices than the aforementioned practice. The main difference arises in the construction stage, as the majority of contractors depend on WEAP analysis for design verification and construction control. Some other contractors drive the pile until refusal, which in some cases could damage the steel pile as well as being over conservative. Figure 2.5 represents the pile design and construction practice in the State of Iowa.

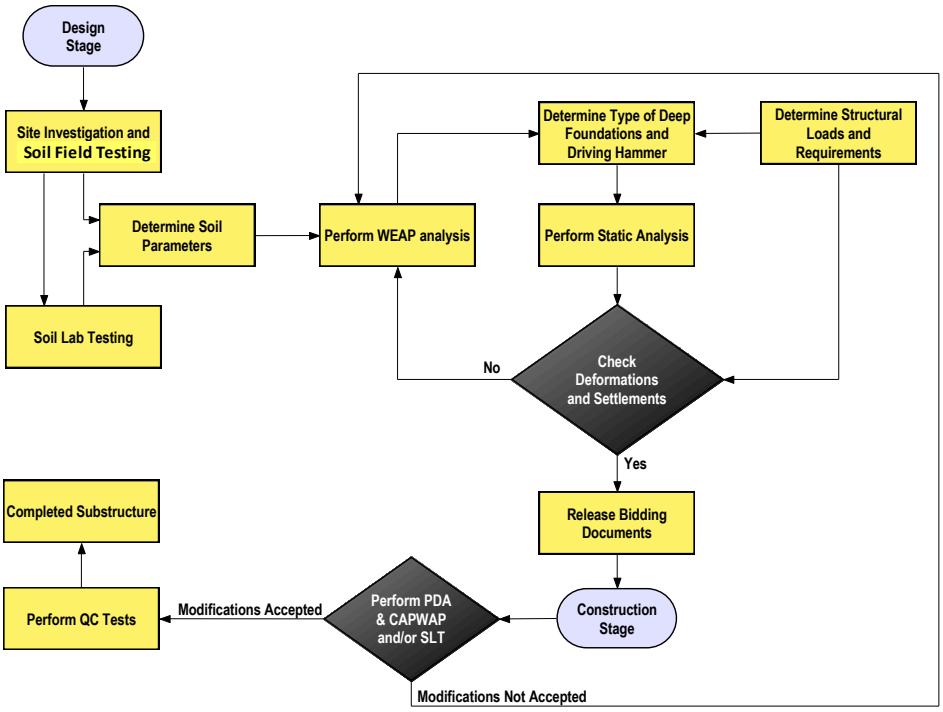

Figure 2.4: Typical design and construction cycle

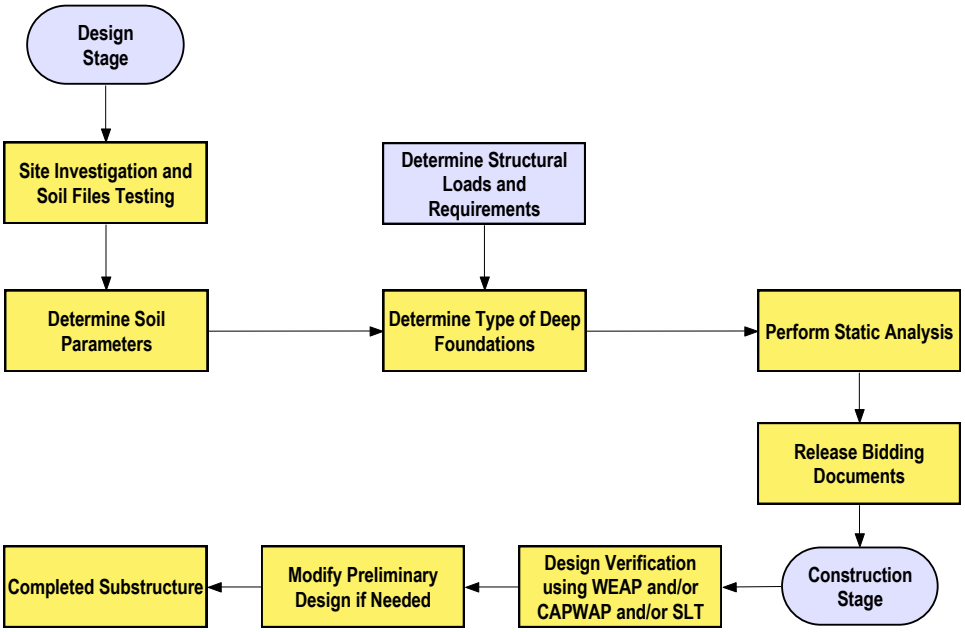

Figure 2.5: Design and construction practice in the state of Iowa

2.6.2. Definition of quality control

Construction control of pile foundations, which can also be referred to as Quality Control (Q.C.), is a general term that accounts for several field-conducted procedures and can be separated into twofold: (1) check/verify the pile design capacity and integrity, and (2) utilize quality assurance (after Paikowsky et al., 2004). According to the previous definition, one can suppose that construction control mainly consists of pile design verification and quality assurance.

Design verification is carried out by means of SLTs, dynamic analysis (e.g., WEAP, PDA, etc.), or dynamic formulas (e.g., ENR, FHWA Gates, etc.). It accounts for soil variability, driving conditions, and any other conditions that could affect the pile capacity. In some cases, design verification depends on engineering judgment and experience by driving the pile to a hard bedrock layer or driving until pile refusal. Although the previous judgmental methodologies are practiced in various regions, it cannot guarantee an acceptable pile final capacity and may lead to unnecessary conservatism. Therefore, it is very important to conduct dynamic analysis or pile SLTs during the construction stage to ensure safe and cost-efficient foundations.

Quality assurance is to guarantee adequate soil investigations and parameter determination during the design stage and to insure pile competence during and after driving. Pile competence can be evaluated by means of conducting verticality tests, Cross Sonic Logging (CSL), Surface Reflection (Pulse Echo Method), Gamma Ray or NX coring, and other tests. The AASHTO recommended LRFD resistance factors for deep foundations are based on a suitable degree of quality control. Therefore, geotechnical engineers should at least assure and maintain the same degree of quality to fully exploit the benefits of the LRFD methodology for geotechnical purposes. Hence, it is important to perform such quality assurance tests and to provide a guideline for the required limits of quality assurance. Paikowsky et al. (2004) proposed a framework for the establishment of knowledge-based factors for both the design and construction capacity evaluation methods. These factors can be accounted for by means of a modifying constant (ξ) multiplied by the LRFD resistance factors. However, this requires additional sophisticated databases.

2.6.3. Combining static and dynamic methods

As previously mentioned, the design stage depends on static analysis. Several static analysis methods could be used for calculating the pile capacity, where each static method has its own LRFD resistance factors, depending on different soil and pile types. On the other hand, construction control tests have their own LRFD resistance factors used for design verification purposes. Combining static and dynamic analyses is not preferable, as the interaction between two different stages is not accurate (Paikowsky et al., 2004).

There is a fact that needs to be highlighted—it is not useful to combine the LRFD resistance factors from two independent pile capacity determination stages (i.e., design and construction stages). This is because normally the construction control tests are not conducted during the design stage. According to Paikowsky et al. (2004), most of the geotechnical LRFD design codes had suffered from different problems, due to combining resistance factors from the two separate stages. Paikowsky reported the AASHTO-LRFD Bridge Design Specifications (2001) were not clear for geotechnical practice, due to the existence of a modifier factor (λ_v), multiplied by the LRFD resistance factors. This modifier accounted for some unnecessary combinations between the design and the construction

stages. In the 2007 AASHTO LRFD (2008 interims), this modifier was removed to fixed the confusing conservatism of the pile design.

However, some state DOTs have adapted a correction factor for static methods. For example, Long et al. (2009) studied the agreement between static methods and dynamic formulas for the Illinois DOT (IDOT). The main criterion was determining the average difference between static methods and dynamic formulas, as some static methods were too inaccurate, based on static load test results. The correction factor developed by IDOT is somewhat different than the previously mentioned modifier factor (λ_v), as it is supposed to be applied to static methods before performing the calibration for the LRFD resistance factors. Therefore, the correction factor modifies the nominal design capacity attained from different static methods. Based on these modified capacities, the LRFD resistance factors are calibrated. In summary, the IDOT combined dynamic and static analyses to determine the most useful method for their region.

2.7. Static Analysis Methods

Several methods are available to predict the nominal axial capacity of driven piles. Among these, the static analysis methods have been developed empirically or semi-empirically using field test data. Static analysis methods are fairly straightforward and typically utilized during the design stage. There are numerous limitations for each method and the selection of the most appropriate method for a specific design problem depends on the site geology, pile type, extent of available soil parameters, and local practice. Static methods only estimate the pile nominal capacity without determining the corresponding movements, i.e., they only determine the strength limit state of a pile foundation and not the vertical settlement. Many soil strength parameters are required for different static analysis methods, where these soil parameters are directly measured or calculated, based on correlations to in-situ and/or laboratory soil tests. The following sections provide a summary of the most commonly used correlations to calculate different soil strength parameters, followed by an overview of the most frequently used static analysis methods for determining the nominal capacity of pile foundations.

2.7.1. Determination of soil properties

Most of the static methods directly or indirectly utilize the soil's shear strength parameters to calculate the capacity of pile foundations. These parameters could be determined using laboratory tests or correlations to field tests, such as the Standard Penetration Test (SPT) or Cone Penetration Test (CPT). Since the SPT is considered as one of the most commonly used soil field tests despite its disadvantages, many soil strength correlations were developed, based on this test. There are several errors that should be considered and corrected while using SPT N-values, where N-value is the number of blows required to drive a standard split spoon sampler a distance of 1.0 ft (30 cm). Cheney and Chassie (1993) studied common SPT errors; among them are the effects of soil overburden pressure as well as the variation in the free fall of the drive weight that affects the driving efficiency. The efficiency of the system can be determined by comparing the Kinetic Energy (KE) with the Potential Energy (PE), meaning the Energy Ratio (ER) is equal to KE/PE. According to the LRFD highway bridge substructures reference manual (2007), the ER is equal to 60% for routine engineering practices in the United States. The N-value corresponding to 60% is termed N60, which can be calculated, if the field efficiency is different than 60%, by using the following equation:

$$N_{60} = (ER/60\%)\ x\ N \qquad [2.27]$$

Peck et al. (1974) have presented a normalization parameter (C_n) that should be multiplied by N60 to correct the N-values to account for the effect of overburden pressure in non-cohesive soils. The corrected SPT N-value is:

$$(N_1)_{60} = C_n\ x\ N_{60} \qquad [2.28]$$

$$C_n = 0.77 \log_{10}\left(\frac{1.92}{\sigma_v'}\right),\ \ C_n < 2.0 \quad (S.I.\ units) \qquad [2.29]$$

$$C_n = 0.77 \log_{10}\left(\frac{40}{\sigma_v'}\right),\ \ C_n < 2.0 \quad (English\ units) \qquad [2.30]$$

where,

σ_v' =Effective vertical stress.

The SPT has been used in correlations for soil unit weight (γ), relative density (D_r), angle of internal friction (ϕ), and unconfined compressive strength (S_u). There are several correlations between the SPT N-values and different soil parameters. These different correlations are presented in Table 2.8. According to Paikowsky et al. (2004), the best correlation for determining ϕ in cohesionless soils is provided by Peck and Thornburn (1974), who recommended limiting ϕ below 36°. Also, the most common correlation used to estimate S_u from SPT is the one provided by Terzaghi and Peck (1967), using the uncorrected N-values. Tables 2.9 and 2.10, after Bowles (1977), summarize different ranges of D_r, ϕ, and γ with respect to corrected and uncorrected N-values, respectively. On the other hand, there are many empirical correlations to estimate the soil's shear strength parameters from the CPT test. As shown in Table 2.11, the S_u and ϕ were mainly calculated, based on the CPT cone tip resistance (q_c), as well as the soil's effective overburden pressure (σ'_v). According to Paikowsky et al. (2004), the best correlation for determining S_u is by Hara (1974), while the correlation used by Robertson and Campanella (1983) is most commonly used for calculating the soil's internal friction angle. There are many empirical correlations to calculate other soil parameters from CPT, which are summarized in Kulhawy and Mayne (1990).

After this preview of different correlations used to determine soil parameters from SPT and CPT, it would be appropriate to indicate that not all of these correlations were used in this study. Only some of them have been chosen, as will be presented later in Chapter 5, according to the recommendations given by the 2007 AASHTO-LRFD specifications, the FHWA LRFD-highway bridge substructures reference manual (2007), as well as the NCHRP 507 LRFD report by Paikowsky et al. (2004).

Table 2.8: Selected correlations between SPT N-values and various soil parameters

Soil Properties	SPT Correlation	Reference
ϕ (deg.)	$\mathbf{54 - 27.6\exp(-0.014(N_1)_{60})}$	Peck, Hanson, and Thornburn (1974)
	$\mathbf{\tan^{-1}[N/(12.2 + 20.3\sigma')]^{0.34}}$	Schmertmann (1975)
S_u (bar) (1 bar = 14.5 psi)	$\mathbf{0.06\ N}$	Terzaghi and Peck (1967)
	$\mathbf{0.29\ N^{0.72}}$	Hara (1974)
D_r	see Mayne and Kulhawy (1990)	

Table 2.9: D_r, ϕ, and γ corresponding to corrected SPT N-values (after Bowles, 1977)

Description	Very Loose	Loose	Medium	Dense	Very Dense
Relative density, D_r	0 – 0.15	0.15 – 0.35	0.35 – 0.65	0.65 – 0.85	0.85 – 1.00
Corrected SPT N-value	0 to 4	4 to 10	10 to 30	30 to 50	50+
Internal friction Angle, ϕ	25 – 30°	27 – 32°	30 – 35°	35 – 40°	38 – 43°
Unit weight, γ (kN/m^3) (1 kN/m^3 = 6.24 pcf)	11.0 – 15.7	14.1 – 18.1	17.3 – 20.4	17.3 – 22.0	20.4 – 23.6

*Use 5% larger values for granular material.

Table 2.10: Ranges of q_u and γ with respect to un-corrected SPT (after Bowles, 1977)

Description	Very soft	Soft	Medium	Stiff	Very Stiff	Hard
S_u (kPa) (1 kPa = 0.145 psi)	0 – 24	24 – 48	48 – 96	96 – 192	192 – 384	384+
Un-corrected SPT N-value	0 to 2	2 to 4	4 to 8	8 to 16	16 – 32	32+
γ (kN/m^3) (1 kN/m^3 = 6.24 pcf)	15.8 – 18.8	15.8 – 18.8	17.3 – 20.4	18.8 – 22.0	18.8– 22.0	18.8 – 22.0

*Correlations should be used for preliminary estimates only

Table 2.11: Correlations between CPT and soil parameters

Soil Properties	CPT Correlation	Reference
ϕ (deg.)	$[0.1 + 0.38 * \log(q_c/\sigma')]$	Robertson and Campanella (1983)
Su (bars) (1 bar = 14.5 psi)	$(q_c - \sigma_o)/N_k$	Hara (1974)

2.7.2. Pile capacity in cohesive soils

Different static methods have been designed empirically or semi-empirically, based on a reasonable agreement with pile load tests. Some of these methods were based on field tests conducted in cohesive soils (i.e., clayey soils), restricting their usage to designs in similar soil types. There are several of these methods, such as the Alpha (α) method, Beta (β) method, Lambda (λ) method, and CPT-method. On the other hand, there are static methods

developed, based on field tests performed in cohesionless soils (i.e., sandy soils). Among these methods are the SPT-method and Nordlund's method. Not all the available static methods in the literature are presented in this Chapter, but only the most commonly used methods and the methods that have been recommended for the design of pile foundations by the 2007 AASHTO-LRFD specifications, the FHWA LRFD-highway bridge substructures reference manual (2007), as well as the NCHRP 507 LRFD report by Paikowsky et al., 2004.

Before using static analysis methods, geotechnical engineers should be familiar with the limitations of each method and should be able to choose the appropriate method that best represents specific soil-pile conditions. Moreover, static methods should not be the only approach used for designing deep foundations, but several verification techniques should be performed regularly to check the design. Many state DOTs have developed their own static analysis methods that better represent their unique soil conditions and construction practices. Such locally developed methods are generally called the "In-house" method. In 1989, the Iowa DOT developed its foundation soils information chart for pile foundation after Dirks and Kam (1989), revised in 1994. The Iowa design charts were given the name "*Bluebook*" (some time referred to as "*BB*"). In summary, the BB is an in-house static analysis approach, especially developed for Iowa soils and mainly combines different static analysis methods together to enhance pile capacity predictions. In the next sections, different static analysis methods, as well as the BB method, are briefly described.

2.7.2.1 The α-API Method

The α-method (API-1974) is a semi-empirical approach of calculating the pile skin friction, based on the total stresses induced in the soil and calculated using the soil's undrained shear strength (S_u). This method was mainly developed for cohesive or clay soils. It has been used for many years and has proven to provide reasonable design capacities for displacement and non-displacement piles. This method depends on the alpha factor (α), which is indirectly related to the soil's undrained shear strength (S_u). The factor was back-calculated from several pile load tests. The main equation used for calculating the pile unit shaft resistance is as follows:

$$f_s = \alpha \,.\, S_u \qquad [2.31]$$

where,

f_s =Unit side-friction resistance.

α =Adhesion factor.

S_u =Undrained shear strength in soil adjacent to the foundation.

There are numerous functions that have been developed to correlate the α-value to different soil properties and pile types. Among the most commonly used functions are those developed by Tomlinson (1957), Peck (1958), the American Petroleum Institute (API-1974), and Tomlinson (1980). Figure 2.6 presents some of the different correlations used to calculate α after Vesic (1977). It is clear from the figure there is a large scatter among the α-values, which requires local experience while selecting the suitable function used in the design of piles. According to Coduto (2001), although the API (1974) function was mainly developed for the design of offshore piles, it is probably the most suitable for the design of driven piles. The equations used to determine α-values based on the API are as follows:

For; $S_u < 25$ kPa (500 psf):

$$\alpha = 1 \qquad [2.32]$$

For; 25 kPa (500 psf) < S_u < 75 kPa (1500 psf):

$$\alpha = 1.0 - 0.5\left(\frac{S_u - 25\ \text{kPa}}{50\ \text{kPa}}\right) \quad (\textit{S.I. units}) \qquad [2.33]$$

$$\alpha = 1.0 - 0.5\left(\frac{S_u - 500\ \text{lb/ft}^2}{1000\ \text{lb/ft}^2}\right) \quad (\textit{English units}) \qquad [2.34]$$

For; $S_u > 75$ kPa (1500 psf):

$$\alpha = 0.5 \qquad [2.35]$$

On the other hand, O'Neill and Reese (1999) have developed a bearing capacity factor (N_c) to calculate the end-bearing resistance of deep foundations in cohesive soil, based on the soil's total undrained shear strength as follows:

$$q'_t = N_c^* \,.\, S_u \qquad [2.36]$$

where,

q'_t =Net unit end-bearing resistance.

S_u =Undrained shear strength of the soil between pile tip and 2B below the tip.

B =Pile diameter.

N_c^* =Bearing capacity factor (after O'Neill and Reese, 1999).

$= 6.5$ if $S_u \leq 25$ kPa (500 psf) [2.37]

$= 8.0$ at $25 < S_u < 100$ kPa (1000 psf) [2.38]

$= 9.0$ at $S_u \geq 100$ kPa (2000 psf) [2.39]

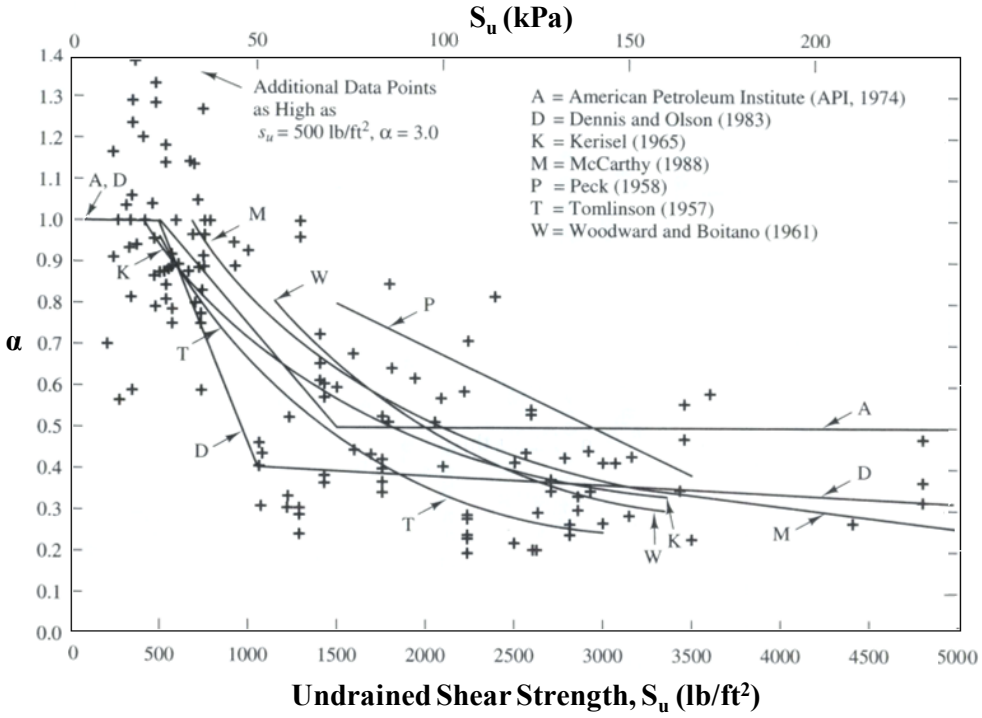

Figure 2.6: Measured values of α as back calculated from full-scale static load tests compared with several proposed functions for α (After Coduto, 2001)

As previously indicated, S_u was calculated, based on the correlation to the uncorrected SPT N-values provided by Terzaghi and Peck (1967). This raised many arguments against the reliability of the α-method, even if S_u was determined, based on laboratory testing, as the soil sampling method can cause significant disturbance to the soil's properties (Jardine et al., 2005). They added that in the case of driven piles, the driving process itself could lead to significant changes in soil properties, such as remolding of the soil next to the pile. This may directly affect the calculated pile skin-friction, based on the α-method. However, the method has been widely used in practice, as it still provides relatively reasonable pile capacities in cohesive soils (Coduto, 2001).

2.7.2.2 The α-Tomlinson Method

Among the common functions developed to correlate the α-value to the soil's undrained shear strength is that developed by Tomlinson (1980). The α-Tomlinson method has been widely used, especially in stiff clays. This method accounts for different pile materials (i.e., concrete, timber, or steel piles) and provides reasonable capacity estimates for large displacement piles; hence, it may not be the most suitable method for driven piles. The method relies on the α-values, which, in-turn, depend on the bearing embedment in stiff clay and the width of the pile. The equation used for calculating skin friction using α -Tomlinson is similar to α-API. The only difference is in the value of α. The equation used is as follows:

$$f_s = \alpha \, . \, S_u \qquad [2.40]$$

where,

f_s =Unit side-friction resistance.

α =Adhesion factor (Figures 2.7 and 2.8 after Tomlinson 1979 and 1980, respectively).

S_u =Undrained shear strength in soil adjacent to the foundation.

The same equations mentioned before with the α-API method are used to calculate the end-bearing resistance of the pile.

2.7.2.3 The β-Method

The β-method (Burland, 1973) is a semi-empirical approach, based on effective stresses calculated from the vertical effective overburden stress. This method was developed to model the long-term drainage shear strength. It can be used for different soil types, such as clay, silt, sand, or gravel, and can even be used for layered soil profiles. According to Fellenius (1991), the beta factor (β) is affected by soil type, mineralogy, density, strength, pile installation technique, as well as other factors. The values of β range between 0.23 and 0.8, but cannot exceed 2 for over consolidated soils, as suggested by Esrig and Kirby (1979). The β-method has been found to work best for piles in normally consolidated and lightly over consolidated soils. However, the method tends to overestimate pile capacity for heavily over consolidated soils (AASHTO-interim 2006). The β-method equation for calculating the unit skin friction is as follows:

$$f_s = \beta \, . \, \overline{P}_o \qquad [2.41]$$

where,

f_s =Unit side-friction resistance.

β =Bjerrum-Burland β coefficient = $K_s \tan \delta$ (or use Table 2.12 and Figure 2.9).

$\overline{P}_o$ =Average effective overburden pressure along the pile shaft (kPa).

K_s =Earth pressure coefficient.

δ =Friction angle between pile and soil.

To calculate the end-bearing resistance of the pile, Eq. [2.42] is used:

$$q_t = N_t \, . P_t \qquad [2.42]$$

where,

N_t =End-bearing capacity coefficient (Table 2.12 and Figure 2.10, after Fellenius, 1991).

P_t =Effective overburden pressure at pile toe (kPa).

Note, N_t and P_t are functions of angle of soil internal friction (ϕ'), which can be calculated using empirical correlations to SPT N-values or from laboratory testing.

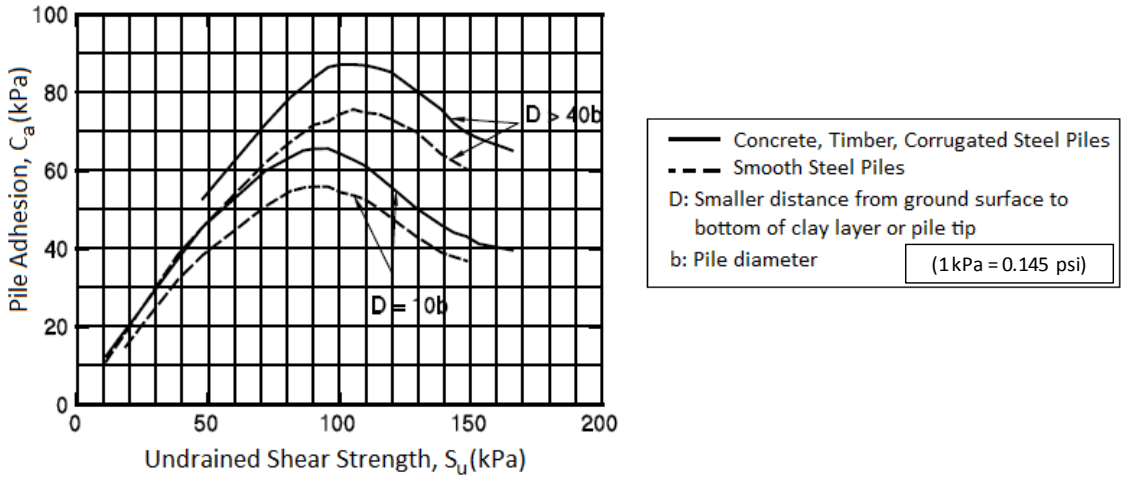

Figure 2.7: Adhesion values for piles in cohesive soils (after Tomlinson, 1979)

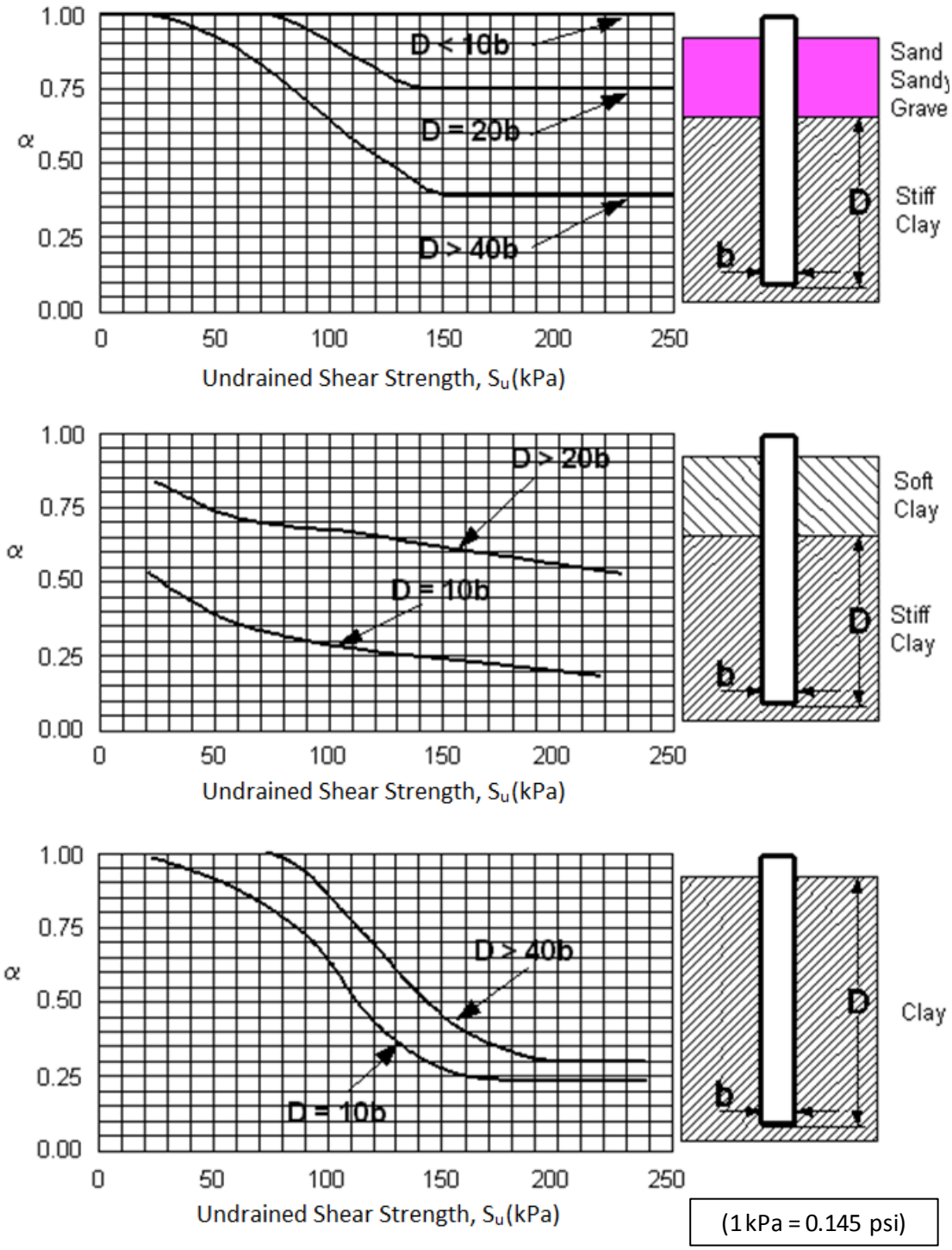

Figure 2.8: Adhesion factors for driven piles in clay soils (after Tomlinson, 1980)

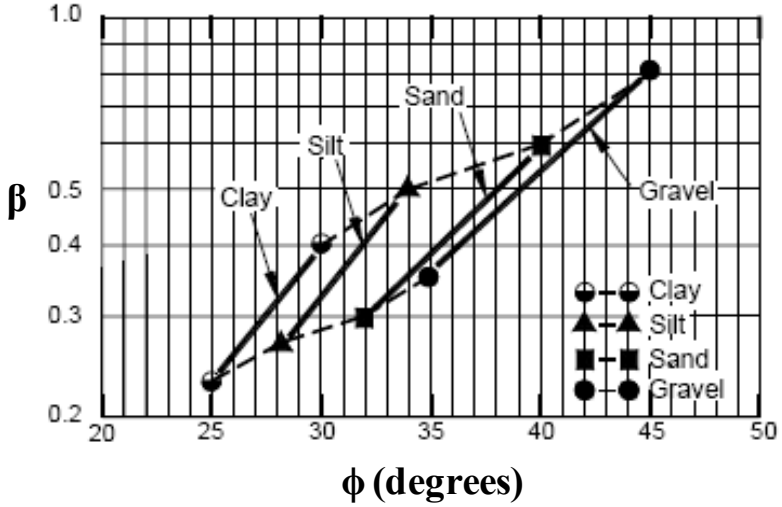

Figure 2.9: The β coefficient versus soil type using ϕ' angle (after Fellenius, 1991)

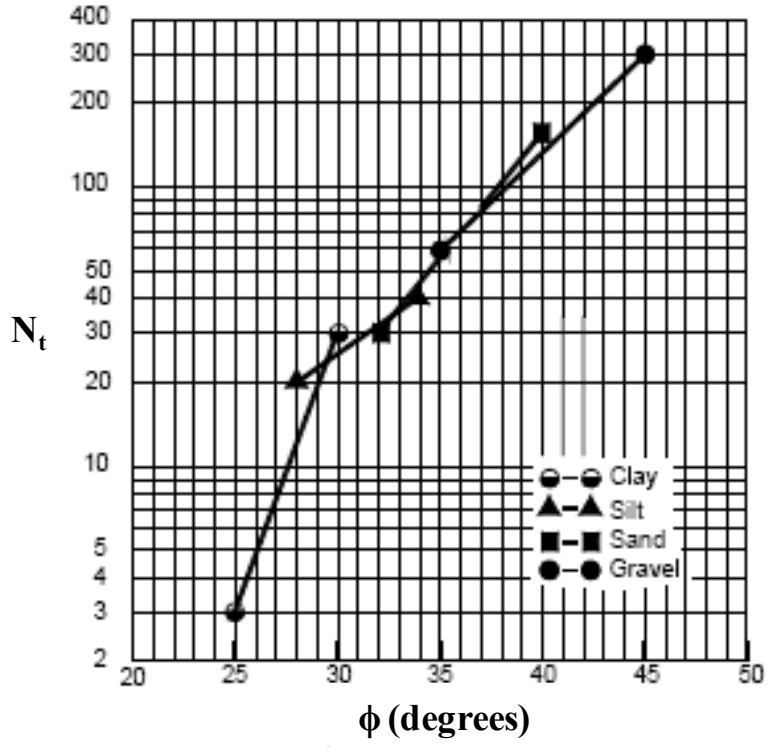

Figure 2.10: The N_t coefficient versus soil type using ϕ' angle (after Fellenius, 1991)

Table 2.12: Approximate range of β and N_t coefficients (after Fellenius, 1991)

Soil type	ϕ' (deg.)	β	N_t
Clay	25 – 30	0.23 – 0.40	3 – 30
Silt	28 – 34	0.27 – 0.50	20 – 40
Sand	32 – 40	0.30 – 0.60	30 – 150
Gravel	35 – 45	0.35 – 0.80	60 – 300

2.7.2.4 The λ-Method

The λ-method (Corps of Engineers, 1992) is an empirical approach, based on effective stresses induced in the soil (calculated from the vertical effective overburden stress) and total soil strength (calculated from undrained shear strength). This method may be used to relate the unit skin friction to the passive earth pressure (AASHTO-interim, 2006). The value of λ was empirically-determined by examining the results obtained from various load tests conducted on steel pipe piles in cohesive soils. Therefore, this method is more accurate, if used for the same soil and pile conditions. Eq. [2.43] is used to calculate the skin friction:

$$q_s = \lambda(\sigma_v' + 2S_u) \qquad [2.43]$$

where,

$\sigma_v' + 2S_u$ =Passive lateral earth pressure (ksf).

σ_v' =Effective vertical stress at midpoint of soil layer under consideration (ksf).

S_u =Undrained shear strength of soil (ksf).

λ =Empirical coefficient (see Figure 2.11 after Vijayvergiya and Focht, 1972).

To calculate the end-bearing resistance of the pile in cohesive soil, the same equations for the α-method previously mentioned can be used (based on O'Neill and Reese, 1999).

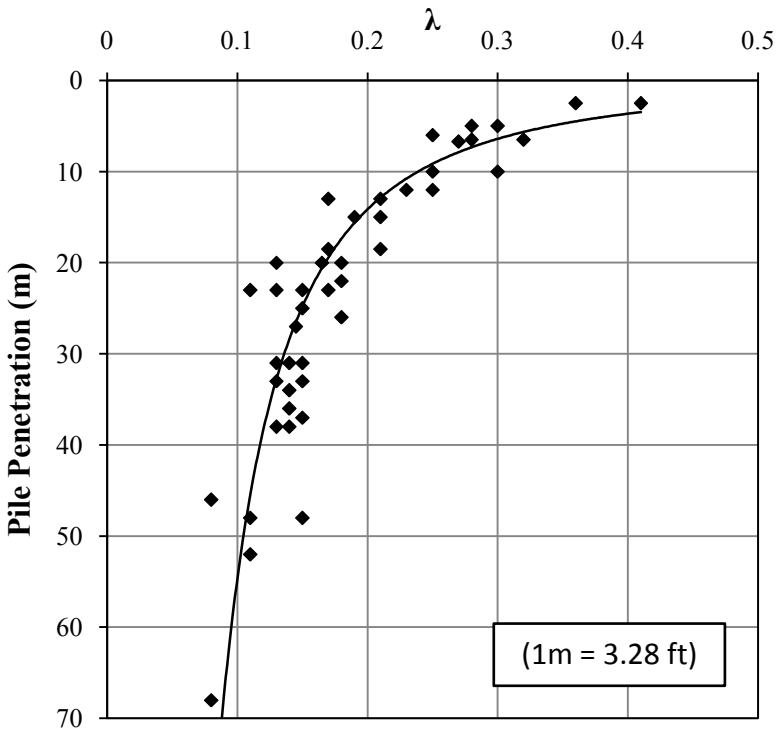

Figure 2.11: Chart for λ factor using pile penetration length (after Vijayvergiya, 1972)

2.7.2.5 The CPT-Method

Nottingham and Schmertmann (1975) developed an empirical approach to calculate pile capacity, based on the CPT applied to cohesive and cohesionless soils. Correlations to CPT provide accurate pile design capacities, especially with driven piles. Moreover, it provides continuous readings for the soil's profile and accordingly can take into consideration the effects of different soil layers. The cone tip resistance (q_c) is used to determine the end-bearing resistance of piles, while the sleeve friction (f_s) is used to determine the skin friction resistance along the shaft. The ultimate shaft resistance in cohesionless soils can be calculated using the following expression:

$$R_s = K\left[\frac{1}{2}\,(\bar{f}_s\,A_s)_{0\text{ to }8b} + (\bar{f}_s\,A_s)_{8b\text{ to }D}\right] \qquad [2.44]$$

If $\bar{f}_s$ is not available, the shaft resistance in cohesionless soils could be determined from the cone tip resistance as follows:

$$R_s = C_f\ \sum q_c\,x\,A_s \qquad [2.45]$$

In the case of cohesive soils, the shaft resistance could be determined using the following expression:

$$R_s = \alpha' \, x \, \bar{f}_s \, x \, A_s \qquad [2.46]$$

where,

K =Ratio of unit pile shaft resistance to unit cone sleeve friction in sands (Figure 2.12).

D =Embedded pile length.

b =Pile width or diameter.

$\bar{f}_s$ =Average unit sleeve friction from CPT at the point considered.

A_s =Pile-soil surface area at the point considered.

C_f =Factor obtained from Table 2.12 after the FHWA-LRFD reference manual, 2007).

q_c =Average cone tip resistance along the pile length.

α' =Ratio of pile shaft to sleeve friction (use Figure 2.13, after Schmertmann, 1978).

The ultimate tip resistance (or pile end-bearing) shall be determined as follows:

$$q_t = \frac{q_{c1}+q_{c2}}{2} \qquad [2.47]$$

where,

qc1 =Average of cone tip resistance over distance xb following the path 1-2-3 using the minimum path rule in the upward direction (Figure 2.14, after Schmertmann, 1978).

b =Pile diameter.

x =Value from 0.7 to 4.0 below pile tip as shown on Figure 2.14.

q_{c2}: =Average of cone tip resistance over distance 8b following the path 3-4 using the minimum path rule as shown on Figure 2.14.

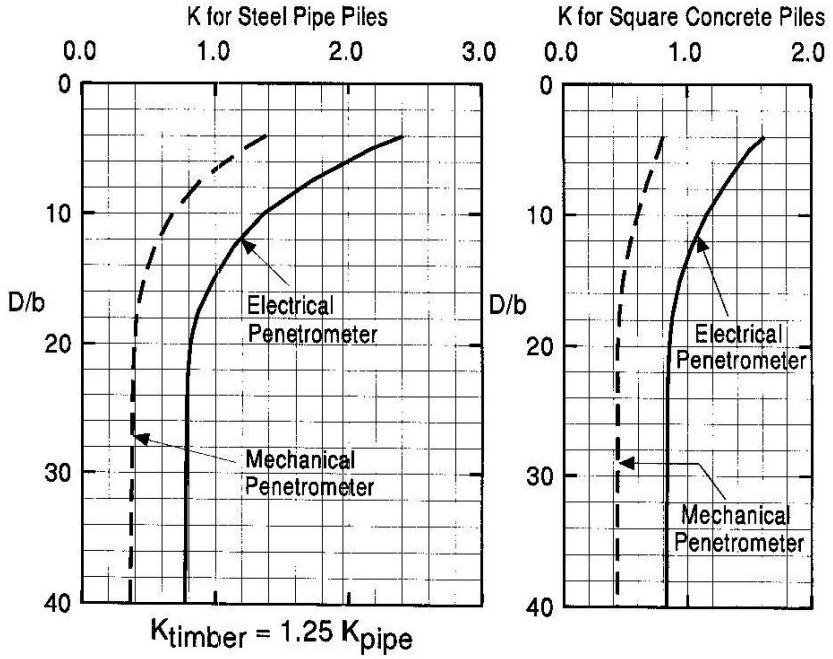

Figure 2.12: Penetrometer design curve for side friction in sand (after FHWA, 2007)

Table 2.13: Representative CPT C_f values (after FHWA, 2007)

Type of piles	C_f
Precast concrete	0.012
Timber	0.018
Steel displacement	0.012
Open end steel pipe	0.008

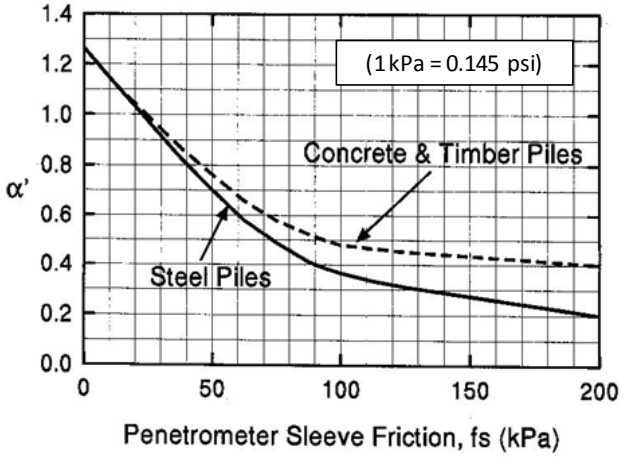

Figure 2.13: Design curve for skin-friction in clays by Schmertmann (1978)

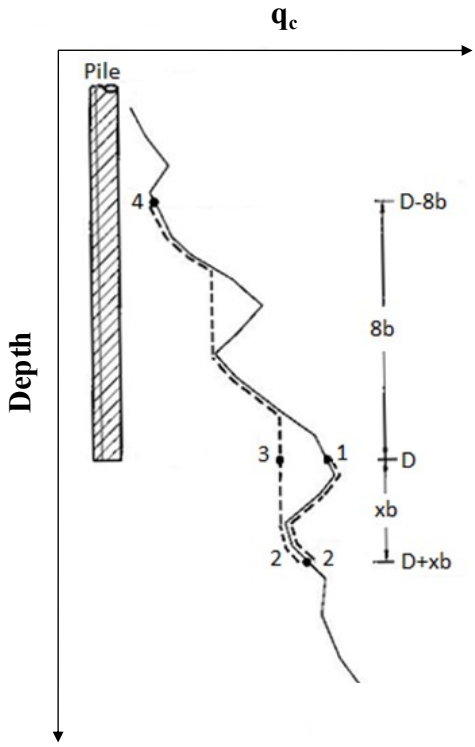

q_{c1}: Average q over a distance xb below the pile tip (path 1-2-3). Sum qc values in both the downwards (path 1-2) and the upward (path 2-3) direction. Use actual q_c values along path 1-2 and the minimum path rule along path 2-3. Compute q_{c1} for x-values from 0.7 to 3.75 below the pile tip and use the minimum q_{c1} value obtained.

q_{c2}: Average q over a distance 8b above the pile tip (path 3-4) using the minimum path rule.

D: Pile embedded length

Figure 2.14: Procedure suggested for estimating the pile end-bearing capacity by Nottingham and Schmertman (1975)

2.7.3. Pile capacity in cohesionless soils

2.7.3.1 SPT-Meyerhof Method

The SPT-Meyerhof method (Meyerhof, 1976/1981) is an empirical approach for calculating the pile capacity, based on SPT tests conducted in cohesionless soils like sands and non-plastic silts. According to the FHWA-LRFD reference manual (2007), the SPT method should be only used for preliminary estimates for pile capacity, not for final design recommendations. This is due to the non-reproducibility of SPT N-values and simplified assumptions contained in the method. Meyerhof (1976) reported different correlations and provided some limitations on shaft and tip resistance, according to pile type (displacement or non-displacement pile). The end-bearing capacity, based on the SPT-Meyerhof method for piles driven to a depth D_b in cohesionless soil, is calculated using the following:

$$q_t = \frac{40\ \bar{N}_b'.D_b}{b} \leq 400\bar{N}_b' \qquad \text{(kPa)} \qquad [2.48]$$

$$q_t = \frac{0.8\ \bar{N}_b'.D_b}{b} \leq \bar{N}_b' \qquad \text{(ksf)} \qquad [2.49]$$

where,

$\overline{N}_b'$ =Average SPT blow counts (blows/1ft) of the bearing stratum extended to 3b below pile tip and corrected for overburden pressure.

b =Pile diameter.

D_b =Pile embedment depth in the bearing stratum.

The skin friction for displacement piles (e.g., closed-end pipe piles) in cohesionless soils for the SPT-Meyerhof method is calculated using the following equations:

$$f_s = 2\overline{N}' \quad \text{(kPa)} \qquad [2.50]$$

$$f_s = \frac{\overline{N}'}{25} \quad \text{(ksf)} \qquad [2.51]$$

The skin friction for non-displacement piles (e.g., Steel H-piles) in cohesionless soils for the SPT-Meyerhof method is calculated using the following equations:

$$f_s = \overline{N}' \quad \text{(kPa)} \qquad [2.52]$$

$$f_s = \frac{\overline{N}'}{50} \quad \text{(ksf)} \qquad [2.53]$$

where,

f_s =Unit skin friction (shaft resistance) for driven pile.

$\overline{N}'$ =Average SPT blow counts along the pile and corrected for overburden pressure.

2.7.3.2 The SPT-Schmertmann Method

The SPT- Schmertmann method (Lai and Graham, 1995) is an empirical approach based on SPT N-values, applicable in sand, clay, and mixed soils. This method is conservative, as it ignores the shaft resistance when the N-value is less than 5blows/ft, as well as limiting the N-value to 60blows/ft. The correlations used for calculating the skin friction for different piles and soil types are presented in Table 2.14. It is clear from Table 2.14 that all correlations depend on the uncorrected SPT N-values. On the other hand, to calculate unit end-bearing, the following equation is used:

$$q_p = \frac{(\text{average } q_p)_{8B \text{ above desired point}} + (\text{average } q_p)_{3.5B \text{ below desired point}}}{2} \qquad [2.54]$$

where,

q_p =Weighted average tip resistance from Table 2.15.

B =Pile diameter.

The ultimate tip resistance is fully mobilized, if the actual bearing embedment length (D_A) is equal to the critical bearing embedment length (D_C). D_C is determined in Table 2.16. In the case for $D_A < D_C$, the mobilized tip resistance for H-piles is reduced. To calculate the exact reduction in tip resistance, the following equations are used:

If $D_A < D_C$ and end-bearing soil layer are stronger than the overlying layer, then:

$$q_p = q_{LC} + \frac{D_A}{D_C}(q_T - q_{LC}) \quad [2.55]$$

$$CSFBL = \frac{SFBL}{q_T}\left[q_{LC} + \frac{D_A}{2D_C}(q_T - q_{LC})\right] \quad [2.56]$$

where,

q_p =Reduced tip resistance.

q_T =Unit tip resistance at layer change.

q_{LC} =Uncorrected unit tip resistance at pile tip.

CSFBL =Reduced side resistance in bearing layer.

SFBL =Uncorrected side resistance in bearing layer.

If $D_A > D_C$ and end-bearing soil layer are stronger than the overlying layer, then:

$$CSFACD = \frac{USFACD}{q_{CD}}[q_{LC} + 0.5(q_{CD} - q_{LC})] \quad [2.57]$$

where,

CSFACD =Corrected side resistance between the top of the layer and the critical depth.

USFACD =Uncorrected side resistance from the top of the bearing layer to critical depth.

q_{CD} =Unit tip resistance at critical depth.

Table 2.14: Side resistance correlations for the SPT-Schmertmann method

Type	Soil Description	Ultimate unit shaft resistance q_p (tsf)		
		Concrete piles	Steel H-piles	Pipe piles
1	Clay	2.0N(110-N) /4006.6	2N(110-N)/5335.94	0.949+0.238lnN
2	Mixed soil	2.0N(100-N) /4583.3	-0.0227+0.033N-$(4.57610^{-1})N^2$+ 2.465(E-6*N^3)	0.243+0.147lnN
3	Sands	0.019N	0.0116N	0.058+0.152lnN
4	Limestone	0.01N	0.0076N	0.018+0.134lnN

Table 2.15: Tip resistance correlations for the SPT-Schmertmann method

Type	Soil Description	Ultimate unit tip resistance q_p (tsf)	
		Concrete and Steel H-piles	Pipe piles
1	Clay	0.7N	0.48N
2	Mixed soil	1.6N	0.96N
3	Sands	3.2N	1.312N
4	Limestone	3.6N	1.92N

Table 2.16: Critical bearing depth ratio for the SPT-Schmertmann method

Type	Soil Description	Critical depth ratio (D_c/B)
1	Clay	2
2	Mixed soil	4
3	Sands ($N \leq 12$)	6
	Sands ($N \leq 30$)	9
	Sands ($N > 30$)	12
4	Limestone	6

2.7.3.3 The Nordlund Method

The SPT-Nordlund method (Nordlund and Thurman, 1963) is a semi-empirical approach based on field observations from pile static load tests. It accounts for different pile shapes (i.e., constant diameter or tapered piles), as well as pile materials and types, including steel H-piles, closed and open end pipe piles, and timber piles. According to Hannigan et al. (2005), this method is preferred in cohesionless soils, such as sandy and gravel soils, as the pile load tests used to develop the Nordlund's design curves were conducted in sandy soils.

Moreover, the load tests were conducted for piles with diameters (widths) less than 500 mm (19.6 inch), which means the method over predicts the capacity for piles with widths larger than 500 mm (19.6 inch). A detailed pile design procedure using the Nordlund method is provided in the FHWA design and construction manual (1997). In the case of tapered piles, the total ultimate pile capacity (shaft resistance and end-bearing) for the Nordlund method is calculated using the following equation:

$$Q_u = \sum_{d=0}^{d=D} K_\delta \,.\, C_f.\, P_d.\, \frac{\sin(\delta+\omega)}{\cos\,\omega} C_d.\, \Delta d + \alpha_t \,.\, N'_q.\, A_t.\, P_t \quad . \qquad [2.58]$$

In the case of piles with uniform cross sections, the capacity is calculated as follows:

$$Q_u = K_\delta.\, C_f.\, P_d.\, \sin\delta \,.\, C_d.\, D + \alpha_t \,.\, N'_q.\, A_t.\, P_t \qquad [2.59]$$

The previous equation can also be written as:

$$Q_u = K_\delta.\, C_f.\, P_d.\, \sin\delta \,.\, C_d.\, D + q_L \,.\, A_t \qquad [2.60]$$

where,

d =Depth.
D =Embedded pile length.
K_δ =Coefficient of lateral earth pressure at depth d (Tables 2.17 and 2.18).
C_f =Correction factor for K_δ when $\delta \neq \phi$ (use Figure 2.15).
P_d =Effective overburden pressure at the center of depth increment d.
δ =Friction angle between soil and pile.
ω =Angle of pile taper from vertical.
C_d =Pile perimeter at depth d.
Δd =Length of pile segment.
α_t =Factor depending on the pile slenderness ratio (use Figure 2.16).
N'_q =Bearing capacity factor (use Figure 2.17).
A_t =Pile toe area.
P_t =Effective overburden pressure at pile toe $\leq$ 150 kPa (3.2 ksf).
q_L =Limiting unit tip resistance (use Figure 2.18).

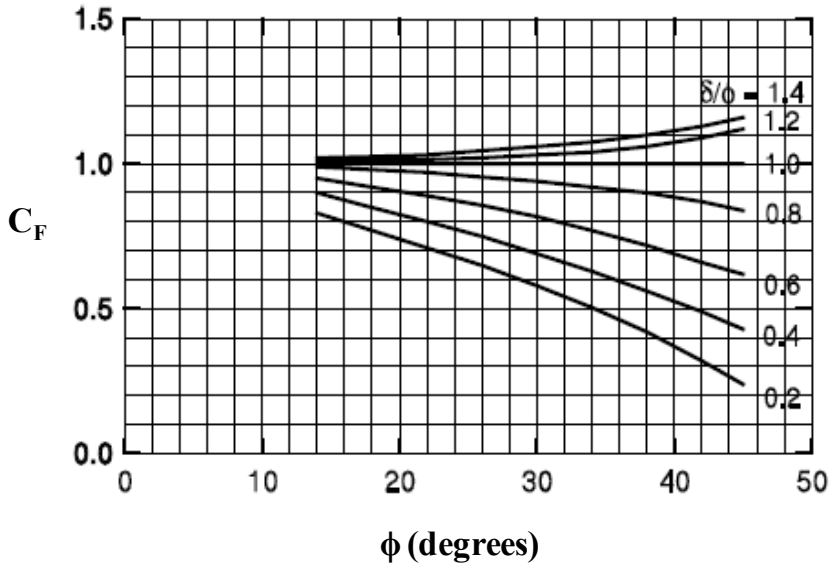

Figure 2.15: Correction factor C_F for K_δ when $\delta \neq \phi$ (after Nordlund, 1979)

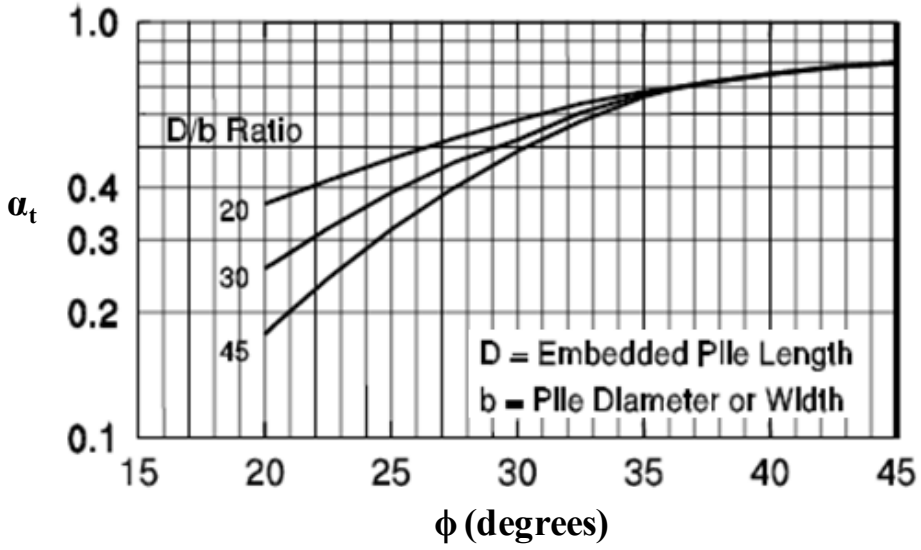

Figure 2.16: Chart for estimating the α_t coefficient from ϕ (after Nordlund, 1979)

Table 2.17: K_δ for piles when $\omega = 0^o$ and V= 0.0093 to 0.093 m^3/m

ϕ	Displaced Volume (V), m^3/m									
	0.01	**0.02**	**0.03**	**0.04**	**0.05**	**0.06**	**0.07**	**0.07**	**0.08**	**0.09**
25	0.70	0.75	0.77	0.79	0.80	0.82	0.83	0.84	0.84	0.85
26	0.73	0.78	0.82	0.84	0.86	0.87	0.88	0.89	0.90	0.91
27	0.76	0.82	0.86	0.89	0.91	0.92	0.94	0.95	0.96	0.97
28	0.79	0.86	0.90	0.93	0.96	0.98	0.99	1.01	1.02	1.03
29	0.82	0.90	0.95	0.98	1.01	1.03	1.05	1.06	1.08	1.09
30	0.85	0.94	0.99	1.03	1.06	1.08	1.10	1.12	1.14	1.15
31	0.91	1.02	1.08	1.13	1.16	1.19	1.21	1.24	1.25	1.27
32	0.97	1.10	1.17	1.22	1.26	1.30	1.32	1.35	1.37	1.39
33	1.03	1.17	1.26	1.32	1.37	1.40	1.44	1.46	1.49	1.51
34	1.09	1.25	1.35	1.42	1.47	1.51	1.55	1.58	1.61	1.63
35	1.15	1.33	1.44	1.51	1.57	1.62	1.66	1.69	1.72	1.75
36	1.26	1.48	1.61	1.71	1.78	1.84	1.89	1.93	1.97	2.00
37	1.37	1.63	1.79	1.90	1.99	2.05	2.11	2.16	2.21	2.25
38	1.48	1.79	1.97	2.09	2.19	2.27	2.34	2.40	2.45	2.50
39	1.59	1.94	2.14	2.29	2.40	2.49	2.57	2.64	2.70	2.75

Table 2.18: K_δ for piles when $\omega = 0^o$ and V= 0.093 to 0.93m^3/m

ϕ	Displaced Volume (V), m^3/m									
	0.093	**0.186**	**0.279**	**0.372**	**0.465**	**0.558**	**0.651**	**0.744**	**0.837**	**0.93**
25	0.85	0.9	0.92	0.94	0.95	0.97	0.98	0.99	0.99	1
26	0.91	0.96	1	1.02	1.04	1.05	1.06	1.07	1.08	1.09
27	0.97	1.03	1.07	1.1	1.12	1.13	1.15	1.16	1.17	1.18
28	1.03	1.1	1.14	1.17	1.2	1.22	1.23	1.25	1.26	1.27
29	1.09	1.17	1.22	1.25	1.28	1.3	1.32	1.33	1.35	1.36
30	1.15	1.24	1.29	1.33	1.36	1.38	1.4	1.42	1.44	1.45
31	1.27	1.38	1.44	1.49	1.52	1.55	1.57	1.6	1.61	1.63
32	1.39	1.52	1.59	1.64	1.68	1.72	1.74	1.77	1.79	1.81
33	1.51	1.65	1.74	1.8	1.85	1.88	1.92	1.94	1.97	1.99
34	1.63	1.79	1.89	1.96	2.01	2.05	2.09	2.12	2.15	2.17
35	1.75	1.93	2.04	2.11	2.17	2.22	2.26	2.29	2.32	2.35
36	2	2.22	2.35	2.45	2.52	2.58	2.63	2.67	2.71	2.74
37	2.25	2.51	2.67	2.78	2.87	2.93	2.99	3.04	3.09	3.13
38	2.5	2.81	2.99	3.11	3.11	3.29	3.36	3.42	3.47	3.52
39	2.75	3.1	3.3	3.45	3.45	3.65	3.73	2.8	3.86	3.91

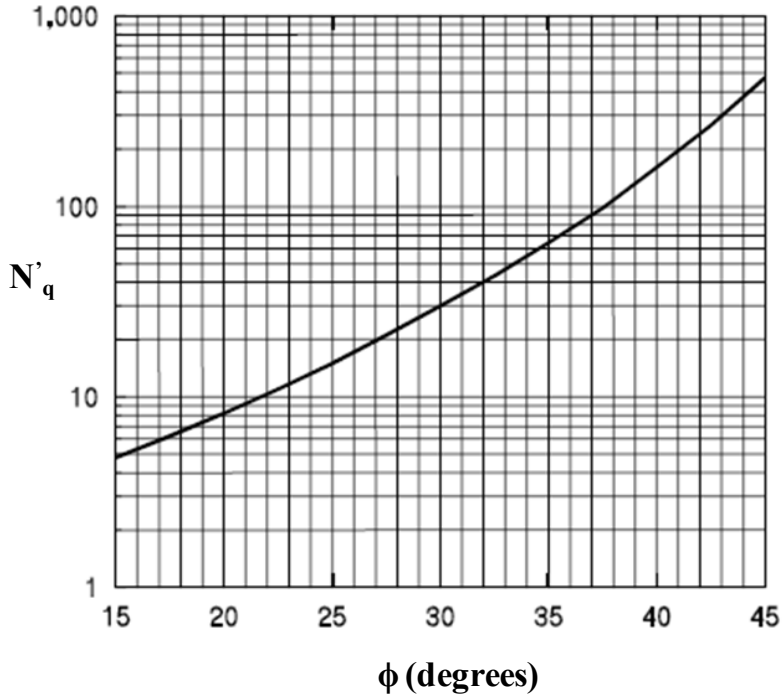

Figure 2.17: Chart for estimating the N'_q coefficient from ϕ (after Bowles, 1977)

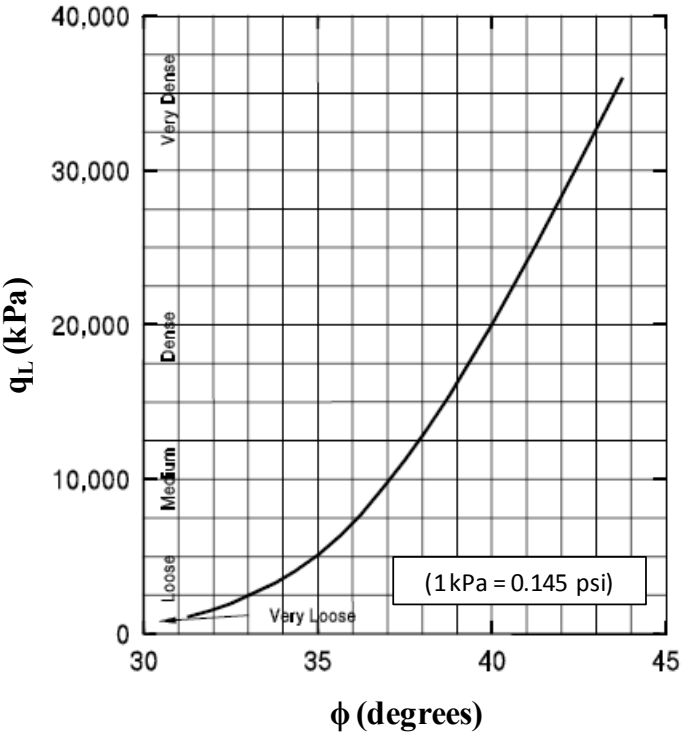

Figure 2.18: Relationship between the toe resistance and ϕ in sand by Meyerhof (1976)

2.7.4. Iowa Bluebook method

The Iowa Foundation soils information chart for pile design (or Iowa Bluebook) was developed in 1989 by Dirks and Kam and revised in 1994. The Bluebook (BB) enables the design engineer to calculate pile skin friction as well as end-bearing, separately. A combination of the SPT-Meyerhof method (Meyerhof, 1976/1981) and α-Tomlinson method (Tomlinson, 1980) were used to develop the pile skin friction design charts for different soil types. On the other hand, wave equation concepts were used to develop the end-bearing charts. The BB was calibrated to more than 280 pile load tests, which have been performed in the state of Iowa since 1968. The BB design chart accounted for different pile materials and geometry. Practically, the only soil parameter required during the pile design using the BB is the SPT corrected N-values; hence, it is considered a simple method. The BB has proven to provide relatively consistent pile designs compared to other complex static analysis methods. The major limitation of the BB is including an embedded factor of safety equal to 2.0, which makes it relatively conservative to other design methods and violates the basic principles of the LRFD approach.

2.7.5. DRIVEN computer program

The DRIVEN computer program was developed by the FHWA in 1998 for calculating pile capacity. This program calculates the capacity of open and closed end pipe piles, steel H-piles, concrete piles, and other pile types. From the DRIVEN user manual by Mathias and Cribbs (1998), the user inputs the soil layer unit weights and strength parameters, including the percentage strength loss during driving. After selecting the pile type, the program calculates pile capacity versus depth for cohesive and cohesionless soils. The methods used for calculating pile capacity in the DRIVEN program are Nordlund method and α-method (previously described in this chapter) for cohesionless and cohesive layers, respectively. Several analysis options are included, as the program automatically subtracts the resistance of unsuitable soil layers and the contribution from scourable soils from the ultimate pile capacity. Using DRIVEN, the capacity can be calculated at the EOD as well as BOR with options that account for pile plugging. This program provides a compatible output data file with the WEAP program to facilitate running drivability studies.

2.7.6. SPT-97

SPT-97 is a windows-based computer program developed by FDOT and the University of Florida. It calculates pile capacity, based on the SPT-Schmertmann method (Lai and Graham, 1995) described earlier in this chapter. This method was used in the NCHRP Report 507 (Paikowsky et al., 2004) in LRFD resistance factor calibration. According to Paikowsky et al. (2004), this computer program proved to provide reasonable results, except for the two following cases: 1) there is a problem in correcting pile resistance, when $D_c < D_a$ (critical bearing depth is smaller than actual), this problem might occur for Iowa soils, due to the relatively low D_c (because the main geological formation in the state is glacial clay with low SPT N-values); and 2) the capacity is incorrectly computed for pipe piles. This program is available online for geotechnical engineers at the FDOT official website.

2.7.7. Comparison of different static methods

It is important to compare and select the right static analysis method for a specific design problem. This should be based on soil and pile types, as well as the extent of available soil parameters and the degree of accuracy needed from the design. Table 2.19 summarizes the most commonly used static analysis methods and provides a brief description of the approach used to derive each method, the recommended soil type, design parameters, and in-situ tests needed, as well as the advantages and limitations corresponding to different methods. Table 2.20 summarizes the required equations for calculating the shaft and tip resistances, using different static analysis methods, and clearly indicates the appropriate soil type recommended for each method, as well as the required soil parameters or in-situ tests required for the analysis.

Table 2.19: Comparison of the commonly used static analysis methods for calculating pile capacity

Method	Approach	Recommended soil type	Design Parameters needed	Advantages	Limitations
SPT	Empirical	Cohesionless soils (i.e., sand)	Results from SPT test (i.e., N-blow counts).	Uses the common SPT test. Simple method to use.	The SPT test is not a reliable test compared to other lab and/or in-situ tests.
Nord-lund	Semi-empirical	Cohesionless soils (i.e., sand and gravel)	Charts by Nordlund and Thurman (1979).	It accounts for pile shape, pile material, and type.	ϕ is calculated using the SPT test. The method over-predicts the capacity for piles with widths larger than 600 mm.
α-method	Semi-empirical	Cohesive soils (i.e., clay)	Total stress soil parameters are needed.	Widely used method, which gives reasonable results for displacement and non-displacement piles.	There are several relations for the α-factor, which give large scatter.
β-method	Semi-empirical	Cohesive and Cohesionless soils (i.e., clay, silt, sand or gravel)	Effective stresses calculated from the vertical effective overburden stress.	The method was developed to model the long-term drainage shear strength. It can be used for different soil types and for layered profiles.	The method tends to overestimate the pile capacity for heavily overconsolidated soils.
CPT	Empirical	Cohesive and Cohesionless soils (i.e., clay, silt and sands)	Results of CPT test (sleeve friction and cone tip resistance).	CPT is an accurate test. The CPT method is satisfactory, especially for driven piles. It can be used in layered soils.	CPT test is considered to be an expensive test.

Table 2.20: Summary of the equations required for different static methods

Soil Type	Method	Shaft Resistance	Tip Resistance	Required Soil Parameters
Cohesive	α-API (API-1974)	$f_s = \alpha \, . \, S_u$	If: $S_u \leq 25$ kPa $q_t = 6.5 \, S_u$ If: $25 < S_u < 100$ kPa $q_t = 8.0 \, S_u$ If: $S_u \geq 100$ kPa $q_t = 9.0 \, S_u$	S_u (undrained shear strength)
	α-Tomlinson (Tomlinson, 1980)			S_u; D_b (pile embedment)
	λ- Method (US Army Corps of Engineers, 1992)	$f_s = \lambda(\sigma_v' + 2S_u)$		S_u; γ (soil unit weight)
Cohesive/ Cohesion-less	β-Method (Burland, 1973)	$f_s = \beta \, . \, \overline{P}_o$	$q_t = N_t \, . \, P_t$	ϕ; γ
	CPT-Method (Nottingham and Schmertmann, 1975)	$f_s = K\left[\frac{1}{2}\,(\bar{f}_s \, A_s)_{0 \text{ to } 8b} + (\bar{f}_s \, A_s)_{8b \text{ to } D}\right]$	$q_t = \frac{q_{c1} + q_{c2}}{2}$	CPT; D_b
Cohesion-less	SPT-Meyerhof Method (Meyerhof, 1976/1981)	$f_s = \frac{\overline{N}'}{25}$ (ksf)	$q_t = \frac{0.8 \, \overline{N}_b' \, . \, D_b}{b} \leq \overline{N}_b'$ (ksf)	SPT; D_b
	SPT-Schmertmann Method (Lai and Graham, 1995)	$f_s = f(N)$ (see section 2.7.3.2)	$q_t = f(N)$	SPT
	Nordlund Method (Nordlund and Thurman, 1963)	$q_{total} = K_\delta . C_f . P_d . \sin\delta \, . C_d . D + \alpha_t \, . N_q' . A_t . P_t$		ϕ; γ; D_b
In-house for cohesive/ cohesion-less	Iowa Bluebook Method (Dirks and Kam, 1989)	Use the revised design charts for different soil and pile types		SPT

2.8. Pile Static Load Test

Static Load Tests (SLTs) accurately measure the actual behavior of pile foundations in the field when subjected to axial vertical compressive loading and characterize the load-settlement relationship at the pile head. Load testing is the most definitive method of determining the nominal capacity of a pile, which provides valuable information to the design engineer and is recommended for design verification purposes. SLTs can also assist in calibrating sophisticated design models, such as finite element models, ensuring these models provide safe results, and eliminating excess conservatism. In difficult soil and bedrock conditions, the SLT results are the only means of identifying the actual pile capacity. SLTs can also help generating databases for advanced research.

2.8.1. SLT methods and procedures

There are several SLT methods, procedures, and equipment used for routine pile testing and proof-testing purposes described in the ASTM D-1143 standards (ASTM, 2007). Among the different methods are the Slow Maintained Testing Method (SM) and the Quick Maintained Testing Method (QM). According to the *Canadian Foundation Engineering Manual* (1985), the ST method is time consuming and can lead to complex SLT data evaluation and interpretation. Also, the SM test could affect the pile true load movement behavior during testing. Conversely, the QM test is faster, more efficient in determining the pile capacity, and provides accurate results. Therefore, this method is preferable to the SM method.

Acceptance of the pile SLT is generally governed by building codes reviewed by structural and geotechnical engineers. The structural engineer determines the maximum deflection that a structure can sustain without losing its function, while the geotechnical engineer determines the pile bearing capacity and limits the soil-pile resistance to a certain extent, such that the deformations do not exceed the plastic behavior. There are several methods for determining the ultimate pile capacity from a SLT, which can be called the SLT acceptance criteria. The commonly used acceptance criteria are briefly described in the following sections.

2.8.2. Acceptance criteria

As previously described, the static load test is the most accurate test that represents the actual response of the piles. Hence, it is vital to select a suitable method of determining the pile nominal (maximum non-factored) capacity from the load-displacement curve. There are several methods for determining the nominal pile capacity from a SLT. These methods have advantages, limitations, and applications, which should be addressed. Some of these methods are represented in this section because they are the most commonly used, according to design codes.

2.8.2.1 Davisson's Method

The Davisson's criterion (Davisson, 1972) is one of the most popular methods and seems to work best with data from the QM test (Coduto, 2001). The criterion is applied by drawing a parallel line to the elastic compression line (base line) offset by a specified amount of displacement, depending on the pile size. This parallel line is then called the Davisson line. As can be seen in Figure 2.19, the point of intersection between the Davisson line and the load displacement curve is considered the pile nominal capacity. Equation [2.61] is used to plot the base line on the load-displacement curve:

$$\Delta = \frac{Q_{va} \cdot L}{AE} \qquad [2.61]$$

where,

Δ =Elastic movement of base line.

Q_{va} =Applied load.

A =Cross sectional area of pile.

E =Modulus of elasticity of pile material.

L =Embedded length of pile.

To draw the Davisson line parallel to the base line, the following expression is used:

$$X = 0.15 + \frac{D}{120} \qquad [2.62]$$

where,

X =Offsite displacement from the base line (inch).

D =Pile diameter (inch).

Davisson' criterion was originally recommended for different types of driven piles (Prakash et al., 1990). In the NCHRP report-507 by Paikowsky et al. (2004), different methods of determining the pile capacity from the load-displacement curve were used and compared with the static-cyclic capacity of 75 piles. Paikowsky et al. (2004) indicted that the distribution of the ratio between the capacities determined using Davisson's criterion and the static-cyclic test yielded the closest mean to unity and the least standard deviation compared to the distributions using other determination methods. Thus, the Davisson criterion was the only method that was selected to determining the pile nominal capacity from the load-displacement curve in the NCHRP report-507. One of the main advantages of Davisson's criterion is being an objective method that can be used as an acceptance criterion for the static load test, as the Davisson parallel line can be predicted even before starting the test. However, Hannigan et al. (2005) indicated that this method has some limitations, as it under-predicts pile capacity for piles with diameters larger than 24 inches. Table 2.21 provides a comparison between Davisson's method and other determination methods, presenting the appropriate pile types for each method, the recommended static load test type, advantages, limitations, and applicability.

2.8.2.2 Shape of Curvature Method

As shown in Figure 2.20, the nominal pile capacity in the shape of the curvature method (Butler and Hoy, 1977) can be defined as the point of intersection between the elastic compression line and the line tangent to the plastic portion of the load-displacement curve. According to Prakash et al. (1990), this method is applicable for QM tests. The disadvantage of this method is that it penalizes long piles because they will have larger elastic movements; hence, it underestimates the capacity of longer piles. Table 2.21 provides a comparison between the shape of curvature method and other determination methods.

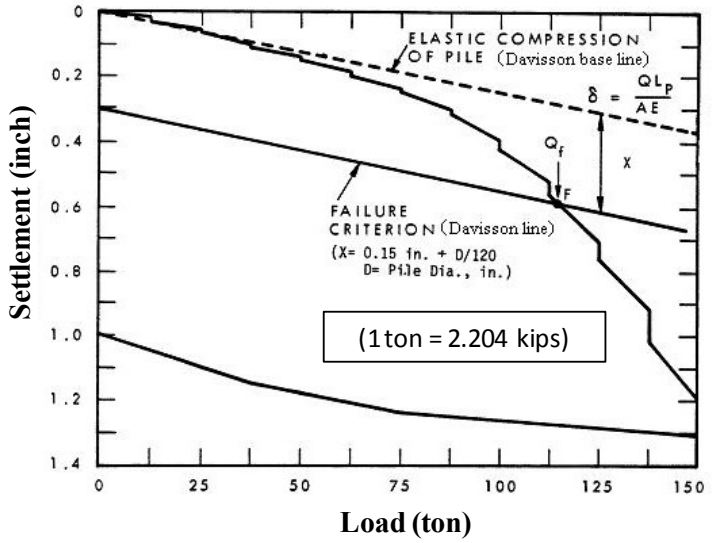

Figure 2.19: Determining the pile capacity using Davisson's method

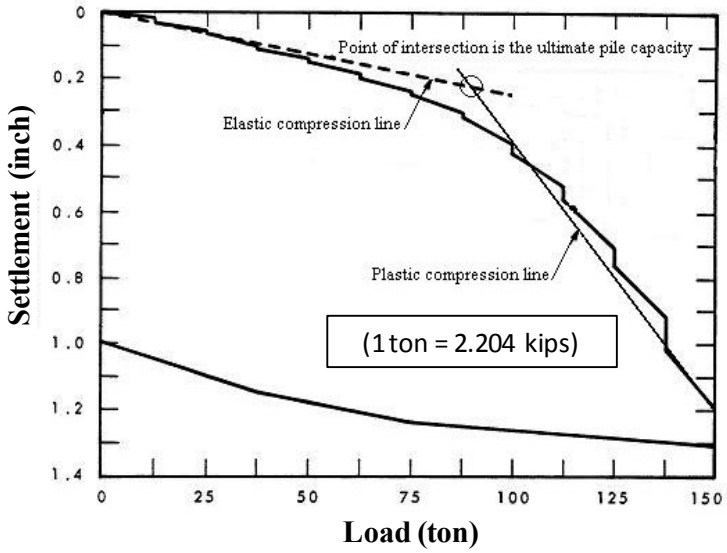

Figure 2.20: Determining the pile capacity using the shape of curvature

2.8.2.3 Limited Total Settlement Method

The pile capacity can be limited at a point where the settlement of the pile is the smallest of 0.1 times the pile diameter or 1 inch. This method is an objective method. It could be used as an acceptance criterion for the static load test, as the limited total settlement line can be predicted even before starting the test. Also, this method is simple and does not require any sophisticated equations. However, the method is not suitable for long piles, as elastic settlement exceeds the limit without inducing plastic deformations. Additionally, the

pile may fail before reaching the settlement limit of the method. Figure 2.21 provides an example of using the limited total settlement method. Table 2.21 provides a comparison between the limited settlement method and other methods.

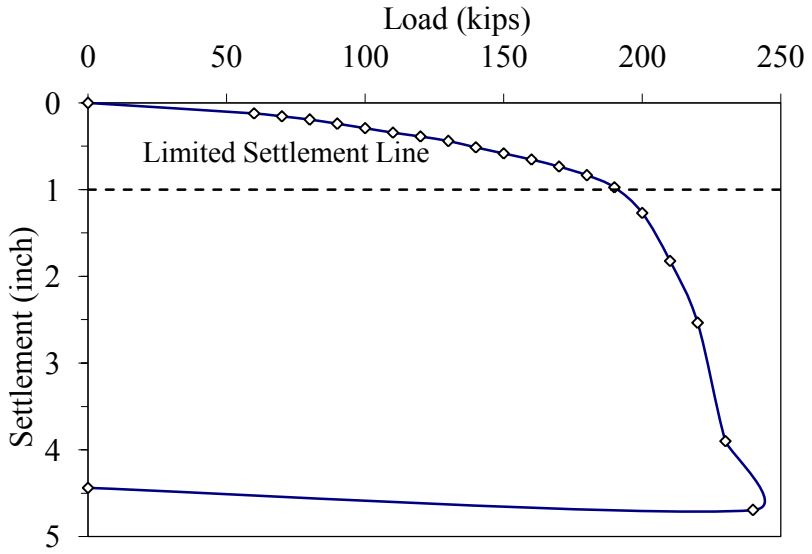

Figure 2.21: Determining the pile capacity using the limited total displacement

2.8.2.4 De Beer's Method

In the De Beer's Method (adapted from Bowles, 1996), the load test data is plotted in a log-log scale, at which the intersection between the two straight portions of the graph will be equal to De Beer's capacity as shown in Figure 2.22. This method was originally proposed for SM tests (Prakash et al., 1990). One of the most common problems with this method is the two straight portions in the graph cannot be clearly determined. Table 2.21 provides a comparison between De Beer's method and other determination methods.

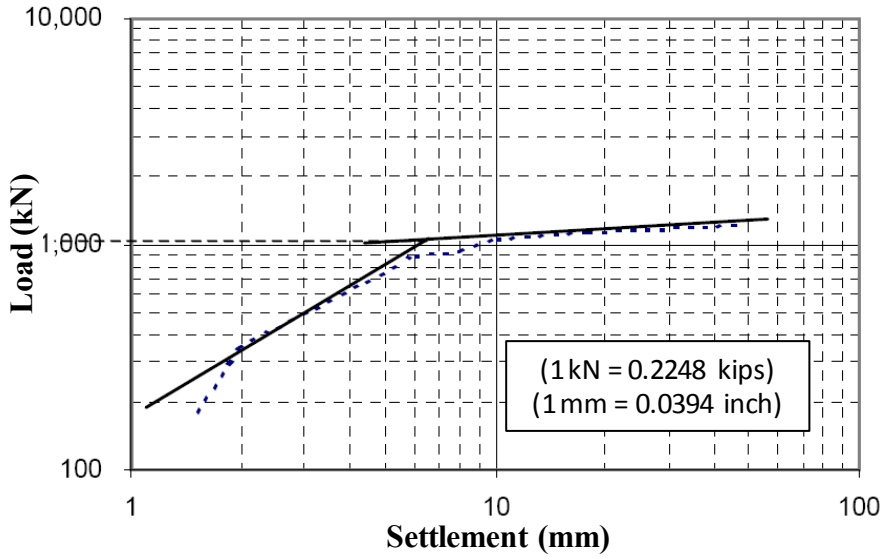

Figure 2.22: An Example of determining the pile capacity using De Beer's method

2.8.2.5 Chin's Method

In Chin's method (Chin 1970/1971) shown in Figure 2.23, a straight line between Δ/Q_{va} and Δ is plotted where Δ is the displacement and Q_{va} is the corresponding load. Then, the Q_{ult} is equal to $1/C_1$, where C_1 is explained in the figure. Chin's method was developed for both QM and SM tests. However, it has several disadvantages. It assumes the load-moment curve is approximately hyperbolic. Also, Chin's method requires constant time increments used when conducting the SLT. Moreover, a problem could occur while selecting the straight line passing through the points shown in the figure, as sometimes the points do not appear to fall in a straight line. This could occur unless the test has passed Davisson's failure criterion. According to Prakash et al. (1990), this method may not provide good results for static load tests performed according to the ASTM standards, as the tests may not have exactly constant time load increments.

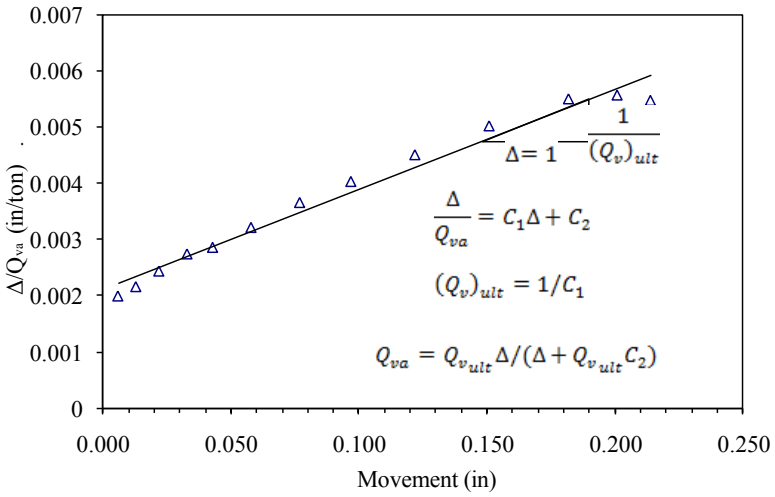

Figure 2.23: Determining the capacity using Chin's method (after Prakash et al., 1990)

2.8.2.6 Iowa DOT Method

The Iowa Foundation Pile Design Chart (Dirks and Kam, 1989) was developed, based on determining the pile actual failure load, using the Louisiana method. The Louisiana method is defined as the intersection between the tangent of the linear portion of the load-displacement curve and a line with a slope of 0.05 inches per ton at the yield point. The yield point is defined as the intersection between the load-displacement curve and a parallel line to the recovery line at 0.25 inches settlement. This method was essentially adapted for Louisiana soils and is not frequently used in general geotechnical practices. Moreover, the method is relatively sophisticated and not recommended by any design codes for the LRFD calibration. On the other hand, Davisson's criterion is an uncomplicated method that has proven to perform better in the case of driven steel H-piles and was recommended for a consistent LRFD calibration framework by AASHTO and NCHRP.

Table 2.21: Comparison between pile ultimate capacity determination methods including appropriate pile types for each method, recommended static load test type, advantages, limitations, and applicability for each method

Method	Recommended pile types	SLT[(1)] type	Advantages	Limitations	Comments
Shape of Curvature (Fuller and Hoy, 1977)	Bored, belled, and small diameter driven concrete piles as well as Franki piles.	QM[(2)] test	It yields failure loads near to actual test failure loads.	It is a subjective method; hence, results could greatly vary from one to other.	Easy method. It is a conservative method not suitable for long piles.
Davisson's (1972)	Driven piles as well as Franki piles.	QM test	An objective method, which can be used as a SLT acceptance.	For piles with diameters more than 24 inches, this method under-predicts the capacity.	Easy method. A conservative method (recommended by specifications).
Chin's (1970-1971)	N/A	QM and SM[(3)] tests	N/A	Constant time load increments required for accuracy. Also, assumes hyperbolic load-settlement relation. Gives failure loads higher than that of actual test failure loads.	Easy method. Loads must be higher than those of Davisson's acceptance load.
De Beer's (1967-1972)	N/A	SM tests	N/A	Subjective method.	Moderate method. Drawn on log scale.
Hansen's 90 (1963)	Small diameter driven concrete piles.	CRP[(4)] tests	N/A	Trial and error.	Moderate method
Hansen's 80 (1963)	N/A	QM and SM tests	Criteria agree well with plunging failure.	Not suitable for tests that include unloading cycles or unachieved plunging.	Moderate method. Assumes that the load-displacement curve is parabolic.
Limited Total Settlement	N/A	N/A	Objective method	Not suitable for long piles. as elastic settlement exceeds limit without inducing plastic deformations.	Easy method. Pile may fail before reaching settlement limit of the method.

[(1)] Static load test type; [(2)] QM: Quick Maintained test2; [(3)] SM: Slow Maintained test; and [(4)] CRP: Constant Rate of Penetration Test.

2.9. References

AASHTO LRFD Bridge and Construction Specifications (1994). Washington, DC.

AASHTO LRFD Bridge Design Specifications (2004). Washington, DC

AASHTO LRFD Bridge Design Specifications (2006). Washington, D.C.

AASHTO LRFD Bridge Design Specifications (2007). Customary U.S. Units, 4th edition (2008 Interim), American Association of State Highway Transportation Officials, Washington, D.C.

AbdelSalam, S. S., Sritharan, S., and Suleiman, M. T. (2008). "Current design and construction practices of bridge pile foundations." *Proceeding: The International Foundations Congress and Equipment Expo*, March 2009, Orlando, Florida.

Abu-Hejleh, N., DiMaggio, J., and Kramer, W. (2009). "AASHTO Load and Resistance Factor Design Axial Design of Driven Pile at Strength Limit State." *Transportation Research Board 88th Annual Meeting*, 2009, Paper #09-1034, Washington DC.

Allen, T. M., Nowak, A. S., and Bathurst, R. J. (2005). "Calibration to Determine Load and Resistance Factors for Geotechnical and Structural Design." *Transportation Research Circular Number E-C079*, TRB, Washington, DC, 83p.

Allen, T. M. (2005). "Development of the WSDOT Pile Driving Formula and Its Calibration and Resistance Factor Design (LRFD)." *FHWA Report, WA-RD 610.1*, Washington State Department of Transportation.

American Concrete Institute (1974). "Recommendations for Timber Piles Design, Manufacture and Installation of Concrete Piles," *ACI Report No. 543R-74*.

Argo, D. E. (1987). "Dynamic Formulas to Predict Driven Pile Capacity." Department of Civil and Environmental Engineering, Washington State University, Pullman, WA.

ASTM D1143 (2007). "Standard Test Methods for Deep Foundations under Static Axial Compressive Load." *American Society for Testing and Materials, ASTM*, Philadelphia, PA.

Baecher, G. (2001). "Contribution to a progress research report as part of Project NCHRP 24-17, LRFD Deep Foundations Design." unpublished document.

Barker, R., Duncan, J., Rojiani, K., Ooi, P., Tan, C., and Kim, S. (1991). "NCHRP Report 343: Manuals for the Design of Bridge Foundations." *TRB, National Research*

Council, Washington, D.C.

Becker, D. E. and Devata, M. (2005). "Implementation and Application Issues of Load and Resistance Factor Design (LRFD) for Deep Foundations." *ASCE Conf. Proc. 156, 1 (2005)*, DOI:10.1061/40777(156)1

Becker, D. E. (1996). "Eighteenth Canadian Geotechnical Colloquium: Limit States Design for Foundations, Part I: An overview of the foundation design process." *Canadian Geotechnical Journal*, Vol. 33, No. 6, December, pp. 956–983.

Belcher, D. J., and Flint, R. F. (1946). "Soil deposits map of United States and Canada." *Geological Society of America*, Washington, D.C.

Bowles, J. (1977/1996). "Foundation Analysis and Design." McGraw-Hill, New York.

Broms, B. (1964). "Lateral Resistance of Piles in Cohesive Soils." *Journal of the Soil Mechanics and Foundations Division*, ASCE, Vol. SM2, March, pp. 27–63.

Burland, J. B., (1973). "Shaft Friction of Piles in Clay." Ground Engineering, London, Vol.6., No.3, pp.3042.

Butler, H. D., and Hoy, H. E. (1977). "Users Manual for the Texas Quick-Load Method for Foundation Load Testing." *FHWA-IP- 77-8, FHWA*, Office of Development, Washington, DC.

Canadian Foundation Engineering Manual, (1985). "Second Edition, Part 3: Deep Foundations." *Canadian Geotechnical Society*, BiTech Publishers, Vancouver.

Chang, N. Y. (2006). "CDOT Foundation Design Practice and LRFD Strategic Plan." *Colorado DOT Research Branch*, Report No. CDOT-DTD-R-2006-7.

Chellis, R. D. (1949). "The Relationship Between Pile Formulas and Load Tests." ASCE: *American Society of Civil Engineers*, Transactions 114:290-320.

Cheney, R. S. and Chassie, R. G. (1993). "Soils and Foundations Workshop Manual." *FHWA Report No. FHWA-HI-88-009*.

Chin, F. V. (1970). ''Estimation of the Ultimate Load of Piles Not Carried to Failure.'' *Proceeding: The 2nd Southeast Asian Conference on Soil Engineering*, pp. 81–90.

Coduto, D. P. (2001). "Foundation design: principles and practices." Prentice-Hall Inc., Englewood Cliffs, N.J.

Cummings, A. E. (1940). "Dynamic Pile Driving Formulas." *Journal of the Boston Society of*

Civil Engineers, No. 27:6-27.

Davisson, M. (1972). "High Capacity Piles." *Proceeding: Soil Mechanics Lecture Series on Innovations in Foundation Construction*, ASCE, IL Section, Chicago, IL, pp. 81–112.

DiMaggio, J., Saad, T., Allen, T., Barry, R., Al Dimillio, Goble, G., Passe, P., Shike, T., and Person, G. (1999). "FHWA International Technology Exchange Program." *FHWA Report Number FHWA-PL-99-013*.

Dirks, K. and Kam P. (2003). "Foundation Soils Information Chart – Pile Foundation*." Iowa Department of Transportation*, Office of Road Design, Ames, Iowa, United States.

Ellingwood, B., Galambos, T. V., Macgregor, J. G., and Cornell, C. A. (1980). "Development of a Probability Based Load Criterion for American National Standard A58 - Building code requirements for minimum design loads in buildings and other structures." *National Bureau of Standards*, Washington, D.C.

Esrig, M. I., and Kirby, R. C. (1979). "Soil Capacity for Supporting Deep Foundation Members in Clay." *ASTM*, STP. No. 670, pp. 27–63.

Fellenius, B. H., (1991). "Summary of Pile Capacity Predictions and Comparison with Observed Behavior." ASCE: American Society of Civil Engineers, ASCE, *Journal of Geotechnical Engineering*, Vol. 117, No. 1, pp. 192 - 195.

FHWA (1997). "Design and Construction of Driven Pile Foundations." *Workshop manual*, Volumes I, publication FHWA-HI-97-013.

FHWA (2007). "Load and Resistance Factor Design (LRFD) for Highway Bridge Superstructures." *FHWA Publication number*: FHWA-NHI-07-034

Foye, K. C., Abou-Jaoude, G., Prezzi, M., and Salgado, R. (2009). "Resistance Factors in Load and Resistance Factor Design of Driven Pipe Piles in Sand." *Journal of Geotechnical and Geoenvironmental Engineering,* ASCE, v 135, n 1, 2009, p 1-13.

Fragaszy, Richard J., Douglas E., Argo, and Higgins, J. D. (1989). "Comparison of Formula Predictions with Pile Load Tests." Transportation Research Record: *Journal of the Transportation Research Board,* TRR 1219:1-12.

Gates, M. (1957). "Empirical Formula for Predicting Pile Bearing Capacity." *Civil Engineering*, 65-66.

Gibbs, H. J. and Holtz, W. G. (1957). "Research on Determining the Density of Sands by

Spoon Penetration Testing." *Proc. of the 4th Int. conference of Soil Mechanics and Foundation Engineering*, London 1,35-39.

Green, R. (1994). "LRFD Code for Ontario Bridge Substructures." *Transportation Research Record*, ISSN 0361-1981, 1994, no1447, pp. 73-79.

GRL, Inc. (1999). "Pile-Driving Analyzer, PAK Users Manual." Goble, Rausche, Likins and Associates, 1999.

Gulhati, Sahashi, K., and Manoj, D. (2005). "Geotechnical Engineering." New Delhi, Haryana India: Tata McGraw-Hill Publishing Company Limited.

Hannigan, P. J., Goble, G. G., Thendean, G., Likins, G. E., and Rausche, F. (2005). "Design and Construction of Driven Pile Foundations." Vol. I and II, *Federal Highway Administration Report No. FHWA-HI-05*, Federal Highway Administration, Washington, D.C.

Hannigan, P. J., Goble, G. G., Thendean, G., Likins, G. E., and Rausche, F. (1998). "Design and Construction of Driven Pile Foundations." Volumes I and II, *FHWA-HI-97-013. National Highway Institute*, Federal Highway Administration, U.S. Department of Transportation, Washington, D.C. in Geotechnical Load and Resistance Factor Design." Journal of Geotechnical and Geoenvironmental Eng., Vol. 129, No. 4, April 2003, pp. 287-295.

Hansen, J. B. (1963). "Hyperbolic Stress-strain Response: Cohesive Soils," *Discussion Journal of the Soil Mechanics and Foundations Division*, American Society of Civil Engineers, New York, NY, Vol. 89, No. SM4.

Hara, A., Ohta, T., Niwa, M., Tanaka, S., and Banno, T. (1974). "Shear Modulus and Shear Strength of Cohesive Soils." *Soils and Foundations*, Vol. 14, No. 3, Sept. 1974.

Iowa DOT (2008). "Standard Specifications with GS-01014 Revisions." *Iowa DOT Electronic Reference Library*, http://www.erl.dot.state.ia.us/Apr_2008/GS/frame.htm.

Iowa DOT LRFD Design Manual (2009). "Office Policies and Procedures, Office of Bridges and Structures." *Iowa DOT Electronic Reference Library.*

Jardine R. J, Chow, F. C, Overy, R., and Standing, J. (2005). "ICP Design Methods for Driven Piles in Sands and Clays." Publishers Thomas Telford Inc.

Kerkhoff, G. O., Oehler, L. T., and Housel, W. S. (1965). "A Performance Investigation of

Pile Driving Hammers and Piles." Lansing, Michigan State Highway Commission.

Kulhawy, F., and Phoon, K. (1996). "Engineering Judgment in the Evolution from Deterministic to Reliability-Based Foundation Design." *Proceeding: The 1996 Conference on Uncertainty in the Geologic Environment, UNCERTAINTY'96*. Part 1 (of 2), July 31–Aug. 31, Madison, WI, ASCE, NY, pp. 29–48.

Kulhawy, F. H. and Mayne, P. W., (1990). "Manual on Estimating Soil Properties for Foundation Design." *Report. EL-6800*, Electric Power Research Ins., Palo Alto.

Kuo, C. L., McVay, M. C., and M., Birgisson, B. (2002). "Calibration of Load and Resistance Factor Design: Resistance factors for drilled shaft design." *Transportation Research Record ISSN 0361-1981*, 2002, no 1808, pp. 108-111.

Kyung, K. J., Gabr, M. A., and Shamimur, M. R. (2002). "Development of Resistance Factors for Axial Capacity of Driven Piles in North Carolina." PhD Dissertation, North Carolina State University, Raleigh, North Carolina, October, 2002.

Lai, P., and Graham, K. (1995). "Static Pile Bearing Analysis Program." *SPT94:* http://www.dot.state.fl.us/structures/manuals/spt94.zip.

Lai, P., McVay, M., Bloomquist, D., and Badri, D. (2008). "Axial Pile Capacity of Large Diameter Cylinder Piles." *Proceeding: From Research to Practice in Geotechnical Engineering Congress*, 2008.

Mathias D., and M. Cribbs (1998). "DRIVEN 1.0: A Microsoft Windows Based Program for Determining Ultimate Static Pile Capacity." *Federal Highway Administration*.

McVay, M., Birgisson, B., Zhang, L., Perez., A, and Putcha, S. (2000). "Load and Resistance Factor Design (LRFD) for Driven Piles Using Dynamic Methods - A Florida Perspective." *Geotechnical Testing Journal*, Vol. 23, No. 1, pp. 55–66.

McVay, M., Klammler, H., Bloomquist, D., Otero, J., and Farone, M. (2010). "Modification of LRFD Resistance Factors Based on Site Variability." *NTIS website*, accessed March 2010.

Mertz, D. R. (2007). "AASHTO-LRFD Background to the Specifications." *Aspire, Precast/Prestressed Concrete Institute.*

Meyerhof, G. (1970). "Safety Factors in Soil Mechanics." *Canadian Geotechnical Journal*, Vol. 7, No. 4, pp. 349–355.

Meyerhof, G. (1976). "Bearing Capacity and Settlement of Pile Foundations." ASCE: American Society of Civil Engineers, *Journal of the Geotechnical Engineering Division*, Vol. 102, No. 3, March, pp. 195–228.

Misra, A. and Roberts, L. A. (2006). "Probabilistic Analysis of Drilled Shaft Service Limit State Using the t-z Method." *Canadian Geotechnical Journal*, 1324-1332 (2006).

Misra, A., Roberts, L. A. and Levorson, S. M. (2007). "Reliability of Drilled Shaft Behavior using Finite Difference method and Monte Carlo simulation." *Geotechnical and Geological Engineering,* no.25, 65-77.

Moore, J. (2004/2005). "AASHTO LRFD Oversight Committee (OC) survey 2004 and the Update 2005." New Hampshire DOT, AASHTO Load and Resistance Factor Design (LRFD) Bridge Specifications information website, accessed May, 2008.

Moore, J. (2007). "AASHTO LRFD Oversight Committee (OC) Update 2007." New Hampshire DOT, AASHTO Load and Resistance Factor Design (LRFD) Bridge Specifications information website, accessed May, 2008.

Nordlund, R. L. (1963/1979). "Bearing Capacity of Piles in Cohesionless Soils." *Journal of Soil Mechanics and Foundation Engineering*, JSMFE, Vol. 89, SM 3, pp 1-36.

Nottingham, L., and Schmertmann, J. (1975). "An Investigation of Pile Capacity Design Procedures." Final Report D-629 to Florida Department of Transportation, Department of Civil Engineering, University of Florida, pp 159.

Nowak A. S. and Collins K. R. (2000). "Reliability of Structures." Publisher: McGraw-hill.

Nowak, A. S. (1999). "NCHRP Report 368: Calibration of LRFD Bridge Design Code." TRB, Washington, DC.

Olson, R. E., and Flaate, K. S. (1967). "Pile-Driving Formulas for Friction Piles in Sand." *ASCE Journal of Soil Mechanics and Foundation Division* 93 (No. SM 6):279-296.

O'Neill, M. W. and Reese, L. C. (1999). "Drilled Shafts: Construction Procedures and Design Methods." *FHWA Report No. IF-99-025*, Federal Highway Administration, Washington, D.C.

Paikowsky, S. G. with contributions from Birgisson, B., McVay, M., Nguyen, T., Kuo, C., Baecher, G., Ayyub, B., Stenersen, K., O'Malley, K., Chernauskas, L., and O'Neill, M. (2004). "Load and Resistance Factor Design (LRFD) for Deep Foundations."

NCHRP Report, no. 507, TRB, Washington D.C.

Passe, P. (1997). "Florida's Move to the AASHTO LRFD Code." *STGEC 97*, Chattanooga. Tennessee.

Peck, R. B., W. E. Hanson, and T. H. Thornburn (1974). "Foundation Engineering." John Wiley & Sons, pp. 514.

Pile Dynamics, Inc. (2000). "CAPWAP for Windows Manual." Cleveland, Ohio: Pile Dynamics, Inc.

Prakash, S., and Sharma, H. D. (1990). "Pile Foundations in Engineering Practice." Wiley, New York.

Ramey, G. E., and Hudgins, A. P. (1975). "Modification of Pile Capacity and Length Prediction Equations Based on Historical Alabama Pile Test Data." Montgomery, AL: State of Alabama Highway Department - Bureau of Research and Development.

Rausche, F., and Goble, G. (1979). "Determination of Pile Damage by Top Measurements." ASTM: American Society for Testing and Materials, Philadelphia, PA

Roberts, L. A., Gardner, B. S., and Misra, A. (2008). "Multiple Resistance Factor Methodology for Service Limit State Design of Deep Foundations using t-z Model Approach." *Proceeding: The Geo-Congress 2008*, New Orleans, LA.

Robertson, P. K., and Campanella, R. G. (1983). "Interpretation of Cone Penetration Tests." *Canadian Geotechnical Journal*, Vol. 20, No. 4, Nov. 1983.

Schmertmann, J. H. (1975). "Measurement of in-situ Shear Strength, State-of-the-art Report." *Proceeding: The American Society of Civil Engineers Conference on In Situ Measurements of Soil Properties*, Raleigh, North Carolina, 2, 57–138.

Schmertmann, J. H. (1978). "Guidelines for Cone Penetration Test, Performance and Design." *FHWA Report No. FHWA-TS-78-209*, U.S. DOT, Washington, D.C.

Scott, B., Kim, B. and Salgado, R. (2003). "Evaluation of Load Factors for Use in Geotechnical Design." *Journal of Geotechnical and Geoenvironmental Engineering*, ASCE, 129(4), 287-295.

Skempton, A.W. (1951), "The Bearing Capacity of Clays." *Proc. Building Research Congress*, vol. 1, pp. 180-189.

Tang, W. (1993). "Recent Developments in Geotechnical Reliability." *Proceeding: The*

Conference on Probabilistic Methods in Geotechnical Engineering.

Terzaghi, K., and Peck, R. B. (1967). "Soil Mechanics in Engineering Practice." Wiley.

Thibodeau, E., and Paikowsky, S. (2005). "Performance Evaluation of a Large Scale Pile Load Testing Program in Light of Newly Developed LRFD Parameters." *Proceeding: Session of the Geo-Frontiers 2005 Congress*, January 24-26, 2005, Austin, Texas.

Tomlinson, M. J. (1957). "The Adhesion of Piles Driven in Clay Soils." *Proceeding: The 4th International Conference on Soil Mechanics and Foundation Engineering*, Vol. 2, 1957, pp. 66-71, Butterworth Scientific Publications, Ltd. London, England.

Tomlinson, M. J. (1980/1995). "Foundation Design and Construction." *6th Edition*. Longman Scientific & Technical, Essex, England.

U.S. Army Corps of Engineers, (1992). "Pile Layout to Minimize Interference." *Engineer Technical Letter ETL 1110-8-17(FR)*, Department of the Army, US Army Corps of Engineers, Washington, DC, 20314-1000.

VanderVeen, C. (1953). "The Bearing Capacity of a Pile." *Proceeding: The 3rd International Conference on Soil Mechanics and Foundation Engineering*, Vol. 2.

Vesic, A. S. (1977). "Design of Pile Foundations." *National Cooperative Highway Research Program Synthesis of Highway Practice No. 42*, Transportation Research Board, Washington, D.C.

Vijayvergiya, V. N., and Focht, J. A. (1972). "A New Way to Predict Capacity of Piles in Clay." *Proceeding: The 4th Annual Offshore Technology Conference*, Houston, TX, Offshore Technology.

Withiam, J. L., Voytko, E. P., Barker, R. M., Duncan, J. M., Kelly, B. C., Musser, S. C., and Elias, V. (1998). "Load and Resistance Design LRFD for Highway Bridge Substructures." *Federal Highway Administration*, Washington, D.C.

CHAPTER 3: CURRENT DESIGN AND CONSTRUCTION PRACTICES OF BRIDGE PILE FOUNDATIONS WITH EMPHASIS ON LRFD IMPLEMENTATION

Sherif S. AbdelSalam[1]; Sri Sritharan, M. ASCE[2]; Muhannad T. Suleiman, M. ASCE[3]

A paper accepted for publication in the *Journal of Bridge Engineering*, ASCE

3.1. Abstract

The Federal Highway Administration mandated the use of the Load and Resistance Factor Design (LRFD) approach in the U.S. for all new bridges initiated after September 2007. This paper presents bridge deep foundation practices established through a nationwide survey of more than 30 state Departments of Transportation (DOTs) from 2008. Highlighted by this study are the benefits of the LRFD, as well as how its flexibility is exploited in design practice. This study collected information on current foundation practices, pile analysis and design, pile drivability, pile design verification, and quality control. Since this is the first nationwide study conducted on the LRFD topic following the FHWA mandate, the status on the implementation of LRFD for bridge foundation design was also examined. This study determined: 1) more than 50% of the responded DOTs use the LRFD for pile design, while 30% are still in transition to the LRFD; and 2) about 30% of the DOTs, who use the LRFD for pile foundations, utilizes regionally-calibrated resistance factors to reduce foundation costs.

CE Database keywords: LRFD, Implementation, Survey, Bridge, Deep Foundations, Pile Analysis, and Design.

[1] Graduate Student and Research Assistant, Dept. of Civil, Construction, and Environmental Engineering, Iowa State University, 355 Town Engineering, Ames, IA 50011-3232, E-mail:ssabdel@iastate.edu

[2] Wilson Engineering Professor and Associate Chair, Dept. of Civil, Construction and Environmental Engineering, Iowa State University, 376 Town Engineering, Ames, IA 50011-3232, E-mail: sri@iastate.edu

[3]Assistant Professor, Dept. of Civil and Environmental Engineering, 321 Acopian Engineering Center, Lafayette College, Easton, PA, 18042. E-mail: suleimam@lafayette.edu

3.2. Introduction

It has long been recognized that standard bridge design specifications, based on the allowable (or working) stress design (ASD) approach, do not promote a consistent reliability for design; thus, they fail to ensure uniform levels of performance for bridges. Since the mid-1980s, the Load and Resistance Factor Design (LRFD) approach has been progressively developed with the objective of ensuring a uniform reliability for bridges. In LRFD specifications, the targeted reliability index (β) defines the measure of safety associated with a probability of failure (P_f) in a limited range of 3 to 3.6 for different types of foundations (Meyerhof, 1970). According to Barker et al. (1991), a reduced β value in the range between 2.0 to 2.5 could be used for redundant piles, such as those in a pile group. This is because failure of a pile in a pile group does not necessarily lead to failure of the foundation. For this reason, Paikowsky et al. (2004) recommended a reliability index of 2.33 (corresponding to a P_f = 1%) for redundant piles as opposed to a value of 3.00 (corresponding to P_f = 0.1%) suggested for non-redundant piles. In comparison, the reliability indices corresponding to the factors of safety (FS) used in the ASD of bridge foundations ranged from 1.5 to 4.7 (Mertz, 2007), indicating a large variation in the probability of failure for this approach.

Although the LRFD approach to designing structural elements has been well established and implemented in design codes around the world, its application to geotechnical design has been relatively slow (DiMaggio, 1999). This caused the Federal Highway Administration (FHWA) to mandate the use of the LRFD approach in the design of state bridges initiated in the United States after October 1, 2007. Despite the FHWA mandated deadline, not all State Departments of Transportation (DOTs) have adopted the LRFD in their foundation designs. This could be due to the potential conservatism of the LRFD bridge design specifications with a likely anticipation of increase in the foundation cost. This is more likely the case when resistance factors used in design account for the large variation in soil parameters, as well as different levels of uncertainty associated with determining the capacity of deep foundations (Paikowsky et al., 2004). Consequently, regionally-calibrated resistance factors are permitted in LRFD to minimize the unnecessary conservatism built into the design, provided these factors are developed in a consistent manner with the approach suggested in the 2007 LRFD Specifications by the American

Association of State Highway and Transportation Officials (AASHTO).

As part of an ongoing research project for the Iowa Highway Research Board (IHRB) aimed at establishing LRFD resistance factors for the design of deep foundations in the state of Iowa by accounting for the local soil conditions, a study was conducted through a web-based survey to determine current design and construction practices of deep foundations nationwide. In addition to the basic questions relevant to the implementation of the LRFD methods in bridge foundation design practice, information on design and construction practices of bridge deep foundations was gathered and analyzed in the following topic areas: pile analysis and design, pile drivability, pile design verification methods, and quality control of pile construction.

Two features of this survey are: 1) this was the first survey conducted after the October 1, 2007 deadline imposed by the FHWA, and 2) it focused on collecting detailed information on the design and construction practices of bridge deep foundations. The outcomes of this survey are presented in this paper, which encourage bridge designers to adopt the LRFD method for pile foundation design and highlight the benefits of utilizing regionally-calibrated resistance factors.

3.3. Background

With an anticipation of implementing the LRFD methodology to new bridge foundations in the United States, several questionnaires and surveys have been conducted over the past decade to monitor the degree of LRFD implementation. In 1999, the FHWA developed a questionnaire concerning the design and construction practices for deep foundations and distributed it to State Highway officials, Transportation Research Board (TRB) representatives, and FHWA geotechnical engineers via the Internet (Paikowsky et al., 2004). A total of 45 responses were received. According to this survey, 37% of the respondents used the ASD method for foundation design with a factor of safety ranging from 2.0 to 3.0. Among these respondents, 35% used the AASHTO Load Factor Design (LFD) method and only 28% used the AASHTO-LRFD method. This survey also collected useful information about the design and construction considerations for both driven piles and drilled shafts.

In 2004, The AASHTO-LRFD Oversight Committee (OC) conducted a survey among the State Departments of Transportation (DOTs) to monitor the degree of implementation of the LRFD approach for bridge substructure design (Moore, 2004), with a follow-up survey in 2005. The committee found that 12 states had fully implemented the LRFD method for foundation design in 2004 and this number increased to 16 in 2005. In 2006, researchers at the University of Colorado sent a questionnaire to all state DOTs as part of developing the LRFD strategic plan for foundation design practice in Colorado (Chang, 2006). Only 28 DOTs responded to the questionnaire, which revealed less than 22% of the respondents had either implemented or started the implementation of LRFD for bridge foundations, while the remaining 78% had not even attempted LRFD implementation. In 2007, the AASHTO-LRFD OC updated the LRFD implementation survey in their progress report (Moore, 2007), which indicated 44 states would have fully implemented the LRFD approach for all new bridges by October 1, 2007—the FHWA mandated deadline.

Based on the outcomes of the aforementioned questionnaires and surveys conducted before the October 1, 2007 deadline, it was observed the focus of past surveys was to examine the degree of LRFD implementation for foundation design. The construction issues and/or details of the design procedures adopted for the bridge foundations were not examined. Consequently, the previous surveys did not provide any information on the use of regionally-calibrated resistance factors nor did they address the design verification and quality control practices adopted for pile foundations.

3.4. Data Collection

The data for the study reported in this paper were collected through a web-based survey developed in January 2008 and distributed to DOT officials from different states as well as FHWA engineers. A total of 33 completed surveys were received during the first quarter of 2008.One response was received from the FHWA-Eastern Federal Lands Highway Division (EFLHD), one from the Alberta Infrastructure & Transportation, Canada, and the remainder came from 31 different state DOTs. With input from the Iowa DOT officials, the survey was designed as user-friendly and aimed at gathering information on current design and construction practices of pile foundations—emphasizing LRFD and ASD design

approaches. Although nearly 100 questions were included, the survey utilized several logical branches to minimize the time required to complete the survey; i.e., respondents were not exposed to questions unrelated to their design and construction practice.

3.5. Goals and Topic Areas

The goal of the survey was to determine the current design and construction practices of deep foundations nationwide, focusing on the LRFD implementation for bridge substructure design and the current usage of regionally-calibrated LRFD geotechnical resistance factors. The survey had four topic areas: 1) foundation practice, 2) pile analysis and design, 3) pile drivability, and 4) design verification and quality control.

The foundation practice section contained general questions that acquired information about typical soil formations, average depths to bedrock, routine in-situ and laboratory tests performed in soil, frequency of using deep foundations for bridges, as well as the types and sizes of frequently used piles. The pile analysis and design section was next, which included questions about the use of various design methods, the extent of implementation of the LRFD method, load and geotechnical resistance factors used in accordance with LRFD, factors of safety used with the ASD method, and load factors used with the LFD method. Information about the different analysis methods used to calculate pile capacity (i.e., static methods, dynamic methods, and dynamic formulas) was also collected.

The third section on pile drivability focused on questions related to soil setup and relaxation, and their effect on pile capacity in different soil types. Furthermore, this section gathered information on determining the required pile penetration length during driving and the definition of pile refusal. The final section on design verification and quality control obtained information on pile design verification tests conducted during the construction stage, the frequency of performing the Static Load Test (SLT) on pile foundations, and different methods used for determining the pile nominal capacity based on SLT. At the end of the survey, respondents were asked to share information about available SLT databases and to provide general comments on the survey as well as their contact details.

3.6. Major Findings

Presented in this section is a summary of analysis results of responses received from the 31 state DOTs in the four main topic areas of the survey. In addition, the responses received from FHWA-EFLHD and Alberta Infrastructure & Transportation are highlighted in the presentation of results where appropriate.

3.6.1. Foundation practice

Figure 3.1 presents a summary of results obtained for the common foundation practice in different states. Included in this figure are the most common soil formations; average depth to bedrock; the most commonly used category of deep foundations, pile types, and sizes; and the static analysis methods used in pile design. Respondents were allowed to identify up to three different soil formations for each state. Consequently, the soil formation shown for each state in Figure 3.1 was based on survey responses. For a few respondents who opted not to answer this question and the state DOTs who did not respond to the survey, the soil formation shown was based on geological maps (Belcher and Flint, 1946).

For questions about commonly used in-situ and laboratory tests used to define soil parameters, 94% of the respondents reported use of the Standard Penetration Test (SPT), 52% use the Cone Penetration Test (CPT), 16% use the Vane Shear Test (VST), and around 20% perform some other uncommon tests. Note, the respondents were allowed to identify an unlimited number of tests in this category. Furthermore, all respondents reported performing basic laboratory soil tests, such as Atterberg limits and soil classification, while 42% stated they perform triaxial tests, 35% reported performing the unconfined compression test, 29% perform the direct shear test, and 16% perform some other uncommon laboratory tests. Despite the subjective nature of the test, the survey confirmed a majority of respondents depend on SPT tests to determine the basic soil parameters.

The next set of questions gathered information about the use of different foundation types associated with bridges, the most commonly used categories of deep foundations, as well as details about the commonly used types of driven piles and drilled shafts. For the choice of foundation type, about 91% of the respondents indicated they more frequently use deep foundations than shallow foundations in different soil types, while shallow foundations

are used primarily for low volume bridges in shallow bedrock or gravel. Among deep foundation users, 76% use driven piles, 18% use drilled shafts, and 6% use a combination of both types. Figures 3.2 and 3.3 highlight the percentage of usage of different types of driven piles and drilled shafts, respectively. Among the driven pile users, all respondents indicated they use steel H-piles, while 80% use closed-end pipe piles, 40% use open-end pipe piles, 32% use precast/prestressed concrete piles, 8% use precast concrete piles, 4% use timber piles, and about 12% of the respondents reported using other pile types (e.g., monotube piles, tapered tube piles, and a combination of prestressed concrete and steel H-piles).Among the drilled shaft users, it was determined 83% use cast-in-drilled-hole shafts (CIDH), 50% use soldier piles, 33% use continuous flight auger (CFA), and 33% use micropiles.

Furthermore, the respondents were asked to identify the most common pile size(s) they use. This information is included in Figure 3.1, which revealed steel H-piles and precast/prestressed concrete piles are more commonly used on the East Coast of the United States, where soil formation is mainly composed of coastal plain and glacial tills. On the West Coast, where the soil profile is mainly composed of alluvium soil, open-end pipe piles are more commonly used. Most of the states in the Midwest use steel H-piles, where the main soil profile is composed of glacial tills. In specific areas of the West, the CIDH shafts are also widely used, presumably due to the seismic requirements and the possibility of forming dependable plastic hinges in this foundation type.

The bridge foundation practices reported by FHWA-EFLHD and the Alberta Infrastructure & Transportation were similar to those of the state DOTs. Both indicated they depend on SPT and CPT for determining the in-situ soil parameters and they mainly perform Atterberg limits and the unconfined compression test as the basic laboratory soil tests. The FHWA-EFLHD indicated they frequently use deep foundations for bridge construction, especially driven steel H-piles and precast concrete piles. Alberta Infrastructure & Transportation indicated the usage of the same foundation type for bridge construction, but with emphasis on driven steel H-piles and open-end pipe piles.

3.6.2. Pile analysis and design

The questions for this section were aimed at understanding the deep foundation design and analysis process practiced by different state agencies. This section began with questions directed at determining the pile resistance criterion in cohesive and cohesionless soils. In cohesive soils, it was found 88% of the respondents depend on both skin friction and end bearing, 6% of the respondents depend only on skin friction, and 6% of them indicated they ignore end bearing only when the average SPT N-value is less than 12 blows per 30.5 cm (1 ft). In cohesionless soils, it was found 87% of the respondents depend on combining the resistances obtained through skin friction and end bearing, 9% depend only on skin friction, and 4% include the resistance from end bearing only when the average SPT N-value is greater than 25 blows per 30.5 cm (1 ft).

Furthermore, the most preferred method for designing deep foundations was determined the ASD method, confirmed by 45% of the respondents. The primary reasons for this choice are their familiarity with the ASD method and possible increase in foundation cost when the AASHTO-LRFD specifications are used, due to the built-in conservatism. However, the LRFD approach was reported to be the most commonly used method, due to the imposed FHWA mandate. About 52% of the survey respondents are currently using LRFD, while 33% of them are in a transition stage from ASD to LRFD, and about 15% of respondents are still using ASD with a factor of safety ranging from 2 to 2.5.

Figure 3.4 shows the current extent of LRFD implementation in the design of bridge foundations in the United States. This figure was created by combining the 31 responses collected from the state DOTs with the results of the AASHTO-LRFD OC survey (Moore, 2007) to obtain data for the 19 DOTs who did not respond to the recent survey. Even though the FHWA mandate was implemented in October 2007, 15 state DOTs, who responded to the survey, and 11 of those, who only responded to the AASHTO-OC survey, are believed to be either still using the ASD method or in a transition stage to the LRFD approach for designing bridge foundations. Among the DOTs who responded using the LRFD method for foundation design, 46% are using regionally-calibrated resistance factors based on SLT database and reliability theory, 23% are using regionally-calibrated factors by fitting to the ASD factor of safety, while 31% are using the geotechnical resistance factors as specified in the current

AASHTO Specifications (2007). Information on the assumed risk or probability of failure (P_f) for the LRFD approach to pile foundations was also requested. Since they are currently not using LRFD or in transition to LRFD, 15 of the respondents did not answer this question. Another nine respondents reported they were unaware of the assumed probability of failure. However, four respondents indicated they rely on a P_f value of less than 1/100 for the piles, while three reported using a P_f value in the range of 1/5000 to 1/1000. Although no specific question was asked relating the pile redundancy to P_f, the reported variation in P_f is believed to be due to the assumed redundancy of the piles.

The next set of questions collected information about the different static analysis methods, dynamic analysis methods, and dynamic formulas used for determining pile capacity. It was found about 2/3 of the respondents employ a combination of static and dynamic methods. Respondents, who reported using this combination, essentially deploy the static analysis methods for determining the number of piles and dynamic analysis methods or dynamic formulas for finalizing the penetration length.

As shown in Figure 3.5, the most common static analysis method used for piles in cohesive soils is the α-method at 42% (Tomlinson, 1957; API, 1974). About 32% of the respondents reported using the β-method (Esrig and Kirby, 1979), 11% use the CPT method (Nottingham and Schmertmann, 1988), and 9% follow the λ-method (US Army Corps of Engineers, 1992). Figure 3.5 also reveals the most popular static analysis method for piles in cohesionless soils is Nordlund's method (Nordlund and Thurman, 1963) by 63%. About 40% of the respondents use the SPT method (Meyerhof, 1976/1981) and 6% use in-house methods for piles in cohesionless soils. Most of the respondents chose the Nordlund's method as the most accurate static method for sandy soils, and the α-method as the most accurate static method for clayey soils. Note; the survey permitted multiple answers for this particular set of questions. Complete descriptions of the different static analysis methods identified above may be found in Hannigan et al. (1998).

For dynamic analysis methods, all respondents reported using the Wave Equation Analysis Program (WEAP) for determining pile capacity. The most commonly used software for this purpose was GRLWEAP (GRL, 1999), where 41% define the soil parameters using the soil type based method (ST), 28% use the SPT N-values based method (SA), 21% use the

Driven software (Hannigan et al., 1998), and 10% follow some other unspecified approaches. Figure 3.6 represents the use of other dynamic analysis methods—74% of the respondents indicated they use the Pile Driving Analyzer (PDA) and the CAse Pile Wave Analysis Program (CAPWAP), while 16% use other uncommon methods. Information collected on the frequently used dynamic formulas in the design of deep foundations is presented in Figure 3.7. About 57% of the respondents prefer the FHWA-modified Gates formula, 21% use the ENR formula, 14% use the Gates formula, and more than 43% use in-house formulas. Complete descriptions of the different dynamic formulas identified above may be found in Hannigan et al. (1998). More than 80% of the respondents chose the dynamic analysis methods as more accurate and reliable than static analysis methods and dynamic formulas in determining the capacity of deep foundations.

In this part of the survey, the different extreme load types used in the design of bridge foundations, as well as the different methods used for estimating the lateral displacement demand of piles, were also inquired. For the extreme load consideration, it was found that 37% of the respondents account for scour load in their design, 25% include earthquake load, 20% account for loads due to collision, and 18% use a combination of extreme loads. All respondents reported lateral displacement is a design consideration for piles. However, the method used for determining pile displacement demand varied—72% of the respondents use p-y curves, 14% use the Broms method (Broms, 1964), and 14% use other methods, such as the FB-Pier strain wedge theory, point of fixity method, and empirical methods. In the context of lateral demand on piles, it is worth noting the expected pile displacement is significantly influenced by the abutment type chosen for the bridge. For example, integral abutments designed without any expansion joints are becoming an increasingly popular choice among various DOTs. When bridges are designed with integral abutments, the superstructure loads in the longitudinal and traverse direction may not only be distributed over more supports, thus increasing the design efficiency of the foundations, but they also increase the pile redundancy (Mistry 2005).

In general, the FHWA-EFLHD pile design practice was found to be similar to that of the State DOTs. The FHWA-EFLHD indicated that they are still in a transition stage from ASD to LRFD and that they are currently using the resistance factors from the 2007

AASHTO LRFD Specifications for the LRFD approach. For the design of bridge pile foundations, they indicated the use of static analysis methods such as α-, β-, and Nordlund. As for the pile design verification, the FHWA-EFLHD response noted that the use of the SLT less frequently and the preferred approach being the dynamic analysis methods (i.e., PDA and CAPWAP) and dynamic formulas (i.e., ENR, Gates, and FHWA-modified Gates). A point of contrast between the FHWA-EFLHD bridge foundation design practice and that of the state DOTs is that FHWA-EFLHD considers the static analysis methods to be more accurate than the dynamic methods as long as the soil strength parameters are adequately obtained. On the other hand, the Alberta Infrastructure & Transportation pile design practice was quite different from that of the state DOTs in that they have already implemented the LRFD approach for the design of bridge foundations and depend on the Canadian Highway Bridge Design Code for determining the appropriate LRFD resistance factors. They mainly use the static analysis methods in the design of bridge deep foundations and the appropriate static method for a given site is reported to be selected by the consulting firm chosen for the project. They also indicated to be using the ENR dynamic formula for design verification.

3.6.3. Regionally-calibrated LRFD resistance factors

As previously indicated, among those who have already implemented the LRFD approach to their design of bridge foundations, 12 DOTs use regionally-calibrated resistance factors that are more suitable for the local soil types. These resistance factors were calibrated based on local SLT data and using statistical approaches based on reliability theory. Of the DOTs, who are still in transition to the LRFD, six of them have adopted preliminary, regionally-calibrated resistance factors, which were established using their local design and construction experience as well as the recommended load factors to retain the factor of safety used for the ASD method. This information, together with details about soil formation, deep foundation practice, and design methodology is summarized in Table 3.1. Of the respondents, 11 of them indicated that they have a collection of SLT data for their state, as identified in the table.

Note that the First Order Second Moment (FOSM) and the First Order Reliability Method (FORM) are two common reliability approaches that can be used for the LRFD

calibration. According to Allen et al. (2005), FOSM is the most straightforward technique, in which the random variables are represented by their first two moments, i.e., the mean (μ) and standard deviation (σ), while the Coefficient of Variation (COV) is defined by σ/μ. Paikowsky et al. (2004) performed the LRFD calibration for the resistance factors using both methods and concluded that the difference between them is around 10%, with FOSM providing slightly conservative resistance factors. Moreover, the 2007 AASHTO-LRFD specifications are based on the FOSM assuming a lognormal distribution of the load and resistance density functions. Although specific questions about the selected reliability approach used for the LRFD calibration were asked, most tend to follow the FOSM approach because it was used in the 2007 AASHTO-LRFD specifications.

All the reported regionally-calibrated resistance factors for different soil and pile types were examined using statistical means, in order to establish a representative mean and standard deviation so that benefits of the reported resistance factors could be realized. The minimum sample size (N) for these statistical analyses was limited to three. For all datasets, the mean and standard deviation were determined as a function of the soil type, pile type, and static analysis method. For those datasets with $N < 3$, only the average resistance factors were determined. All of these results are summarized in Tables 3.2 and 3.3. Figure 3.8 presents the histograms and frequency distributions as well as the confidence intervals for the Probability Density Functions (PDFs) of the reported resistance factors for steel H-piles in different soil types. As shown in Figure 3.8, the PDFs of different datasets follow a normal distribution, while the probability of the upper and lower limits of the true mean of each dataset were found within 95% confidence intervals. As indicated by the standard deviations in Table 3.2, it appears that the mean of the reported regionally-calibrated resistance factors for a given soil type are somewhat consistent, especially for the steel H-piles. Also note in this table that the mean resistance factor of the open-end pipe piles is greater than those established for the steel H-piles and CIDH shafts. However, it is noted that the resistance factor of the pipe piles is based only on two data points. For resistance factors reported for different static analysis methods in Table 3.3, smaller standard deviations are again observed, indicating smaller variations in the reported resistance factors for a given method and soil type. Furthermore, it is noted that the in-house methods lead to higher resistance factors than

those determined for routinely used static analysis methods.

Table 3.4 compares the mean values of the regionally-calibrated resistance factors from Tables 3.2 and 3.3 with those reported in the National Corporative Highway Research Project (NCHRP) report number 507 by Paikowsky et al. (2004) and the 2007 AASHTO-LRFD Specifications. In most cases, it is observed that the AASHTO recommendations are more conservative than those proposed by Paikowsky et al. (2004). Furthermore, the mean of the reported regionally-calibrated resistance factors by different DOTs in all cases are equal to or greater than the recommended values in NCHRP 507 and the AASHTO Guidelines. In some cases, the regionally-calibrated factors are twice as high as those recommended for design practice by AASHTO. Therefore, it is clear that the LRFD regional calibration could result in higher resistance factors as previously shown, thus optimizing the pile design and reducing the foundation costs.

The benefits of using regionally-calibrated resistance factors in pile design can be realized through a simple design example. Consider a bridge pier with a maximum factored axial load of 8900 kN (2000 kips) that is to be designed with a deep foundation consisting of 18.3 m (60 ft) long steel HP 254 mm (depth) x 62.4 kg/m (self-weight) (10 in. x 42 lbs/ft), connected with a concrete cap. The soil formation at the site is firm to very firm glacial clay with silt seams and boulders, with medium soil variability. If the α-API (API, 1974; Coduto, 2001) static analysis method is used for the design of the pile foundation, the axial capacity of a single pile is 567 kN (127 kips). Using the LRFD resistance factor of 0.35 provided in the 2007 AASHTO specifications, the design capacity of a single pile is 198.5 kN (42 kips), requiring a minimum of 45 piles. If the average regionally-calibrated resistance factor of 0.47 for the α-API method is used from Table 3.3, the design capacity of each pile is 266.5 kN (60 kips), needing a total of only 34 piles. This 25% reduction in number of piles will significantly reduce the foundation cost as it reduces the construction costs of both the piles and the pile cap.

3.6.4. Pile drivability

In the design stage, the pile penetration length required in the field is estimated using the chosen static analysis method. However, the penetration length may be readjusted at the

construction site using the pile driving data. It was found that 31% of the respondents depend on a WEAP analysis and field observations to readjust the pile penetration length, 20% employ dynamic formulas to make the adjustments, and 15% rely on the initial static analysis results and make no adjustments to pile length in the field (see Figure 3.9). Interestingly, 6% of the respondents noted that they drive the pile until refusal, while 4% prefer to drive the piles until the bedrock is reached. The remaining 24% of respondents indicated that they use a combination of the aforementioned methods depending on the site conditions and design requirements.

Effects of soil relaxation and setup on the pile capacity were also addressed in this section of the survey and it was found that more than 50% of the respondents believe that the pile capacity is unaffected by relaxation in cohesive soils. The responses of those who indicated that the pile capacity is affected by relaxation were grouped based on the most predominant soil formation that they indicated for their region. Accordingly, 40% of respondents noted that the change in pile capacity would not exceed 5% of the value expected at End of Driving (EOD) in silty sands, 6% indicated that the effect varies from 5 to 10% in sandy soils, and only 2% assumed that the effect exceeds by 20% of the pile capacity in silts. Similarly, as for the influence of soil setup on the pile capacity, 34% of the respondents indicated that the pile capacity increases above 20% of the value at EOD due to setup in clays and silty clays, 25% indicated that the effect varies from 5 to 10% in glacial tills and clays, 25% indicated that the effect varies from 11 to 20% in clayey silts, 6% indicated that the soil setup effect does not exceed 5% on the pile capacity, and 10% of the respondents assume that the pile capacity is unaffected by soil setup in cohesionless soils.

3.6.5. Design verification and quality control

This final section of the survey focused on design verification and quality control issues. All but one respondent indicated that they perform field tests on 5 to 10% of the installed piles to verify the design capacity. Among several different techniques, about 45% of respondents have used the SLT for design verification, while others predominantly use the dynamic monitoring approach especially for friction piles (i.e., use of WEAP, PDA and CAPWAP). Usually for small projects, the WEAP analysis is considered as an adequate pile

design verification technique, but for large scale projects, the PDA and CAPWAP are preferred. Among those who use SLT, 73% responded that they use the Davisson's criterion (Davisson, 1972) to define the pile nominal capacity, 26% use the limited total settlement method, 7% use the shape of curvature method, and 13% follow other unspecified methods.

The most commonly used quality control (QC) tests in the field were found to be: gamma-gamma test (which is used with drilled shafts installed using the slurry displacement method), cross hole sonic test, pile verticality measures, and weld/placement inspection. More than 45% of respondents reported that they perform such QC tests on 5% of installed piles, another 45% of them perform QC tests less frequently, and the remaining 10% never perform such tests.

3.7. Conclusions

This paper has presented results from an important survey on the current design and construction practices of deep foundations for bridges, which is one of the first surveys to be completed following the FHWA mandate on the use of the LRFD approach in the U.S. on all new bridges initiated after October 1, 2007. The outcomes of the survey are significant in that they give an overview of the current bridge foundation practices and highlight how frequently the state DOTs take advantage of the provision in the AASHTO-LRFD Specification to improve the deep foundation design by employing regionally-calibrated geotechnical resistance factors and the associated benefits. Based on the responses received, the conclusions drawn from the study are as follows:

1. As of June 2008, 52% of the DOTs who responded to the survey have adopted the LRFD approach for the design of bridge deep foundations, 33% of them were in a transition phase from ASD to LRFD, and the remaining 15% still followed the ASD approach with a factor of safety ranging from 2 to 2.5. Of those using the LRFD method, six DOTs use geotechnical resistance factors by fitting to ASD, eight are following the 2007 AASHTO-LRFD recommended values, while 12 DOTs have adapted their own regionally-calibrated factors based on reliability theory.
2. The mean of the reported regionally-calibrated geotechnical LRFD resistance factors were statistically analyzed and presented in Tables 3.1 through 3.4. The LRFD

regionally-calibrated resistance factors reported for sands and clays are either equal to or greater than the AASHTO recommended values. In sand, the resistance factors are as much as 50% above those recommended by AASHTO, while values as much as 100% above the recommended values are used for clay. Such large increases in resistance factors will likely reduce the overall cost of bridge deep foundations.

3. In the design stage, state DOTs are using static analysis methods for determining the pile capacity. The most commonly used methods in cohesive soils are the α- and β-methods. On the other hand, the most commonly used static methods in cohesionless soils are the Nordlund and SPT methods. Most of the respondents chose the α-method and the Nordlund method to be the most accurate method for determining the pile capacity in cohesive and cohesionless soils, respectively.
4. During the construction of deep foundations, the DOTs employ either dynamic analysis methods or dynamic formulas to verify the pile capacity estimated by a static analysis method. Although all of the respondents noted that they use WEAP as a dynamic analysis method, 75% indicated that they use a combination of PDA and CAPWAP in addition to WEAP. Of those who use dynamic formulas for pile capacity verification, the majority of respondents either use the FHWA-modified Gates formula or a locally developed formula.

3.8. Acknowledgments

The study reported in this paper was conducted by the authors as part of the ongoing research project *TR-573: Development of LRFD Design Procedures for Bridge Pile Foundations in Iowa*, which is funded by the Iowa Highway Research Board (IHRB). The authors also express their gratitude to 1) all respondents of the survey; 2) Sandra Larson and Mark Dunn, Research and Technology Bureau of Iowa DOT, for their coordination and support of the project; 3) Norm McDonald, State Bridge Engineer for Iowa, for inviting other DOTs to participate in the survey; and 4) the following members of the project Technical Advisory Committee for their guidance and advice: Ahmad Abu-Hawash, Dean Bierwagen, Lyle Brehm, Ken Dunker, Kyle Frame, Steve Megivern, Curtis Monk, Michael Nop, Gary Novey, John Rasmussen and Bob Stanley. The members of this committee represent Office

of Bridges and Structures, Soils, Design Section, and Office of Construction of the Iowa DOT, FHWA Iowa Division, and Iowa County Engineers.

3.9. References

AASHTO LRFD Bridge Design Specifications (2007). Customary U.S. Units, 4th edition, 2008 Interim, American Association of State Highway and Transportation Officials, Washington, D.C.

Allen, T. M., Nowak, A.S., and Bathurst, R. J. (2005). "Calibration to Determine Load and Resistance Factors for Geotechnical and Structural Design." *Transportation Research Circular Number E-C079*, TRB, Washington, DC, 83p.

Barker, R., Duncan, J., Rojiani, K., Ooi, P., Tan, C., and Kim, S. (1991). "NCHRP Report 343: Manuals for the Design of Bridge Foundations." *Transportation Research Board*, National Research Council, Washington, D.C.

Belcher, D.J., and Flint, R. F. (1946). "Soil Deposits Map of United States and Canada." *Geological Society of America*, Washington.

Broms, B. (1964). "Lateral Resistance of Piles in Cohesive Soils." *Journal of the Soil Mechanics and Foundations Division*, ASCE, Vol. SM2, March, pp. 27–63.

Chang, N. Y. (2006). "CDOT Foundation Design Practice and LRFD Strategic Plan." Colorado DOT Research Branch, Report No. CDOT-DTD-R-2006-7

Davisson, M. (1972). "High Capacity Piles." *Proceeding: Soil Mechanics Lecture Series on Innovations in Foundation Construction*, ASCE, Illinois Section, Chicago, IL, pp. 81–112.

DiMaggio, J., Saad, T., Allen, T., Barry, R., Al Dimillio, Goble, G., Passe, P., Shike, T., and Person, G. (1999). FHWA International Technology Exchange Program, report number FHWA-PL-99-013.

GRL, Inc. (1999). "Pile-Driving Analyzer, PAK Users Manual." Goble, Rausche, Likins, and Associates.

Hannigan, P.J., Goble, G.G., Thendean, G., Likins, G.E. and Rausche, F. (1998). "FHWA-HI-97-013: Design and Construction of Driven Pile Foundations-Volume I and II." National Highway Institute, Federal Highway Administration, U.S. Department of

Transportation, Washington, D.C.

Moore, J. (2004/2005). AASHTO LRFD Oversight Committee (OC) survey 2004 and the Update 2005, New Hampshire DOT, AASHTO - LRFD Bridge Specifications information website. (http://www.ridot.us/aashto/agenda.htm), accessed May, 2008.

Moore, J. (2007). AASHTO LRFD Oversight Committee (OC) Update 2007, New Hampshire DOT, AASHTO Load and Resistance Factor Design (LRFD) Bridge Specifications information website (http://www.transportation.org/sites/bridges), accessed May, 2008.

Mertz, D. R. (2007). "AASHTO-LRFD Background to the specifications." Aspire, Precast/Prestressed Concrete Institute.

Meyerhof, G. (1970). "Safety Factors in Soil Mechanics." *Canadian Geotechnical Journal*, Vol. 7, No. 4, pp. 349–355.

Mistry, V. (2005). "Integral Abutments and Joint-less Bridges," *Proceeding: The Integral Abutment and Joint-less Bridges Conference*, FHWA, Baltimore, 3-11.

Paikowsky, S. G. with contributions from Birgisson, B., McVay, M., Nguyen, T., Kuo, C., Baecher, G., Ayyub, B., Stenersen, K., O'Malley, K., Chernauskas, L., and O'Neill, M. (2004). "NCHRP Report, 507: Load and Resistance Factor Design (LRFD) for Deep Foundations." TRB, Washington D.C.

Table 3.1: Reported factors sorted according to pile types, static methods, and soil types

State	Pile Type	Static Analysis		Dynamic Analysis	Dynamic Formulas	Resistance Factors		
		Cohesive	Cohesionless			Sand	Clay	Mix
CA*	Steel H-piles	CPT-method	Nordlund	P + C + W[(1)]	F-G[(2)]	0.45	0.35	N/A
CO	CIDH	SPT-method	SPT-method	P + C + W	ENR, G[(3)], F-G	0.1	0.9	0.5
CT*	Prestressed	In-house	In-house	P + C + W	Not used	0.65	0.65	0.65
ID*	Steel H-piles	β-method	SPT-method	P + C + W	F-G	0.45	0.45	0.45
MA*	Open-pipe	In-house	Nordlund	P + C + W	Not used	0.65	0.65	0.65
NH*	Closed-pipe	α-method	Nordlund	P + C + W	Not used	0.45	0.35	N/A
NJ*	CIDH	α-method	Nordlund	P + C + W	Not used	0.45	0.35	0.4
NM*	Steel H-piles	β-method	Nordlund	P + C + W	ENR, G, F-G	0.35	0.45	N/A
NV	Steel H-piles	α-method	Nordlund	Not used	Not used	0.35	0.25	N/A
PA*	Steel H-piles	β-method	Nordlund	P + C + W	Not used	0.5	0.5	0.5
UT*	Steel H-piles	α-method	Nordlund	Not used	Not used	0.5	0.7	0.7
WA	Steel H-piles	In-house	In-house	WEAP	F-G	0.5	0.5	0.5
WY	Steel H-piles	CPT-method	Nordlund	Not used	Not used	0.45	0.35	0.35

*Pile Load Test Database available; [(1)] P + C + W: PDA, CAPWAP, and WEAP; [(2)] F-G: FHWA Modified Gates method; [(3)] G: Gates method.

Table 3.2: Mean values and standard deviations of the reported regional resistance factors according to different pile and soil types

Pile Type	Reported Factors in Sand			Reported Factors in Clay			Reported Factors in Mixed Soils		
	N[(1)]	Mean	S.D.[(2)]	N	Mean	S.D.	N	Mean	S.D.
Steel H-pile	11	0.48	0.11	12	0.48	0.15	8	0.55	0.13
CIDH	4	0.4	0.23	3	0.6	0.28	3	0.5	0.13
Open-end Pipe	2	0.65	N/A	2	0.67	N/A	2	0.67	N/A

[(1)] Sample Size; and [(2)] Standard Deviation.

Table 3.3: Mean values and standard deviations of the reported regional resistance factors according to different static analysis methods and soil types

Static Analysis Method	Reported Factors in Sand			Reported Factors in Clay			Reported Factors in Mix Soil		
	N	Mean	S.D.	N	Mean	S.D.	N	Mean	S.D.
Nordlund	11	0.5	0.12		N/A		4	0.53	0.17
SPT method	3	0.45	0.25		N/A		3	0.53	0.11
α-method		N/A		6	0.47	0.19		N/A	
β-method		N/A		4	0.49	0.13		N/A	
CPT method		N/A		3	0.45	0.17		N/A	
In-house	3	0.62	0.11	4	0.63	0.10	3	0.62	0.11

Table 3.4: Comparison between the reported resistance factors and the recommended factors in NCHRP 507 and 2007 AASHTO-LRFD Specifications

Soil Type	Static Analysis Method	NCHRP	AASHTO-Specifications	Mean of Reported Resistance Factors
Sand	SPT- method	0.45	0.3	0.45
	β-method	0.3	N/A	0.65
	Nordlund	0.45	0.45	0.5
	In-house	N/A	N/A	0.62
Clay	α-method	0.45	0.35	0.47
	β-method	0.2	0.25	0.49
	In-house	N/A	N/A	0.63

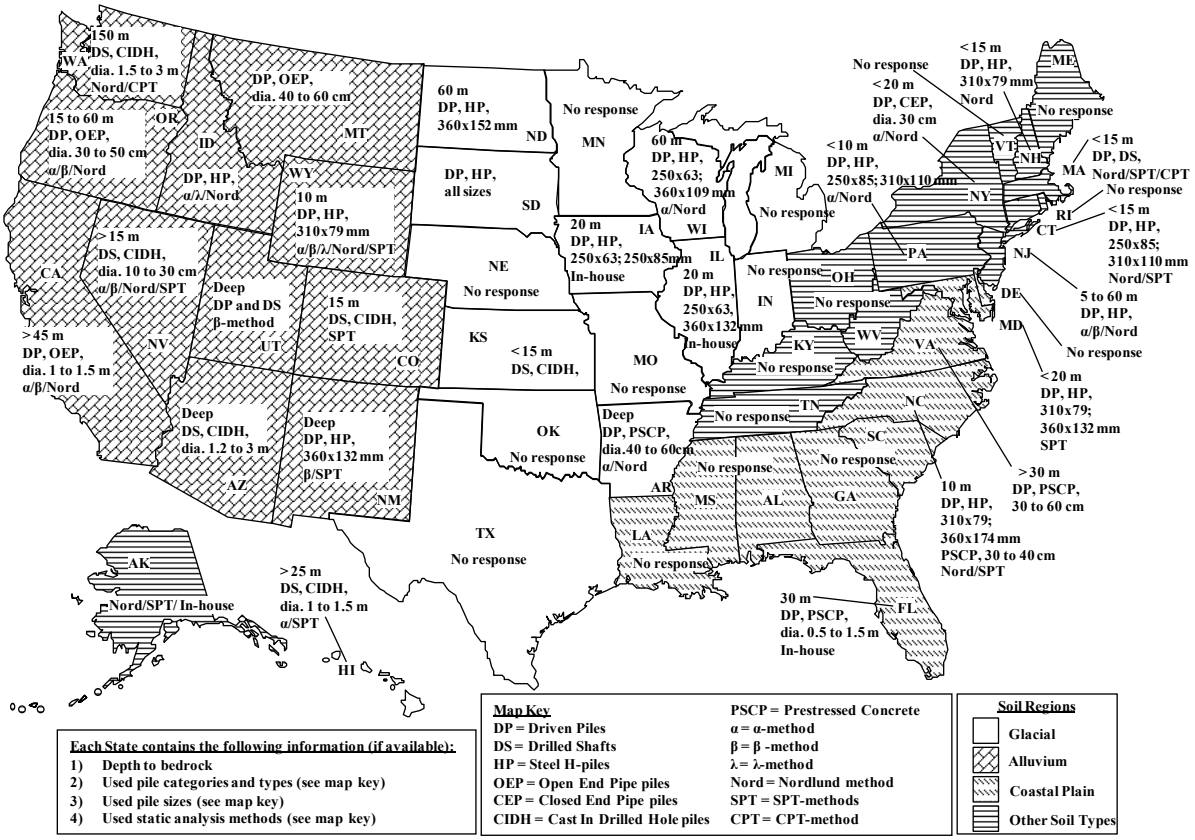

Figure 3.1: U.S. Map for soil formations, average bedrock depth, commonly used deep foundation categories, types and sizes, and static methods used in different States

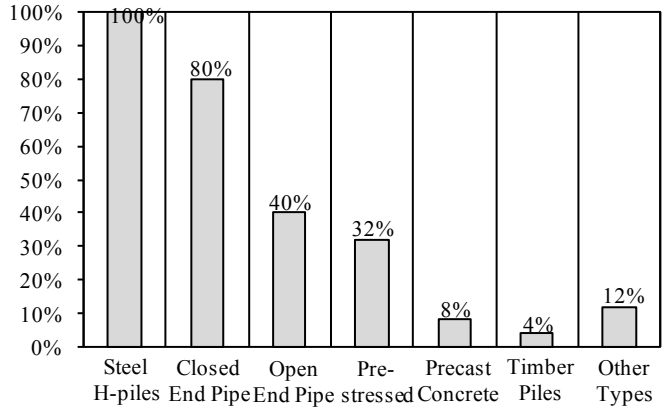

Figure 3.2: Distribution of the most commonly used driven pile types for bridge foundations

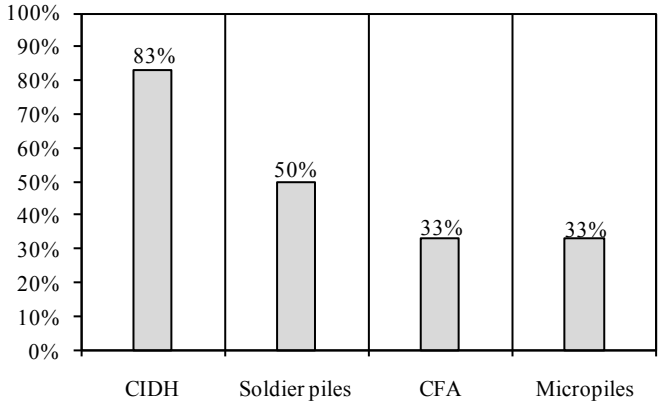

Figure 3.3: Distribution of the most commonly used drilled shaft types for bridge foundations

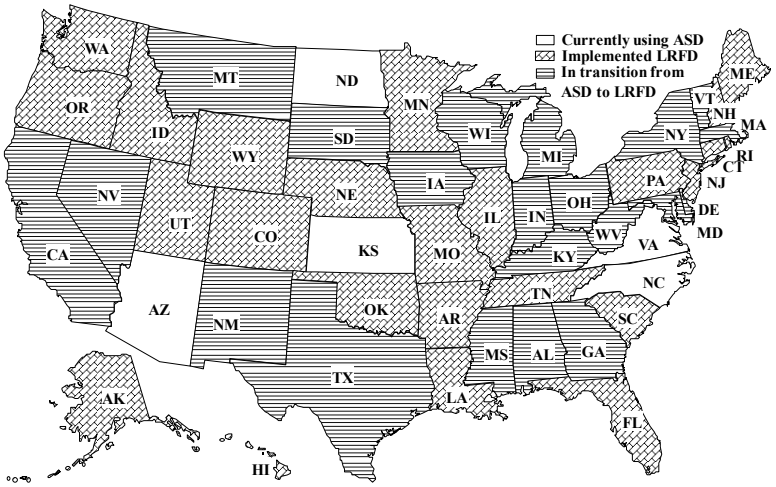

Figure 3.4: Current extent of LRFD implementation

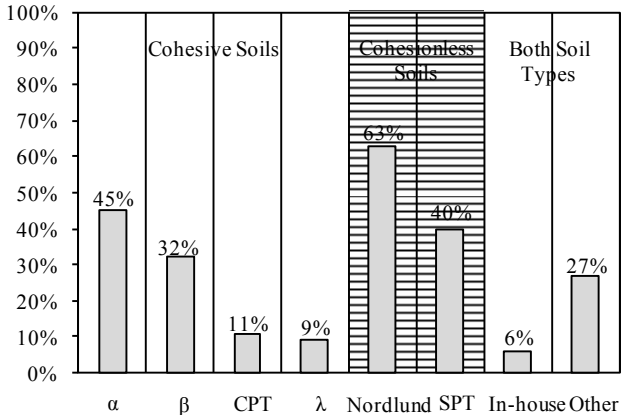

Figure 3.5: Most commonly used static analysis methods for the design of deep foundations

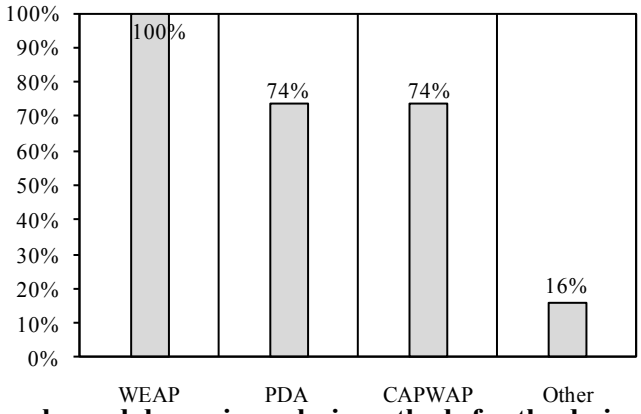

Figure 3.6: Commonly used dynamic analysis methods for the design of deep foundations

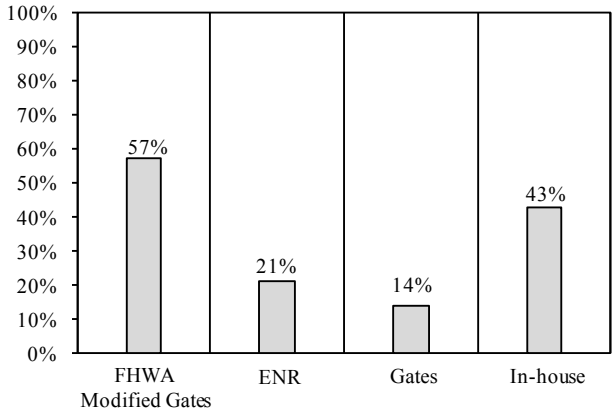

Figure 3.7: Most commonly used dynamic formulas for deep foundations

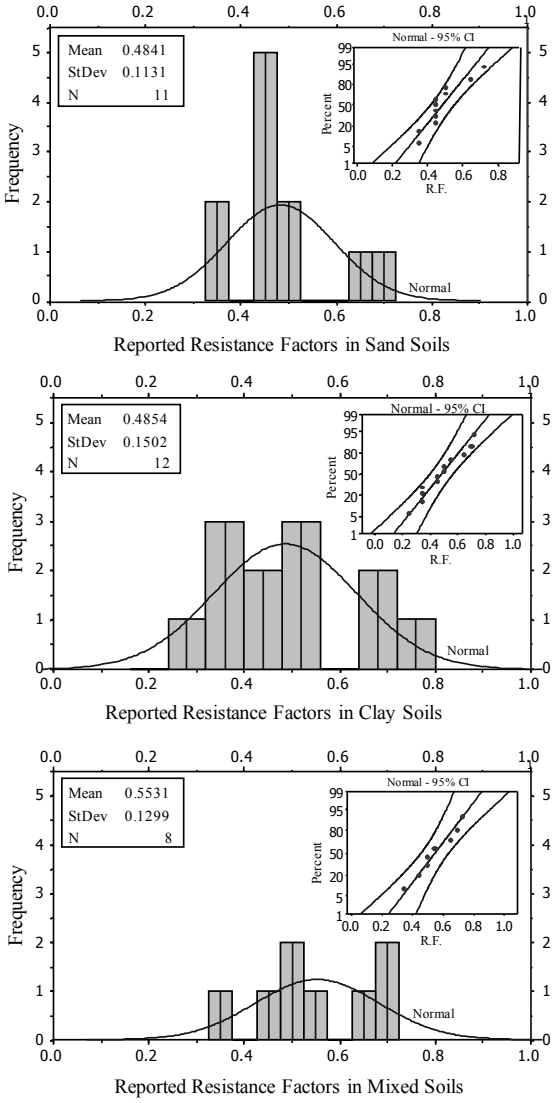

Figure 3.8: Histograms, frequency and 95% CI of the reported regional LRFD resistance factors for steel H-pile in different soil types

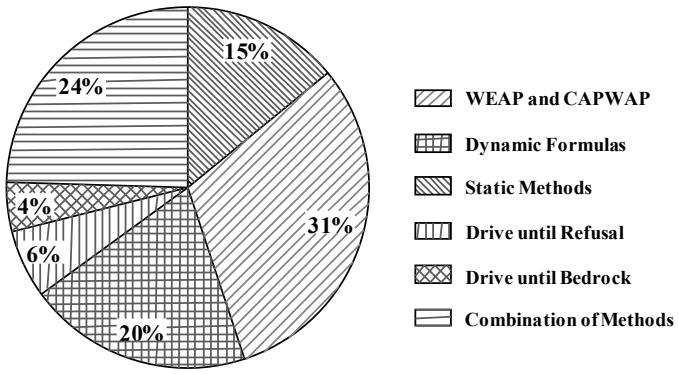

Figure 3.9: Methodologies used for readjusting the pile penetration length

CHAPTER 4: UTILIZING A MODIFIED BOREHOLE SHEAR TEST TO IMPROVE THE LOAD-TRANSFER ANALYSIS OF AXIALLY-LOADED FRICTION PILES IN COHESIVE SOILS

Sherif S. AbdelSalam[1]; Muhannad T. Suleiman, M. ASCE[2]; Sri Sritharan, M. ASCE[3]

A paper to be submitted to the *Geotechnical Testing Journal*, ASTM

4.1. Abstract

This study focuses on the use of a proposed *Modified* Borehole Shear Test (mBST) to improve the prediction of the load-displacement relationship and the load distribution for axially-loaded friction piles in cohesive soils using load-transfer analysis (*t-z* method). Until now, empirical formulas with a soil laboratory or in-situ tests, such as the Cone Penetration Test (CPT), have been used for deriving the *t-z* curves required for this analysis, but the proposed mBST enables direct field measurement of these curves along the soil-pile interface. As part of this study, three full-scale instrumented static vertical load tests were conducted on steel H-piles. The t-z analysis was used to model these three piles utilizing TZPILE software. Different *t-z* curves were used in the models: (1) based on empirical correlations with CPT and (2) based on direct measurements from the proposed mBST. When compared to the measured responses from the static vertical load tests, the mBST-based models showed a significant improvement in prediction accuracy compared to the CPT-based models. The findings in this paper may help incorporate serviceability limits into the design of deep foundations.

CE Database Keywords: Load-Transfer; t-z Analysis; t-z curve; Load-Displacement; Borehole Shear Test; Pile foundation; Soil-structure interaction; Pile modeling.

[1] Graduate Student and Research Assistant, Dept. of Civil, Construction, and Environmental Engineering, Iowa State University, 355 Town Engineering, Ames, IA 50011-3232, E-mail:ssabdel@iastate.edu

[2] Assistant Professor, Dept. of Civil and Environmental Engineering, Lafayette College, 321 Acopian Engineering Center, Easton, PA, 18042. E-mail: suleimam@lafayette.edu

[3] Wilson Engineering Professor and Associate Chair, Dept. of Civil, Construction and Environmental Engineering, Iowa State University, 376 Town Engineering, Ames, IA 50011-3232, E-mail: sri@iastate.edu

4.2. Introduction

Several numerical methods have been used to characterize soil-structure interaction of vertically-loaded driven piles and drilled shafts. Among them is the load-transfer analysis technique, known as the "*t-z*" analysis, used to calculate the vertical load-displacement response, as well as the vertical load distribution along the pile's length. Although this approach has been considered acceptable for modeling deep foundations subjected to axial compressive loads (Misra and Chen, 2004; Alawneh, 2006), load-transfer curves, *t-z* and *q-w* curves, that, respectively, describe the skin friction between the pile and surrounding soil along the length and the end bearing at the pile's tip, the selection of these curves effectively controls the accuracy of the analysis. These curves are currently obtained, based on empirical or semi-empirical correlations, with soil properties estimated using laboratory and/or in-situ tests (Roberts et al., 2008).

The objective of this study is to improve the load-transfer analysis used for vertically loaded friction piles in cohesive soils, using *t-z* curves obtained by direct in-situ measurements, avoiding the use of empirical correlations. Driven steel H-piles were selected to demonstrate the proposed approach. A significant benefit of improving the load-transfer analysis is that it can facilitate incorporation of vertical settlement and serviceability limits into the design of deep foundations using the Load and Resistance Factor Design (LRFD) approach. In the proposed approach, the *t-z* curves along the soil-pile interface are directly captured in the field, using a *modified* Borehole Shear Test (mBST) device. The conventional Borehole Shear Test (BST) device and its testing procedure were designed to only measure soil shear strength parameters. However, the proposed modifications to the BST enable direct field measurement of the *t-z* curves in a simple and cost-effective way.

In this paper, mBST was implemented to directly measure the *t-z* curves along the soil-pile interface at three different test sites. The measured *t-z* curves were then used with commercial software, TZPILE v.2.0, developed by ENSOFT, Inc. (Reese et al., 2005) to calculate the load-displacement response at the pile's head and the load distribution along the pile's length. Furthermore, because CPT is widely used to model vertically-loaded piles (Abu-Farsakh and Titi, 2004), *t-z* curves developed by commonly used empirical correlations with CPT data were also used to model the three test piles. The results of these *t-z* models

were then compared with the experimentally-measured responses from the three vertical static load tests conducted on full-scale instrumented steel H-piles driven into cohesive soils at three different test sites in Iowa. Due to the limited space in this paper, the experimental and analytical investigations for one test site are presented in detail, but include general summaries for the other two tests.

4.3. Background

The most accurate method to obtain the load-displacement relationship at the pile's head and the load distribution along the pile's length is to conduct an instrumented pile Static Load Test (SLT). However, according to a survey conducted by AbdelSalam et al. (2008) on the current design and construction practices of bridge deep foundations, the majority of the Departments of Transportation (DOTs) do not perform the SLT due to its high cost.

Another approach to characterize the behavior of vertically-loaded piles is to use analytical methods. According to Guo and Randolph (1998), the analytical methods used to characterize pile behavior can be classified into three categories: (1) approximate closed-form solutions, (2) one-dimensional numerical algorithms, and (3) boundary or finite element approaches. The first two categories depend on the load-transfer response, which does not require significant soil testing to develop the soil model in comparison to the effort needed for the third category of analysis (El-Mossallamy, 1999). Regardless of the analysis method used, the soil-pile interface properties largely dictate the load-displacement relationship and the load distribution as a function of depth for deep foundations (De-Gennaro et al., 2006; Engin et al., 2007). Due to its efficiency, simplicity, and potential use in the development of serviceability limits for the design of deep foundations according to the LRFD approach, the one-dimensional load-transfer numerical analysis using the *t-z* method was selected for this study, which is an iterative technique that solves nonlinear differential equations using the finite difference approach (Misra and Chen, 2004; Alawneh, 2006).

As shown in Figure 4.1, the pile in the t-z analysis is divided into several segments and is replaced by elastic springs. The soil surrounding the pile along the shaft is also represented by a set of non-linear springs. One spring at the pile's tip represents soil resistance from end bearing. The initial t-z model was developed by Coyle and Reese (1966)

and Suleiman and Coyle (1976) in cohesive and cohesionless soils, respectively. Reddy et al. (1998) modified the model to account for pile elastic deformation in computing the mobilized skin friction using an elastoplastic soil-pile interface model. The model was then improved to include a hyperbolic response for the springs representing the soil-pile interface by Misra and Roberts (2006). However, the major shortcoming of this method is no in-situ test was used to accurately measure the *t-z* and *q-w* curves in the field. Therefore, researchers have been estimating the *t-z* and *q-w* curves, based on empirical correlations to laboratory or in-situ test data, such as the SPT or CPT (Coyle and Reese, 1966; Roberts et al., 2008). Although CPT is considered more accurate than SPT for cohesive soils and many empirical correlations have been widely used in predicting pile capacity with a fairly acceptable accuracy, it may require extensive work to determine which correlation is most appropriate for a specific soil and pile condition (Abu-Farsakh and Titi, 2004).

4.4. Proposed Modified Borehole Shear Test

The original BST was initially designed by Handy and Fox (1967). It provides a direct, cost effective measurement for determining drained soil strength parameters, such as effective cohesion (c') and effective internal angle of friction (ϕ'). As shown in Figure 4.2a, the BST equipment consists of two main parts—the dynamometer and the shear head. On the shear head, grooved shear plates are used on both sides. To conduct the BST, the shear head is inserted into an open borehole (or through a hollow stemmed auger) and a constant stress (P_n) normal to the surface of the borehole is applied for a period of time to allow for consolidation. The range of applied normal stresses is usually determined using the estimated effective lateral earth pressures at the test depth. The consolidation time for one shear test ranges from 5to 15 minutes depending on soil type and ground water conditions to allow for dissipation of excess pore water pressure (Handy, 1986). After consolidation is completed, the soil in the borehole is sheared by applying an upward pulling stress (T) to the shear head and the stress is measured using a gauge attached to the dynamometer (see Figure 4.2a). In the original test procedure, only the maximum shear stress is recorded during the test. Using the grooved shear plates, the test is repeated at the same depth under different normal stresses, after rotating the shear head by approximately 45^o, to obtain a series of normal stress

versus shear strength values for the soil (Handy and Fox, 1967), representing the Mohr-Coulomb failure envelope of the soil resulting in measured soil effective shear strength parameters.

To directly measure the *t-z* curves at the soil-pile interface for vertically-loaded piles, the original BST equipment and testing procedure were modified. These modifications are as follows: (1) a dial gauge was added to the apparatus' base plate to measure the vertical displacement of the shear head during shearing as shown in Figure 4.2b; (2) the grooved shear plates shown in Figure 4.2c were replaced with smooth steel shear plates (see Figure 4.2d) to better represent the friction surface of the steel H-piles; hence, capturing the soil-pile interface properties; and (3) the data collection procedures were modified to record the shear resistance as a function of vertical displacement (see Figure 4.2e) at different normal stresses, representing the effective lateral earth pressure on the driven pile at the time of SLT, after rotating the shear head by approximately 45^{o}. The effective lateral earth pressure was determined, based on the calculations of friction angle and overconsolidation ratio using commonly used SPT and CPT correlations, and on readings of two push-in pressure cells installed next to the test pile, which account for the effect of pile driving and pore water pressure dissipation at the time of SLT. The calculation and measurement procedures of the lateral earth pressure are described in more details later in this paper.

4.5. Field Testing

Three vertical SLTs were conducted on full-scale instrumented steel HP 10x42 piles driven into cohesive soils at three different Iowa counties: Clarke County (test site T-1), Jasper County (test site T-2), and Poweshiek County (test site T-3). The test piles were loaded using a 2000 kN (440 kips) hydraulic jack and the applied load was measured using a 1300 kN (290 kips) load cell. In addition to using four 25.4 cm (10 inch) displacement transducers to measure the vertical displacement at the top of the test piles, the piles were instrumented with strain gauges along the shaft and near the pile's tip. All of the piles were load tested following the "Quick Test" procedure outlined in the ASTM D 1143 (ASTM, 2007). In all cases, the test pile was loaded in 5% increments beyond the estimated maximum capacity. The load was kept relatively constant at the end of each load increment for a

duration ranging from 5 to 15 minutes, until deflection readings stabilized, as required by ASTM D 1143.After the pile experienced excessive vertical displacement at approximately constant load (i.e., pile plunging), the pile was unloaded in five equal load decrements. Soil profiles at the test sites were characterized using in-situ SPT, CPT, BST, and mBST, and several laboratory tests including soil classification, Atterberg limits, and consolidation tests. Based on in-situ and laboratory test results, the cohesive soil shear strength at the three sites indicated a range of stiff to hard cohesive soils. At each site, two push-in pressure cells were used to monitor the lateral earth's pressure before and after driving the piles, as well as during the SLT.

The purpose of conducting these soil and pile tests is to acquire the data necessary to model the test piles and to validate the analytical results, respectively. In this paper, the investigation procedure, results, and analysis for test site T-1 will be discussed in detail. However, the other two tests (T-2 and T-3), which produced similar findings to that of T-1, will not be discussed in detail (for more details about soil and pile field test results for T-2 and T-3, see Ng et al., in process).

4.5.1. Characterization of soil and soil-pile interface

Test Site T-1

The bridge site was located at the intersection of Interstate-35 and U.S. Highway-34 near Osceola, Iowa. An 18.3 m (60 ft) long, steel HP 10×42 test pile with 17.4 m (57 ft) embedded length was driven into the ground at the site. In addition, two HP 10x42, 18.3m (60 ft) long piles with 16.4 m (54 ft) embedded length, were driven into the ground, and used as reaction piles for the loading frame. Ten strain gauges were installed on each side of the web centerline of the test pile. The locations of strain gauges along the pile length were determined, considering different soil layers at the site and included two gauges (one on each side) near the bottom of the pile to quantify the resistance at the pile's tip (see Figure 4.3).

SPT and CPT soil investigation

The typical geological formation at test site T-1 consists of a loess soil deposit on top of slightly overconsolidated glacial clay. During drilling, the loess soil layer was found to

extend to 9.25 m (30.3 ft) below the ground's surface. Using laboratory tests conducted on disturbed samples collected during drilling, the two soil layers (loess and glacial clay) were classified as low plasticity clay (CL) per the Unified Soil Classification System. The groundwater table at the time of in-situ testing was located at 10 m (32.8 ft) below the ground's surface. In addition to basic soil properties, Figure 4.3 summarizes the measured CPT tip resistance (q_c) and skin friction (f_s), as well as the soil's undrained shear strength (S_u) estimated according to the CPT commonly used correlation recommended by Schmertmann et al. (1978), using $N_k = 15$. Also included in this figure are the SPT blow counts corrected to account for the effect of the soil overburden pressure, the locations of the BST and mBST tests, and the effective shear strength parameters obtained from the BST tests (discussed in detail in a subsequent section). Table 4.1 provides a summary of the soil classification and the cone parameters from CPT results after considering the effect of the pore water pressures.

Monitoring lateral earth pressure

At each site, conventional and modified BSTs at different normal stresses were conducted at different depths to measure soil shear strength parameters and adequately capture *t-z* curves for the soil-pile interface for main soil layers. To determine normal stresses used in the BSTs and mBSTs conducted at each depth, the expected range of lateral earth pressures on the surface of the pile along its length was required. For each test site, several 1-D consolidation tests were conducted to cover the main soil layers along the pile's embedded length. From laboratory consolidation tests, the coefficient of consolidation (C_v) and the overconsolidation ratio (OCR) were calculated and summarized in Table 4.1 for the three test sites. From the OCR values, the soil was mainly found to be from normally to slightly over consolidate for the three test sites. Consequently, the at-rest lateral earth pressure coefficient (K_o) was then determined using the equations recommended by Jaky (1944) for clays. The values of K_o for NC soils and slightly OC soils ranged from 0.44 to 0.47 for all soil layers along the length of the pile at T-1.

In addition to all in-situ tests used to estimate the lateral earth pressures, two push-in pressure cells, which measure total lateral earth pressure and pore water pressure, were

installed near the test piles to: (1) validate the estimated lateral earth pressure calculated from different in-situ tests, (2) ensure the applied normal stresses during the mBST represented the lateral earth pressure on the pile, and (3) examine the effect of pile driving, if any, on the lateral earth's pressure. The pressure cells were installed approximately two days before the start of pile driving to allow for pressure readings to stabilize as recommended by Suleiman et al. (2010) and data were continuously recorded as a function of time during pile driving, restrikes, and SLT.

At test site T-1, the two push-in pressure cells were installed at distances of 20 cm (8.0 inch) and 45.72 cm (18 inch) from the test pile flange, both at the same depth of 7.0 m (23.25 ft) from the ground's surface. At the time of the SLT, the effective lateral earth pressure, using the pressure cell closer to the pile, matches the estimated lateral earth's pressure from SPT and CPT data, while the effective lateral earth's pressure, using the far pressure cell, was higher than the range of the expected pressures. However, it was observed the far pressure cell was broken when retrieved after testing, indicating damage that could have occurred during installation. Consequently, the lateral earth pressure readings obtained from the second pressure cell were disregarded and the average of measured and calculated lateral earth pressures were used in this study.

BST and mBST soil investigation

The conventional and modified BSTs were conducted at depths of 2.7 m (8.8 ft), 7.2 m (23.6 ft), and 11.0 m (36.1 ft) below the ground's surface. The locations of conventional and modified BST tests were selected to cover the main soil layers at the site. Based on the lateral earth's pressure calculations and measurements presented above, the values of the normal stresses along the test pile were determined, and the BST and mBST were conducted accordingly. The Mohr-Coulomb failure envelope for the soil and the soil-pile interface obtained from the BST and mBST results, respectively, are indicated as shown in Figure 4.4 at a depth equal to 11.0 m (36.1 ft) below the ground's surface. As expected, the figure shows smaller values for adhesion (a) and friction angle (α) at the soil-pile interface, when compared to the soil's shear strength parameters. Table 4.2 summarizes the measured soil's shear strength parameters (i.e., c' and ϕ') and soil-pile interface properties (i.e., adhesion, a, and friction angle, α), using BST and mBST, respectively. The table also summarizes the

selected values of normal stresses conducted with each test.

For test site T-1, the measured *t-z* curves obtained using the mBST at the soil-pile interface are presented in Figure 4.5 for different depths along the pile embedded length, using the corresponding appropriate normal stresses indicated in Table 4.2. Other *t-z* curves measured, using the mBST based on different normal pressures and for other test sites, are available but not presented in this paper due to size limitations; for more details see Ng et al. (in process). In the "*t-z* Analysis" section of this paper, the *t-z* curves measured, using the mBST, are compared with those developed, based on the CPT test and the curves back-calculated from strain gauge readings obtained during the SLT.

Test Sites T-2 and T-3

The typical geological formation at test sites T-2 and T-3 consists of loess soil deposit on top of slightly overconsolidated glacial clay. Similar to T-1, the soil profiles at test sites T-2 and T-3 were characterized using in-situ SPT, CPT, BST, and mBST, and laboratory tests such as soil classification, Atterberg limits, and consolidation tests. Furthermore, two push-in pressure cells were used to monitor the lateral earth's pressure. Soil classification and CPT results at both sites are summarized in Table 4.1, which show a predominant cohesive soil profile at both sites with the soil profile mainly consisting of clay and silty clay for T-2 and clay to sandy silt for T-3. Table 4.1 shows CPT tip resistance (q_c) at the three sites ranges from 1249 kPa (26 ksf) to 9731 kPa (203 ksf) with estimated undrained shear strength from 79 kPa (1.7 ksf) to 288 kPa (6 ksf), indicating stiff to hard cohesive soils.

In-situ BST sand mBSTs were conducted, following the same procedures used forT-1 at different normal stresses as summarized in Table 4.2. In summary, a total of 16 and 18 conventional and/or modified BSTs were conducted at T-2 and T-3, respectively. Field testing results showed similar trends to those found at T-1 and the *t-z* curves for both test sites were developed using the same approach described previously. For the three sites, the effective cohesion ranges from 13.3 kPa (278 psf) to 72.6 kPa (1517 psf).

4.5.2. Pile static load tests

For test site T-1, the load-displacement response measured at the pile's head is

presented in Figure 4.6, while the load distribution along the pile, established using the strain gauge data recorded at the end of each load increment is shown in Figure 4.7. Figure 4.6 indicates the vertical load-displacement of the pile was approximately linear up to an applied load of 1043 kN (236 kips), with the maximum applied load reached during testing, 1170 kN (263 kips). The rate of load transfer in the pile during the last few loading steps, indicated by the slope of the curves in Figure 4.7, was almost constant in both soil layers with the slope for the top soil layer smaller than that of the bottom soil layer (i.e., 30 kN/m (2.1 kip/ft) vs. 90 kN/m (6.2 kip/ft)). Furthermore, the load transferred to the pile's tip during the test ranged from 0 to 54 kN (0 to 12 kips), within 6% of the maximum applied load, confirming the tested pile was essentially a friction pile.

The load-displacement along the pile shaft was determined by integrating strain gauge data using Simpson's numerical integration rule. The pile tip load-displacement curve was then back-calculated by subtracting the total load-displacement measured at the pile's head from the integrated load-displacement along the pile's shaft. The total load-displacement response measured at the pile's head, as well as separated shaft and tip displacements are presented in Figure 4.6, showing the pile capacity was approximately 1100 kN (243 kips), based on Davisson's criterion (Davisson, 1972).

Similar to T-1, an instrumented steel HP 10x42 test pile, with a length of 18.3 m (60 ft), was driven into the ground after conducting the BSTs at T-2 and T-3 test sites. For T-2 and T-3, the rate of load transfer during the last few loading steps for the loess and glacial clay soil layers was comparable to that measured at T-1. Using Davisson's criterion, the pile capacity at T-2 and T-3 was 685 kN (154 kips) and 700 kN (157 kips), respectively. Using the strain gauge measurement, the maximum percent of load resisted by the pile's tip was 2% for T-2 and 17% for T-3, confirming that the test piles mainly resisted the applied loads by skin friction. Detailed soil properties, test results, and developed *t-z* curves for T-2 and T-3 can be found in Ng et al. (in process).

4.6. T-z Analysis

In each t-z model developed for the field tested piles, the HP 10x42 pile was divided into 50 segments with each segment represented by an elastic spring of constant stiffness

term, AE=3.596x10^8 kN, where E and A are the elastic modulus and the cross-sectional area of the pile, respectively. Given the test piles were mainly friction piles, as confirmed by the percent of the load resisted by end-bearing (which ranged from 2 to 17% for the three sites), the model was analyzed, based on *t-z* curves developed from different in-situ tests (i.e., CPT and mBST), and compared to the pile measured response from SLT results. Four major analyses discussed in this paper are: 1) *t-z* curves based on empirical correlations to CPT and no end bearing (TZ-CPT); 2) *t-z* and *q-w* curves based on empirical correlations to CPT (TZ-CPT*); 3) *t-z* curves based on the mBST and no end-bearing (TZ-mBST); and 4) *t-z* curves based on the mBST, with the *q-w* curve obtained from the SLT (TZ-mBST-SLT) strain gauge data.

Test Site T-1

The main goal of the *t-z* analysis is to evaluate the load-displacement relationship at the pile's head as well as the load transfer along the pile's length, using *t-z* curves measured with the proposed mBST. However, it is appropriate to first compare the *t-z* curves obtained from CPT and mBST data to see how closely they match the *t-z* curves back-calculated from strain gauge data.

T-Z Curves

For the mBST test, the *t-z* curves at different depths were directly measured in the field in the form of shear stress versus displacement. An example of the *t-z* curves measured using the mBST for T-1 was previously presented in Figure 4.5. However, the *t-z* curves were also determined, based on S_u, q_c, f_s, and strain at 50% of soil strength (ε_{50}), with S_u and ε_{50}estimated, based on empirical correlations with the CPT test results—cited and summarized in Table 4.1. The CPT-based soil parameters were input into the TZPILE software as recommended by Reese et al. (2005). Reese et al. (2005) also indicated the TZPILE internally develops the t-z curves using a procedure similar to that suggested by Coyle and Reese (1966).

At test site T-1, Figures 4.8a and 4.8b compare the *t-z* curves developed from CPT and mBST data for the two main soil layers at depths of 7.0 m (23 ft) and 11.0 m (36 ft) below the ground surface, respectively. To validate the curves obtained from different in-situ

tests, the *t-z* curves at the same depths were back-calculated using the strain gauge data. When compared to the *t-z* curves from mBST and CPT data, Figure 4.8 shows that the *t-z* curves measured, using mBST, provide a reasonable match with the curves back-calculated from the strain gauge data. The *t-z* curves obtained, using CPT, did not match the back-calculated curves, especially for the soil's layer at 11.0 m (36 ft). This confirms the mBST data better represents the soil-pile interface properties when compared with the CPT data and it can be used to directly measure the *t-z* curves required for the load-transfer analysis.

Analysis and results

The calculated load-displacement relationships using the *t-z* curves developed from CPT and mBST data compared with the measured SLT response for the friction steel H-pile at test site T-1 are summarized in Figure 4.9. The key values of the calculated responses are compared with the measured responses and have been summarized in Table 4.3. For test site T-1, the slope of the first portion of the load-displacement curve (i.e., the load-displacement curve before the start of plunging failure) calculated from the TZ-CPT model provided a 37% stiffer response when compared with the slope of the first portion of the measured curve from the SLT. The pile capacity estimated using Davisson's criterion for the TZ-CPT analysis was 1654 kN (372 kips), 50% higher than the measured pile capacity of 1100 kN (247 kips). This significant overestimation of the CPT-based approach is consistent with observations for T-2 and T-3. When including the effect of the end bearing component using a *q-w* curve developed based on CPT data, the results of the TZ-CPT* analysis showed an insignificant difference of 3% compared to the TZ-CPT model, where end-bearing was ignored. Therefore, considering the *q-w* curve, based on CPT data, did not significantly affect the calculated response.

The analysis using the *t-z* curves directly measured in the field, using mBST (TZ-mBST) did not include the *q-w* curve for end-bearing. They show a slope of the first portion of the load-displacement response approximately 3% softer than the measured response (see Figure 4.9). Furthermore, the pile capacity estimated using Davisson's criterion from the TZ-mBST analysis was 25% smaller than the pile capacity estimated from the measured response (see Table 4.3). However, when the TZ-mBST predicted capacity was compared with the measured capacity based on skin friction only, the difference is reduced from 25 to

19%. Therefore, the TZ-mBST has provided a conservative, yet acceptable, prediction of pile capacity, when compared to the significantly overestimated capacity provided by the TZ-CPT model. Generally, it is clear the TZ-mBST analysis has improved the prediction of pile behavior and provided a better load-displacement response compared to that calculated, based on empirical correlations using CPT data.

Although not practical for prediction purposes, an additional analysis similar to TZ-mBST was conducted, where the end-bearing component back-calculated from strain gauge data was included. In this analysis, referred to as TZ-mBST-SLT, it was found that incorporating the end-bearing component slightly improves the prediction of the slope of the first portion of the load-displacement curve, reducing the difference between the measured and calculated responses from 3 to 1% (see Figure 4.9 and Table 4.3). Pile capacity obtained from the TZ-mBST-SLT model was 980 kN (220 kips), only 11% smaller than the measured capacity.

In conclusion, although the t-z analysis, based on mBST data, was slightly conservative when estimating pile capacity, it provided a very good match of the slope of the first portion of the load-displacement curve (i.e., the load-displacement curve before the start of plunging). Ignoring the end-bearing component in the TZ-mBST model could have caused this conservatism, which was reduced in the TZ-mBST-SLT model. However, the TZ-mBST as well as the TZ-mBST-SLT models better represent the pile measured load-displacement relationship compared to the TZ-CPT model. This improved prediction of the first portion of the load-displacement curve, which represents the range of working stresses for these piles, could be used to incorporate serviceability limits into the LRFD approach for deep foundation design.

In addition to comparing the load-displacement responses, the load distribution along the length of the pile calculated, using different *t-z* models was compared with the measured load distributions obtained from strain gauge data. Figure 4.10 represents the load distribution along the pile's length at an applied load of 880 kN (198 kips), using different *t-z* analyses compared to the measured distribution. This figure shows the TZ-mBST and TZ-mBST-SLT models provide a very good prediction of the load distribution along the pile's length compared to the TZ-CPT model. It should be noted the inaccurate load-displacement

relationship and load distribution prediction of the CPT-based approach may be improved by conducting extensive field and laboratory tests to determine the most appropriate empirical correlation to use for a specific site and pile condition. However, using the proposed mBST-based approach avoids this problem.

Test Sites T-2 and T-3

Figures 4.11 and 4.12 show the load-displacement curves for the piles at test sites T-2 and T-3, respectively, using the same four t-z models discussed above, and compared with the measured responses from the SLT results. Figure 4.11 shows similar responses to those presented in Figure 4.9 at test site T-1. Table 4.3 also summarizes the characteristics of the calculated load-displacement curves at test sites T-2 and T-3 compared with the measured responses obtained from SLTs. The load-displacement curve resulting from the TZ-CPT model provided a significantly higher slope of the first portion of the load-displacement curve compared to SLT results and a significantly higher pile capacity, based on Davisson's criterion (see Table 4.3). On the other hand, the analysis using the TZ-mBST model provided a very good match to the first portion of the measured load-displacement curve as well as closer Davisson pile capacities when compared to the TZ-CPT results. Moreover, Figures 4.11 and 4.12 represent the results of the TZ-mBST-SLT model. They are clear, considering the end-bearing component did not significantly affect the calculated load-displacement relationship. In summary, a similar soil-pile response to that observed at T-1 was observed at T-2 and T-3.

4.7. Summary and Conclusions

Although t-z analysis has proven a practical method for modeling vertically-loaded deep foundations, the *t-z* and *q-w* curves are typically based on empirical or semi-empirical correlations with soil properties measured or estimated using laboratory or in-situ soil tests. To improve the load-transfer analysis used to predict the load-displacement and load transfer along the pile's length, a modified Borehole Shear Test (mBST) is proposed to directly measure the *t-z* curves in the field. For steel H-piles, the mBST uses smooth steel plates to measure the shear stress as a function of displacement at the soil-pile interface at different

normal stresses. In this study, a load-transfer analysis was conducted, based on the measured soil-pile interface properties using the mBST, and the empirically correlated interface properties from CPT results.

Three full-scale instrumented load tests were conducted on driven friction steel HP 10x42 piles at three sites with mainly cohesive soil profiles. The measured responses of the load tests included vertical load-displacement at the pile's head and load transfer along the length of the pile. The soil's profiles at the three sites were characterized using SPT, CPT, BST, and mBST tests. The *t-z* curves were developed using CPT and mBST for soil layers at three different sites. The calculated responses, using the *t-z* models, were compared with the measured responses. Four major *t-z* models were analyzed for each test pile: TZ-CPT, TZ-CPT*, TZ-mBST, and TZ-mBST-SLT. The first and the third models ignored the end-bearing component (since the test piles were mainly friction piles), while the second and the fourth models consider end-bearing, based on CPT and SLT, respectively. When compared with measured responses for the three sites, the major findings from this study can be summarized as follows:

- The pile load-displacement relationship predicted using *t-z* curves, based on empirical correlations with CPT data (TZ-CPT), significantly overestimated the soil-pile interface properties, the first portion of the load-displacement response, and the pile capacity by as much as 50%.
- The pile load-displacement response calculated using *t-z* curves obtained from mBST data (TZ-mBST) provided a very good match of the slope of the first portion of the measured load-displacement responses (i.e., the load-displacement curve before the start of plunging) and an acceptable estimate of the pile's capacity (with differences ranging from 17 to 25% for the three test sites).
- Ignoring the end-bearing component (*q-w* curve) in the *t-z* analysis did not significantly affect the results in the case of friction steel H-piles.
- Based on overall response predictions for the three test sites, the TZ-mBST model has proven to provide a better match of the measured SLT results when compared with TZ-CPT model.

  Finally, the proposed mBST is a simple, cost effective in-situ test that captures the

soil-pile interface properties and can be directly used in the load-transfer analysis to simulate load-displacement behavior at the pile's head and the load distribution along the pile's length. This study focused on friction steel H-piles in cohesive soils. However, it can be extended to other types of deep foundations such as concrete piles. The proposed procedure can also help incorporate serviceability limits into the LRFD for deep foundation design.

4.8. Acknowledgments

The study reported in this paper was conducted by the authors as part of the ongoing research project TR-573: Development of LRFD Design Procedures for Bridge Pile in Iowa, funded by the Iowa Highway Research Board (IHRB). The authors express their gratitude to the IHRB and members of the project Technical Advisory Committee for their guidance and advice. The members of this committee represent Office of Bridges and Structures, Soils, Design Section, and Office of Construction of the Iowa DOT, FHWA Iowa Division, and Iowa County Engineers. Finally, special thanks to Kam Weng Ng and Matthew Roling for their help during conducting the field/laboratory tests and interpretation of data.

4.9. References

AbdelSalam, S. S., Sritharan, S., and Suleiman, M. T. (2008). "Current Design and Construction Practices of Bridge Pile Foundations." *International Foundation Congress and Equipment Expo 09*, ASCE and Geo-Institute, Orlando, Florida.

Abu-Farsakh, M. Y. and Titi, H. H., (2004). "Assessment of Direct CPT Methods for Predicting the Ultimate Capacity of Friction Driven Piles." *ASCE Journal of Geotechnical and Geoenvironmental Engineering*, volume 130, No. 9, pp. 935 - 944.

Alawneh, A. S. (2006). "Modeling Load–Displacement Response of Driven Piles in Cohesionless soils under Tensile Loading." *Computers and Geotechnics* 32, 578–586.

American Society for Testing of Materials (2007)."Standard Test Methods for Deep Foundations under Static Axial Compressive Load." *ASTM D1143 – 07*.

Coyle, H. M. and Reese, L. C. (1966). "Load Transfer for Axially-loaded Piles in Clay." *Journal of Soil Mechanics and Foundation Engineering Division*, 92(2), 1- 26.

Davisson, M. (1972). "High Capacity Piles." *Proceeding: Soil Mechanics Lecture Series on*

Innovations in Foundation Construction, ASCE, IL Section, Chicago, IL, pp. 81–112.

De Gennaro, V., Said, I., and Frank, R. (2006).“Axisymmetric and 3D Analysis of Pile Test using FEM.” *Numerical Methods in Geotechnical Engineering*, 2006 Taylor & Francis Group, London, ISBN 0-4 15-40822-

El-Mossallamy, Y. (1999). “Load-Settlement Behavior of Large Diameter Bored Piles in Over-consolidated Clay.” *Proceeding: The 7th International Symposium on Numerical Models in Geotechnical Engineering* - NUMOG VII, Graz, 1-3 September 1999, 433-450. Rotterdam, Balkema.

Engin, H. K., Septanika, E. G., and Brinkgreve, R. B. (2007). “Improved Embedded Beam Elements for the Modeling of Piles.” *Proceeding: 10thInternational Symposium on Numerical Models in Geotechnical Eng.* – NUMOG X, Rhodes (Greece). April 2007.

Guo, W. D. and Randolph M. F. (1998). “Vertically Loaded Piles in Non-homogeneous Media.” *Inter. Jl. for Numerical and Analytical Methods in Geomechanics*, Vol. 21.

Handy, R. L. (1986). “Borehole Shear Test and Slope Stability.” *Proceeding: The ASCE Specialty Conference on In Situ tests*: Use of In Situ Tests in Geotechnical Engineering, Blacksburg, Virginia, pp. 161-175.

Handy, R. L. (2008). “Evaluation of Geotechnical soil Testing I. Field Tests.”*International Journal of Geotechnical Engineering*, 1, pp. 11-28.

Handy, R. L. and Fox, N. S. (1967). “A Soil Borehole Direct Shear Test Device.” *Highway Research News, Transportation Research Record*, No.27, p. 42-51.

Jaky, J. (1944). “The Coefficient of Earth Pressure at Rest.”*Journal of Society of Hungarian Architects and Engineers*, Budapest, Oct. 1944, pp. 355-358.

Mayne, P. W. and Kulhawy, F. H. (1990). “Manual on Estimating Soil Properties for Foundation Design.” Rpt. EL-6800, Electric Power Research Inst., Palo Alto, 306 p.

Misra, A. and Chen, C. H. (2004). “Analytical Solutions for Micropile Design under Tension and Compression.” *Geotechnical and Geological Engineering*, 22(2), 199-225.

Misra, A. and Roberts, L. A. (2006). “Probabilistic Analysis of Drilled Shaft Service Limit State Using the “t-z” Method.” *Canadian Geotechnical Journal*, 1324-1332 (2006).

Ng, K. W., Sritharan, S., Suleiman, M., AbdelSalam, S. S., & Roling, M. (in process).“Development of LRFD Design Procedures for Bridge Pile Foundations in

Iowa - *Soil Investigation and Full-Scale Pile Tests*." Final Report Vol. II. IHRB Project No.TR-573, TR-583 and TR-584.Iowa State University, Ames, Iowa.

Reddy, E. S., O'Reilly, M., and Chapman, D. A. (1998). "Modified t-z Model- A Software For Tension Piles." *Computers and Structures*, 68: 613–25.

Reese, L. C., Wang, S. T., and Arrellage, J. (2005). "Analysis of Load Versus Settlement for an Axially-loaded Deep Foundation - TZPILE v.2.0 Software User Manual." ENSOFT, INC.3003 West Howard Lane, Austin, Texas 78728.

Roberts, L. A., Gardner, B. S., and Misra, A. (2008). "Multiple Resistance Factor Methodology for Service Limit State Design of Deep Foundations using a t-z Model Approach." *Proceeding: The Geo-Congress 2008,* New Orleans, LA.

Robertson, P. K., and Campanella, R. G. (1983). "Interpretation of Cone Penetration Tests." *Canadian Geotechnical Journal*, Vol. 20, No. 4, Nov. 1983.

Schmertmann, I. B. (1978). "Guidelines for Cone Penetration Test, Performance, and Design." *Report No. FHWA-TS-78-209, U.S. DOT*, Washington, D.C., pp. 145.

Suleiman, I. B. and Coyle, H. B. (1976). "Uplift Resistance of Piles in Sand." *Journal of Geotechnical Engineering*, ASCE 1976; 102(GT5):559–62.

Suleiman, M. T., Conway, W. M. Stevens, L. Jahren, C. T., Ceylan, H. (2010). "Identification of Practices, Design, Construction, and Repair Using Trenchless Technology." Institute of Transportation, Final Research Report. Iowa Department of Transportation Project Number IHRB-06-09.

Table 4.1: Soil properties measured in laboratory and estimated using SPT and CPT

Test #	Layers m	Soil Type[1]	γ[2] kN/m^3	q_c kPa	f_s kPa	OCR[3]	C_v[3] in^2/min	K_o[4]	S_u[5] kPa	ϕ[6]	ε_{50}[7]
T-1	0 – 8.5	CL	17.5	1673	102	1.11	0.031	0.47	107	--	0.0050
	8.5 – 17.4	CL	22	2908	153	< 1.0	0.024	0.44	180	--	0.0045
T-2	0 - 1.5	Fill	17	1543	64	1.0	0.042	0.42	101	--	0.0050
	1.5 - 5.5	CL-ML	18.2	1614	12	1.41	0.026	0.44	102	29	--
	5.5 - 10.7	CL	18.9	2815	172	< 1.0	0.026	0.47	177	--	0.0045
	10.7 – 17	CL	19.5	2165	74	< 1.0	0.035	0.51	129	--	0.0050
T-3	0 – 6.6	CL	17.5	1249	62	N/A	N/A	0.48	79	--	0.0070
	6.6 -11.4	ML	19.0	9731	62	4.43	0.044	0.44	638	32	--
	11.4 – 15	CL	21.0	3771	74	< 1.0	0.067	0.45	236	--	0.0040
	15 – 17.4	CL	22.0	4628	206	< 1.0	0.024	0.44	288	--	0.0040

For unit conversion: 1 m = 39.37 inch; 1 kN/m^3 = 6.24 lb/ft^3; and 1 kPa = 0.145 psi.
[1] CL is low plastic clay, CL-ML is silty clay, and ML is sandy silt (according to the USCS);[2]Soil total unit weight calculated in the laboratory; [3] OCR and coefficient of consolidation (C_v) measured based on a laboratory conducted 1-D consolidation tests; [4]K_o calculated for normally consolidated clays after Jaky (1944) based on CPT results; [5]After Schmertmann et al. (1978), assuming N_k=15; [6] After Robertson and Campanella; and[7] After Reese et al. (2005) used for the TZ-CPT analysis.

Table 4.2: Soil and soil-pile interface shear strength parameters measured using the BST and mBST at different depths showing the range of normal stress

Test#	Depth (m)	Range of Normal Stress P_n (kPa)				BST[1]		mBST[2]	
						c' (kPa)	ϕ'	a (kPa)	α
T-1	2.7	22	30*	40	60	14.9	25	15.1	22
	7.2	50	70	90	110*	26.2	7	18.1	7
	11.0	110	130	150	170*	72.6	27	42.2	15
T-2	8.2	60	80	100	120*	22.7	8	12.6	16
	14.0	150	180	200	220*	13.6	12	14.4	10
T-3	2.7	20	40*	80	N/A	7.0	33	1.5	27
	7.0	50	100	150*	N/A	13.3	14	22.0	5
	13.7	100	150	250*	N/A	48.6	3	38.3	15

For unit conversion: 1 m = 39.37 inch; and 1 kPa = 0.145 psi.
[1] Conventional BST, using test procedures after Handy (1986) to allow for pore water pressure dissipation; [2] Modified BST, using similar testing procedures to the conventional test to allow for pore water pressure dissipation; and *Represents the normal stress corresponding to measured lateral earth pressure and selected for the TZ-mBST analysis.

Table 4.3: Summary of the major t-z analyses used to compare the calculated responses with the measured responses from SLT

Test #	Model	Model Description		Load-Displacement Curve		% Difference to SLT[1]	
		t-z curves (skin-friction)	*q-w curve (end-bearing)*	Slope of First Portion (kN/m)	Davisson Capacity (kN)	Slope of First Portion	Davisson Capacity
T-1	SLT	Strain Gauges		193116	1100	Measured	
	TZ-CPT	CPT	Ignored	265054	1654	37% stiffer	50% higher
	TZ-CPT*	CPT	CPT	265054	1680	37% stiffer	53% higher
	TZ-mBST	mBST	Ignored	184257	830	3% softer	25% lower
	TZ-mBST-SLT	mBST	SLT	190415	980	1% softer	11% lower
T-2	SLT	Strain Gauges		198451	685	Measured	
	TZ-CPT	CPT	Ignored	297159	1140	50% stiffer	66% higher
	TZ-CPT*	CPT	CPT	297159	1150	50% stiffer	68% higher
	TZ-mBST	mBST	Ignored	195377	566	2% softer	17% lower
	TZ-mBST-SLT	mBST	SLT	187526	570	6% softer	17% lower
T-3	SLT	Strain Gauges		168481	700	Measured	
	TZ-CPT	CPT	Ignored	242613	1015	44% stiffer	45% higher
	TZ-CPT*	CPT	CPT	242613	1036	44% stiffer	48% higher
	TZ-mBST	mBST	Ignored	177972	840	5% stiffer	20%higher
	TZ-mBST-SLT	mBST	SLT	176870	920	5% stiffer	31% higher

[1] Difference between the load-displacement curves adapted from different t-z analyses and the pile measured response during SLT.

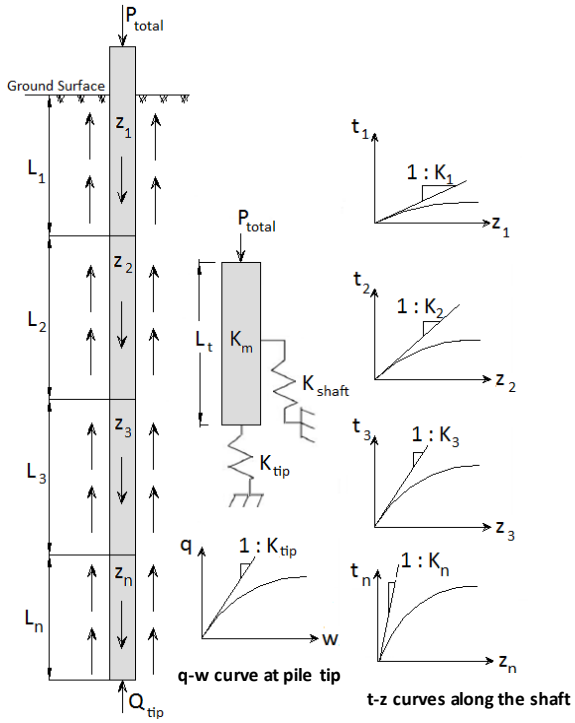

Figure 4.1: Idealized load-transfer model showing t-z curves for the pile segments and *q-w* curve at the pile tip (modified after Alawneh, 2006)

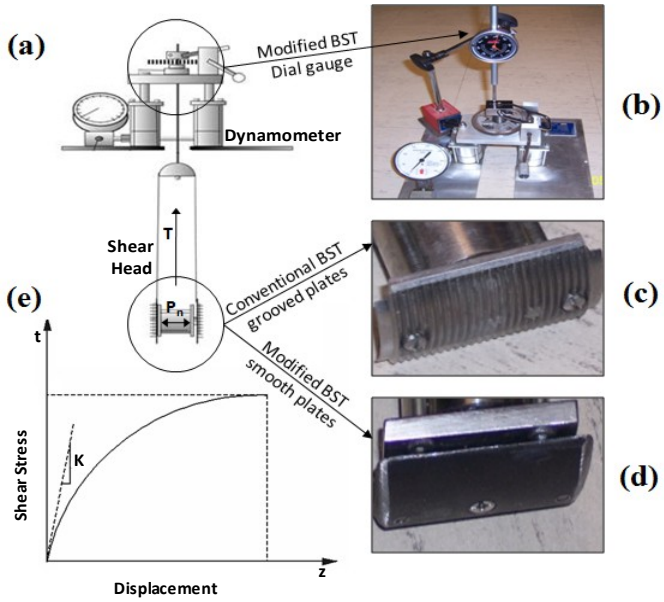

Figure 4.2: (a) BST components (modified after Handy, 2008, courtesy of Handy Geotechnical Instruments, Inc.); (b) added dial gauge; (c) grooved shear plates used in conventional BST; (d) new smooth plates; and (e) sample t-z curve

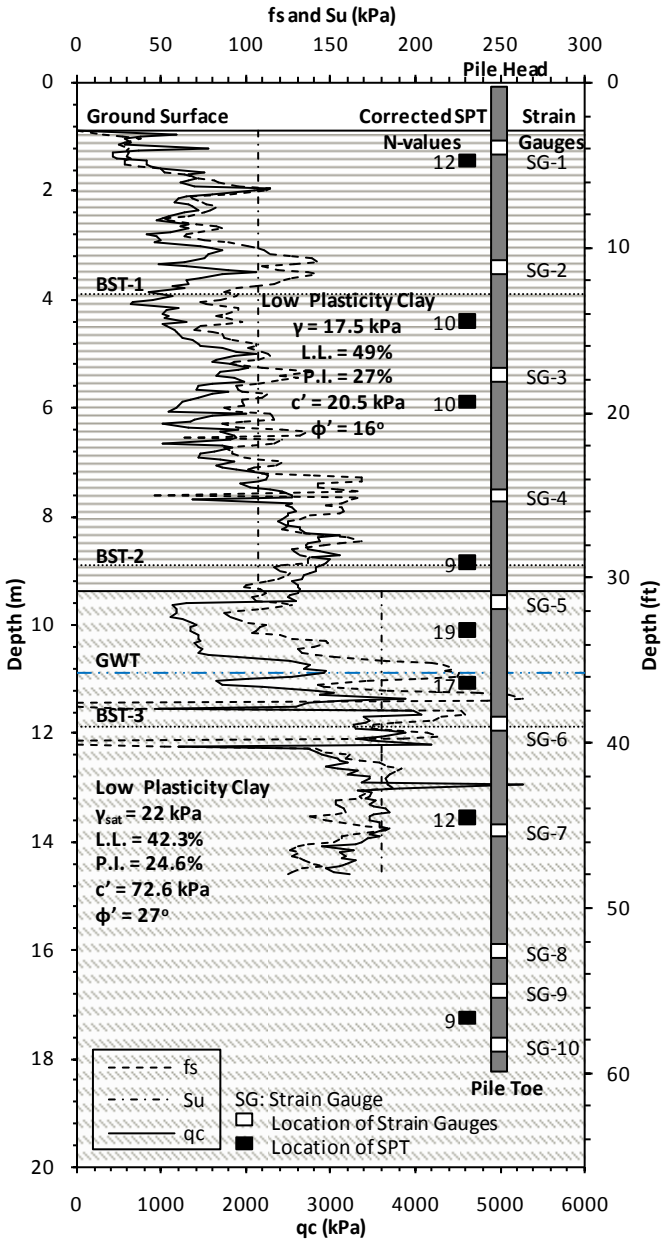

Figure 4.3: Summary of soil tests conducted at T-1 including: tip resistance (q_c), skin friction (f_s), and undrained shear strength (S_u) from CPT; corrected SPT N-values; depths of BST/mBST, and soil shear strength parameters from BST; soil classification; and strain gauges locations

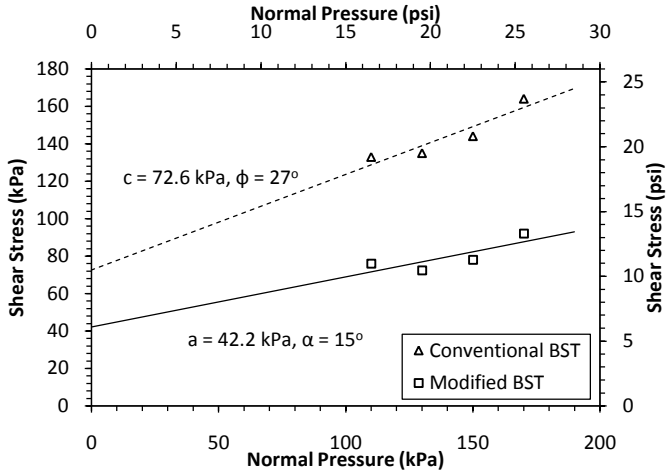

Figure 4.4: Failure envelopes for the soil and soil-pile interface measured using BST and mBST, respectively, at a depth of 11.0 m below the ground surface for T-1

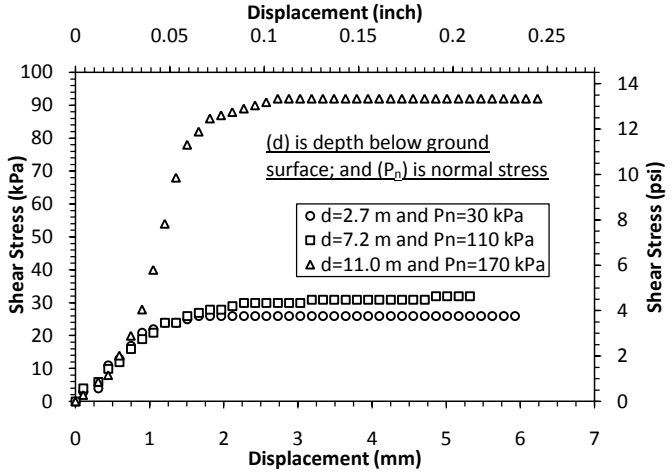

Figure 4.5: Shear stress vs. displacement curves for the soil-pile interface measured using mBST at different depths below ground surface and at the normal stresses used in the t-z analysis for T-1

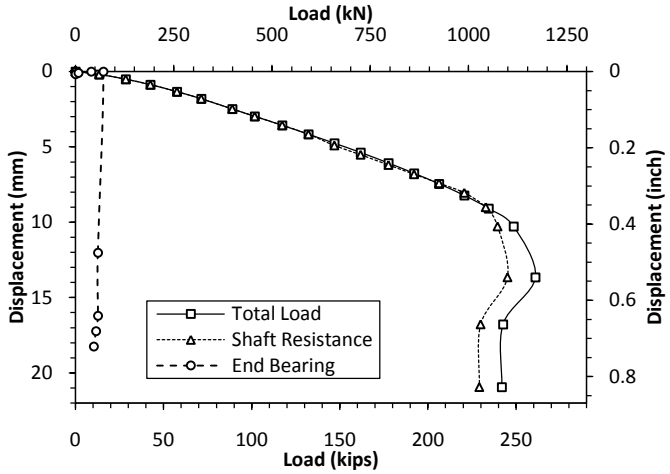

Figure 4.6: Measured pile load-displacement response at the pile head during static load test and calculated pile shaft and pile tip displacement for test site T-1

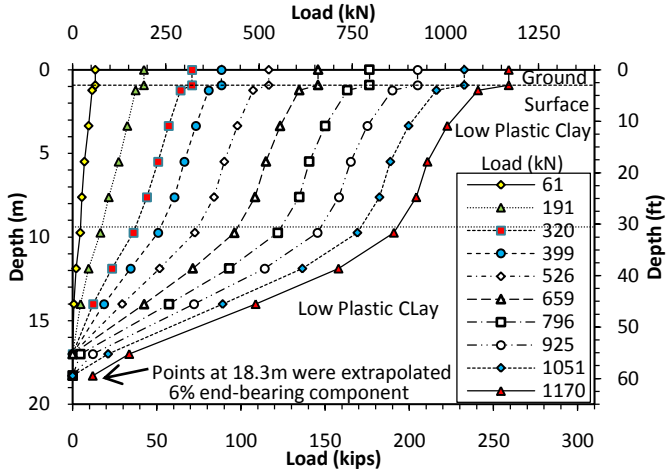

Figure 4.7: Load distribution along the pile length calculated from measured strains at different applied loads for test site T-1

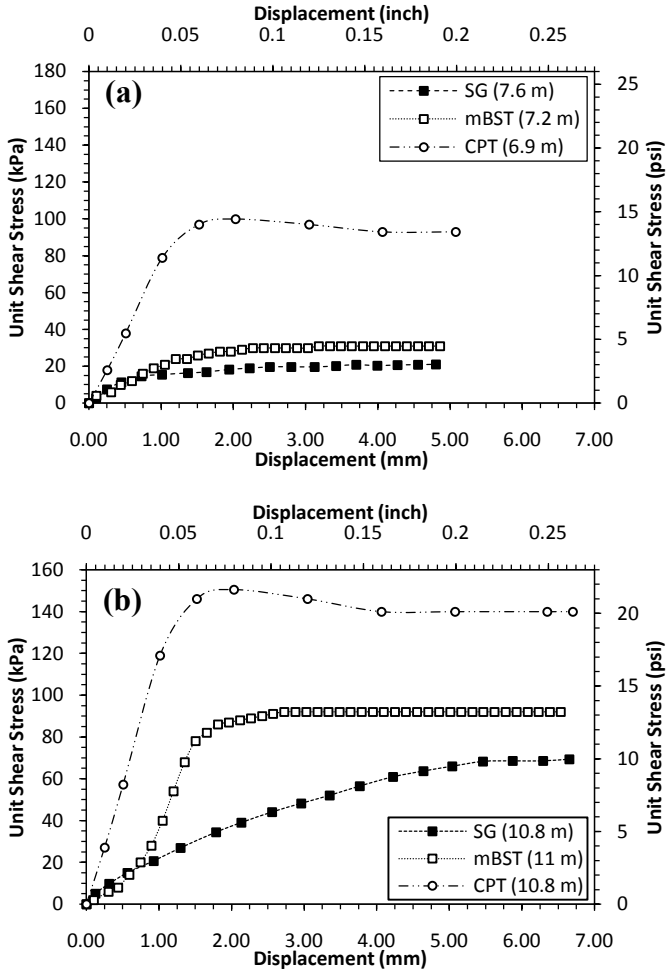

Figure 4.8: t-z curves developed from mBST and CPT compared with t-z curves back-calculated from strain gauge data within the two major soil layers at depths of 7.0 and 11.0 m for test site T-1

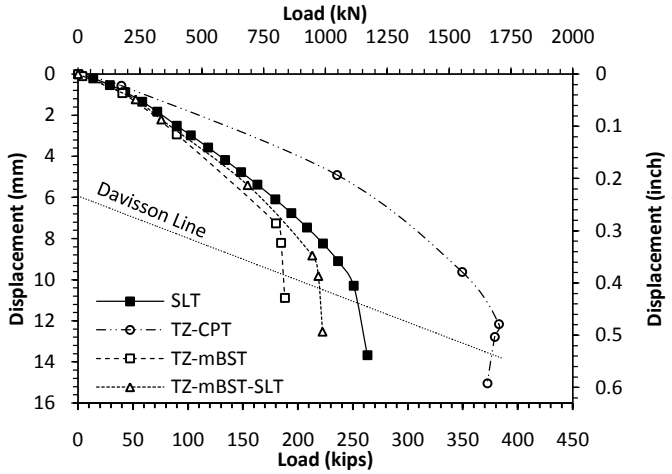

Figure 4.9: Load-displacement responses based on different t-z analyses compared with measured response for test site T-1

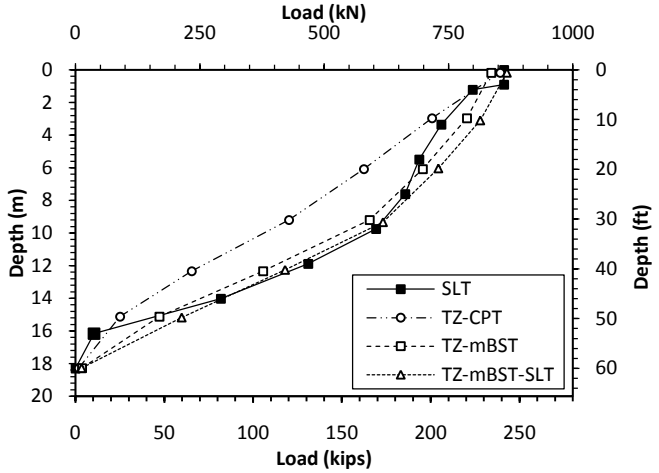

Figure 4.10: Load distribution along the pile length calculated using different t-z analyses compared with measured values at test site T-1

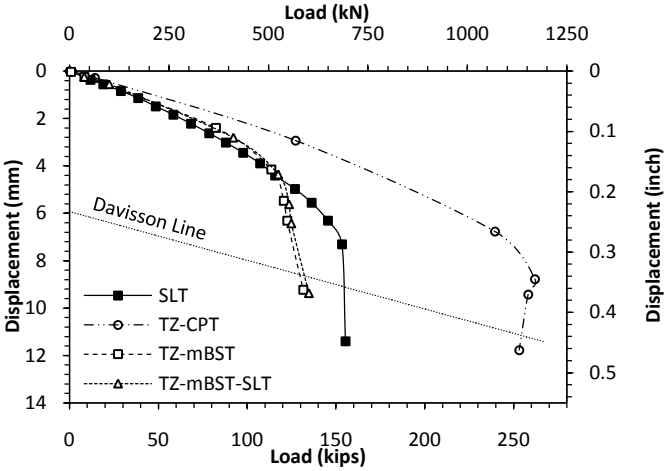

Figure 4.11: Load-displacement responses based on different t-z analyses compared with measured response for test site T-2

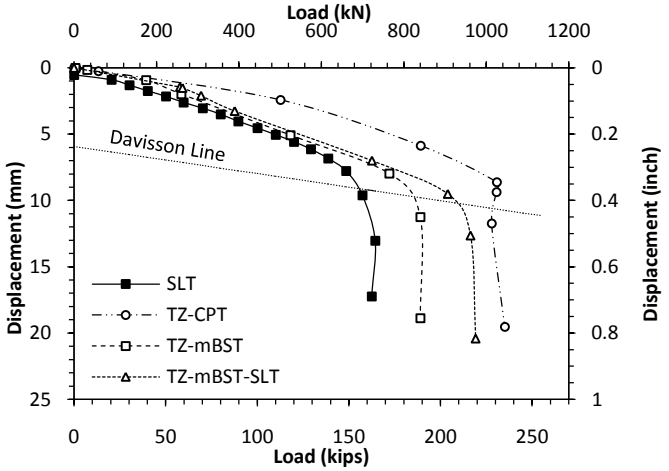

Figure 4.12: Load-displacement responses based on different t-z analyses compared with measured response for test site T-3

CHAPTER 5: IMPROVED T-Z ANALYSIS FOR VERTICALLY LOADED PILES IN COHESIONLESS SOILS BASED ON LABORATORY TEST MEASUREMENTS

Sherif S. AbdelSalam[1]; Muhannad T. Suleiman, M. ASCE[2]; Sri Sritharan, M. ASCE[3]

A paper to be submitted to the *Journal of Geotechnical and Geoenvironmental Eng*., ASCE

5.1. Abstract

Load transfer analysis (or t-z analysis) has been used to predict load-displacement response of axially-loaded piles. The *t-z* curves along pile length and *q-w* curve at pile tip are routinely obtained, based on empirical correlations using soil field or laboratory tests. This study focuses on the use of a *modified* Direct Shear Laboratory Test (mDST) to directly measure the *t-z* and *q-w* curves for steel piles driven into cohesionless soils. As part of this study, two full-scale instrumented steel H-piles driven into sandy soils were load tested and soil layers at the two sites were characterized using in-situ and laboratory soil tests. Load transfer analyses, with *t-z* and *q-w* curves directly measured using the mDST, were conducted to predict the response of full-scale load tests utilizing the TZPILE v.2.0 program. When compared to the measured load-displacement response and load distribution as a function of depth from the static load tests, the t-z models, based on mDST measurements, showed very good match with the measured responses. The proposed method presents a simple and cost-effective procedure to predict the pile response to aid in incorporating serviceability limits into the design of deep foundations.

CE Database keywords: Load-transfer; t-z analysis; *t-z* and *q-w* curves; Load-displacement; Direct shear test; Pile foundation.

[1] Graduate Student and Research Assistant, Dept. of Civil, Construction, and Environmental Engineering, Iowa State University, 355 Town Engineering, Ames, IA 50011-3232, E-mail:ssabdel@iastate.edu

[2] Assistant Professor, Dept. of Civil and Environmental Engineering, Lehigh University, STEPs Building, Room 326, 1 West Packer Avenue, Bethlehem, PA, 18015. E-mail: suleimam@lafayette.edu

[3] Wilson Engineering Professor and Associate Chair, Dept. of Civil, Construction and Environmental Engineering, Iowa State University, 376 Town Engineering, Ames, IA 50011-3232, E-mail: sri@iastate.edu

5.2. Introduction

In the United States, bridges and their foundations are now designed using the Load and Resistance Factor Design (LRFD) approach. In support of this, significant efforts have been directed towards the development of LRFD resistance factors for deep foundations. The current American Association of State Highway and Transportation Officials (AASHTO) specifications and several locally-developed design guidelines provide resistance factors to calculate pile resistance at the strength limit state, while the serviceability requirements that may be needed to prevent excessive pile settlements are typically checked after determining pile resistance. Thus, the typical design approach may not be efficient and may lead to several design iterations to satisfy the strength and serviceability requirements, especially when the serviceability limit state governs the design (Misra and Roberts, 2006). Therefore, a design methodology, based on predicting pile load-displacement response can incorporate both strength and serviceability limits in the design process (Misra et al., 2007; Roberts et al., 2008). However, the analytical approach for predicting the load-displacement response needs to be simple, yet it should produce acceptable accuracy for practicing engineers and designers to use. Due to its efficiency, simplicity, and potential in developing the serviceability limits for the design of deep foundations using the LRFD approach, load-transfer numerical analysis, using the t-z method, was selected as an iterative technique that solves nonlinear differential equations using the finite difference approach (Misra and Chen, 2004; Alawneh, 2006; Roberts et al., 2008).

The major shortcoming of the t-z analysis has been that no laboratory test was used to accurately measure the load-transfer curves, *t-z* and *q-w* curves, to describe the skin-friction between the pile and surrounding soil, and end-bearing at the pile's tip, respectively. Therefore, the *t-z* and *q-w* curves have been estimated, based on empirical correlations to in-situ soil tests, such as the Standard Penetration Test (SPT) or Cone Penetration Test (CPT) (see Coyle and Reese, 1966; Roberts et al., 2008). Recently, AbdelSalam et al. (2010) developed a modified Borehole Shear Test (mBST) that directly measures the *t-z* curves in the field for the interface between the steel pile and cohesive soil. Given these test piles were mainly friction piles, AbdelSalam et al. (2010) focused on measuring the *t-z* curves required for modeling shaft resistance of the pile. When compared to measured responses from three

full-scale vertical load tests conducted on steel H-piles installed in cohesive soils, the t-z analysis using load-transfer curves and mBST, showed good agreement with measured load-displacement response at the pile's head and load transfer along pile length. However, conducting mBST in cohesionless soils is not easy, due to the tendency of borehole collapse and/or the risk of losing the mBST shear head during testing. In addition, the mBST can only capture the *t-z* curves required for calculating the skin-friction component of the pile resistance, acceptable in the case of friction piles driven into mainly cohesive soil profiles, but in the case of cohesionless soils, the end-bearing component cannot be neglected.

The main objective of this study is to utilize the t-z analysis method to accurately predict the load-displacement response of vertically-loaded steel H-piles driven into cohesionless soils. For this purpose, a *modified* Direct Shear Test (mDST) was developed to measure the *t-z* curves for different soil layers in the laboratory. In addition, the box for the Direct Shear Test (DST) apparatus was used in a laboratory Pile Tip Resistance (PTR) test to measure the *q-w* curve for the end-bearing soil layer. The proposed mDST and PTR laboratory tests offer a simple and cost-effective method to directly measure the *t-z* and *q-w* curves, respectively. These measured curves can be used with commercial software, TZPILE v.2.0, developed by ENSOFT, Inc. to predict pile response using the t-z method. To validate the proposed approach, two vertical static load tests (SLTs) were conducted on full-scale instrumented steel H-piles driven into cohesionless soils at two different sites in Iowa and the predicted responses were compared with those field measured.

5.3. Background

The use of DST to measure the soil-pile interface friction angle for steel piles was initially proposed by Reddy et al. (2000) to estimate shaft capacity of steel piles driven into sandy soils. Later, Pando et al. (2002) performed a series of tests to measure the fiber reinforced polymer composite pile-soil interface friction angle. Pando et al. (2002) also conducted comparisons to the static shaft capacity, based on the Nordlund static method (Nordlund, 1963) and concluded the static calculated capacity using the interface angle measured, using DST, showed comparable values with the measured capacity. However, none of the studies cited above used DST to measure the *t-z* curves required for the load-

transfer analysis, or used the measured curves to predict pile load-displacement response and compared the analysis with field measured responses from pile static load test results.

For the end-bearing mechanism, numerous studies have investigated soil response under the pile tip utilizing small-scale models or calibrated chambers; several have focused on measuring the load-penetration response that represents the *q*-*w* curve at the pile's tip. For example, Houlsby and Evans (1988) studied steel pile bearing capacity in layered silts and sands, using a soil-pile laboratory model to determine the effect of different pile types on the load-penetration response. Yasufuku and Hyde (1995) investigated the relationship between the soil stress-strain properties at the pile's tip and the corresponding end-bearing capacity. However, neither of the previous studies used the laboratory measured load-penetration curve to conduct a load-transfer analysis or compared their results to measured responses from large-scale SLTs. Furthermore, determining the minimum permissible size of a soil-pile laboratory model with respect to the pile diameter or size (D) is not detailed in the aforementioned studies and has no clear design standards.

Nevertheless, Bowles (1996) indicated that soil stresses and corresponding displacements at a pile tip bearing on dense sand or sand-gravel deposits can be evaluated, with reasonable accuracy, assuming a fictitious rigid footing placed on the bearing stratum. To model a rigid footing in a test pit or a small soil box, the ASTM D 1194 standards (ASTM, 2006) states that the soil box size should be at least four times the width of the model footing. Given the depth of stresses influence below the pile tip ranges from 2D to 4D in different soils and is approximately 1.5D in the case of coarse sand deposits (Houlsby and Evans, 1988), the minimum required depth of the soil box should be at least 1.5D below the model rigid footing, bearing on dense sand or sand-gravel deposits. The summary provided above shows that for piles installed in dense sand or sand gravel deposits, a laboratory test with model rigid footing placed in a soil box with a width greater than 4D and depth greater than 1.5D can be used. However, when using small-scale rigid footings to represent pile tip response in dense sand or sand gravel deposits, the measured *q*-*w* curves for the model footing must be scaled or converted to represent the *q*-*w* of the large-scale pile as will be discussed later.

5.4. Field Testing

As part of an ongoing research project aimed at establishing LRFD resistance factors for the design of deep foundations in the state of Iowa by accounting for local soil conditions, ten vertical SLTs were conducted on full-scale instrumented steel HP 10x42 piles. The last two SLTs were conducted on piles driven into cohesionless soil profiles (mainly sand) at Des Moines County (test site ISU-9) and Cedar County (test site ISU-10). For ISU-9, the bridge site was located southeast of Huron close to the Mississippi River. As for ISU-10, the bridge was located south of Tipton at the intersection of Interstate-80 and the Iowa River. For both test sites, a 15.8 m (52 ft) long test pile with 14.9 m (49 ft) embedded length was driven between two anchor piles, 18.3m (60 ft) long with 16.4 m (54 ft) embedded length each. The test piles were loaded, using a 2000 kN (440 kips) hydraulic jack, and the applied load was measured using a 1300 kN (290 kips) load cell. The "Quick Test" procedure outlined in the ASTM D 1143 (ASTM, 2006) was used to load test the piles. In all cases, the load was applied in 5% increments of the estimated nominal capacity and the load was kept relatively constant at the end of each load increment for a duration ranging from 5 to 10 minutes until the pile vertical displacement readings stabilized. After excessive vertical displacement at approximately constant load was experienced, the piles were unloaded in five equal load decrements. In addition to using four 25.4 cm (10 inch) displacement transducers to measure the vertical displacement at the top of the two test piles, they were instrumented with strain gauges along the shaft and near the tip.

Figures 5.1 and 5.2 show the locations of strain gauges installed on each side of the web centerline of test piles ISU-9 and ISU-10, respectively. The locations of strain gauges presented in the figures were determined, considering different soil layers at the two test sites and included at least two gauges near the bottom of the piles to quantify tip resistance. The soil profiles at the test sites were characterized, using in-situ SPT and CPT tests in addition to several laboratory tests, including soil classification, Atterberg limits, as well as DST and mDST. At ISU-10, a push-in pressure cell was used to monitor the lateral earth pressure before and after driving of the piles as well as during SLT.

5.4.1. Soil investigation

SPT and CPT results

The typical geological formation at ISU-9 consists of normally consolidated Alluvium deposits of clay, sand, and gravel deposits. As shown in Figure 5.1, four different soil layers were found during drilling. The first layer consisted of clay deposits extending to 4.8 m (15.7 ft) below the ground surface, followed by sand deposits up to 13.4 m (43.9 ft),underlain by a 2.6 m (8.5 ft) of granular material, and the bottom layer consisted of firm silty clay material. The groundwater table at the time of in-situ testing was located at 5.2 m (17.1 ft) below the ground's surface. Using laboratory tests conducted on soil samples collected at ISU-9, the top soil layer was classified as low plasticity clay (CL) per the Unified Soil Classification (USCS), the second layer was classified as well-graded sand (SW), the third as well-graded gravelly sand (SW), and the bottom layer as inorganic clay of high plasticity clay (CH). In addition to the basic soil properties, Figure 5.1 summarizes the measured CPT tip resistance (q_c) and skin friction (f_s) for ISU-9. Also included in Figure 5.1 are the SPT blow counts corrected for the effect of the soil's overburden pressure and the corresponding relative density (D_r %) after Terzaghi and Peck (1967).

The soil profile at ISU-10 was divided into three layers, where the first layer consisted of sandy fill material extending to 4.6 m (15.1 ft) below the ground surface followed by a 10.4 m (34.1 ft) layer of coarse sand with gravel as presented in Figure 5.2. The bottom layer consisted of sand and boulders, and the groundwater table was located 3 m (9.8 ft) below the ground surface at the time of in-situ testing. Using laboratory tests conducted on the soil samples from ISU-10, the top soil layer was classified as well-graded sand (SW) per the USCS, the second layer was classified as well-graded sand with gravel seam (SW), and the bottom layer as well-graded gravelly sand (SW). As shown in Figure 5.2, a 1.0 m (3 ft) layer of boulders was located almost in the middle of the second layer, which prevented the CPT from penetrating to the desired depth. Figure 5.2 summarizes the basic soil properties, the measured q_c and f_s from the CPT results, the corrected SPT blow counts, and the relative density (D_r %) of different soil layers at ISU-10.

5.4.2. Monitoring lateral earth pressure

In preparation for conducting conventional and modified laboratory DSTs at different normal stresses to measure soil shear strength parameters and adequately capture the *t-z* and *q-w* curves along the soil-pile interface, expected ranges of lateral earth pressure (σ_h) acting along the test piles were required to determine the appropriate normal stresses for use in the DST and mDST tests. Figures 5.1 and 5.2 represent the location of DST/mDST for different soil layers at ISU-9 and ISU-10. To complete this task, the angle of soil internal friction (ϕ) and the over consolidation ratio (OCR) of soil layers were estimated, based on empirical correlations with SPT and CPT in-situ tests. Based on SPT results, the ϕ and the OCR were estimated after Peck, Hanson, and Thornburn (1974) and Mayne and Kemper (1988), respectively. For CPT-based estimates, recommendations by Robertson and Campanella (1983) and Mayne and Kulhawy (1990) were used. The at-rest lateral earth pressure coefficient (K_o) was then determined by using the equations recommended by Jaky (1944) and Mayne and Kulhawy (1990) for Normally Consolidated (NC) and Over Consolidated (OC) soils, respectively. Figures 5.1 and 5.2 summarize the K_o, OCR, and the corresponding effective σ_v along the pile length for NC and OC soils for ISU-9 and ISU-10.

To validate the estimated lateral earth pressure calculated based on SPT and CPT tests, a push-in pressure cell was installed at ISU-10 at 20 cm (8.0 inch) from the test pile flange and 3.1 m (10 ft) below the ground surface. The pressure cell data were continuously recorded during pile driving, re-striking, and SLT. On average, the effective lateral earth pressure measured by the pressure cell at the time of SLT was 22 kPa (3.2 psi), very close to the calculated value for NC soils at the same depth, using the theoretical correlations with SPT and CPT results (see Figure 5.2).

5.4.3. Pile static load tests

For test pile ISU-9, the load distribution along the pile length was established and presented in Figure 5.3, using the strain gauge data recorded at the end of each load increment during SLT. Figure 5.3 shows the rate of load transferred in the pile during the last nine load steps represented by the slope of the curves was almost zero within the top soil layer, indicating the cohesive material did not significantly contribute to pile resistance.

Within the second and third soil layers, an average rate of load transfer of 30 and 75 kN/m (2.1 and 5.1 kips/ft) was observed, respectively. Furthermore, the load transferred to the pile's tip during the test ranged from 0 to 210 kN (0 to 47.2 kips), indicating an end-bearing of approximately 28% of the maximum applied load.

The measured total load-displacement response of the ISU-9 pile is presented in Figure 5.4. Accordingly, pile response was approximately linear up to 521 kN (117.1 kips) and sustained a maximum applied load of 754 kN (169.5 kips). Based on Davisson's criterion (Davisson, 1972), the pile nominal capacity was determined 704 kN (158.3 kips). The *shaft* load-displacement was determined by integrating strain gauge data, using Simpson's numerical integration rule (Figure 5.3). The load-displacement curve at the pile tip was then back-calculated by subtracting the skin friction component from the total response measured at the pile's head. A similar procedure was used for the test pile at ISU-10, although the strain gauges were not functioning properly. This precluded an accurate separation of the skin friction and the end-bearing components from the pile's total capacity. Figure 5.4 represents the load-displacement response measured at the pile's head for ISU-10, indicating an approximate total nominal capacity of 580 kN (130.4 kips), based on Davisson's criterion.

5.5. Direct Measurement of Load-Transfer Curves

5.5.1. Modified direct shear test to measure the t-z curves

Conventional DST was modified to directly measure the *t-z* curves at the soil-pile interface for steel H-piles at ISU-9 and ISU-10. A square steel plate, with the same grade of the steel piles, was fabricated to fit into the lower half of the DST mold with dimensions equal to 100 mm (3.94 inch) in width and 40 mm (1.57 inch) in height. As shown in Figure 5.5, the steel plate is placed in the lower half of the shear box, while the upper half is filled with soil material compacted to match the soil unit weight and estimated relative density summarized in Table 5.1. Soil samples collected below the ground water table were submerged in de-aired water during testing. A normal stress equal to the estimated horizontal stresses on the surface of the pile at the depth of the tested sample was applied. The mDST was conducted following the ASTM D3080-98 (ASTM, 2006). While performing the mDST, the shear stress versus horizontal displacement was recorded after correction of the reduced

shear contact area, which represents the interface properties between the soil and the steel plate, or the *t-z* curve at the soil-pile interface.

For the test pile at ISU-9, conventional and modified DSTs were conducted on soil samples collected at depths of 2.6 m (8.5 ft), 7.0 m (23 ft), and 13.7 m (45 ft) below the ground's surface, covering the main soil layers at the test site. As an example of the measured properties, Figure 5.6 shows the Mohr-Coulomb failure envelope for the soil and the soil-pile interface obtained from DST and mDST results, respectively, at 7.0 m (23 ft) below the ground surface at ISU-9. As expected, the figure shows smaller values for adhesion (a) and friction angle (α) at the soil-pile interface, when compared to soil shear strength parameters. For all soil layers at ISU-9, Table 5.1 summarizes the values of the water content, dry and total soil unit weights, relative density, and normal stresses used during laboratory testing, in addition to the measured soil shear strength parameters (i.e., c' and ϕ'), and soil-pile interface properties (i.e., adhesion, a, and friction angle, α), using the DST and the mDST, respectively.

Figure 5.7 presents the measured *t-z* curves obtained using mDST at the soil-pile interface compared to those back-calculated from the strain gauge readings obtained from the SLT data at ISU-9. As can be observed from the figure, there is a good match between the laboratory and field measured t-z curves, especially when comparing the maximum shear stress values of the top and bottom soil layers, as the difference did not exceed 5%. The *t-z* curves presented in Figure 5.7 were measured at normal stresses corresponding to the measured and/or estimated lateral earth pressure in the field (see Table 5.1). For test site ISU-10, DST and mDST tests were conducted following the same procedures used for ISU-9 at different normal stresses as summarized in Table 5.1. The table also summarizes the soil shear strength parameters and soil-pile interface properties measured for the test pile at ISU-10. The test results for ISU-10 showed similar trends to those observed for ISU-9.

Using the load transfer analysis, the *t-z* curves were measured by utilizing mDST to predict pile load-displacement response. However, to include the end-bearing component, the *q-w* curve at the pile tip is needed. In the following section, another modification is proposed to the DST apparatus to measure the *q-w* curve at the pile's tip.

5.5.2. Pile tip resistance test to measure the q-w curves

As previously discussed, the response of the tip of a pile installed in sand deposits can be modeled as rigid footing in the laboratory. A small-scale steel plate (representing a fictitious rigid footing) was used to model the vertical load-displacement relationship (*q*-*w* curve) under the pile's tip for ISU-9 and ISU-10. The box with the DST apparatus, dimensions of 100 mm (3.94 inch) in width and 60 mm (2.36 inch) in height (see Figure 5.8), was used in a laboratory Pile Tip Resistance (PTR) test to measure the *q*-*w* curve for a small-scale steel plate.

To confirm the suggested relative dimensions between the soil box and the model plate summarized in the background section, steel plates with different sizes and shapes were tested. The box width to plate width ratios of 4 and 5.7 and box depth to plate width ratios of 2.4 and 3.4 were used. These plates were embedded by 10 mm (0.40 inch) in the compacted soil. For the model representing ISU-9, the soil sample collected at a depth of 15 m (49.2 ft) (i.e., the depth of the pile tip) was compacted inside the box to match the estimated D_r of 68%. For ISU-10, the sample collected at the pile's tip was compacted to achieve a D_r% of 76%. For both PTR tests at ISU-9 and ISU-10, the loads were applied in controlled steps equal to one-twentieth of the estimated maximum load, following testing procedures provided by Yasufuku and Hyde (1995). For each loading increment, the corresponding vertical displacement was measured until the rate of settlement was less than 0.01 mm/min.

When comparing the measured responses of different plates, the difference in the load-displacement curves measured using both steel plate sizes was determined less than 10%. Furthermore, the effect of placing the plate on the soil's surface was evaluated and found its effect is also less than 10%. Therefore, using different sizes and placement locations of steel plates did not significantly affect PTR test results. Hence, the box's dimensions relative to the used steel plates were considered acceptable.

In addition to the previous laboratory checks on box dimensions, a finite element (FE) analysis representing the used box in the PTR test, the soil, and the steel plate (with a box to plate width ratio of 4.0) was conducted to confirm the dimensions of the box and the plate have minimal effects on the measured responses. An axisymmetric FE model was used to simulate the behavior, based on the Mohr-Coulomb constitutive model for the soil material,

using the commercial computer program, PLAXIS 7.2. In the axisymmetric analysis, the model plate diameter of 28 mm (1.12 inch) was selected to provide the same cross-sectional area of the actual steel plate. The plate was modeled as a non-porous linear-elastic material with elastic modulus equal to $2x10^8$ kPa ($2.9x10^7$psi) and Poisson's ratio equal to 0.2. The soil's shear strength measurements from the DST laboratory test results (see Table 5.1) were used for the required parameters of the Mohr-Coulomb soil constitutive model. The FE model was manually adjusted to match the stress-displacement behavior measured from the laboratory model. Presented in Figure 5.9 is the evaluated normal stress corresponding to the prescribed vertical displacement of 7.0 mm (0.28 inch) for ISU-9. As seen from the figure, the maximum stresses induced in the soil were concentrated directly below the steel plate and degraded towards the bottom horizontal boundary to less than 18% of the maximum stress. Moreover, the maximum vertical displacement under the plate did not exceed 1.4D, where D is the diameter of the steel plate, even less than the minimum required depth of the soil box specified in the literature. Thus, based on experimental results and finite element analysis, the dimensions of the used box in the PTR test are large, compared to plate dimensions, and insignificantly affect the vertical load-displacement response of the load tested plates.

The load-displacement response of the PTR model plate with box to plate width ratio of 4.0 was used in the t-z analyses for ISU-9 and ISU-10. The measured load-displacement curves for the model plate were converted to load-penetration curves (*q*-*w* curves) for the full-scale pile at ISU-9 and ISU-10. According to Bowles (1988), the following expression can be practically used to extrapolate the model plate loads in the case of cohesionless soils.

$$q_{pile} = q_{model}\left(\frac{A_{pile}}{A_{model}}\right)$$

The q_{pile} and q_{model} represent the applied load on the full-scale pile and the model plate, respectively. A_{pile} and A_{model} represent the full-size and the model pile cross-sectional areas, respectively. By using the cross-sectional area ratio in the previous equation, the square shaped PTR model pile can be practically converted for the full-size actual pile (H-shaped). For displacement (*w*) calculations, Terzaghi and Peck (1967) provided an equation to convert the measured tip displacement of the model pile to that of the full size pile in

cohesionless soils as follows:

$$w_{pile} = w_{model} \left(\frac{2A_{pile}}{A_{pile} + A_{model}} \right)^2$$

The w_{pile} and w_{model} represent the vertical displacement of the full-scale pile and the model plate, respectively. In Figure 5.10, the *q*-*w* curves for the two test piles are presented after extrapolation from laboratory model tests. As seen in Figure 5.10, both piles failed in end-bearing at about the same maximum applied load of 52 kN (11.7 kips), corresponding to an approximate vertical displacement of 5.08 mm (0.2 inch).

5.6. Load-transfer Analysis

In this section, the *t*-*z* and the *q*-*w* curves measured, utilizing the mDST and the PTR tests, respectively, were used to model the skin-friction and the end-bearing components of the test piles using the load-transfer analysis (or the t-z model). The responses of ISU-9 and ISU-10 tests were predicted, using the t-z models and compared with measured responses.

5.6.1. Model description

In the t-z model, the pile is divided into several segments and is replaced by elastic springs. The surrounding soil is represented as a set of non-linear springs, with one spring depicting soil behavior at the pile's tip. The initial t-z model was developed by Coyle and Reese (1966) and Suleiman and Coyle (1976) in cohesive and cohesionless soils, respectively. Reddy et al. (1998) modified the model to account for pile elastic deformation in computing the mobilized skin friction, using an elastoplastic soil-pile interface model. The model was then improved to include a hyperbolic response for the springs representing the soil-pile interface by Misra and Roberts (2006). In each t-z model developed for the tested piles at ISU-9 and ISU-10, the HP 10x42 pile was divided into 50 segments with each segment represented by an elastic spring of constant stiffness term, AE=3.596x108 kN, where E and A are the elastic modulus and the cross-sectional area of the pile, respectively. To model the soil and soil-pile interface in the t-z models, the *t*-*z* and the *q*-*w* curves, respectively, were measured by using the mDST and the PTR tests.

5.6.2. Load-displacement curves

For ISU-9, the response of the full-scale test was evaluated using two different t-z analyses. Initially, the analysis was conducted using only the *t-z* curves measured by utilizing the mDST (i.e., assuming no end-bearing and only including shaft resistance in the analysis), called TZ-S-mDST, to compare the predicted response with the *shaft* load-displacement relationship calculated using strain gauge data. The analysis was then conducted, including both the *t-z* and *q-w* curves (TZ-T-mDST) to compare the predicted response with the measured *total* load-displacement relationship (i.e., measured load-displacement at the pile head). Figure 5.11 shows the predicted shaft and total load-displacement relationships compared with the measured responses. As shown in Figure 5.11, the predicted shaft load-displacement curve, using the TZ-S-mDST model, perfectly matches the measured relationship (with a difference of only 3.3% on the conservative side). On the other hand, the predicted total load-displacement relationship also provides a very good match of the measured total response along the first portion of the curve and a difference of 4% in the nominal capacity at the plastic portion, based on Davisson's criterion (see Table 5.2). In addition to comparing load-displacement responses, Figure 5.12 represents the load distribution along pile length at an applied load of 754 kN (170 kips), which represents the maximum applied load in the field, calculated by using the TZ-T-mDST model and compared to the measured pile response. This figure shows TZ-T-mDST provides a very good prediction of the load distribution along pile length compared to the loads based on strain-gauge measurements. Hence, the t-z analysis succeeded to accurately capture the load-displacement response and load transfer along pile length for ISU-9.

The total load-displacement response of the test pile at ISU-10 was predicted using the t-z model based on the *t-z* and *q-w* curves attained from the mDST and PTR tests, respectively (see Figure 5.13). As shown in the figure, the slope of the first portion of the predicted load-displacement response is about 12% stiffer than the measured response. Furthermore, the capacity estimated using Davisson's criterion from the TZ-T-mDST analysis was about only 4% higher than the pile capacity estimated from the measured response (see Table 5.2). Therefore, the TZ-T-mDST analysis matches the measured load-displacement response for ISU-10 with acceptable accuracy. Based on comparisons with

measured responses for ISU-9 and ISU-10, it is evident the load-transfer analysis, based on laboratory measured *t-z* and *q-w* curves, respectively, using the mDST and PTR tests, provided an accurate and effective means of predicting the load-displacement response of vertically-loaded steel piles in sandy soils.

5.7. Summary and Conclusions

The main goal of this study was to improve the prediction of the load-displacement response of steel H-piles driven into cohesionless soils. The t-z analysis was used for this purpose, utilizing TZPILE v.2.0 software. A laboratory *modified* Direct Shear Test (mDST) and Pile Tip Resistance (PTR) test were proposed to improve t-z analysis by measuring load transfer curves. The mDST and PTR basically provided a measure for the *t-z* and *q-w* curves, respectively, required for t-z analysis and represent the skin-friction and the end-bearing of steel piles driven into sand soils. As part of this study, two static load tests were conducted on full-scale instrumented steel H-piles at two locations (ISU-9 and ISU-10) with cohesionless soil profiles. The soil investigation program for both test sites included in-situ tests, such as SPT, CPT, and push-in-pressure-cells, as well as laboratory tests, such as soil classification and DST. The t-z analysis, based on mDST and PTR measurements, provided the shaft load-displacement response (TZ-S-mDST), as well as the total load-displacement response (TZ-T-mDST). The results were compared to the responses measured in the field. A summary of the major findings is presented below.

- The laboratory measured *t-z* curves obtained, using mDST, were compared to those measured in the field using strain gauges readings. It was found the differences between them at the maximum shear stress did not exceed 5%.
- The PTR test was conducted to measure the *q-w* curve, using different sizes and placements of the small-scale steel plate. It was determined the effect of changing these factors on the results is minimal and did not exceed 10%.
- A FE model was utilized to assess the effect of the PTR box boundaries on the small-scale steel plate behavior, where the displacements induced in the model soil did not exceed 1.4D. Hence, the PTR box dimensions are acceptable.

- For the test pile at ISU-9, the predicted load-displacement relationship for the shaft using the TZ-S-mDST model perfectly matches the measured response.
- When adding the end-bearing component to the ISU-9 analysis (i.e., TZ-T-mDST), the model provided a very good match of the measured load distribution as a function of depth, as well as the total load-displacement curve, with only 3.3% softer response along the elastic portion of the curve and 4% lower capacity at the plastic portion.
- The TZ-T-mDST model also showed very good prediction of the measured total load-displacement response for ISU-10 with an acceptable error of about 12% along the elastic portion of the curve and about 4% at the plastic portion.
- Based on overall response predictions for the two test piles, the load transfer analysis, with *t-z* and *q-w* curves measured using the mDST and PTR tests, respectively, has proven to provide a very good match of the measured responses, which offer a simple and cost-effective procedure to predict steel pile responses.

Finally, similar studies can be conducted for other pile types, such as concrete piles, and the proposed procedure can help incorporate serviceability limits into the LRFD design of deep foundation, based on predicting pile load-displacement response.

5.8. Acknowledgments

The study reported in this paper was conducted by the authors as part of the ongoing research project TR-573: Development of LRFD Design Procedures for Bridge Pile Foundations in Iowa funded by the Iowa Highway Research Board (IHRB). The authors express their gratitude to the IHRB and members of the project Technical Advisory Committee for their guidance and advice. The members of this committee represent Office of Bridges and Structures, Soils, Design Section, and Office of Construction of the Iowa DOT, FHWA Iowa Division, and Iowa County Engineers. Finally, special thanks to Kam Weng Ng and Matthew Roling for their help during the field/laboratory tests.

5.9. References

AbdelSalam, S. S., Suleiman, M. T., and Sritharan, S. (2010). "Modeling Axially-loaded Friction Steel H-Piles using the Load-Transfer Approach Based on a Modified Borehole Shear Test." Submitted to *Geotechnical Testing Journal*, ASTM.

Alawneh, A. S. (2006). "Modeling Load–Displacement Response of Driven Piles in Cohesionless Soils under Tensile Loading." *Computers and Geotechnics*, 32.

ASTM (2006). "Annual Book of ASTM Standards, Soil and Rock (I)." *American Society for Testing and Materials*, Vol. 4.08, ASTM, Philadelphia, PA.

Bowles, J. (1988). "Foundation Analysis and Design." 4th Edition, McGraw-Hill, New York.

Coyle, H. M. and Reese, L. C. (1966). "Load Transfer for Axially-loaded Piles in Clay." *Journal of Soil Mechanics and Foundation Engineering Division*, 92(2), 1- 26.

Davisson, M. (1972). "High Capacity Piles." *Proceeding: Soil Mechanics Lecture Series on Innovations in Foundation Construction*, ASCE, IL Section, Chicago, IL, pp. 81–112.

De Gennaro, V., Said, I., and Frank, R. (2006)."Axisymmetric and 3D Analysis of Pile Test using FEM." *Numerical Methods in Geotechnical Engineering*, 2006 Taylor & Francis Group, London, ISBN 0-4 15-40822-

El-Mossallamy, Y. (1999). "Load-Settlement Behavior of Large Diameter Bored Piles in Over-consolidated Clay." *Proceeding: The 7th International Symposium on Numerical Models in Geotechnical Engineering*, September 1999, 433-450. Rotterdam, Balkema.

Engin, H. K., Septanika, E. G., and Brinkgreve, R. B. (2007). "Improved Embedded Beam Elements for the Modeling of Piles." *Proceeding: The 10th International Symposium on Numerical Models in Geotechnical Eng.* – NUMOG X, Rhodes (Greece).

Houlsby, G. T., Evans, K. M., and Sweeney, M. (1988). "End bearing capacity of model piles in layered carbonate soils."*Proc. Int. Conf. on Calcareous Sediments*, Perth, Australia, Balkema, Vol. 1, 209–214.

Jaky, J. (1944). "The Coefficient of Earth Pressure at Rest." *Journal of Society of Hungarian Architects and Engineers*, Budapest, Oct. 1944, pp. 355-358.

Mayne, P. W. and Kemper, J. B. (1988). "Profiling OCR in Stiff Clays by CPT and SPT." *Geotechnical Testing Journal*, ASTM, Vol. 11, No. 2, pp. 139-147.

Mayne, P. W. and Kulhawy, F. H. (1990). "Manual on Estimating Soil Properties for Foundation Design." Rpt. EL-6800, Electric Power Research Inst., Palo Alto, 306 p.

Misra, A. and Chen, C. H. (2004). "Analytical Solutions for Micropile Design under Tension and Compression." *Geotechnical and Geological Engineering*, 22(2), 199-225.

Misra, A. and Roberts, L. A. (2006). "Probabilistic Analysis of Drilled Shaft Service Limit State Using the "t-z" Method." *Canadian Geotechnical Journal*, 1324-1332 (2006).

Nordlund, R. L. (1963). "Bearing capacity of piles in cohesionless soils."*Journal of Soil Mechanics and Foundation Engineering*, JSMFE, Vol. 89, No. SM 3.

Pando, M., Filz, G., Dove, J., and Hoppe, E. (2002). "Interface Shear Tests on FRP Composite Piles." *ASCE International Deep Foundations Congress*, Orlando, FL, Vol.2, 1486-1500.

Peck, R. B., Hanson, W. E., and Thornburn, T. H. (1974). "Foundation Engineering."John Wiley & Sons.

Reddy, E. S., Chapman, D. N., and Sastry, V. V. (2000). "Direct Shear Interface Test for Shaft Capacity of Piles in Sand." *Geotechnical Testing Journal*, Vol. 23, No. 2.

Reddy, E. S., O'Reilly M., and Chapman, D. A. (1998). "Modified t-z Model - A Software for Tension Piles." *Computers and Structures*, 68: 613–25.

Roberts, L. A., Gardner, B. S., and Misra, A. (2008). "Multiple Resistance Factor Methodology for Service Limit State Design of Deep Foundations using a 't-z' Model Approach." *Proceeding: The Geo-Congress 2008, New Orleans, LA*.

Robertson, P. K. and Campanella, R. G. (1983). "Interpretation of Cone Penetration Tests." *Canadian Geotechnical Journal*, Vol. 20, No. 4, Nov. 1983.

Schmertmann, J. B. (1978)."Guidelines for Cone Penetration Test, Performance and Design." *Report No. FHWA-TS-78-209, U.S. DOT*, Washington, D.C., pp. 145.

Suleiman, I. B. and Coyle, H. B. (1976). "Uplift Resistance of Piles in Sand." *Journal of Geotechnical Engineering*, ASCE 1976; 102(GT5):559–62.

Terzaghi, K. and Peck, R. B. (1967). "Soil Mechanics in Engineering Practice." John Wiley & Sons.

Yasufuku, N. and Hyde, A. F. (1995). "Pile End-bearing Capacity in Crushable Sands." *Geotechnique* 45, No.4, pp. 663-676.

Table 5.1: Soil and soil-pile interface shear strength parameters measured using the SPT, CPT, DST, and mDST at different depths

Test Site	Depth (m)	w_c%	γ_{dry} kN/m^3	γ_{bulk} kN/m^3	D_r%[ɣ]	Normal Stress Range			DST		mDST	
						P_n (kPa)			c' (kPa)	ϕ'	a (kPa)	δ
ISU-9	2.6	24%	18.8	23.4	163[†]	10	20[*]	30	N/A	N/A	9.7	14.2
	7.0	23%	18.5	22.9	38%	60	100[*]	128	0	37.0	1.6	25.5
	13.7	18%	21.4	25.2	68%	108	206[*]	295	0	39.1	0	28.2
ISU-10	2.1	15%	17.6	20.2	40%	25[*]	40	60	7.2	37.6	3.6	28.7
	7.6	18%	20.3	24.0	70%	60[*]	120	170	32.2	29.6	0	31.5
	13.7	7%	22.2	23.7	76%	120[*]	220	310	0.2	41.3	0	33.5

For unit conversion: 1 m = 39.37 inch; 1 kN/m^3 = 6.24 lb/ft^3; and 1 kPa = 0.145 psi.
[ɣ] Calculated based on SPT data after Terzaghi and Peck (1967); [*] Represents the normal stress corresponding to measured lateral earth pressure and selected for TZ-mDST analyses; and †Value of the undrained shear strength in kPa for the clay layer calculated based on CPT test results using correlations from Schmertmann et al. (1978), assuming N_k=15.

Table 5.2: Summary of the t-z model findings compared to the field test results

Test Site	Model	Model Description		Load-Displacement Curve		% Difference to SLT[*]	
		t-z curves *(skin-friction)*	*q-w* curve *(end-bearing)*	Slope of First Portion (kN/m)	Davisson Capacity (kN)	Slope of First Portion	Davisson Capacity
ISU-9	SLT	Strain Gauges Readings		132,178	704	Measured Pile Response	
	TZ-S-mDST	mDST	Ignored	127,779	550	3.3% softer	22% lower
	TZ-T-mDST	mDST	PTR	127,779	675	3.3% softer	4% lower
ISU-10	SLT	Strain Gauges Readings		87,391	580	Measured Pile Response	
	TZ-S-mDST	mDST	Ignored	98,036	484	12% stiffer	17% lower
	TZ-T-mDST	mDST	PTR	98,036	603	12% stiffer	4% higher

For unit conversion: 1 m = 39.37 inch; and 1 kN = 0.224 kips.
[*]Difference between the load-displacement curves adapted from the t-z analyses and the pile measured response during SLT.

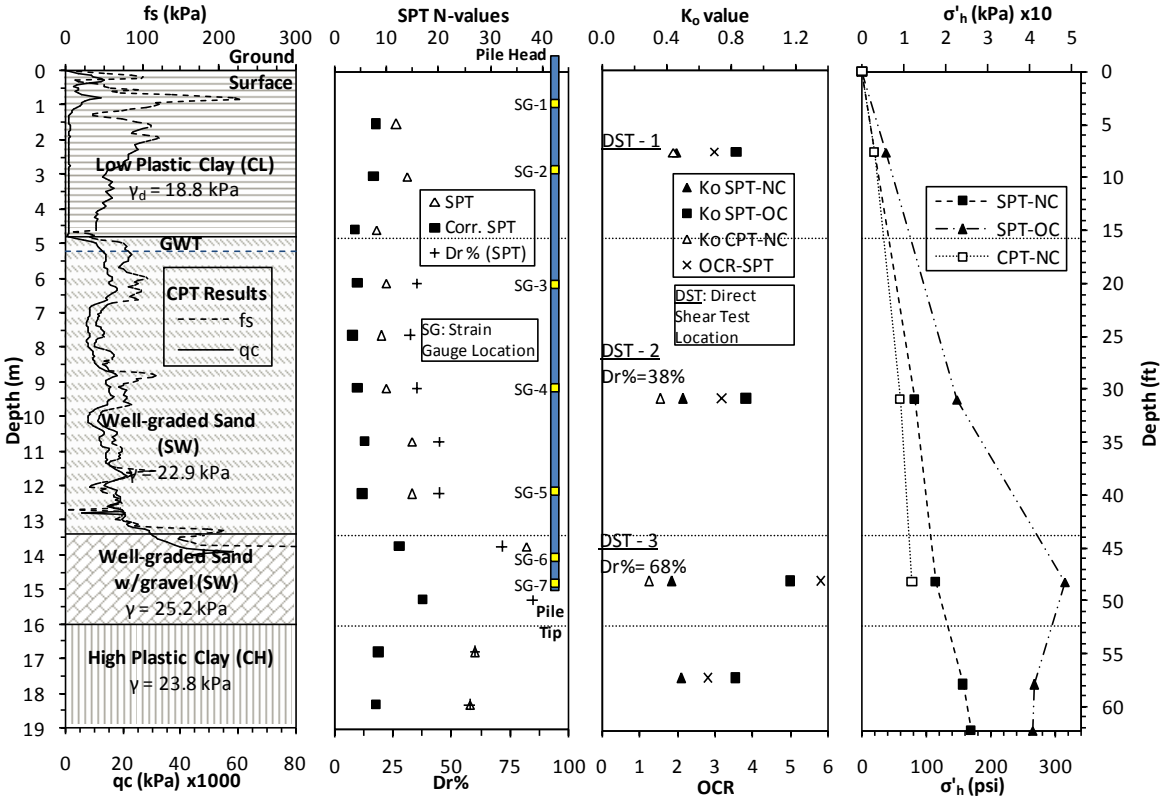

Figure 5.1: Summary of soil tests conducted at ISU-9 including: tip resistance (q_c) and skin friction (f_s) from CPT;SPT N-values and corresponding D_r%;soil classification; calculated K_o and OCR for NC and OC soils; corresponding effective lateral earth pressure; depths of DST/mDST; and strain gauge locations along the test pile

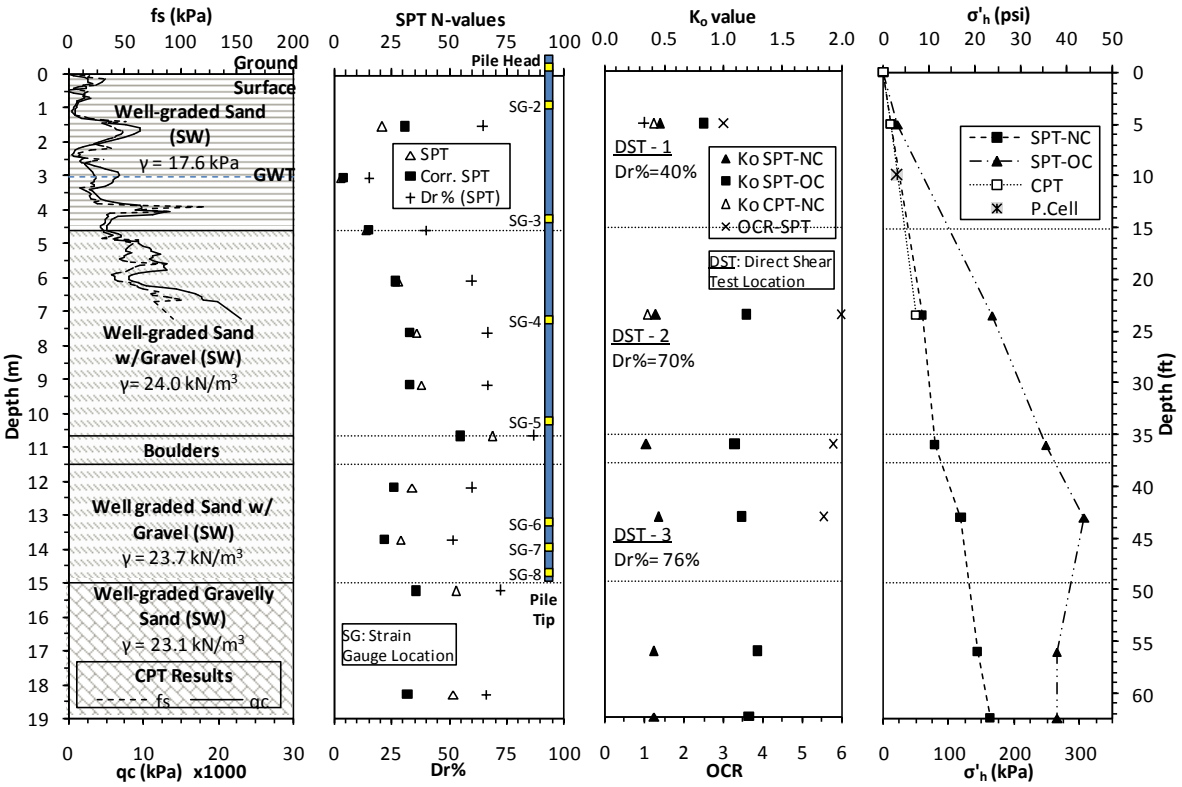

Figure 5.2: Summary of soil tests conducted at ISU-10 including: tip resistance (q_c) and skin friction (f_s) from CPT;SPT N-values and corresponding D_r%;soil classification; calculated K_o and OCR for NC and OC soils; corresponding effective lateral earth pressure; depths of DST/mDST; and strain gauge locations along the test pile

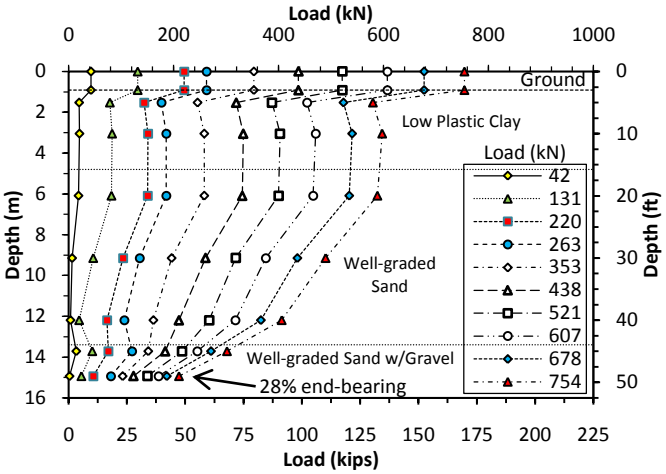

Figure 5.3: Load distribution along the pile length calculated from measured strains at different applied loads for test site ISU-9

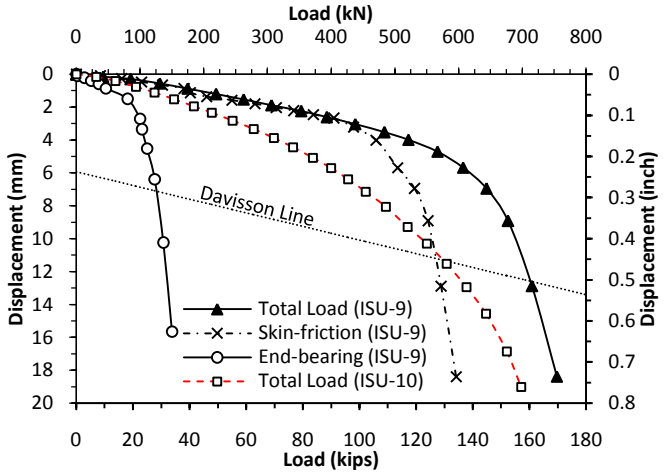

Figure 5.4: Measured load-displacement response at the pile head during SLT for ISU-9 and ISU-10, and separated skin-friction and end-bearing components for ISU-9

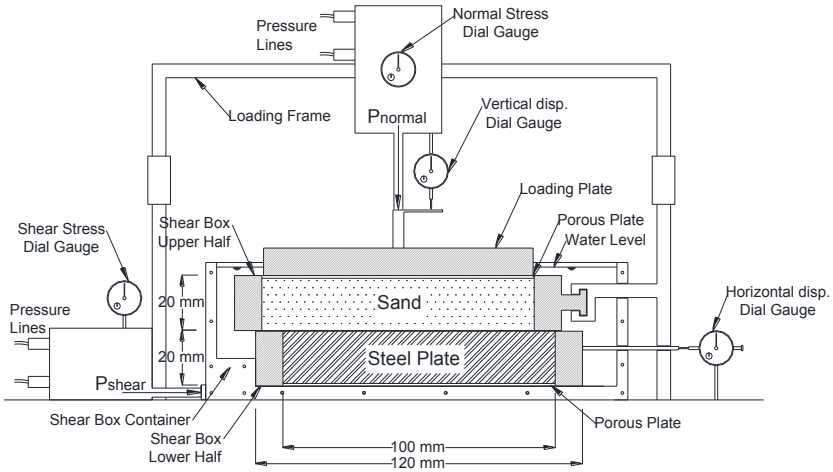

Figure 5.5: Overview of the mDST unit as used to measure the *t-z* curves

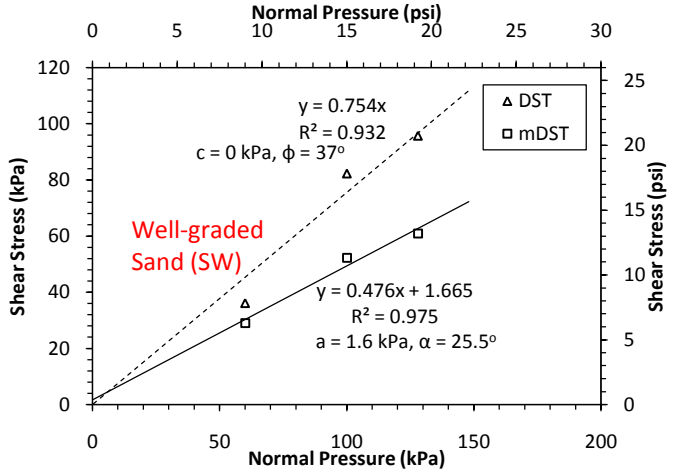

Figure 5.6: Mohr-Coulomb failure envelope for the soil and the soil-pile interface obtained using DST and mDST, respectively, at depth of 7 m forISU-9

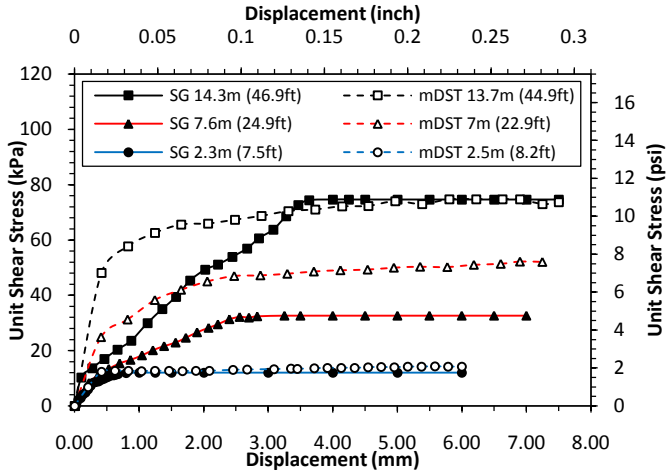

Figure 5.7: Comparison of *t-z* curves developed from mDST with those back-calculated from strain gauges(SG)for the soil layers at test site ISU-9

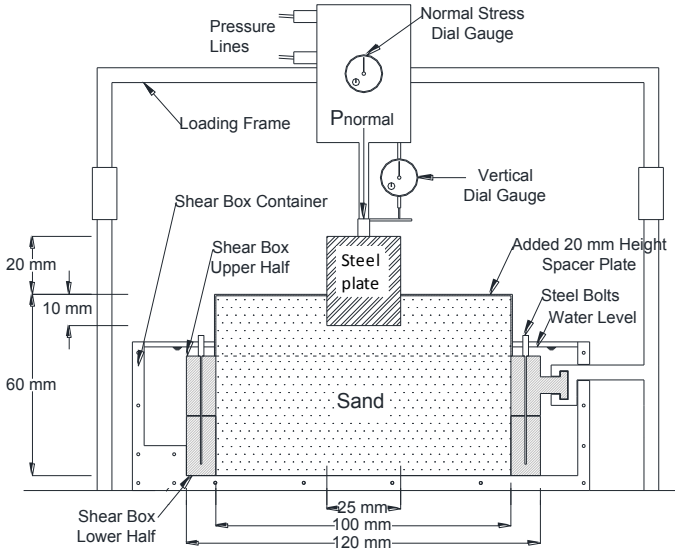

Figure 5.8: Overview of the PTR unit as used to measure the *q-w* curves

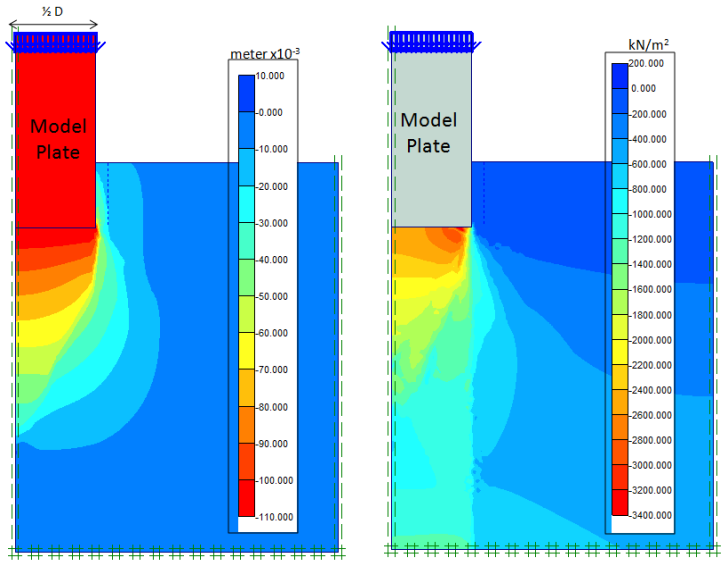

(a) Max. vertical displacement **(b) Max. effective normal stresses**

Figure 5.9: FE model results representing the PTR test conducted for ISU-9

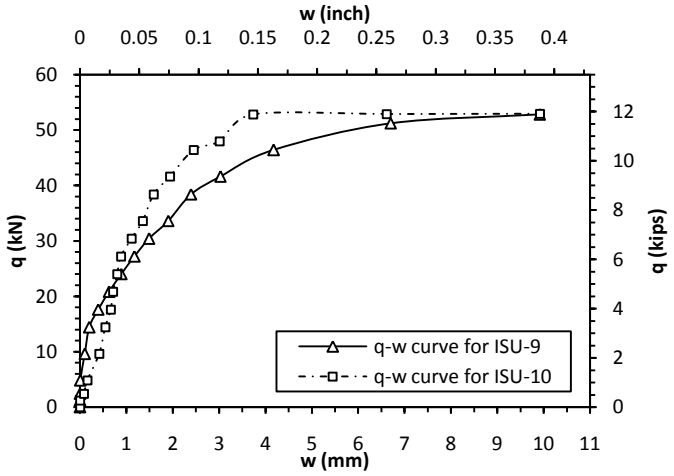

Figure 5.10: Comparison of the *q-w* curves obtained for the two test piles after extrapolation from the PTR test results

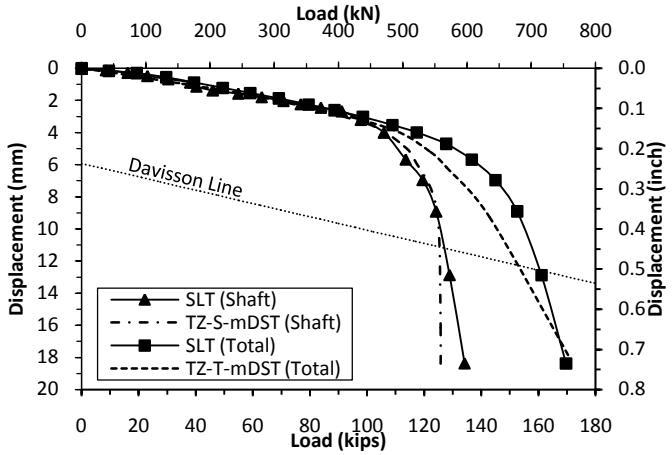

Figure 5.11: Load-displacement responses based on different t-z analyses and compared with measured response for test site ISU-9

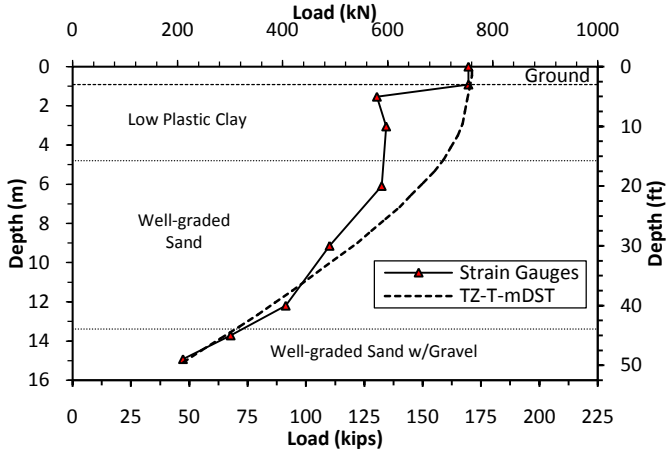

Figure 5.12: Load distribution along the pile length calculated using TZ-T-mDST and compared with measured values at test site ISU-9

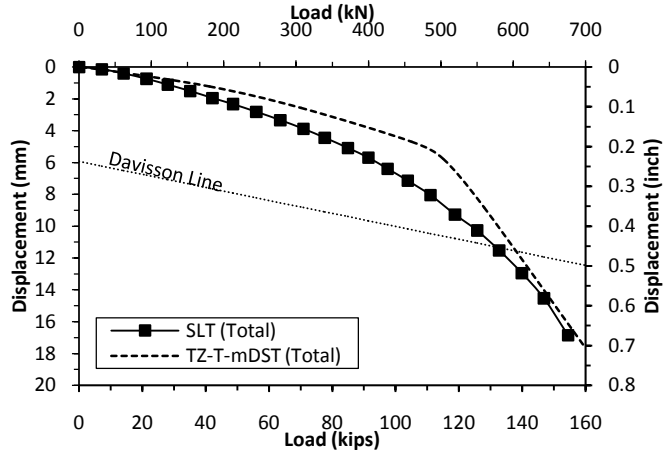

Figure 5.13: Load-displacement responses calculated using TZ-T-mDST and compared with measured values at test site ISU-10

CHAPTER 6: PILE RESPONSE CHARACTERIZATIONUSING A FINITE ELEMENT APPROACH

Sherif S. AbdelSalam[1]; Sri Sritharan, M. ASCE[2]; Muhannad T. Suleiman, M. ASCE[3]

A paper to be submitted to a conference proceeding

6.1. Abstract

The study presented herein focused on improving the accuracy and efficiency of simplified two-dimensional finite element (FE) models in simulating the response of vertically-loaded steel piles driven into cohesive and cohesionless soils. For this purpose, data from four static load tests (SLTs) conducted on instrumented steel H-piles driven into clay and sand soil profiles accompanied by various in-situ and laboratory soil tests were used. The behavior of the load-tested piles was simulated using axisymmetric FE analyses, based on the Mohr-Coulomb soil constitutive model by means of PLAXIS 7.2. Following identification that the elastic modulus of cohesive soils and the soil-pile interface properties are poorly represented in the analysis, these capabilities were improved first. The modulus of clay soil was obtained from a Consolidated Undrained (CU) Triaxial soil laboratory test, while the *modified* Direct Shear Test (mDST) was utilized to provide an accurate laboratory measurement of the soil-pile interface properties. With these refinements, the FE model provided an improved prediction for the load-displacement response of the four test piles without using sophisticated soil constitutive models that require conducting costly and time consuming tests.

Keywords: Finite Element; Pile Foundations; Soil-structure Interaction; Load-displacement; Interface Element; Soil Elastic Modulus.

[1] Graduate Student and Research Assistant, Dept. of Civil, Construction, and Environmental Engineering, Iowa State University, 355 Town Engineering, Ames, IA 50011-3232, E-mail:ssabdel@iastate.edu

[2] Wilson Engineering Professor and Associate Chair, Dept. of Civil, Construction and Environmental Engineering, Iowa State University, 376 Town Engineering, Ames, IA 50011-3232, E-mail: sri@iastate.edu

[3] Assistant Professor, Dept. of Civil and Environmental Engineering, Lehigh University, STEPs Building, Room 326, 1 West Packer Avenue, Bethlehem, PA, 18015. E-mail: suleimam@lafayette.edu

6.2. Introduction

An analysis approach to predict the load-displacement response of axially-loaded piles can facilitate incorporation of both strength and serviceability limit states in routine design of deep foundations. According to Guo and Randolph (1998), analytical methods used to characterize pile behavior can be classified into three major categories: (1) approximate closed-form solutions, (2) one-dimensional numerical algorithms, and (3) boundary or finite element methods. The first two categories depend on load-transfer analysis, an iterative technique for solving the nonlinear differential equations of load-transfer using the finite-difference method (Coyle and Reese, 1966; Suleiman and Coyle, 1976). The third category depends on a more comprehensive modeling technique and accurate characterization of material behavior.

Recently, numerous studies have successfully adapted the load-transfer analysis (t-z analysis) to model the pile behavior under axial loads (Misra and Chen, 2004; Misra and Roberts, 2006; Roberts et al., 2008; AbdelSalam et al., 2010). Although the t-z analysis provides the load-displacement response at the pile head and load transfer as a function of pile depth, it does not provide the stresses and strains induced in the surrounding soil medium. Consequently, the t-z method may not provide insight into the response of soil and pore water pressure development around the pile (Wathugala and Desai, 1989). The repercussion of not having this knowledge is that the influence of the load transferred through one pile on adjacent piles in a pile group or nearby shallow or deep foundations may not be known. In these cases, it is important to use a detailed model to examine the load transfer in a pile. For vertically-loaded piles, the soil properties and the interface element behavior are the most important parameters that control the accuracy of the finite element (FE) analysis outcomes. More specifically, De-Gennaro et al. (2006) and Engin et al. (2007) reported soil-pile interface properties and the soil modulus typically estimated, based on empirical correlations, largely dictate FE analysis results. Therefore, utilizing more detailed laboratory tests to obtain the soil constitutive properties may be appropriate (De-Gennaro et al., 2006; Engin et al., 2007). The accuracy of the FE analysis results is also dependent on the pile material and construction techniques (El-Mossallamy, 1999).

The objective of this study is to examine the accuracy and efficiency of a simplified

Mohr-Coulomb soil constitutive model in simulating the response of vertically-loaded steel H-piles driven into cohesive and cohesionless soils by utilizing a two-dimensional axisymmetric FE analysis using PLAXIS 7.2. For this purpose, data from four vertical static load tests (SLTs) conducted on instrumented steel H-piles accompanied with various in-situ and laboratory soil tests were used. In the preliminary FE analysis, the soil constitutive parameters were estimated, based on empirical correlations with Cone Penetration Test (CPT) data. Two parameters were determined to represent the main potential sources for error in the FE model. These two parameters were the soil-pile interface properties and the soil elastic modulus. To improve the determination of these parameters, the soil-pile interface properties were measured in the laboratory using a *modified* Direct Shear Test (mDST), which directly measures the shear stress versus displacement relationship at soil-steel contacts without the use of empirical correlations. In addition, the soil elastic modulus was measured by means of a Consolidated Undrained (CU) Triaxial soil test. Measured soil constitutive properties were used in the FE model, which showed significant improvement in predicting the pile load-displacement behavior compared with the field measured responses of the four load tested piles. A significant benefit of improving the simplified FE model is that it can facilitate incorporation of the vertical settlement and serviceability limits into the design of deep foundations.

6.3. Preliminary FE Model

For soil-structure interaction problems, the commercially-available finite element code, PLAXIS, has been widely used and reported by many researchers to model the behaviour of deep foundations with an acceptable accuracy (Prakoso and Kulhawy 2001; Sellountou et al., 2005; Oh et al., 2008). In this study, PLAXIS was used because it is capable of solving non-linear plasticity problems using a “staged construction” operation, which allows for changing the load configuration on the model pile head, pore water pressure distribution, and pile geometry. Ideally, a three-dimensional analysis is preferable to simulate the behaviour of steel H-piles, but as iterated before, this is the first attempt to analyze steel H-piles using a simplified axisymmetric model in sand and clay soils. The H-pile was represented in the axisymmetric model assuming the cross-section of the actual pile is

circular. However, the model pile diameter was selected to provide the same surface area of the actual H-pile along the shaft, while the cross-section of the model pile was gradually reduced at the tip to reflect the actual area of the pile's tip. The H-pile was modeled using a non-porous linear-elastic constitutive model with properties summarized in Table 6.1. To eliminate the effects of the FE model vertical boundaries on the soil-pile response, the model diameter was selected equal to 7.0D, where D is the model pile diameter. Also, a length equal to 5D was defined between the model pile tip and the bottom horizontal boundary of the FE model.

The preliminary FE analysis was conducted to model the behavior of four statically load tested piles. Two of the test piles with identification numbers (ISU-4 and ISU-5) were driven into cohesive soil layers and the other two test piles (ISU-9 and ISU-10) were driven into mainly cohesionless soil layers. Table 6.1 summarizes soil layers and soil properties for all test sites. As can be seen in the table, the unit weights of different soil layers were measured in the laboratory, while the remaining soil constitutive parameters were estimated using correlations with the CPT results. All the empirical correlations with the CPT data used to estimate the soil properties are referenced in Table 6.1. In all cases, the Mohr-Coulomb model was used to describe the constitutive soil behavior utilizing an unstructured very fine mesh consisting of 15-node triangular elements. The Mohr-Coulomb elastic perfectly plastic model was selected for this preliminary FE analysis because it is one of the most widely used constitutive models and has proven to be quite accurate and efficient in simulating soil-structure interaction problems (Tan and Bui, 2006). In addition to the elastic soil modulus and Poisson's ratio, E_s and ν, respectively, the Mohr-Coulomb model incorporates the use of three plastic parameters, φ, c, and ψ, which denote the friction angle, cohesion, and dilatancy angle of the soil material, respectively. The angle of dilatancy can be defined as the tendency of soil to expand in volume due to shear. Table 6.1 includes all the required soil constitutive parameters for this analysis based on the Mohr-Coulomb model.

In the preliminary FE models, the ground water table was defined for all test sites, using the phreatic surface option of the program and the initial stresses were generated using the predefined K_o values based on the friction angle of the soil. For the interface element between the soil and the pile, the PLAXIS code uses a virtual zero thickness element with

reduced properties that connect pile elements with surrounding soil elements. The reduced interface properties are defined for each soil layer by determining the strength reduction factor for interfaces (R_{inter}). This factor relates the strength of the interface (in terms of friction angle, α, and adhesion, a) to the soil cohesion and friction angle. Based on the PLAXIS user manual recommendations, the R_{inter} can be assumed equal to 0.50 and 0.67 for clay-steel and sand-steel contacts, respectively. Table 6.1 summarizes the used values of the R_{inter} in the preliminary FE analysis for different soil layers presented at the four test sites.

Table 6.1: Constitutive soil parameters estimated using empirical correlations to CPT

Test Site	Soil Layers[(1)]	Thickness m	γ_{dry} kN/m^3	γ_{wet} kN/m^3	S_u[(2)] kPa	c[(3)] kPa	ϕ[(4)]	ν[(5)]	E_s[(6)] kPa	R_{inter}
ISU-4 (GWT: 4.5m)	Clay	0 - 1.5	17	21.3	101	50	34	0.3	9347	0.5
	Clay	1.5 - 5.5	18.2	21.3	102	51	29	0.25	10586	0.5
	Clay	5.5 - 11	18.9	21.3	177	88	33	0.35	13662	0.5
	Clay	11 - 18	19.5	22.4	129	64	31	0.35	10366	0.5
ISU-5 (GWT: 10.0m)	Clay	0 - 7.6	17.5	21.1	107	54	32	0.30	9753	0.5
	Clay	7.6 - 12	19.5	22.9	148	74	32	0.30	13638	0.5
	Clay	12 - 18	20.5	23.8	180	90	34	0.35	16464	0.5
ISU-9 (GWT: 5.2 m)	Clay	0 - 4.8	18.8	23.4	216	108	34	0.25	17070	0.5
	Sand	4.8 - 13	18.5	22.9	0	0	40	0.45	28560	0.67
	Sand	13- 16	21.4	25.2	0	0	44	0.45	19490	0.67
ISU-10 (GWT: 3.0 m)	Sand	0 - 4.6	17.6	20.2	0	0	36	0.45	9248	0.67
	Sand	4.6 - 15	20.3	24.0	0	0	40	0.45	24390	0.67
	Boulder	15 -17	24	24.0	0	0	44[(7)]	0.25	270000[(7)]	0.67

For unit conversion: 1 m = 39.37 inch; 1 kN/m^3 = 6.24 lb/ft^3; and 1 kPa = 0.145 psi.
[(1)] An undrained soil condition was used for the cohesive layers, while a drained condition was used for cohesionless layers; [(2)] After Schmertmann et al. (1978) using N_k = 15; [(3)] c = S_u/2; [(4)] After Robertson and Campanella (1983); [(5)] After Das (1998); [(6)] After Mayne and Kulhawy (1990) using M=8.25 (q_t-σ_{vo}); and[(7)]CPT not available, ϕ and E_s were extrapolated. Pile: Linear-Elastic model; γ=50 kN/m/m; E_s=2.0E8 kPa; υ=0.2; Shaft radius=0.16m; Tip radius=0.05m; R_{inter}=1.0.Steel Plate: Elastoplastic model; EA=1.6x10E8 kN/m; EI=9000 kN m2/m; d=0.026m; w=0.57 kN/m/m; υ=0.25.

6.3.1. Piles in cohesive soils

The two test piles referred to as ISU-4 and ISU-5 were selected for the preliminary FE analysis in cohesive soils. Figure 6.1a shows different soil layers, boundary conditions, and the interface elements used along the pile length for the preliminary FE model representing the test pile ISU-4 (FE-ISU4-1 model). As can be seen from the figure, the bottom boundary was totally fixed in both directions, while the side boundaries were only

fixed in the horizontal direction. The figure also shows the positive interface elements connecting the soil and pile elements along different soil layers. The positive interface means the interface is connecting the outer surface of the pile with the soil. Figure 6.1b shows a view of finite element mesh generated for this analysis.

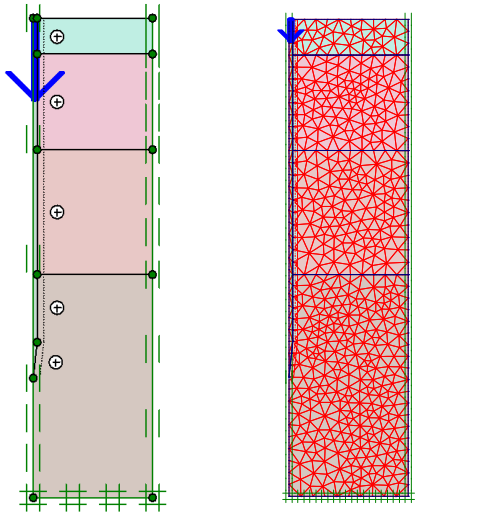

Figure 6.1: FE model representing the test pile at ISU-4

The FE analysis was performed based on controlled vertical displacement increments that represented the same displacement values collected during the static load test on the test piles. Using the staged construction option of the program, the displacements and stresses were reset for each loading increment to avoid convergence issues that could take place in the analysis. For the FE-ISU4-1 model, Figures 6.2a and 6.2b, respectively, show the deformed mesh and the distribution of the total displacement corresponding to an extreme prescribed vertical displacement of 40 mm (1.6 inch) at the model's pile head. As can be seen from the figure, the maximum total displacement around the model's pile was limited to around 2.5D, where D is the model pile diameter; hence, the FE model boundaries had no effect on total displacement. Moreover, Figure 6.2c shows the plastic zone by means of the effective normal stresses developed in the soil medium at the extreme total displacement. As can be seen from the figure, the maximum effective normal stress induced in the soil is 410.6 kPa (59.6 psi), concentrated at an approximate distance of around 3D below the pile tip and degrading towards the bottom horizontal boundary. Thus, the bottom boundary has a

negligible effect on the stresses induced in the soil below the pile tip.

Figures 6.3a and 6.3b show the predicted load-displacement response at the pile head compared to the measured response for the test piles ISU-4 and ISU-5, respectively. From Figure 6.3a, it can be seen the predicted load-displacement curve is less stiff by about 60% compared to the measured response along the elastic portion. Moreover, the predicted load-displacement curve underestimated the pile nominal capacity at the plastic portion by 43% when compared with the measured pile nominal capacity. For each case, the measured pile nominal capacity was defined using the Davisson criterion (Davisson, 1972) represented in the figures by a dot line referred to as the Davisson line. For the FE model that represented the test pile ISU-5 (FE-ISU5-1 model), Figure 6.3b shows the predicted load-displacement curve has stiffness 64% less than that of the measured curve along the elastic portion, and 65% lower nominal capacity compared to the measured capacity. Thus, the preliminary FE analyses for vertically-loaded piles driven into cohesive soils generally show poor correlations compared to field measured responses. The previous conclusion was expected, as several studies reported estimated soil-pile interface properties and soil elastic modulus, based on empirical correlations that could lead to biased FE results (El-Mossallamy 1999; De-Gennaro 2006; Engin 2007).

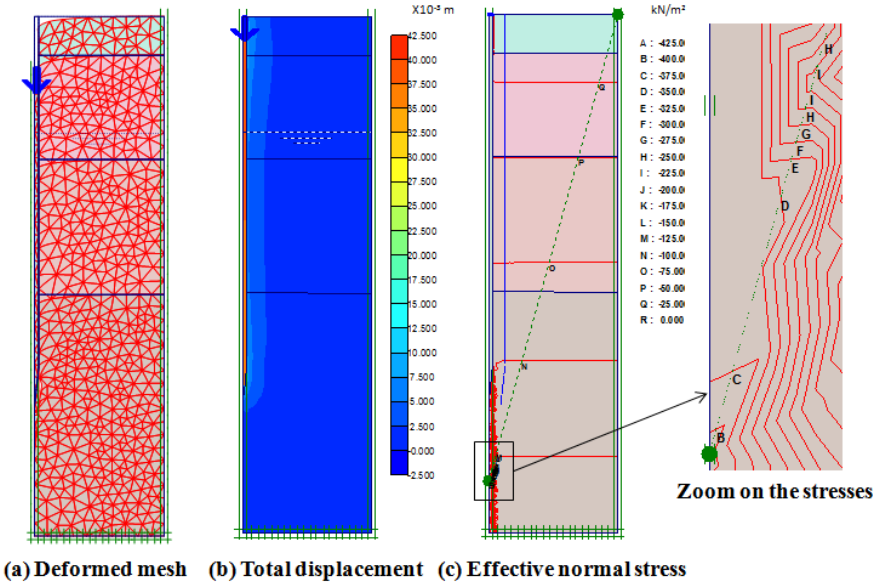

Figure 6.2: FE model results for the test pile at ISU-4

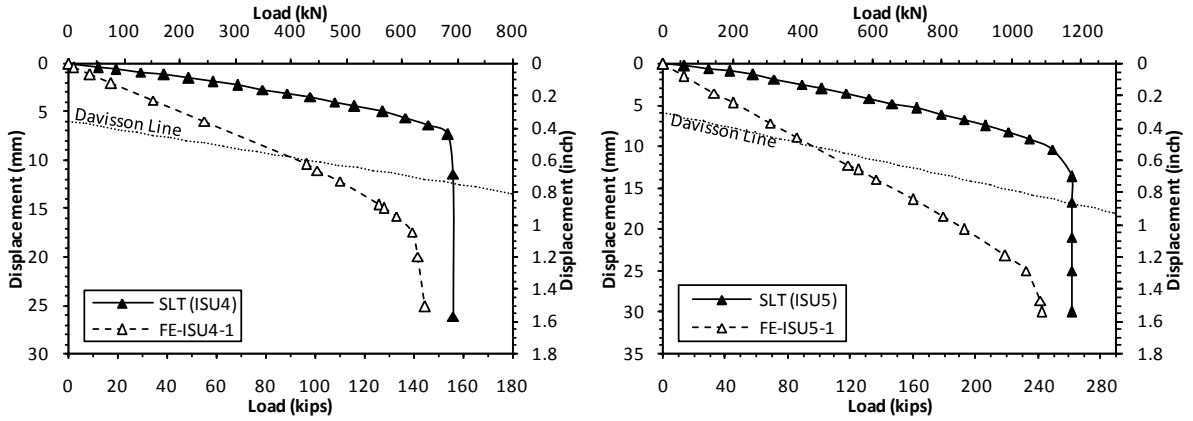

(a) Test pile at ISU-4 (clay) **(b) Test pile at ISU-5 (clay)**

Figure 6.3: Predicted versus measured pile load-displacement responses for piles in clay

6.3.2. Piles in cohesionless soils

The same axisymmetric FE model was utilized to simulate the behavior of the other two test piles driven into mainly cohesionless soil layers and referred to as ISU-9 and ISU-10. However, the top soil layer at ISU-9 was classified as low plastic clay with thickness equal to 4.8m (15.74 ft). As summarized in Table 6.1, all the constitutive parameters were established for the soil material, based on empirical correlations to the CPT conducted at each test site. This table also summarizes the selected R_{inter} values for each soil layer, based on the recommended values in the PLAXIS user manual. Figure 6.4a shows different soil layers, boundary conditions, and the interface elements used along the pile length for the preliminary FE model representing ISU-9 (FE-ISU9-1 model). Moreover, Figure 6.4b shows a view of finite element mesh used for the analysis.

For the FE-ISU9-1 model, Figures 6.5a and 6.5b, respectively, show the deformed mesh and the distribution of the total displacement corresponding to the extreme prescribed vertical displacement of 18.4 mm (0.72 inch) at the model's pile head. As can be seen from Figure 6.5a, the maximum total displacement around the model's pile was concentrated in the top clay layer and below the model's pile tip. However, the displacement did not extend laterally more than around 5.0D. Hence, the FE model boundaries had minimal effects on total displacements. Moreover, Figure 6.5c shows the plastic zone by means of effective normal stresses developed in the soil medium at the extreme total displacement. As seen in this figure, the maximum effective stress induced in the soil is 421.9 kPa (61.2 psi), which is

concentrated directly below the model pile tip and degrading towards the bottom horizontal boundary.

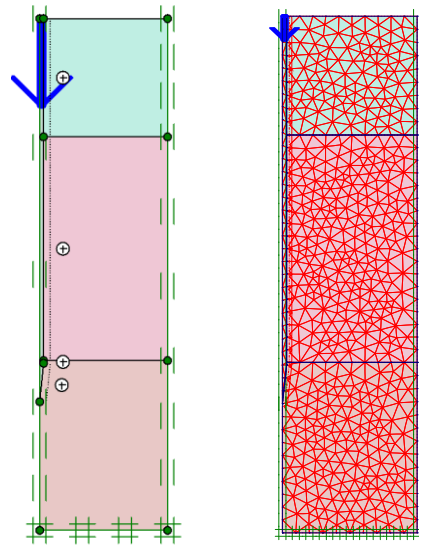

(a) Model overview (b) Fine unstructured mesh

Figure 6.4: FE model representing the test pile at ISU-9

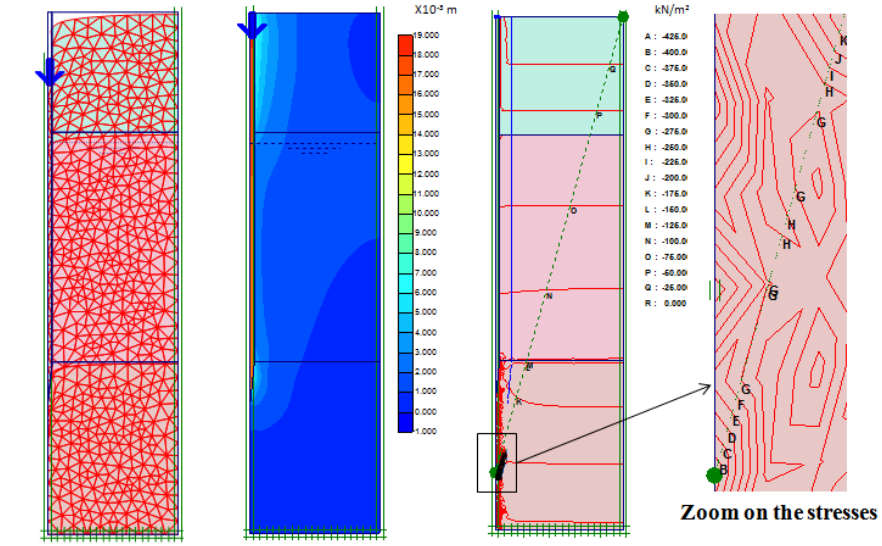

(a) Deformed mesh (b) Total displacement (c) Effective normal stress

Figure 6.5: FE model results for the test pile at ISU-4

From Figure 6.6a, it can be seen that the predicted load-displacement curve using the FE-ISU9-1 model is about 41% less stiff than the field measured response along the elastic

portion. However, the predicted ultimate capacity of the pile was about 26% conservative compared to the measured nominal capacity using Davisson's criterion. This difference between the predicted and the measured responses for ISU-9 could be due to the top clay layer at the test site. For the FE model representing the test pile ISU-10 (FE-ISU10-1 model), Figure 6.6b shows a relatively better prediction of the load-displacement curve along the elastic and plastic portions compared to the field measured pile response. The observation here is the FE model provided a very good match with the actual measurements for the test pile ISU-10 (pile driven into sand soil layers), which is relatively better compared with the predicted behaviors for the test pile ISU-9 (pile driven into mainly sand layers with one clay layer at the top) and the test piles ISU-4 and ISU-5 (piles driven into clay soil layers). Therefore, it is obvious the FE model prediction for the load-displacement behavior is better in the case of piles driven into cohesionless soil layers compared to those predicted for piles driven into cohesive soil layers.

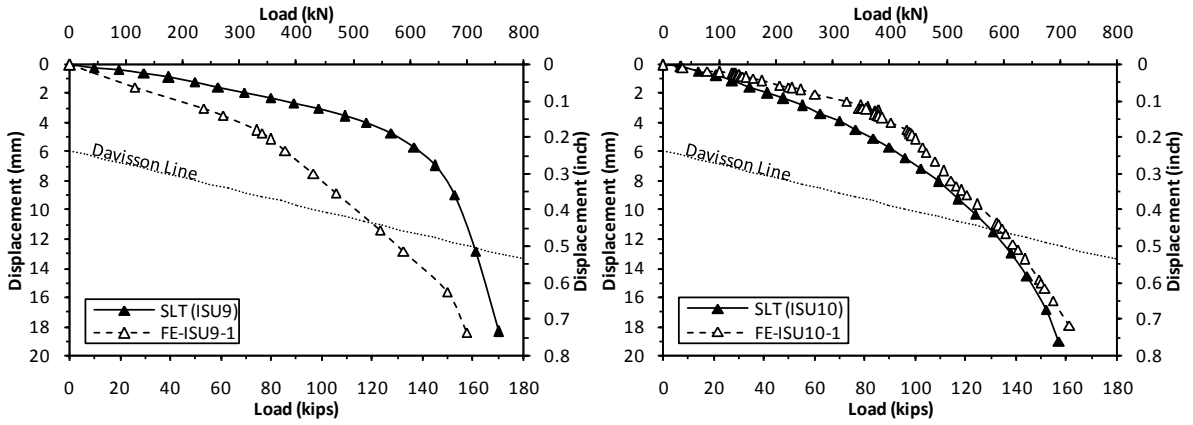

(a) Test pile at ISU-9 (sand + clay) **(b) Test pile at ISU-10 (sand)**

Figure 6.6: Predicted versus measured pile load-displacement responses

6.4. Investigation of the Soil and Interface Properties

As previously indicated, the bias in the FE analysis results in the case of piles driven into cohesive soils could be due to: 1) the use of inappropriate interface based on general recommendations from the PLAXIS user manual and 2) the subjective estimate of the soil elastic modulus based on empirical correlations to CPT results. In this section, the effect of changing the properties of the soil-pile interface element was first studied separately in the

case of cohesive soils. After this, the soil modulus was measured in the laboratory for clay. The difference between the measured and predicted values of the soil modulus was used in the final FE model to improve the analysis as will be discussed in the next sections.

6.4.1. Interface properties

Recently, AbdelSalam et al. (2010) *modified* the Direct Shear Test (mDST) to measure the shear-displacement curves, or the *t-z* curves that represent the soil-pile interface properties, by shearing a steel plate with respect to soil within the direct shear box. The accuracy of the soil-steel interface response for clay soils was first investigated in PLAXIS by examining the reproducibility of the mDST test data. For this purpose, a plane strain two-dimensional FE model was adapted, where the steel plate of the mDST was modeled using a non-porous linear-elastic constitutive model. The soil medium was modeled using the Mohr-Coulomb constitutive model, where the soil shear strength properties were determined, based on actual laboratory measurements from a conventional Direct Shear Test (DST) conducted on the sample collected from the top clay layer for ISU-9. The soil elastic modulus for clay was determined, based on CPT test results, while the only changeable parameter was the R_{inter} along the contact surface between the soil and the steel plate. The values of the R_{inter} used in the analysis were equal to 0.3, 0.4, 0.5, and 0.7. Table 6.2 summarizes the soil and interface parameters used in the four FE models representing the mDST test conducted for the clay layer from ISU-9.

As shown in Figure 6.7a, a constant vertical normal stress was applied on top of the soil during the FE analysis. Controlled horizontal displacement increments were applied to the lower half of the shear box, following the same normal stress and horizontal displacements collected while conducting the mDST laboratory test. Figure 6.7a also shows the plastified zone by means of the effective normal stresses developed in the soil medium, due to an applied constant normal stress of 30 kPa (4.35 psi) and horizontal displacement of 10 mm (0.4 inch) to the lower half of the shear box, and that for the FE model ISU-9/3. As seen from the figure, the maximum normal effective stress induced in the soil was equal to 14.44 kPa (2.09 psi), concentrated at the interface between the upper and lower shear boxes with higher intensity towards the vertical boundaries. Furthermore, Figure 6.7b represents the

shear stresses induced along the interface element, indicating a maximum shear stress value of 15.40 kPa (2.23 psi).

Figure 6.8 represents the shear stress-displacement curves adapted from the FE models for the clay soil sample using different R_{inter} values and compared with the measured curve from the mDST laboratory test. From Figure 6.8, it was found that: 1) R_{inter} equal to 0.5 better represents the behavior at the clay-steel interface, indicating the recommended value in the PLAXIS user manual is appropriate; and 2) the effect of the changing the R_{inter} was not significant on the shear-displacement response, when it exceeded a value of 0.5. From previous observations, it is clear the interface element in PLAXIS is considered acceptable in the case of clay-steel contacts. Therefore, bias in results of the FE model representing axially-loaded steel pile driven into clay could be due to improper estimates of the soil elastic modulus, not the soil-pile interface properties. Thus, the soil modulus significantly controls the soil-pile behavior and needs to be investigated separately.

Table 6.2: Summary of the soil parameters, and R_{inter} values used in the sensitivity analysis for the soil-steel interface

Model ID	Soil type	P kPa	γ_{dry} kN/m^3	γ_{wet} kN/m^3	c$^{(1)}$ kPa	$\phi^{(1)}$	$\nu^{(2)}$	$E_s^{(3)}$ kPa	R_{inter}
ISU-9/1	mDST test for Clay	30	18.8	23.4	10	24	0.25	E_s=17070	0.3
ISU-9/2									0.4
ISU-9/3									0.5
ISU-9/4									0.7
ISU-5-CPT	Triaxial test for Clay	120	17.5	21.1	54	32	0.3	E_1=9753	Not used
ISU-5/1							0.3	E_2=14629	
ISU-5/2							0.3	E_3=19506	

For unit conversion: 1 kN/m^3 = 6.24 lb/ft^3; and 1 kPa = 0.145 psi.
(1) Measured, using the DST results in the case of FE models for ISU-9, and estimated based on CPT results in the case of FE models for ISU-5; (2) Estimated, based on Das (1998); and (3) E_s and E_1 were estimated using CPT data based on correlations after Mayne and Kulhawy (1990), where $E_2 = E_1$ x 1.5, and $E_3 = E_1$ x 2.

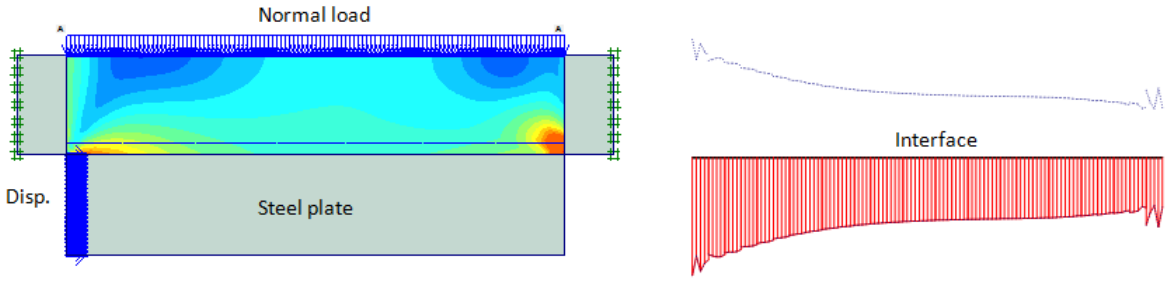

(a) Effective normal stresses in the soil medium (max. = 14.44 kPa)

(b) Shear stresses along the interface element (max. = 15.40 kPa)

Figure 6.7: FE model representing the mDST test for clay soils

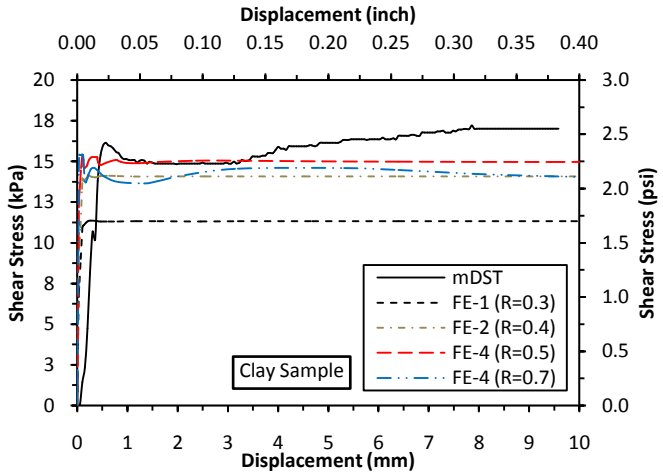

Figure 6.8: Comparison between the shear stress-displacement curves adapted from the FE models using different R_{inter} values and the laboratory measured curve using the mDST for clay

6.4.2. Soil modulus

Empirical correlations for estimating the soil modulus from the CPT results, such as the equation provided by Mayne and Kulhawy (1990), are not complex, and settlements can be estimated relatively quickly from these correlations. However, Lunne and Powell (1997) indicated the estimation of drained consolidation or deformation parameters, such as the constrained modulus, M, and Young's Modulus, E_s, for cohesive soils, based on the undrained CPT test results, may lead to serious errors by as much as ± 100%, especially when based on empirical correlations from the literature. Abu-Farsakh and Titi (2004) indicated that using the CPT test results to estimate the E_s requires extensive work to determine which correlation is the most appropriate to use. However, with local experience individual site/area specific correlations can be developed for certain soil types with greater

reliability.

In this study, a CU triaxial test was conducted on an undisturbed clay soil sample collected at a depth of 7.0 m (23 ft) below ground surface from the test site at ISU-5. A confining stress of 120 kPa (17.4 psi), estimated to represent the effective lateral earth pressure in the field, was used to consolidate the sample. As presented in Figure 6.9, the stress-strain curve was measured and the soil maximum effective stress was around 135 kPa (19.6 psi) and the elastic soil modulus was around 40000 kPa (5801.5 psi). However, the direct use of measured value of the soil modulus in the FE model may still not yield the same measured stress-strain behavior. This is because there are several other factors and parameters that affect FE analysis in addition to the soil modulus. Thus, to improve the FE model to match the actual measured stress-strain response from the CU triaxial test, an investigation that addresses the effect of changing the soil modulus on the overall stress-strain behavior was conducted for the clay soil sample. The objective for this analysis was to determine an adjustment factor that needs to be multiplied by the typically estimated soil modulus using empirical correlations with CPT data and to improve the overall FE model results for similar soil and pile conditions.

For the first model in this sensitivity analysis (ISU-5-CPT model), soil strength, and elastic modulus were calculated, based on empirical correlations with the soil CPT test results previously presented in Table 6.1. An axisymmetric FE model was adapted to simulate the behavior of the soil sample inside the CU triaxial chamber. The FE model was conducted using 10 controlled vertical displacement increments, but before running the load increments, the soil was consolidated using the Automatic Time Stepping (ATS) option from the PLAXIS program. In ATS analysis, the program uses smaller time steps while applying the confinement stress until the soil sample is fully consolidated. Figures 6.10a and 6.10b, respectively, show the deformed mesh of the soil sample and the distribution of the total displacement corresponding to the maximum prescribed vertical displacement of 0.2 mm (0.008 inch) that represents a vertical strain of about 0.15%. Furthermore, Figure 6.10c shows the plastic zone by means of the effective normal stresses developed in the soil medium, with a maximum value equal to around 157 kPa (22.77 psi) at the maximum prescribed displacement. On the other hand, Figure 6.11 shows the predicted stress-strain

curve, limited to an elastic strain of about 0.2%, adapted from the ISU-5-CPT model, and compared to the laboratory measured curve using the CU-triaxial test. As seen from the figure, the difference between the slope of the predicted and measured stress-strain curves is about 41%. Therefore, the predicted E_s, based on empirical correlations using CPT, may be misleading in case of clay soils. This was expected, according to several previous studies conducted by Mayne and Kulhawy (1990), Lunne and Powell (1997), and Abu-Farsakh and Titi (2004).

To improve the estimation of the soil elastic modulus used in the FE model to match the laboratory measured results, two additional models were adapted (ISU-5/1 and ISU-5/2) using increased E_s values by 50 and 100%, respectively, compared to the previously estimated values from the CPT. All soil parameters used in the FE models are summarized in Table 6.2. The results from ISU-5/1 and ISU-5/2 are presented in Figure 6.11, which shows the stress-strain curve adapted using the doubled E_s matches the initial portion of the measured curve at low strain levels (i.e., strain less than 0.2%). Hence, the estimated values for the initial elastic modulus of clay soils, based on empirical correlations to the CPT test results, must be increased by 100%.

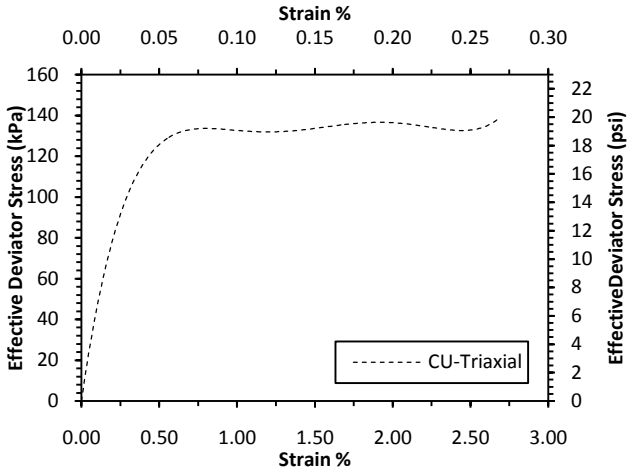

Figure 6.9: Stress-strain curve from the CU-triaxial results for the soil sample at ISU-5

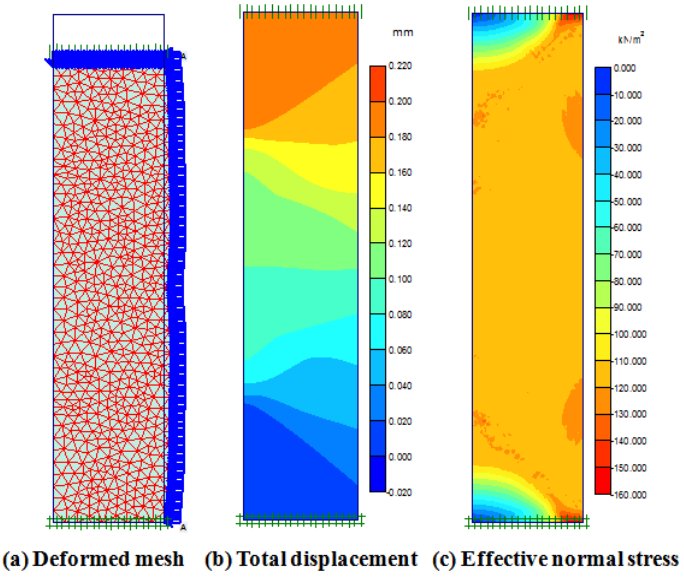

(a) Deformed mesh (b) Total displacement (c) Effective normal stress

Figure 6.10: FE model for the CU-triaxial test conducted on a clay soil sample

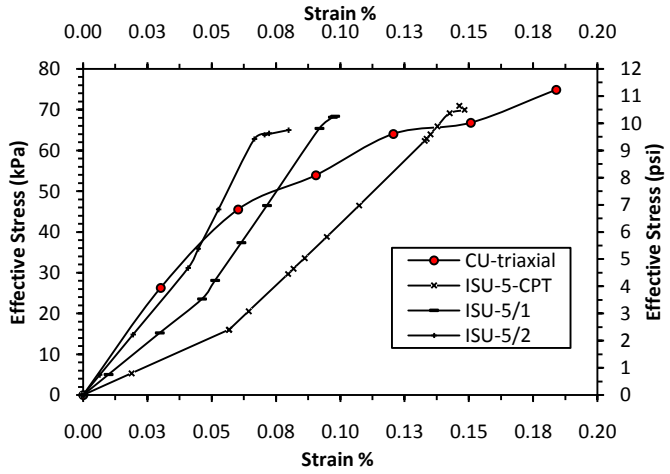

Figure 6.11: Stress-strain curve from different FE models and the triaxial test

6.5. Improved FE Models

This section presents an improved FE analysis for modeling the axially-loaded piles embedded in cohesive soil layers. This was attained by addressing the bias in the values of the estimated elastic modulus of clay soil layers, based on CPT data, increased by 100% based on laboratory CU-Triaxial measurements. However, the interface properties were found appropriate, and were not changed in the improved analysis. Out of the four test sites previously modeled (i.e., ISU-4, ISU-5, ISU-9, and ISU-10), three sites contained clay layers.

Accordingly, the soil elastic modulus used for clay layers in the FE models for ISU-4, ISU-5, and ISU-9 were adjusted by doubling the previously estimated values of E_s based on CPT data.

The analysis was first conducted for the two test piles embedded in mainly clay soil layers at ISU-4 and ISU-5. As seen from Figure 6.12a that represents test pile ISU-4, the difference within the elastic portion of the load-displacement curves predicted, using the earlier FE model (FE-ISU4-1) and the improved model (FE-ISU4-2), was reduced from 60% to 27%, compared to the measured response. Moreover, using the improved model reduced the difference between the predicted and measured pile ultimate capacity using Davisson's criterion from 43 to 11%. This significant enhancement in the estimated load-displacement behavior of test pile ISU-4 was attained after using the correct value of the soil modulus for clay layers. For pile ISU-5, the difference between the predicted and measured load-displacement responses was reduced from 64 to 33% along the elastic portion of the curve, and from 65 to 9% at the ultimate capacity, based on Davisson's criterion (see Figure 6.13b). Hence, the improved FE models for both test sites satisfactorily simulated the behavior of the test piles embedded in mainly cohesive soil layers.

As previously indicated, the FE model used to simulate the behavior at ISU-10 has provided an accurate prediction of load-displacement response for the axially load tested pile embedded in sand soil layers. However, this was not the case for the test pile at ISU-9 embedded in sand and clay soil layers. Accordingly, an improved FE model (FE-ISU9-2) with doubled soil elastic modulus for the top clay layer at ISU-9 was used. As can be seen from Figure 6.14a, the differences between the predicted and measured load-displacement responses for the test pile at ISU-9 was reduced from 41 to 30% along the elastic portion of the curve, and from 26 to 7.5% at the ultimate capacity based on Davisson's criterion. To confirm this improvement in the FE model prediction, the load distribution along the pile length was also adapted from the model's results and compared to the measured response, based on the strain gauges data. Figure 6.14b provides the measured versus the predicted load distribution curves along the pile length from ISU-9. From this figure, it is obvious the improved FE model satisfactorily simulated the load distribution along the pile embedment length in different soil layers.

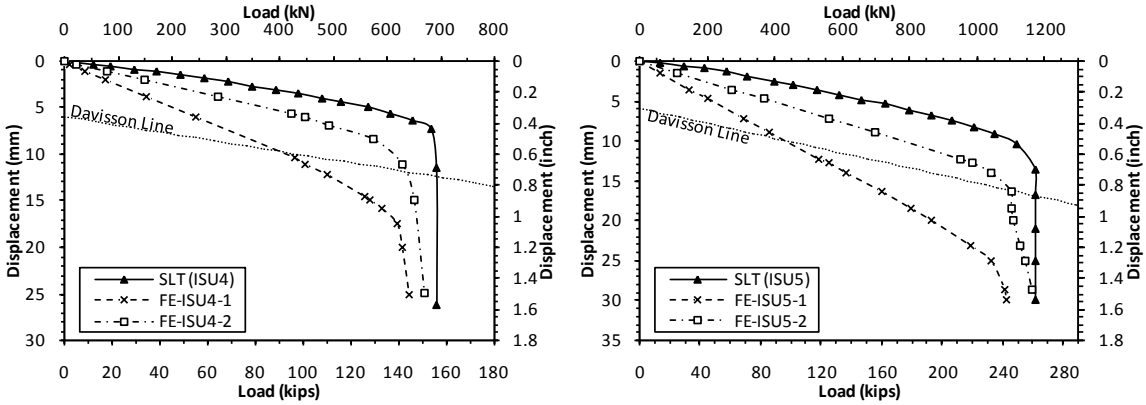

(a) Test pile at ISU-4 **(b) Test pile at ISU-5**

Figure 6.12: Load-displacement behavior using the preliminary and improved FE models versus the measured response

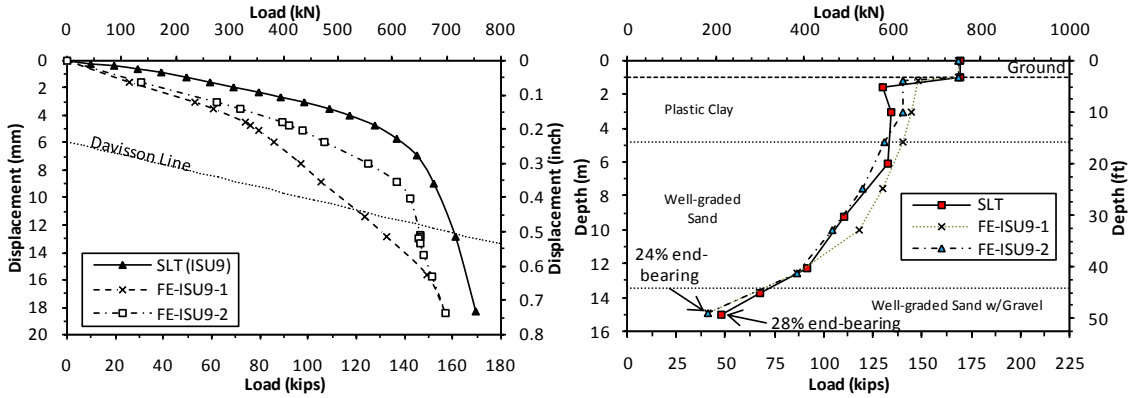

(a) Load-displacement **(b) Load-distribution along the pile length**

Figure 6.13: Pile behavior at ISU-9 using the preliminary and improved FE models versus the measured response

6.6. Summary and Conclusions

A simplified two-dimensional axisymmetric FE analysis using Mohr-Coulomb soil constitutive model was utilized to simulate the behavior of four load tested steel H-piles using PLAXIS 7.2. The soil constitutive properties were first established, based on empirical correlations to the CPT data. A preliminary analysis showed the model can adequately characterize the behavior of the steel piles driven into cohesionless soil layers. However, the model did not accurately capture the load-displacement response for the piles driven into cohesive layers. The properties of the soil-pile interface element and the soil elastic modulus were investigated using the mDST and CU-Triaxial soil laboratory tests, respectively, aimed

at improving the overall FE model results. A summary of the major findings is presented below.

- The preliminary FE model provided adequate prediction of the load-displacement response for the test pile driven into sand soil layers at ISU-10. The preliminary FE analysis for the pile at ISU-9, embedded in sand and clay soil layers, provided a 41% softer load-displacement response along the elastic portion of the curve and a 26% lower pile capacity. However, the FE models for the test piles ISU-4 and ISU-5 driven into clay soil layers provided biased results.
- The interface investigation showed a value of 0.5 for the R_{inter} factor should be used to represent the soil-pile interface element properties in PLAXIS for clay-steel contacts.
- The soil modulus investigation showed the estimated elastic modulus, based on empirical correlations with the CPT results for clay soils, was underestimated by 100%. Based on the CU-Triaxial test measurements; the estimated value of the elastic modulus was increased by 100% for all clay layers to improve the FE models for ISU-4, ISU-5, and ISU-9.
- The improved FE model for ISU-4 showed the differences between the predicted and measured load-displacement responses were reduced from 60 to 27% along the elastic portion of the curve, and from 43 to 11% at the ultimate capacity. For ISU-5, the difference between the predicted and measured load-displacement responses was reduced from 64 to 33% along the elastic portion of the curve, and from 65 to 9% at the ultimate capacity. For ISU-9, the difference between the predicted and measured load-displacement responses was reduced from 41 to 30% along the elastic portion of the curve and from 26 to 7.5% at the ultimate capacity.
- Overall, the improved FE model provided satisfactory results compared with the field measurements for the tested piles. The improved FE analysis is based on the simple Mohr-Coulomb constitutive model, which avoids using sophisticated soil models that require conducting costly and time consuming soil tests.

6.7. Acknowledgments

The study reported in this paper was conducted by the authors as part of the ongoing research project TR-573: Development of LRFD Design Procedures for Bridge Pile Foundations in Iowa funded by the Iowa Highway Research Board (IHRB). The authors express their gratitude to the IHRB and members of the project Technical Advisory Committee for their guidance and advice. The members of this committee represent Office of Bridges and Structures, Soils, Design Section, and Office of Construction of the Iowa DOT, FHWA Iowa Division, and Iowa County Engineers. Finally, special thanks to Kam Weng Ng and Matthew Roling for their help during field/laboratory tests.

6.8. References

AbdelSalam, S. S., Suleiman, M. T., and Sritharan, S. (2010). "Improved t-z Analysis for Vertically Loaded Piles in Cohesionless Soils based on Laboratory Test Measurements." To be submitted to the *ASCE Journal of Geotechnical and Geoenvironmental Engineering* (July 2010).

Abu-Farsakh, M. Y. and Titi, H. H. (2004). "Assessment of Direct CPT Methods for Predicting the Ultimate Capacity of Friction Driven Piles." *ASCE Journal of Geotechnical and Geoenvironmental Engineering*, volume 130, No. 9, pp. 935 - 944.

ASTM D4767 (2004). "Standard Test Method for Consolidated Undrained Triaxial Compression Test for Cohesive Soils." doi:10.1520/D4767-0.

Coyle, H. M. and Reese, L. C. (1966). "Load Transfer for Axially-loaded Piles in Clay." *Journal of Soil Mechanics and Foundation Engineering Division*, 92(2), 1- 26.

Das B. M. (1998). "Principles of foundation engineering." 4th edition, PWS publishing Inc.

Davisson, M. (1972). "High Capacity Piles." *Proceeding: Soil Mechanics Lecture Series on Innovations in Foundation Construction*, ASCE, IL Section, Chicago, IL, pp. 81–112.

De-Gennaro, V., Said, I., and Frank, R. (2006). "Axisymmetric and 3D Analysis of Pile Test using FEM." *Numerical Methods in Geotechnical Engineering*, 2006 Taylor & Francis Group, London, ISBN 0-4 15-40822-

El-Mossallamy, Y. (1999). "Load-Settlement Behavior of Large Diameter Bored Piles in Over-consolidated Clay."*Proceeding: The 7th International Symposium on Numerical*

Models in Geotechnical Engineering, September 1999, 433-450. Rotterdam, Balkema.

Engin, H. K., Septanika, E. G., and Brinkgreve, R. B. (2007). "Improved Embedded Beam Elements for the Modeling of Piles." *Proceeding: The 10th International Symposium on Numerical Models in Geotechnical Eng.* – NUMOG X, Rhodes (Greece).

Guo, W. D. and Randolph, M. F.(1998). "Vertically Loaded Piles in Non-homogeneous Media." Inter. Journal *for Numerical and Analytical Methods in Geomechanics*, Vol. 21, 507-532.

Lunne, P. K., and Powell, J. J. (1997). "Cone Penetration Testing in Geotechnical Practice." Rout ledge, New York, NY.

Mayne, P. W. and Kulhawy, F. H. (1990). "Manual on Estimating Soil Properties for Foundation Design." Rpt. EL-6800, Electric Power Research Inst., Palo Alto, 306 p.

Misra, A. and Chen, C. H. (2004). "Analytical Solutions for Micropile Design under Tension and Compression." *Geotechnical and Geological Engineering*, 22(2), 199-225.

Misra, A. and Roberts, L. A. (2006). "Probabilistic Analysis of Drilled Shaft Service Limit State Using the t-z Method." *Canadian Geotechnical Journal*, 1324-1332 (2006).

Oh, E. Y., Huang, M., Surarak, C., Adamec, R., and Balasrbamaniam, A. S. (2008). "Finite Element Modeling for Piles Raft Foundation in Sand." 11th *East Asia-Pacific Conference on Structural Engineering & Construction* (EASEC-11), Building a Sustainable Environment, November 19-21, 2008, Taipei, Taiwan.

Prakoso, W. A. and Kulhawy, F. H., (2001). "Contribution to Piled Raft Foundation Design." *Journal of Geotechnical and Geoenvironmental Engineering*, ASCE, 127(1), 17-24.

Roberts, L. A., Gardner, B. S., and Misra, A. (2008). "Multiple Resistance Factor Methodology for Service Limit State Design of Deep Foundations using a t-z Model Approach." *Proceeding: The Geo-Congress 2008,* New Orleans, *LA*.

Robertson, P. K. and Campanella, R. G. (1983). "Interpretation of Cone Penetration Tests." *Canadian Geotechnical Journal*, Vol. 20, No. 4, Nov. 1983.

Schmertmann, J. B. (1978). "Guidelines for Cone Penetration Test, Performance and Design." *Report No. FHWA-TS-78-209, U.S. DOT*, Washington, D.C., pp. 145.

Sellountou, E. A., O'Neill, M. W., and Vipulanandan, C. (2005). "Construction Effects on

ACIP Pile Behaviour in Texas Coastal Soils." *Geotechnical special publication*, ISSN 0895-0563, Vol. 130, pp. 631-647.

Suleiman, I. B. and Coyle, H. B. (1976). "Uplift Resistance of Piles in Sand." *Journal of Geotechnical Engineering*, ASCE 1976; 102(GT5):559–62.

Tan, S. and Bui, T. (2006). "Interpretation of Pile Load Test Failure using FEM Simulation." *Numerical Methods in Geotechnical Engineering*. Aug 2006.

Wathugala, G. W. and Desai, C. S. (1989). "An Analysis of Piles in Marine Clay under Cyclic Axial Loading." *Offshore Technology Conference*, May 1989, Houston, Texas.

CHAPTER 7: AN INVESTIGATION OF THE LRFD RESISTANCE FACTORS WITH CONSIDERATION TO SOIL VARIABILITY AND PILE SETTLEMENT

Sherif S. AbdelSalam[1]; Sri Sritharan, M. ASCE[2]; Muhannad T. Suleiman, A. M. ASCE[3]

A paper to be submitted to the *Journal of Bridge Engineering*, ASCE (*LRFD special edition*)

7.1. Abstract

The main goal of this study is to examine the Load and Resistance Factors Design (LRFD) approach for pile design in different soil types, based on using combinations of static analysis methods. First, reliability-based regional LRFD resistance factors for the design of bridge pile foundations were developed for clay, sand, and mixed soils in the Midwest. The framework used for this calibration included an efficient in-house static design method developed by the Iowa Department of Transportation. Then, the benefits of conducting the calibration, using combinations of static methods giving due consideration to soil variability along the pile length, are presented. Finally, a displacement-based LRFD pile design approach that simultaneously accounts for strength and serviceability limit states is suggested. From the findings, it is shown: 1) using combinations of static methods improves design efficiency, especially in mixed soils; 2) utilizing a more refined soil categorization, based on the actual soil profile along the pile embedded length on a site-by-site basis, provides significantly more efficient LRFD approach for the piles; and 3) using the suggested displacement-based LRFD approach can effectively determine the pile capacity and limit the vertical settlement to a pre-defined value.

CE Database keywords: LRFD, Resistance Factors, Deep Foundations, Static Methods, Soil Variability, Serviceability Limit State, Pile Settlement, Load-Displacement.

[1] Graduate Student and Research Assistant, Dept. of Civil, Construction, and Environmental Engineering, Iowa State University, 355 Town Engineering, Ames, IA 50011-3232, E-mail:ssabdel@iastate.edu

[2] Wilson Engineering Professor and Associate Chair, Dept. of Civil, Construction and Environmental Engineering, Iowa State University, 376 Town Engineering, Ames, IA 50011-3232, E-mail: sri@iastate.edu

[3] Assistant Professor, Dept. of Civil and Environmental Engineering, Lehigh University, STEPs Building, Room 326, 1 West Packer Avenue, Bethlehem, PA, 18015. E-mail: suleimam@lafayette.edu

7.2. Introduction

As acknowledged by Kyung et al. (2002), the American Association of State Highway and Transportation Officials (AASHTO) specifications for the LRFD design of bridge deep foundations do not provide resistant factor recommendations for all static methods, different combinations of methods, or local "in-house" methods developed by the Departments of Transportation (DOTs) in different states. The obvious reason for this limitation is AASHTO specifications are aimed at establishing design guidelines at the national level, accounting for large variations in soil properties, which yield unnecessarily conservative pile designs (Paikowsky et al., 2004). Another limitation associated with the AASHTO specifications is the recommended resistance factors only account for the design of axially-loaded piles at the strength limit state. Scott and Salgado (2003) identified the importance of this issue, especially for cohesive soils, where settlement is not immediate and using the unity resistance factor recommended by the AASHTO for serviceability checks may not be adequate. Moreover, Abu-Hejleh et al. (2009) indicated pile vertical settlement may control the design of bridge foundations, due the existence of large structural loads that must be adequately supported without experiencing excessive deformations, especially when the piles are embedded in highly deformable soils.

Towards achieving more cost-effective bridge foundations, the Federal Highway Administration (FHWA) permitted establishing regional LRFD resistance factors to minimize any unnecessary conservatism built into pile design, provided these factors are developed in a manner consistent with the 2007 AASHTO LRFD calibration framework. This framework was used to develop recommendations for three general soil groups—sand, clay, and mixed soils. Although it is atypical to only have clay or sand at a given site, suitable criteria for defining the extent of a specific soil type to classify the site as sand or clay site is not defined in AASHTO. Foye et al. (2009) stated the framework used to develop the recommended AASHTO resistance factors was based on a lumped database that discarded various sources of uncertainties contributing to the observed scatter in soil properties and soil variation along pile length. Recently, McVay et al. (2010) indicated the current design code involved spatial averaging, due to the reliance placed on constant

resistance factors that ignored the effects of soil variation along the shaft embedment. Consequently, McVay et al. (2010) developed the LRFD resistance factors as a function of pile length and soil geostatistical characteristics, showing that separating the soil profile into subzones would lead to increased pile resistance.

To include the vertical serviceability limit state into the LRFD approach for piles, several studies have been conducted during the last few years based on predicting the pile load-displacement relationship, and selecting the design capacity and the corresponding settlement in a reliability-based manner (Misra and Roberts, 2006). The load-transfer method (i.e., t-z method) has been extensively used to model the load-displacement curve at the pile's head required to perform the reliability analysis of deep foundations (Misra et al., 2007). In 2008, Robert et al. developed a practical LRFD approach that simultaneously account for strength and serviceability limit states using the t-z model and the empirically-correlated soil-pile interface properties, based on conventional field soil tests. Recently, AbdelSalam et al. (2010) have reduced the bias in the t-z analysis by measuring the soil-pile interface properties, using a modified Borehole Shear Test (mBST) and a modified Direct Shear Test (mDST) in cohesive and cohesionless soils, respectively, which can be effectively used to incorporate the serviceability limits into the LRFD pile design.

Presented in this paper are findings of a research project aimed at establishing LRFD recommendations for driven steel H-piles, considering local practices and soil conditions. The project focuses on developing regional resistance factors for different static analysis methods in sand, clay, and mixed soils, using a newly developed electronic database that contains 264 pile static load test results, pile driving information, and adequate soil data. Starting with the strength limit state, the resistance factors were developed following the reliability-based AASHTO LRFD calibration framework. Additionally, ten (10) vertical static load tests (SLTs) were conducted on instrumented steel H-piles driven into different soil types to evaluate and verify the performance of regionally-developed recommendations. Using the new field test information, an investigation was undertaken to overcome the aforementioned limitations of the currently used calibration framework that places emphasis on classification of the soil profile along pile length at a given site. In this approach, a unique soil categorization was used, based on the percent of cohesive material present at each site. In

addition, two combinations of static methods were explored in terms of increasing pile design efficiency. Finally, a displacement-based LRFD pile design approach that accounts for pile strength and serviceability limit states, following a one-step design procedure, was suggested. This approach depends on modeling the load-displacement behavior of axially-loaded steel H-piles, using the load-transfer analysis method. To attain an improved t-z analysis, the mBST and mDST were utilized to directly measure the t-z model parameters at the soil-pile interface for clay and sand soils, respectively. The suggested displacement-based design approach aims at determining pile capacity for a target vertical settlement.

7.3. Development of the LRFD Resistance Factors

The development of regionally-calibrated resistance factors requires the existence of adequate local pile SLT data as well as quality information on soil properties. Between 1966 and 1989, 264 pile SLTs conducted on steel H-shaped, timber, pipe, monotube, and concrete piles were collected by the Iowa DOT. The entirety of the collected information included details concerning site location, subsurface conditions, pile type, driving hammer characteristics, and pile load-displacement response. After ensuring the quality of data, an electronic database known as the PIle LOad Tests in Iowa (PILOT-IA) was developed by Roling et al. (2010) to house the test information and allow for efficient analyses performed on the amassed dataset. In PILOT-IA, the number of SLTs conducted on steel H-piles with sufficient information for calculating the pile capacity by means of static methods was 82.

To sort PILOT-IA for different soil types, the same soil groups used in the 2007 AASHTO LRFD specifications were utilized for consistency. Since AASHTO did not provide a criterion to establish the different soil groups, an examination of defining sand and clay sites was undertaken using different rules (see Roling et al., in process). It was concluded that soil layers can be satisfactorily categorized into sand or clay, using the 70% rule for determining the average soil profile along the shaft embedment length. Accordingly, each site in PILOT-IA is classified as sand or clay, based on the most predominant soil that existed more than 70% along the shaft length, in which the soil type for each layer is identified according to the Unified Soil Classification System (USCS). If the percentage of the predominant soils is less than 70% sand or clay, then that site is considered to have mixed

soil. Accordingly, PILOT-IA contained 35 sites in sand, 15 in clay, and 32 in mixed soils that can be used for LRFD resistance factors calibration for different static analysis methods of pile design. In all cases, the measured load capacity of the piles is determined, based on Davisson's criterion (Davisson, 1972), which defines pile nominal capacity from the load-displacement curve.

The analytical capacities of the piles available from PILOT-IA were calculated, using different static analysis methods to develop the LRFD resistance factors. However, it was important to determine the most appropriate static methods to use for the regional calibration, as there are various static methods available in the literature. As part of this study, AbdelSalam et al. (2008) and Roling et al. (2010) surveyed different State DOTs and Iowa county engineers, respectively, to identify the most commonly-used static methods for the design of pile foundations, as well as to learn of current local practices. Based on the survey's outcomes, five static methods were selected for the LRFD calibration—the α-API (API, 1974) method, the β-method (Burland, 1973), the Iowa pile design chart (or Bluebook method) developed by Dirks and Kam (1989) for clay soils, the Nordlund (Nordlund and Thurman, 1963), the SPT-Meyerhof (Meyerhof, 1976), as well as the Bluebook method for sand soils. The Bluebook is an "in-house" method, locally developed by combining the SPT-Meyerhof and α-Tomlinson (Tomlinson, 1980) methods to calculate pile skin-friction and uses the wave equation concepts to develop the end-bearing component.

7.3.1. Calibration method

There are several statistical approaches with different degrees of sophistication that can be used for the LRFD calibration. According to Kyung et al. (2002), the most commonly used approaches are the First Order Second Moment (FOSM) method and First Order Reliability Method (FORM). Paikowsky et al. (2004) conducted the analysis using both methods and concluded the difference in the outcomes of using the two methods is relatively small (i.e., less than 10%) with the FOSM producing slightly lower resistant factors. Nowak and Collins (2000) as well as Allen (2005) have shown that advanced statistical approaches produce results similar to the FOSM, indicating the need for a less sophisticated approach for the LRFD calibration. Consequently, the FOSM was selected herein to develop resistance

factors for pile design, using PILOT-IA database. Moreover, current AASHTO LRFD specifications are based on FOSM, assuming a lognormal distribution for the Probability Density Functions (PDFs) of loads and resistances. According to Scott and Salagado (2003), the lognormal distribution better represents transient loads that piles are subjected to as well as their resistances. Scott and Salagado (2003) also added lognormal distribution adequately characterizes the product of PDFs representing loads and resistances by their first two moments (i.e., mean and standard deviation). As presented in the following section of this paper, PDFs for different groups of piles in PILOT-IA were examined to ensure they follow the lognormal distribution.

Using LRFD specifications, the target reliability index (β) is defined as the measure of safety associated with a probability of failure (P_f), needed for the resistance factors calibration using the FOSM method. Paikowsky et al. (2004) recommended the use of β values of 2.33 and 3.00 for redundant and non-redundant piles, respectively. Consequently, the main target values selected for this study were $\beta = 2.33$ (i.e., $P_f = 1\%$) for redundant pile groups having five or more piles/cap and $\beta = 3.0$ ($P_f = 0.1\%$) for non-redundant pile groups with less than five piles/cap. As for the Dead Load to Live Load (DL/LL) ratio required for the FOSM analysis, no specific recommendations are provided in AASHTO. This ratio is typically controlled by the bridge span, traffic volume, and importance of the structure. Paikowsky et al. (2004) used a DL/LL ratio ranging from 2.0 to 2.5, while Allen (2005) used a conservative ratio of 3.0. Locally, the DOT uses a DL/LL ratio of 1.5, due to frequent use of short span bridges in the state. Nevertheless, Nowak and Collins (2000) and Paikowsky (2004) indicated the effect of the DL/LL ratio is not significant on the resistance factors. Without adding excessive conservatism, a DL/LL ratio of 2.0 was selected for this study.

7.3.2. Resistance factors

In this study, the Anderson-Darling (AD) and the 95% confidence interval (95% CI) statistical tests were used to check the normality of the PDFs of different groups (see Shapiro 1980, for more details on the tests). Each group represents the resistances of steel H-piles driven into a specific soil type and calculated, using a specific static method. As seen in Figure 7.1, using the AD and the 95% CI tests confirmed the lognormal best-fits the

probability distribution for the resistances of 35 piles calculated using the Bluebook method in sand soil profiles and represented by the mean bias ratios (i.e., pile measured capacity using Davisson/calculated capacity using Bluebook or K_{sx}). The same goodness-of-fit tests were conducted for other probability distributions representing the resistances calculated using other static analysis methods in sand, clay, and mixed soil profiles. It was found the lognormal distribution best fits all of them. Furthermore, Figure 7.2 shows the frequency distribution for all the PDFs representing the piles resistances calculated using five different static methods in sand soil profiles. As seen in the figure, the SPT-Meyerhof method provides the largest scatter in comparison to other static methods. Another observation to note here is the normally distributed PDFs are always extended below the zero value on the x-axis, which is not a valid value for the K_{sx} ratio. This strengthens the use of the lognormal distribution in the FOSM calibration of the LRFD resistance factors.

Table 7.1 summarizes the regional LRFD resistance factors for different static methods of designing piles in the three main soil groups, developed for the lognormal PDFs using the FOSM reliability method. This table includes the following statistical parameters: the sample size (N), mean (λ), standard deviation (σ), and the coefficient of variation (COV). For redundant pile groups, the results presented in Table 7.1 indicate the highest resistance factor (φ) in sandy soils was obtained from the Bluebook method followed by SPT-Meyerhof, β-method, and Nordlund method, with φ values of 0.51, 0.43, 0.33, and 0.30, respectively. It can also be noted from Table 7.1, the highest φ in clay soils was also obtained for the Bluebook method, followed by α-API and β-method, in this order, with φ values equal to 0.7, 0.52, and 0.35, respectively. For mixed soils, the SPT-Meyerhof yielded the highest φ, followed by the Bluebook, β-method, α-API, and Nordlund methods, with φ values equal to 0.45, 0.41, 0.33, 0.32, and 0.31, respectively. For non-redundant pile groups, it was found the resistance factors on average were reduced by 30%. Nevertheless, it should be noted that higher resistance factors do not indicate the true efficiency and economy of the design method, as the different static methods lead to different nominal pile capacities. To compare the efficiency of different static methods relative to the actual pile behavior, the efficiency factors defined as φ/λ were calculated. The φ/λ factor ranges from 0 to 1.0, where higher φ/λ correlates to more economic design methods. In Table 7.1, the φ/λ factors are

summarized and it was found the Bluebook is the most efficient method for the three soil groups, followed by the β-method in sand, α-method in clay, and β-method in mixed soils.

Furthermore, a sensitivity analysis was conducted to determine the effect of changing the values of β on the resistance factors. As shown in Figure 7.3 for sandy soils, φ was found to reduce with increasing β value. From this figure, a designer can find the appropriate φ for a chosen β that reflects pile redundancy, bridge life time, importance, degree of quality control, and the extent of design conservatism. Also included in the figure is the φ/λ, corresponding to different β values and static methods in sand. From Figure 7.3, the following three observations are apparent: 1) the order of the efficiency remains the same for the different static methods regardless of the β values; 2) the efficiency of the method reduces with increasing β in a nonlinear manner; and 3) as β increases from 1.5 to 4.0, the efficiency of the design significantly decreases by about 77%. Similar observations were made from the same analyses conducted for the piles embedded in other soil groups (i.e., clay and mixed soils). It was found the efficiency of the design significantly decreases by about 74 and 78% in clay and mixed soils, respectively, when β increases from 1.5 to 4.0.

7.3.3. Verification of the resistance factors

As a part of this research project, ten instrumented steel piles HP 254 x 62.4 (HP 10x42) with identification numbers starting ISU-1 to ISU-10 were load tested at different locations in the state of Iowa. These test sites were chosen to cover different soil regions and geological formations within the state. Two tests were conducted in sand soils (based on the 70% rule), five in clay, and three in mixed soils. The instrumented piles were tested to failure and the Davisson criterion was used to establish the pile measured nominal capacity in each case (see Ng et al., in process for more complete information).

To verify and examine the performance of the regionally-developed resistance factors, one of the test sites was randomly selected and the calculated capacity using different static methods was compared to the field measured capacity of the test pile. Figure 7.4 summarizes the nominal as well as the factored capacities calculated using different static analysis methods and measured using Davisson's criterion for the test pile at ISU-5 (clay site). The calculated nominal capacities were multiplied by the corresponding resistance

factors in Table 7.1 to determine the factored design capacities, while the measured nominal capacity was multiplied by 0.8 in accordance with the AASHTO 2007 to account for soil variability in the site. Compared to the pile measured nominal capacity of 1081 kN (243 kips), Figure 7.4 shows that the SPT-Meyerhof method provided the most conservative nominal capacity equal to 391 kN (88 kips), while the β-method was the most overestimating by around 15%. Thus, there was a large variation between the nominal capacities calculated for the test pile using different static methods, which was significantly reduced after multiplying the calculated nominal capacities by the LRFD resistance factors (see Figure 7.4). From the efficiency prospective, the Bluebook method provided the least conservative factored capacity equal to 636 kN (143 kips).

Figure 7.5 summarizes the calculated as well as the measured nominal and factored capacities for the 10test piles, where the x-axis represents the measured capacity using Davisson's criterion and the y-axis represents the calculated capacity using the Bluebook method. The reason for selecting the Bluebook method for this comparison is it provided the highest efficiency compared to other static methods. As noticed from Figure 7.5, the points that represent the nominal capacities are scattered above and below the equal line, meaning that in some cases, the design capacity is higher than the measured capacity. However, it is clear from the figure that the factored pile design capacities did not exceed the factored measured capacities, except for one point that was slightly higher than the equal line, which indicates the regional LRFD resistance factors succeeded to limit the design capacity calculated using the Bluebook method below the factored measured capacity, ensuring reliable designs for the 10 test piles.

Figure 7.6 represents the frequency distributions of three different PDFs representing the mean bias ratios calculated for the test piles as follows: 1) measured capacity divided by the calculated Bluebook nominal capacity (K_1=measured/nominal); 2) measured capacity divided by the calculated Bluebook factored capacity using the LRFD resistance factors (K_2=measured/LRFD); and 3) measured capacity divided by the calculated working stress design (WSD) capacity of the Bluebook method using a factor of safety equal to 2.0 (K_3=measured/WSD). As seen from the figure, the standard deviation (σ) of K_2 ($\sigma_2 = 0.32$) is lower than for K_3 ($\sigma_3 = 0.54$), also the mean (μ) of K_2 ($\mu_2 = 1.63$) is closer to unity compared

with the mean of K_3 ($\mu_3 = 1.99$), while the probability of K_2 to be lower than unity is smaller than for K_3. All of the previous observations indicate that the Bluebook LRFD-based factored pile capacity is more reliable and economic at the same time compared with the WSD-based pile capacity. In summary, the preliminary regionally-calibrated resistance factors for PILOT-IA provided reliable, consistent, and economic pile designs, where the Bluebook in-house method yielded the highest efficiency compared to other static analysis methods.

After verification of the preliminary resistance factors, results from the recently conducted 10 pile load tests were added to the already existing 82 sites from the PILOT-IA database, and the total number of piles SLTs available for sand, clay, and mixed soil groups increased to 37, 20, and 35, respectively. The final calibration was conducted for the increased database. The difference observed between the preliminary and the final LRFD resistance factors is negligible. Table 7.2 represents a comparison between the developed final LRFD resistance factors and the recommended resistance factors from different design specifications. As seen from the table, the resistance factor for the SPT-Meyerhof method in sand is greater than provided in the AASHTO by about 40%. Likewise for the β-method, the developed resistance factor for sand was about 10% greater than recommended by the National Corporative Highway Research Project (NCHRP) report number 507. Moreover, Table 7.2 shows the developed final resistance factors for α-API and β-methods in clay soils were, respectively, about 15 and 40% greater than those recommended by the NCHRP and AASHTO. In mixed soils, an increase in the resistance factor of about 30% was obtained for β-method compared to AASHTO. Although comparing the calculated efficiencies of different static methods would be more appropriate, values of the efficiency factors were not provided in the AASHTO specifications.

7.4. LRFD for Layered Soil Profiles

In the previous sections, the soil profile at each site in PILOT-IA was classified as sand, clay, or mixed, based on the 70% rule. This approach was necessary, since neither the 2007 AASHTO LRFD specifications nor the NCHRP-507 provided a clear definition to determine sand and clay sites. Consequently, this section examines a different soil categorization approach to see if the alternative approach could improve the efficiency of the

resistance factors in layered soils. The proposed approach is intended to determine the actual percentage of cohesive material existing along the pile length at each site. To complete this task, soil materials were classified following the USCS system and the sites were grouped into the following categories: 100, 87.5, 62.5, 37.5, 12.5, and 0% cohesive material along the pile length. After adding the 10 recently conducted SLTs to the already available 82 sites in PILOT-IA, the total number of SLTs available within each group was 12, 12, 16, 20, 17, and 15, respectively.

As noted from the previous sections, the β and α-API methods provided the highest efficiencies following the Bluebook method in sand and clay, respectively, since these methods were originally developed for such soil types. Therefore, combining the two static methods to calculate the capacity of piles embedded in layered soils may improve the design efficiency compared to using one method. It may also provide higher efficiency factors, when compared to the Bluebook method, which already combines static methods that differentiate between cohesive and cohesionless materials in calculating pile capacity. Hence, besides using the aforementioned soil categorization approach, a combination (COMB-1) of the β and α-API methods was created to calculate the capacity of different pile segments imbedded in cohesionless and cohesive soil layers, respectively.

7.4.1. Recalibration of resistance factors

Recognizing the proposed soil categorization approach, a new set of LRFD resistance factors were developed for the six soil groups following the 2007 AASHTO LRFD calibration framework. The resistance factors and their efficiencies were calculated for COMB-1 as a function of percentage cohesive material existing along the pile length. The results are presented in Figure 7.7 and compared to those obtained for the β and α-API static methods individually. It is clear from this figure that COMB-1 provides higher resistance factors compared to the other two static methods, especially towards more clayey profiles. Figure 7.7b represents the efficiency factors for COMB-1, β, and α-API methods as a function of percentage cohesive material existing along the pile length. This figure indicates the efficiency of COMB-1 is more consistent and higher compared to the other two methods, especially in mixed soil layers. This confirms that COMB-1 in layered soil profiles provides

consistent and more economic pile designs, compared with using either of the β or α-API methods. Another combination (COMB-2) of the Nordlund and α-API methods was created to calculate the capacity of pile segments imbedded in cohesionless and cohesive soil layers, respectively. Figure 7.7 shows that COMB-2 provides more consistent and economic designs compared with using either Nordlund or α-API methods.

After identifying the benefits of using a combination of methods, the LRFD resistance and efficiency factors were developed and presented in Figure 7.8 for COMB-1, COMB-2, and the Bluebook method with respect to the percentage of cohesive material existing along the pile embedded length. Figure 7.8a can be used for determining the resistance factors necessary for the design of steel H-piles driven into any soil layers without the need to determine whether the average profile mainly consists of sand, clay, or mixed soils, as it reflects all possible soil materials that could be found during drilling or from a borehole datasheet. On the other hand, Figure 7.8b provides the efficiency factors corresponding to different static methods. From this figure, it was determined the Bluebook method generally provides the highest resistance factors and efficiency among the other combinations of static methods (i.e., COMB-1 and COMB-2). Moreover, the earlier soil groups based on the 70% rule (i.e., sand, clay, or mixed) and the corresponding constant resistance factors for the Bluebook method are included in Figure 7.8 for comparison purposes. From Figure 7.8, it is clear the resistance factors as well as the efficiency factors are not constant within any of the earlier soil groups. The resistance factors were also calculated for other static methods using the proposed soil categorization approach, but not included in Figure 7.8. Focusing on mixed soils, the resistance and efficiency factors at 50% cohesive material were determined from the figure and compared to the constant resistance factors calculated for different static methods, based on the 70% rule (see Table 7.3). As can be seen in Table 7.3, the percent increase in the resistance factors ranges from 15 to 59% for different methods, when utilizing the proposed soil categorization approach. Therefore, the factored design capacity of the piles will increase, leading to a reduced number and/or length of piles.

7.4.2. Design example

The benefits of utilizing the LRFD resistance factors based on the proposed soil categorization approach (exact % cohesive material) in pile design can be realized through a simple design example. Consider the bridge pier at ISU-6 with a maximum factored axial load of 10,000 kN (2248.1 kips) designed with a number of steel piles, HP 254 x 62.4 (10 in. x 42 lbs/ft), end-bearing in a hard soil layer, with length equal to 16.8 m (55 ft) each, and connected with a concrete cap. The pile at ISU-6 was selected in this example because the soil profile has a large variability.

The typical geological formation at ISU-6 consists of normally consolidated loess silty clay and sand deposits on top of glacial clay. As shown in Figure 7.9, three main soil layers were found during drilling, the first layer consisted of silty clay deposits extending to 8.3 m (27.2 ft) below the ground's surface, followed by medium sand deposits up to 14.0 m (45.9 ft), and the bottom layer consisted of firm glacial clay material. The groundwater table at the time of in-situ testing was located at 7.0 m (22.9 ft) below the ground surface. Using laboratory tests conducted on soil samples collected at ISU-6, the top soil layer was classified as low plastic clay (CL) per the USCS, while the second layer was classified as well-graded sand (SW), and the bottom layer was medium plastic clay (CL). In addition to the basic soil properties, Figure 7.9 summarizes the measured Cone Penetration Test (CPT) tip resistance (q_c) and skin friction (f_s) for ISU-6, as well as the Standard Penetration Test (SPT) blow counts corrected for the effect of the soil overburden pressure. From this figure, it was noticed the average soil profile along the pile embedded length at ISU-6 is composed of about 63% clay (or cohesive material) and 37% sand (or cohesionless material). Following the 70% rule of soil categorization consistent with the AASHTO recommendations, the site at ISU-6 is classified as mixed soils site.

Using the Bluebook method for designing pile foundations, the nominal axial capacity of a single pile is 960 kN (216 kips). By adapting the regionally-developed LRFD recommendations for the Bluebook method in mixed soils from Table 7.1 (based on the 70% rule), the resistance factor is equal to 0.41 and the corresponding factored design capacity of a single pile within the pile group is 393.6 kN (88.5 kips), requiring a minimum of 26 piles/cap. By using the regional LRFD recommendations based on the recently proposed soil

categorization approach (based on the exact % cohesive material along the pile length), the resistance factor from Figure 7.8 is equal to 0.71 for the Bluebook method corresponding to 63% cohesive material. Therefore, the factored design capacity of a single pile is 681.6kN (153.3kips), requiring a total of only15 piles/cap as indicated in Figure 7.9. This 40% reduction in number of piles/cap will significantly reduce the foundation cost, since it reduces the construction costs for both piles and pile cap.

7.5. LRFD Considering Serviceability Limits

The pile serviceability limit state is defined by the prescribed permissible settlements and/or differential settlements, based on the structural serviceability requirements. According to the 2007 AASHTO LRFD specifications, the pile serviceability limits should be checked during the design stage and consistent with the bridge type, magnitude of transient loads, and the bridge's anticipated service life. However, the design specification only provides resistance factors for axially-loaded piles at the strength limit state. Consequently, pile settlement is typically checked after determining the design capacity, which may cause several design iterations to satisfy pile strength and serviceability requirements (Misra and Roberts, 2006). A design methodology, based on determining the load-displacement behavior of the pile, can easily incorporate both strength and serviceability limit states into the pile design process. The most accurate way to measure the actual load-displacement behavior is to conduct a pile static load test, a very expensive and time consuming field test (AbdelSalam et al., 2008). Another approach would be to establish suitable analytical models that can accurately calculate the pile vertical load-displacement behavior (Misra and Roberts, 2006; Roberts et al., 2008). The calculated pile load-displacement behavior, using any of the analytical models, can be compared to the actual field measured response, and for a dataset of load-tested piles. Consequently, the LRFD resistance factors can be developed based on the calculated load-displacement curves, insuring the pile factored capacity is limited to a pre-specified amount of vertical settlement that cannot be exceeded.

7.5.1. Pile characterization using t-z analysis

In this study, the improved t-z model developed by AbdelSalam et al. (2010) to

reduce the bias in the load-transfer analysis by measuring the soil-pile interface properties using a modified Borehole Shear Test (mBST) and a modified Direct Shear Test (mDST) in cohesive and cohesionless soils, respectively, was utilized to model the load-displacement behavior of seven (7) load-tested steel H-piles out of the recently conducted 10 SLTs. The mBST test was conducted at five (5) test sites and covered all possible soil layers at each of these sites. The five test sites mainly consisted of cohesive materials with identification numbers starting ISU-4 to ISU-8. The field measured *t-z* curves using mBST were integrated into the load-transfer analysis, using commercial software, TZPILE v.2.0, from ENSOFT, Inc. (Reese et al., 2005), which accordingly provided an estimate of the load-displacement relationship at the pile's head. For the other two test sites with identification numbers ISU-9 and ISU-10, mDST was conducted for different cohesionless soil layers and the load-displacement curves were calculated at the pile head using the improved t-z model. Figure 7.10a summarizes the calculated load-displacement curves for the seven steel H-piles using the load-transfer analysis. However, it is important to highlight the fact these load-displacement curves only characterize the skin-friction component of pile resistance, as the modeling process only included *t-z* curves along the pile's shaft. On the other hand, Figure 7.10b summarizes the field measured load-displacement curves for the skin-friction component of the seven load tested piles, where the skin-friction was separated for each pile, using the strain gauge data (see Ng et al., in process, for more complete information).

7.5.2. Displacement-based pile design

As acknowledged by Coduto (2001), Davisson's criterion is one of the most frequently used methods for determining the pile's maximum capacity from the load-displacement relationship. This method was essentially developed for driven piles and was used by Paikowsky et al. (2004) to calculate the LRFD resistance factors in the NCHRP-507, due to its efficiency compared to other methods. With Davisson's criterion, the pile's ultimate capacity is defined as the point of intersection between the load-displacement curve and a line parallel to the pile elastic compression, offset by a particular distance depending on the pile size and length. This parallel line is called the *Davisson line*. Typically, the Davisson line intersects with the load-displacement curve within the transition zone from the pile

elastic to the plastic behaviors. Thus, it can provide an acceptable pile design from the strength and serviceability prospects. In this study, the suggested LRFD displacement-based design approach limits the pile vertical settlement to a particular value relative to Davisson's maximum settlement (D), since D is an acceptable value that simultaneously considers pile strength and serviceability limit states. As shown in Figure 7.10, four different settlement ratios were selected and multiplied by D as follows: ¼ D, ½ D, ¾ D, and 1.0 D. Corresponding to the four settlement ratios, the measured nominal capacities for each of the seven test piles was determined.

Following the typical AASHTO calibration framework and based on the FOSM reliability approach, the LRFD resistance factors were calibrated for the four settlement ratios using the measured and calculated pile capacities from the load-displacement curves. Summarized in Table 7.4 are the LRFD resistance and efficiency factors required for the design of friction steel H-piles (HP 10x42), using t-z analysis and limited to pre-specified vertical settlement ranging from ¼ up to 1.0 D. From this table, it can be noted the displacement-based resistance, as well as the efficiency factors, are significantly higher, compared to the earlier LRFD resistance factors of conventional static analysis methods, which only accounted for the pile's strength limit state.

The proposed LRFD pile design procedures can be summarized as follow: 1) use the t-z model to calculate the pile load-displacement curve and determine the Davisson's maximum settlement(D); 2) choose the maximum allowable pile vertical settlement as a function of D; 3) identify this pre-defined maximum settlement on the load-displacement curve and determine the corresponding pile capacity; 4) use Table 7.4 to determine the LRFD resistance factors corresponding to the pile's pre-defined maximum settlement; and 5) multiply the determined capacity by the corresponding LRFD resistance factor to attain the factored pile design capacity, which will consequently prevent the pile from exceeding the pre-defined maximum settlement. Finally, the proposed LRFD displacement-based approach can be used to efficiently and practically determine the factored capacity of friction steel H-piles using the improved t-z model, and simultaneously limit this design to a pre-defined vertical settlement as a function of Davisson's maximum deformation.

7.6. Summary and Conclusions

This study aimed at establishing regional LRFD design recommendations for bridge pile foundations in the state of Iowa. Following the calibration framework recommended by AASHTO, resistance factors were locally-developed, based on PILOT-IA database for five different static methods, including the Bluebook in-house method. Summarized below are the major findings:

- The regional resistance factors for the SPT and β methods in sand were greater than those provided in the AASHTO by around 40 and 10%, respectively. In clay soils, the regional resistance factors for α and β methods were, respectively, 15 and 40% greater than those recommended by both NCHRP and AASHTO. In mixed soils, a 30% increase was obtained for β-method compared to AASHTO recommendations.
- Increasing the reliability index from 1.5 to 4.0 reduced the LRFD efficiency of static methods nonlinearly by an average of around 76% for different soil groups.
- The Bluebook method provided the highest efficiency compared to other static methods in sand, clay, and mixed soils.
- The regional resistance factors were verified by means of 10 recently conducted pile static load tests, and proved to provide reliable and consistent pile designs.

In addition to using COMB-1 and COMB-2, a special soil categorization approach that depends on the exact percent of cohesive material existing along the pile length was proposed and the corresponding resistance factors were re-developed. It was determined that using COMB-1 and COMB-2 improved the design efficiency in layered soil profiles. Moreover, utilizing a more refined soil categorization approach, based on actual soil profile provided significantly higher LRFD resistance factors, where the percent increase in the resistance factors ranged from 15 to 59% for different static methods. Regarding the suggested LRFD displacement-based pile design approach that depends on determining the load-displacement relationship using the improved t-z model, it was found the proposed approach can be efficiently and practically used to simultaneously determine the pile factored design capacity and limit the vertical settlement to a pre-defined value.

7.7. Acknowledgments

The study reported in this paper was conducted by the authors as part of the ongoing research project TR-573, Development of LRFD Design Procedures for Bridge Pile in Iowa, funded by the Iowa Highway Research Board (IHRB). The authors express their gratitude to the IHRB and members of the project's Technical Advisory Committee for their guidance and advice. The members of this committee represent Office of Bridges and Structures, Soils, Design Section, and Office of Construction of the Iowa DOT, FHWA Iowa Division, and Iowa County Engineers. Finally, special thanks to Kam Weng Ng and Mathew Roling for their help during the field/laboratory tests and data interpretation.

7.8. References

AASHTO LRFD Bridge Design Specifications (2007). Customary U.S. Units, 4th edition (2008 Interim), Washington, D.C.

AbdelSalam, S. S., Sritharan, S., and Suleiman, M. T. (2008). "Current Design and Construction Practices of Bridge Pile Foundations." IFCEE' 09, Orlando, FL.

AbdelSalam, S. S., Suleiman, M. T, and Sritharan, S. (2010a). "Modeling Axially-loaded Friction Steel H-Piles using the Load-Transfer Approach Based on a Modified Borehole Shear Test." To be submitted to the *Geotechnical Testing Journal*, ASTM.

AbdelSalam, S. S., Suleiman, M. T, and Sritharan, S. (2010b). "Improved t-z Analysis for Vertically Loaded Piles in Cohesionless Soils based on Laboratory Test Measurements." To be submitted to: ASCE, *Journal of Geotechnical and Geoenvironmental Engineering*.

Abu-Hejleh, N., DiMaggio, J, and Kramer, W. (2009) "AASHTO Load and Resistance Factor Design Axial Design of Driven Pile at Strength Limit State." *Transportation Research Board 88th Annual Meeting*, 2009, Paper #09-1034, Washington DC.

Allen, T. M. (2005). "Development of the WSDOT Pile Driving Formula and Its LRFD Calibration." FHWA Report, Washington State DOT.

American Concrete Institute - ACI (1974). "Recommendations for Timber Piles Design, Manufacture and Installation of Concrete Piles." ACI Report No. 543R-74.

Burland, J. B., (1973). "Shaft Friction of Piles in Clay." *Ground Engineering*, London, Vol.6., No.3, pp.3042

Coduto, D. P. (2001). “Foundation Design: Principles and Practices.” Prentice-Hall Inc., Englewood Cliffs, N.J.

Coyle, H. M. and Reese, L. C. (1966). “Load Transfer for Axially-loaded Piles in Clay.” *Journal of Soil Mechanics and Foundation Engineering Division*, 92(2), 1- 26.

Davisson, M. (1972). “High Capacity Piles.” *Soil Mechanics Lecture Series on Innovations in Foundation Construction*, ASCE, IL, Chicago, IL, pp. 81–112.

Dirks, K. and Kam, P. (1989). “Foundation Soils Information Chart.” *Iowa DOT, Office of Road Design*, Ames, Iowa, United States.

Foye, K. C., Abou-Jaoude, G., Prezzi, M., and Salgado, R. (2009). “Resistance Factors in LRFD of Driven Pipe Piles in Sand.” *Journal of Geotechnical and Geoenvironmental Engineering*, ASCE, v 135, n 1, 2009.

Kyung, K. J., Gabr, M. A., and Shamimur, M. R. (2002). “Development of Resistance Factors for Axial Capacity of Driven Piles.” North Carolina State University.

McVay, M., Klammler, H., Bloomquist, D., Otero, J., and Farone, M. (2010). “Modification of LRFD Resistance Factors Based on Site Variability.” University of Florida, Gainesville, FL.

Meyerhof, G. (1976). “Bearing Capacity and Settlement of Pile Foundations.” ASCE, *Journal of the Geotechnical Engineering Division*, Vol. 102, No. 3, March, pp. 195–228.

Misra, A. and Roberts, L. A. (2006). “Probabilistic Analysis of Drilled Shaft Service Limit State Using the t-z Method.” *Canadian Geotechnical J*ournal, 1324-1332 (2006).

Misra, A., Roberts, L. A. and Levorson, S. M. (2007). “Reliability of Drilled Shaft Behavior using Finite Difference Method and Monte Carlo Simulation.” ASCE: *Geotechnical and Geoenvironmental Engineering*, No. 25, pp. 65-77.

Ng, K. W., Suleiman, M. T., Roling, M. J., AbdelSalam, S. S., and Sritharan, S. (in process). “Development of LRFD Procedures for Bridge Piles in Iowa- Volume II.” Iowa State University, Ames, IA.

Nordlund, R. L. (1963). “Bearing Capacity of Piles in Cohesionless Soils.” *Journal of Soil Mechanics and Foundation Engineering*, JSMFE, Vol. 89, SM 3, pp 1-36.

Nowak, A. S. and Collins, K. R. (2000). “Reliability of Structures.” McGraw-Hill Inc.

Paikowsky, S. G., McVay, B. M., Nguyen, T., Kuo, C., Baecher, G., Ayyub, B., Stenersen,

K., O'Malley, K., Chernauskas, L., and O'Neill, M. (2004). "LRFD for Deep Foundations." NCHRP-507, TRB, Washington D.C.

Reddy E. S., O'Reilly M., Chapman D. A. (1998). "Modified t-z Model - A Software for Tension Piles." *Computers and Structures*, No. 68: 613–25.

Reese, L. C., Wang, S. T., and Arrellage, J. (2005). "Analysis of Load Versus Settlement for an Axially-loaded Deep Foundation - TZPILE v.2.0 Software User Manual." ENSOFT, INC. 3003 West Howard Lane, Austin, Texas 78728.

Roberts, L. A., Gardner, B. S., and Misra, A. (2008). "Multiple Resistance Factor Methodology for Service Limit State Design of Deep Foundations using a t-z Model Approach." *Proceeding: The Geo-Congress 2008*, New Orleans, LA.

Roling, M. J., AbdelSalam, S. S., Sritharan, S., and Suleiman, M. T. (2010). "An Investigation of Design and Construction Practices for Bridge Pile Foundations in Iowa County Jurisdictions for LRFD Calibration." Submitted to: *The TRB Low-Volume Roads Conference and Journal*, March 2010, under review.

Roling, M. J., Sritharan, S., and Suleiman, M. T. (2010). "Development of LRFD Procedures for Bridge Piles in Iowa- Volume I." Iowa State University, Ames, IA.

Scott, B., Kim, B. and Salgado, R. (2003). "Evaluation of Load Factors for use in Geotechnical Design." *Journal of Geotechnical and Geoenvironmental Engineering*, ASCE, 129(4).

Shapiro, S. S. (1980). "How to Test Normality and other Distributional Assumptions: ASQC Basic References in Quality Control." *Statistical Techniques 3*, pp. 1-78.

Suleiman I. B. and Coyle H. B. (1976). "Uplift Resistance of Piles in Sand." *Journal of Geotechnical Engineering*, ASCE 1976; 102(GT5):559–62.

Tomlinson, M. J. (1980). "Foundation Design and Construction." The 6th Edition, Longman Scientific & Technical, Essex, England.

Table 7.1: Preliminary LRFD resistance factors for different static methods and soil groups

Soil Type	N	Static Analysis Method	Mean (λ)	St. Dev.	COV	β=2.33		β=3.00	
						φ[1]	φ/λ[2]	φ	φ/λ
Sand	35	**Bluebook**	1.22	0.52	0.42	**0.51**	0.42	**0.37**	0.31
	35	**SPT-Meyerhof**	1.72	1.14	0.66	**0.43**	0.25	**0.28**	0.16
	35	**β-Method**	0.87	0.42	0.48	**0.33**	0.37	**0.23**	0.27
	35	**Nordlund**	0.91	0.48	0.53	**0.30**	0.33	**0.21**	0.23
Clay	15	**Bluebook**	1.35	0.44	0.32	**0.70**	0.52	**0.54**	0.40
	15	**α-API Method**	1.30	0.59	0.45	**0.52**	0.40	**0.37**	0.29
	15	**β-Method**	1.13	0.65	0.57	**0.35**	0.31	**0.24**	0.21
Mixed	32	**Bluebook**	1.25	0.67	0.54	**0.41**	0.33	**0.28**	0.23
	32	**SPT-Meyerhof**	1.82	1.22	0.67	**0.45**	0.25	**0.29**	0.16
	32	**α-API Method**	1.20	0.75	0.63	**0.32**	0.27	**0.21**	0.18
	32	**β-Method**	0.98	0.52	0.53	**0.33**	0.33	**0.23**	0.23
	32	**Nordlund**	1.19	0.76	0.64	**0.31**	0.26	**0.21**	0.17

[1] LRFD geotechnical resistance factor for PILOT-IA; and [2] Corresponding efficiency factor.

Table 7.2: Comparison between the recommended resistance factors by general design specifications and the regionally-calibrated factors

Soil	Static Analysis Method	Iowa	AASHTO	NCHRP 507
Sand	**SPT-Meyerhof**	0.42	0.3	0.45
	β-Method	0.32	N/A	0.3
	Nordlund	0.31	0.45	0.45
Clay	**α-API**	0.52	N/A	0.45
	β-Method	0.35	0.25	0.2
Mixed	**α-API**	0.32	N/A	0.35
	β-Method	0.34	0.25	0.2
	Nordlund	0.34	N/A	0.2-0.35

Table 7.3: Resistance factors for mixed soils (using 70% rule) versus 50% cohesive material

Static Method	Mixed Soil (70% rule)		50% Cohesive Material		%Increase*
	φ	φ/λ	φ	φ/λ	
Bluebook	0.41	0.33	0.65	0.57	59%
SPT-Meyerhof	0.45	0.25	0.70	0.50	56%
α-API Method	0.32	0.27	0.47	0.50	47%
β-Method	0.33	0.33	0.38	0.46	15%
Nordlund	0.31	0.26	0.42	0.46	35%

* Percent increase in the resistance factors.

Table 7.4: Resistance factors for the design of friction steel H-piles that account for strength and serviceability limits

Analysis Method	N	Limited[2] Settlement	Mean (λ)	St. Dev. (σ)	COV	β=2.33	
						φ	φ/λ
T-Z[1] analysis	7	1/4D	0.95	0.14	0.15	**0.67**	0.71
	7	1/2D	1.00	0.14	0.14	**0.73**	0.72
	7	3/4D	1.05	0.13	0.13	**0.77**	0.73
	7	D	1.13	0.22	0.20	**0.74**	0.66

[1] Load-transfer analysis using mBST and/or mDST results to model the pile load-displacement response for the skin-friction component; and [2] Limited settlement ratio as a function of Davisson's maximum value (D) for a steel H-piles.

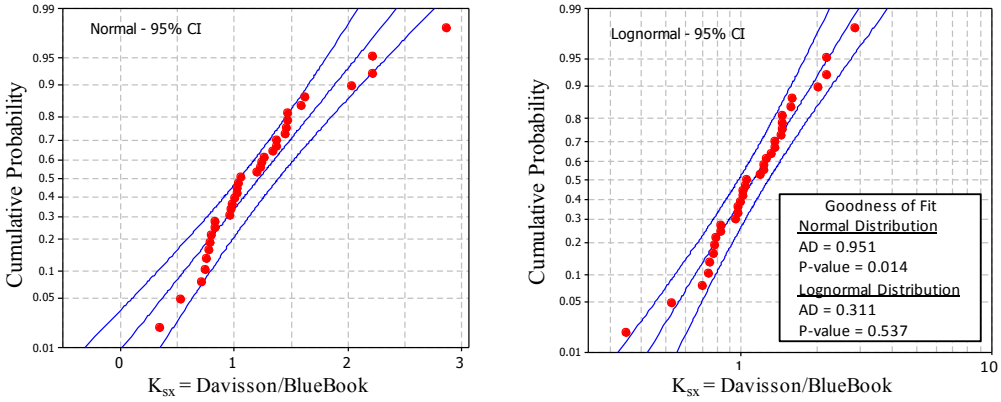

(a) Normal distribution **(b) Lognormal distribution**

Figure 7.1: Goodness-of-fit tests for the Bluebook method in sand

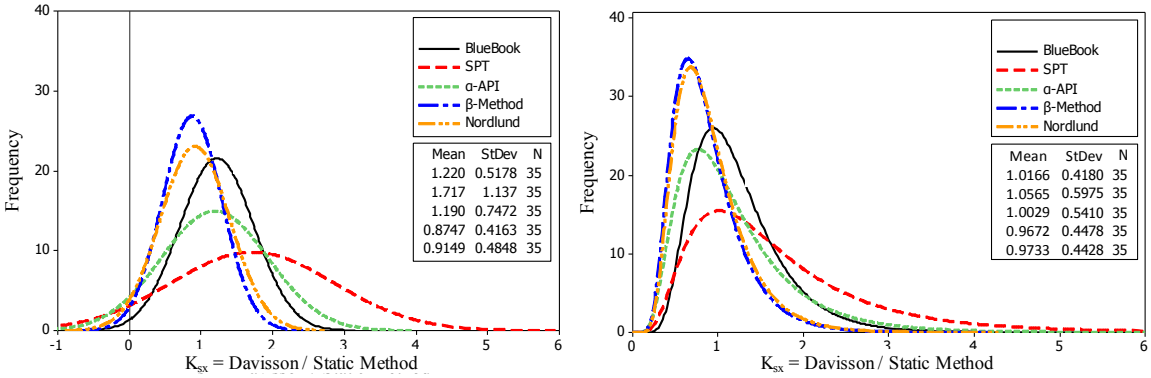

(a) Normal distribution **(b) Lognormal distribution**

Figure 7.2: K_{sx} obtained for 35 piles in sand using different static methods

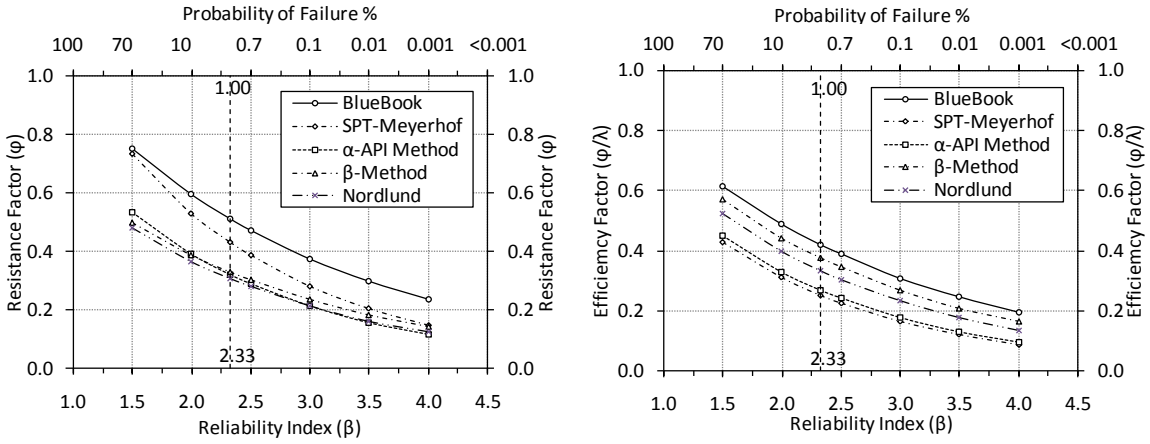

(a) Resistance factors **(b) Efficiency factors**

Figure 7.3: Influence of the reliability index obtained for 35 piles in sand

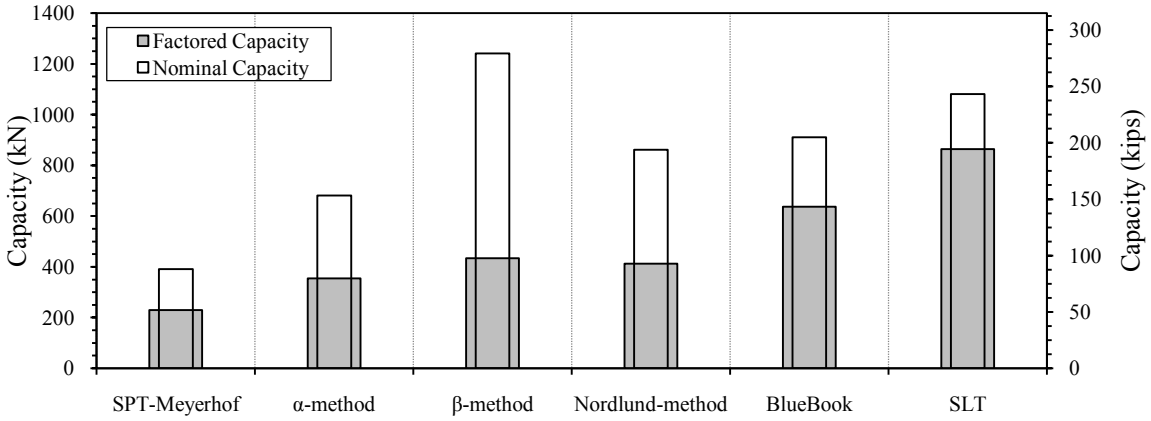

Figure 7.4: Factored and nominal capacities of the test pile driven into clay soil at ISU-5

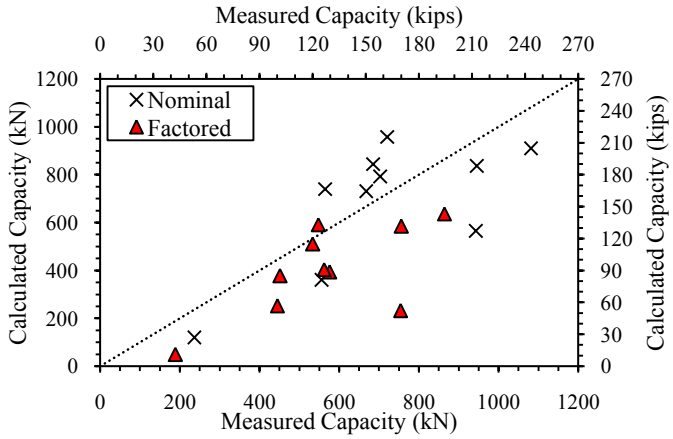

Figure 7.5: Bluebook calculated versus measured capacities for the 10 test piles

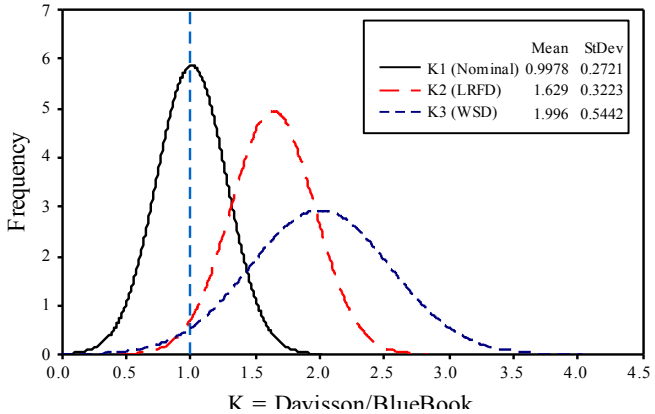

Figure 7.6: Frequency distribution of the PDFs representing the mean bias ratios K_1, K_2, and K_3, calculated for the test piles

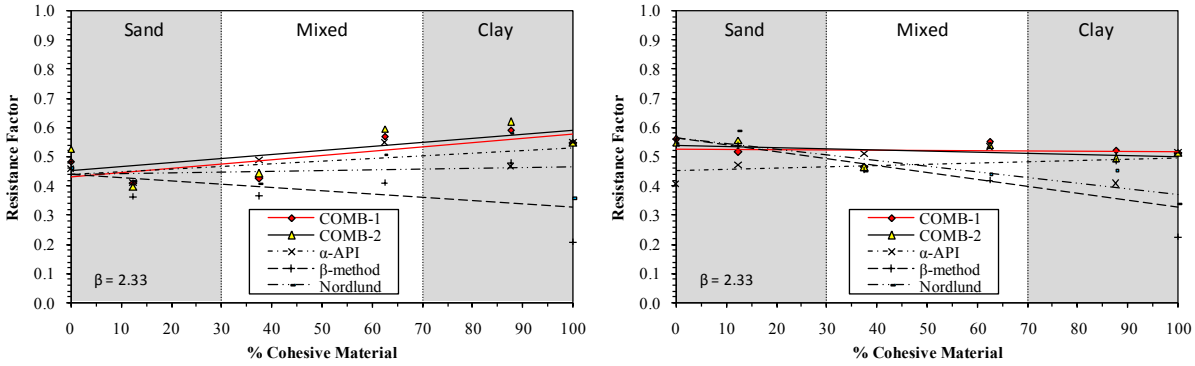

(a) Resistance factors **(b) Efficiency factors**

Figure 7.7: LRFD factors for different static methods and combinations of methods

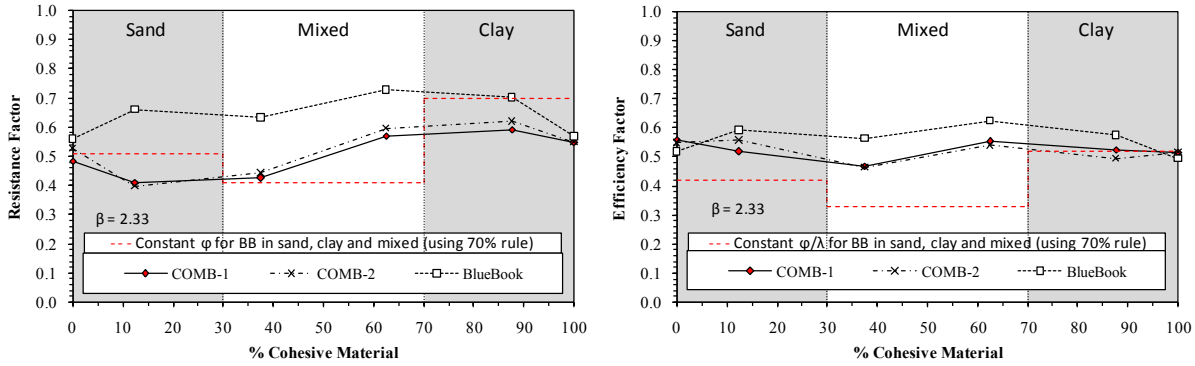

(a) Resistance factors **(b) Efficiency factors**

Figure 7.8: LRFD factors according to the exact %cohesive material along the pile length

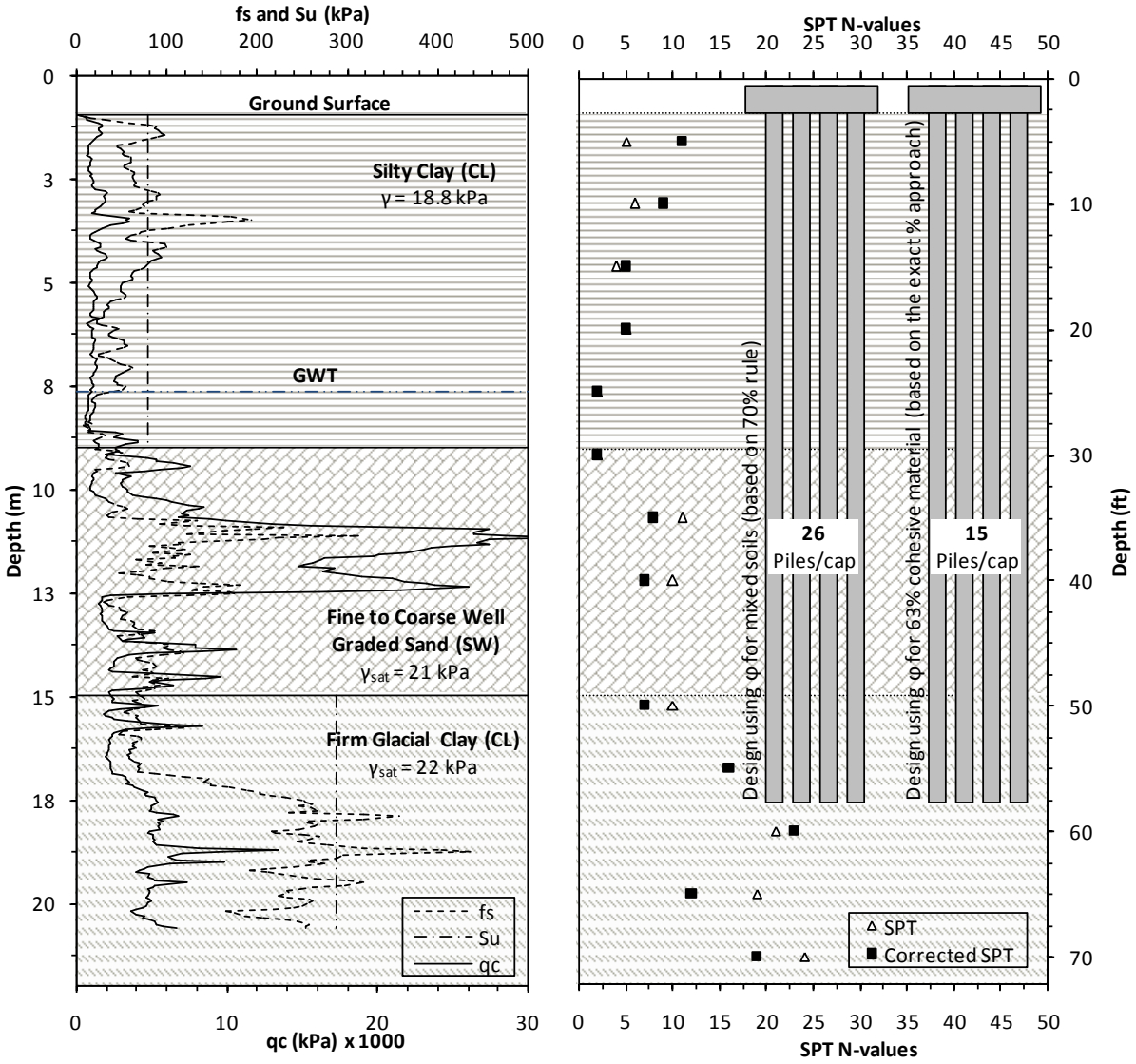

Figure 7.9: Summary of soil tests conducted at ISU-6 including: tip resistance (q_c) and skin friction (f_s) from CPT; SPT corrected N-values; and the required design number of piles/cap using the LRFD recommendations based on the 70% rule versus the exact %cohesive material

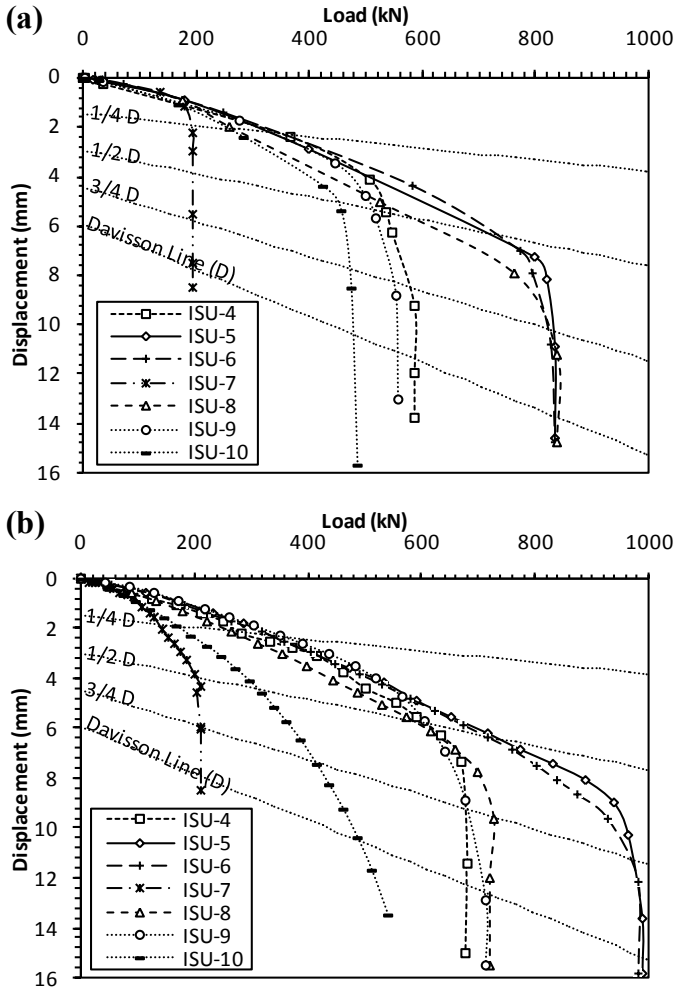

Figure 7.10: Load-displacement curves for the skin-friction component of the seven test piles (a) predicted using TZ-mBST and TZ-mDST models; and (b) measured from SLT

CHAPTER 8: CONCLUSIONS AND RECOMMENDATIONS

8.1. Summary

This dissertation provides regionally-calibrated LRFD resistance factors for the design of bridge pile foundations for soils in Iowa, based on efficient static methods. The resistance factors were calibrated three times using the following approaches: (a) based on the recommended AASHTO LRFD calibration framework; (b) using a specially developed soil categorization approach and combinations of static methods; and (c) based on characterizing the load-displacement response of axially-loaded piles utilizing improved modeling techniques. To provide necessary data to develop the LRFD recommendations for these three approaches, the following information was used: (1) results from a nationwide survey that focused on collecting necessary information regarding the current design and construction practices of bridge deep foundations; (2) historical load test data and soil properties collected for 264 test sites and housed in the electronic database PILOT-IA; and (3) comprehensive load test and soil data collected from ten full-scale instrumented pile static load tests (SLTs) recently conducted as part of this research, and included various in-situ and laboratory soil tests for each site.

In addition, the research presented in this thesis led to: (1) improving the load-transfer analysis in cohesive soils, using a *modified* Borehole Shear Test (mBST); (2) improving the load-transfer analysis in cohesionless soils using the Pile Tip Resistance (PTR) test and the *modified* Direct Shear Test (mDST); and (3) advancing the finite element (FE) analysis to accurately simulate pile and soil behaviors in sand and glacial clay. The results and analysis from this investigation are presented as five dissertation chapters [Chapters 3-7] above.

8.2. Conclusions

For Chapters 3-7, an overview and major conclusions are provided below.

8.2.1. National survey findings

Chapter 3 of this thesis presented results from an important survey on current design and construction practices of bridge deep foundations, one of the first surveys completed

following the Federal Highway Administration (FHWA) mandate on the use of the LRFD approach in the U.S. on all new bridges initiated after October 1, 2007. The outcomes of the survey are significant. They provided an overview of current bridge foundation practices and highlight how frequently the Department of Transportation (DOT) in different states takes advantage of the provisions in the AASHTO-LRFD specifications to improve deep foundation design by employing regionally-calibrated geotechnical resistance factors and their associated benefits. Based on the statistical analysis and responses obtained from the survey, the following conclusions were drawn.

1. About 52% of the 33 state DOTs who responded to the survey adopted the LRFD approach for the design of bridge deep foundations, 33% were in a transition phase from ASD to LRFD, and the remaining 15% still followed the ASD approach with a factor of safety ranging from 2 to 2.5. Of those using the LRFD, six DOTs use geotechnical resistance factors by fitting to WSD, 12 adapted their own regionally-calibrated factors, based on reliability theory, and eight uses the AASHTO.
2. The LRFD regionally-calibrated resistance factors reported for sands and clays are greater by about 50 and 100%, respectively, than the AASHTO's recommended values. This large increase in resistance factors leads to a reduced overall cost of bridge foundations.
3. In the design stage, state DOTs use static analysis methods for determining pile capacity. The most commonly used methods in cohesive soils are the α- and β-methods. On the other hand, the most commonly used static methods in cohesionless soils are the Nordlund and SPT methods. A majority of the respondents chose the α-method and the Nordlund method to be the most accurate method for determining pile capacity in cohesive and non-cohesive soils, respectively.

8.2.2. Improved t-z analysis in clay

Chapter 4 of this thesis introduced an improved t-z analysis in cohesive soils used to characterize the load-displacement response of axially-loaded piles and load transfer along pile length. A new *modified* Borehole Shear Test (mBST) was proposed to directly measure the *t-z* curves in the field, required to model the soil-pile interface in the t-z analysis. For

steel piles, the mBST uses smooth steel plates to accurately measure the shear stress as a function of displacement along the pile's length, which, for the first time, avoids the reliance on empirical correlations with soil tests to estimate the soil-pile interface properties. Three full-scale instrumented load tests were conducted at ISU-5, ISU-6, and ISU-7 on friction steel H-piles driven into mainly cohesive soil profiles. The soil profiles at the three sites were characterized, using SPT, CPT, BST, and mBST tests. Four major t-z models were analyzed for each test pile and compared with measured responses. The major conclusions are summarized below.

1. The pile load-displacement relationship predicted using *t-z* curves, based on empirical correlations with CPT data, significantly overestimated the soil-pile interface properties, the first portion of the load-displacement curve, and the pile capacity by as much as 50%.
2. The load-displacement responses calculated for the three test piles, using *t-z* curves obtained from mBST, provided a very good match along the first portion of the field measured responses, and an acceptable estimate of the capacity with differences ranging from 17 to 25% for the three test piles.
3. Ignoring the end-bearing component (*q-w* curve) in the t-z analysis did not affect the results in the case of steel H-piles driven into clay soil profiles. This is because the test piles were mainly friction piles, as confirmed by the percent of the load resisted by end-bearing that ranged from 2 to 17% for the three test piles.
4. Based on the overall response predictions for the three test sites, the t-z model, based on the proposed mBST test results, proved to provide better assessment for pile behavior compared with the model, based on CPT data.
5. The proposed mBST is a simple and a cost effective in-situ test that captures the soil-pile interface properties in cohesive soils and can be directly used in t-z analysis to simulate the load-displacement and the load distribution along the pile's length.

8.2.3. Improved t-z analysis in sand

Chapter 5 of this thesis introduced two new laboratory tests to improve the t-z analysis of axially-loaded piles in cohesionless soils, since the mBST cannot be conducted in

sandy soil profiles and cannot measure the pile end-bearing properties. The first test is the *modified* Direct Shear Test (mDST), where a steel plate is placed in the lower half of the DST box to accurately measure the shear stress as a function of displacement for different soil layers. The second is the Pile Tip Resistance (PTR) test, which provides a measure of the load-penetration response of the soil under pile foundations, using a small-scale steel plate that represents a fictitious rigid footing. The mDST and PTR basically provide a measure for the *t-z* and *q-w* curves, required for a complete t-z analysis and, respectively, represent the skin-friction and the end-bearing properties of steel piles driven into sand soils. Compared with field results from two pile SLTs conducted at ISU-9 and ISU-10 that represent sandy sites, the t-z analysis based on the mDST and PTR measurements provided an improved shaft load-displacement response (TZ-S-mDST), as well as an improved total load-displacement response (TZ-T-mDST). A summary of the major findings is presented below.

1. Using the mDST, the laboratory measured *t-z* curves compared to those measured in the field using the strain gauges readings. It was determined the differences between them at the maximum shear stress did not exceed 5%.
2. The PTR test was conducted to measure the *q-w* curve using different sizes, shapes, and placements of the small-scale steel plate. It was found the effect of changing these factors on the results is minimal and did not exceed 10%.
3. A finite element model was utilized to assess the effect of the PTR box boundaries on the behavior of the small-scale steel plate. It was determined the PTR box and plate dimensions are appropriate.
4. For the test pile at ISU-9, the predicted load-displacement relationship for the shaft using the TZ-S-mDST model perfectly matches the measured response. When adding the end-bearing component to the ISU-9 analysis (i.e., TZ-T-mDST), the model provided a very good match of the measured load distribution, as a function of depth, as well as the total load-displacement curve, with only a 3.3% softer response along the elastic portion of the curve and a 4% lower capacity at the plastic portion.
5. The TZ-T-mDST model also showed satisfactory prediction of the measured total load-displacement response for ISU-10 with a difference equal to about 12% along the elastic portion of the curve and about 4% for the plastic portion.

6. Based on overall response predictions for the two test piles, the load transfer analysis, based on the *t-z* and *q-w* curves, respectively, measured using the mDST and PTR tests have proven to provide an improved prediction of the field measured load-displacement responses, which offer a simple and cost-effective procedure to characterize the behavior of steel pile driven into sandy soils.

8.2.4. Finite element analysis

Chapter 6 of this thesis presented an adjusted finite element (FE) model to accurately and economically characterize the behavior of axially-loaded steel H-piles using PLAXIS 7.2, since the t-z model does not provide an insight into the stress-strain behavior of the soil continuum surrounding the pile, which may affect adjacent foundations. In the FE analysis, the Mohr-Coulomb soil constitutive properties were established, based on empirical correlations to the CPT data. The preliminary analysis showed the FE model can satisfactorily characterize the behavior of the steel piles driven into cohesionless soil layers. However, the model failed to capture the load-displacement response for the piles driven into cohesive layers. A sensitivity analysis aimed to enhance the overall prediction of the FE model was conducted by means of using mDST and CU-Triaxial soil laboratory test data, which, respectively, amended the properties of the soil-pile interface element and the soil elastic modulus. A summary of the major findings is presented below.

1. The preliminary FE model did not provide accurate prediction for the behavior of the test piles ISU-4, ISU-5, and ISU-9 due to clay layers existing along the pile's length.
2. The interface investigation showed the recommended properties of soil-pile interface element are appropriate for clay-steel contacts. Therefore, the bias in the FE analysis could be due to inappropriate values of the soil elastic modulus.
3. The soil modulus investigation showed the empirically-established elastic modulus values for clay soils, based on CPT data, were underestimated by around 100%. After amending the elastic modulus for clay soils, the improved FE model for ISU-4 showed the differences between the predicted and measured load-displacement responses was reduced from 60 to 27% along the elastic portion of the curve, and from 43 to 11% at the ultimate capacity. For ISU-5, the difference between the

predicted and measured load-displacement responses was reduced from 64 to 33% along the elastic portion of the curve, and from 65 to 9% at the ultimate capacity. For ISU-9, the difference between the predicted and measured load-displacement responses was reduced from 41 to 30% along the elastic portion of the curve, and from 26 to 7.5% at the ultimate capacity.

4. Overall, the improved FE model has provided a satisfactory prediction compared to field test results and for steel H-piles driven into clay and sand soil layers. The improved FE analysis is based on the simple Mohr-Coulomb constitutive model, which avoids using sophisticated soil models that require conducting costly and time-consuming soil tests.

8.2.5. Developed LRFD resistance factors

Chapter 7 of this thesis presented the regionally-calibrated LRFD resistance factors developed for the design of bridge pile foundations in the state of Iowa. Following the calibration framework recommended by AASHTO, the resistance factors were locally developed based on the PILOT-IA database for five different static methods, including the *Bluebook* in-house method. Summarized below are the major conclusions:

1. The regional resistance factors for the SPT and β methods in sand were greater than those provided in the AASHTO by around 40 and 10%, respectively. In clay soils, the regional resistance factors for the α and β methods were, respectively, 15 and 40% greater than those recommended by both NCHRP and AASHTO, while in mixed soils an increase of about 30% was obtained for the β-method compared to AASHTO recommendations.
2. Increasing the reliability index from 1.5 to 4.0 reduced the efficiency of different static methods nonlinearly by an average of approximately 76% for any soil type.
3. The *Bluebook* method provided the highest efficiency compared to other static methods in sand, clay, and mixed soils.
4. The regionally-calibrated resistance factors were verified and confirmed by means of 10 pile static load tests, yielding reliable and consistent pile designs.

Moreover, two new combinations of static methods were developed in this framework (i.e., COMB-1 and COMB-2), in addition to a specially proposed soil categorization approach that depends on the exact percent of cohesive material existing along the pile length. Both advancements to the typical AASHTO calibration framework have increased the values of the LRFD resistance and efficiency factors. Summarized below are the major conclusions:

5. COMB-1 and COMB-2 increased the pile design efficiency in layered soils compared to using a single static method.
6. Utilizing a more refined soil categorization approach, based on the actual soil profile, and provided significantly higher LRFD resistance factors, where the percent increase in the resistance factors ranged from 15 to 59% for different static methods.

The current AASHTO LRFD recommendations provide resistance factors that only account for the pile strength limit state and ignore the serviceability limits. A displacement-based pile design approach was suggested instead. This approach depends on determining the pile load-displacement response, using the t-z method, based on measurements from the mBST and mDST tests. The major conclusions are summarized below.

7. The proposed LRFD displacement-based design approach can be used to simultaneously determine the pile's design capacity and limit the vertical settlement to a pre-defined value.
8. Utilizing the displacement-based pile design approach provided significantly higher LRFD resistance and efficiency factors compared to AASHTO LRFD recommendations.

8.3. Recommendations for Future Work

The investigations presented in this thesis have addressed several challenges associated with the development of the LRFD resistance factors, as well as improving the modeling of axially-loaded steel piles using several analytical methods. A number of issues have become apparent through the course of this investigation, which deserves further investigation as detailed below.

1. Developing the LRFD resistance factors for dynamic analysis methods and dynamic formulas would be helpful to verify the design and monitor pile driving in the field. Using these methods can also provide recommendations that account for the construction control aspects in the design. These topics are examined in companion studies of the same project (see Ng, W. K., in process, and Roling, M. J., 2010).
2. Developing the LRFD resistance factors for the design of drilled shafts would be essential for the Iowa DOT to achieve more comprehensive design guidelines for bridge deep foundations. This requires building a database similar to PILOT-IA, but for drilled shafts.
3. Using results from the 10 SLTs conducted as part of this project, separating the skin-friction and end-bearing components of the pile resistance and developing the corresponding LRFD resistance factors separately may lead to a significant reduction in the cost of bridge deep foundations. For static analysis methods, calibrating the LRFD resistance factors for each component of the pile resistance may also increase the efficiency of the pile's design.
4. The mBST was essentially developed in this study to capture the soil-pile interface properties for steel piles in cohesive soils. However, it would be beneficial to conduct the same modifications to the BST equipment, but using concrete plates instead of the steel plates to capture the interface properties between the soil and concrete drilled shafts. Also, conducting the mBST test in cohesionless soils would provide an improved t-z analysis for all soil types.
5. The adjusted FE model can be used to facilitate incorporation of the vertical settlement and serviceability limits into the design of deep foundations using the LRFD approach. The resistance factors calibration can be conducted following the same approach used in this dissertation for the mBST and mDST.
6. Including the anchor piles, required to support the loading frame to load test the piles, in the FE model would result in a more representative simulation of the problem. In addition, more investigations are needed to properly address the interface properties in the model, which can be attained using the mBST and the mDST actual measurements.

ACKNOWLEDGMENTS

The study reported in this thesis was conducted by the author as part of the ongoing research project TR-573, TR-583 & 584: Development of LRFD Procedures for Bridge Pile Foundations in Iowa funded by the Iowa Highway Research Board (IHRB).

For the course of the doctoral research, the author would like to express deep appreciation and gratitude to the major professor, Dr. Sri Sritharan, for his precious input and guidance throughout this research. The author would also like to state recognition to Dr. Muhannad T. Suleiman for his distinguished contributions and advice during this research. Special thanks to Kam W. Ng and Mathew J. Roling, who have been working on the same research project and significantly contributed to conducting the field and laboratory testing.

For serving on the program of study, the author acknowledges the following committee members for their assistance and advice: Dr. Fouad S. Fanous, Thomas J. Rudolphi, Charles T. Jahren, and Jeramy C. Ashlock. The members of this committee represent the divisions of structural, geotechnical, and construction engineering, at the Department of Civil, Construction, and Environmental Engineering, and the Department of Aerospace Engineering.

For their coordination and support of this research, the author would like to thank Sandra Larson and Mark Dunn, from the Research and Technology Bureau of the Iowa DOT, as well as the following individuals who served on the Technical Advisory Committee: Ahmad Abu-Hawash, Dean Bierwagen, Lyle Brehm, Ken Dunker, Kyle Frame, Steve Megivern, Curtis Monk, Michael Nop, Gary Novey, John Rasmussen, and Bob Stanley. The members of this committee represent Offices of Bridges and Structures, Soils, Design and Construction of the Iowa DOT, FHWA Iowa Division, and Iowa County Engineers.

And finally, many thanks to Douglas Wood for assistance on conducting pile static load tests, Don Davison and Erica Velasco for the assistance with laboratory soil tests, Clinton Halverson from Team Services Inc., and Zach Thomas from Geotechnical Services Inc. (GSI) for conducting soil in-situ tests.